VARIOLITIC BASALTS:

RELATIONS TO ARCHEAN EPIGENETIC GOLD DEPOSITS

IN THE ABITIBI GREENSTONE BELT

by

Murray Ira Jones

A thesis submitted to the School of Graduate
Studies in partial fulfillment of the requirements
for the degree of M.Sc. in Geology

OTTAWA-CARLETON GEOSCIENCE CENTRE
UNIVERSITY OF OTTAWA

Abstract

Variolites are mafic to intermediate volcanic rocks containing centimetre-sized, spherical domains, termed varioles. Varioles are dominantly composed of plagioclase spherulites. Variolitic volcanic rocks host ore in many epigenetic Au deposits within Archean greenstone belts. The geochemistry and alteration of variolitic rocks were studied within the Archean Abitibi Greenstone Belt in Harker Township, Ontario and in the Dome Mine area, Timmins, Ontario. The study demonstrates that there is a connection between the anomalously high Fe/Mg ratio of the variolites and disseminated sulphide-Au mineralization.

Variolites occur dominantly in the upper, more evolved parts of Fe tholeiitic volcanic sequences. They commonly have a more differentiated composition than typical Fe tholeiitic MORB rocks. They have elevated concentrations of incompatible elements, silica, iron, titanium and phosphorous, and lower than expected concentrations of compatible elements such as vanadium and magnesium. In addition, their Fe/Mg ratio is anomalously high, commonly greater than 3.0. Varioles tend to be more concentrated in intermediate-acidic flows, which are characterized by flow banding, extensive development of hyaloclastite, and brittle fracture. Disequilibrium crystal habits, including plagioclase spherulites, branching amphiboles (after pyroxene), and dendritic oxides, are common in variolites and are related to diffusion limited growth conditions. These conditions were likely caused, in part, by the relatively silica-rich nature of the lavas and undercooling.

The differentiation of the variolitic suites is interpreted to be due to fractional crystallization. The compositional range of the suite is similar to other strongly differentiated Archean tholeiitic rocks, such as the Golden Mile Dolerite in Kalgoorlie, Australia. The variolitic suites are also similar to modern evolved, oceanic suites developed in areas of thicker oceanic crust. The variolitic suites are interpreted to result from injection of tholeiitic magma along faults to high levels in the crust where lower temperatures and pressures promoted rapid and extensive differentiation.

Alteration studies of variolites associated with Au mineralization revealed that the alteration mineralogy is partly related to the host rock composition. The upper, more evolved flows of the variolitic suites tend to stabilize a complex mineral assemblage, including albite,

Fe-Ti oxides, and pyrite whereas the lesser evolved flows stabilize a simpler assemblage, generally dominated by carbonate minerals. In both areas, mineralized zones have significant addition of CO_2, S, and Au and depletion of H_2O. Hydrothermal alteration in the Harker Lake area is characterized by oxidation of the host rock with addition of Na_2O and Sr and depletion of Zn, MgO, MnO and, to a minor extent, HREE, whereas alteration at the Dome Mine is characterized by reduction of the host rock, addition of K_2O, Ba, CaO, B, and LREE, and depletion of Na_2O, Sr, and HREE. These results reflect differences between the two areas in the size and intensity of the mineralizing events, the influence of structural styles, and the local rock types.

In variolites, Au is deposited by destabilization of the Au-bisulphide complex largely due to removal of sulphur from solution by reaction with iron in the host rock to form pyrite. Bohlke (1988) has demonstrated that the Fe/Mg ratio of the host rock plays a key role in determining whether Fe-Mg(-Ca) carbonates or pyrite will be formed in the alteration zone. Pyrite will tend to form in host rocks which have a high Fe/Mg ratio. This effect is enhanced when the auriferous hydrothermal fluids have previously equilibrated with high magnesian rocks. The anomalously high Fe/Mg ratio of variolitic rocks (> 2.0) makes them ideal chemical traps for sulphide-Au mineralization. Additionally, their tendency for brittle fracture enables the fluids to affect a greater volume of rock, enhancing the potential for mineralization.

Variolites may be useful in the exploration for epigenetic Au deposits. As a consequence of their composition, variolites have excellent potential to host disseminated sulphide-Au mineralization in association with shear zones or faults, which have provided the pathways for auriferous fluids.

Sommaire

Les variolites sont des roches volcaniques mafiques à intermédiaires contenant des zones sphériques centimétriques appelées varioles. Les varioles sont principalement composées de sphérulites de plagioclase. Les roches volcaniques variolitiques sont typiquement minéralisées dans plusieurs gisements d'or épigénétiques à l'intérieur de ceintures de roches vertes archéennes. La géochimie et l'altération des roches variolitiques furent étudiées à Harker Township, Ontario, et à la mine Dome, Timmins, Ontatio, à l'intérieur de la ceinture de roches vertes de l'Abitibi. Cette étude démontre qu'il y a un lien entre le rapport élevé de Fe/Mg des variolites et la minéralisation disséminée de sulfures et d'or.

Les variolites sont situées principalement dans la partie supérieure et évoluée des séquences volcaniques tholéiitiques riches en fer. Ils ont communément une composition plus différenciée que les roches tholéiitiques riches en fer de type MORB. Les variolites ont des teneurs élévées en éléments incompatibles, silice, fer, titane, et phosphore, et des teneurs faibles en éléments compatibles tel que le vanadium et le magnésium. De plus, leur rapport en Fe/Mg est enrichi (Fe/Mg > 3.0). Les varioles ont tendance à être concentrées dans les coulées intérmediaires à felsiques, lesquelles sont characterisées par la présence de couches rubannées, par l'abondance de hyaloclastite, et par la présence de fractures à comportement fragile. Les cristaux montrant des morphologies à l'état de déséquilibre, tels les sphérulites de plagioclase, les amphiboles (après pyroxene) en forme de branches, et les oxydes dendritiques, sont communs dans les variolites, et furent formés dans des conditions limitées par la diffusion. Ces conditions furent principalement causées par l'enrichissement des coulées en silice, et par un taux élevé de refroidissement.

La différenciation des séquences variolitiques est interpretée comme étant le résultat d'une cristallisation fractionnée. La variation en composition des séquences est semblable à d'autres roches tholéiitiques archéennes fortement différenciées, tel le Golden Mile Dolerite à Kalgoorlie, Australie. Les séquences variolitiques sont également semblables aux roches océaniques modernes évoluées, produites dans les régions où la croûte océanique est épaisse. Les séquences variolitiques sont interprétées comme étant le résultat d'injections de magma

tholéiitique le long des failles, à des niveaux élevés de la croûte, où les températures et pressions réduites ont favorisé une différenciation rapide et considérable.

Les études portant sur l'altération des variolites minéralisées ont démontré que la minéralogie associée à l'altération est reliée à la composition initiale des roches. Les coulées supérieures évoluées des séquences variolitiques ont tendance à stabiliser un assemblage de minéraux complexes, comprenant l'albite, les oxydes riches en fer et titane, et la pyrite. Par contre, les coulées inférieures stabilisent un assemblage plus simple, généralement dominé par des carbonates. Dans les roches encaissantes, la minéralisation est associée à une addition significative de CO_2, S, et Au, et à une réduction de H_2O. L'altération dans la région de Harker Lake est caractérisée par l'oxydation des roches encaissantes, par l'addition de Na_2O et Sr, et par un appauvrissement en Zn, MgO, MnO, et éléments lourds des terres rares. Par contre, l'altération à la mine Dome est représentée par la réduction des roches encaissantes, par l'addition de K_2O, Ba, CaO, B, et des éléments légers des terres rares, et par un appauvrissement en Na_2O, Sr, et en éléments lourds des terres rares. Ces résultats mettent en évidence les différences entre les deux régions, en terme de la grosseur et de l'intensité du gisement, de la géologie structurale, et de la lithologie environnante.

L'or est déposé dans les variolites par la déstabilisation du complexe Au-bisulphide, due principalement à l'enlèvement du soufre en solution pour former de la pyrite. Bohlke (1988) a démontré que la présence de carbonates riches en fer ou de pyrite dans la zone d'altération est relié au rapport initial de Fe/Mg des roches encaissantes, la pyrite se formant quand le rapport de Fe/Mg est anormalement élevé. La formation de pyrite est accentuée lorsque le fluide aurifère hydrothermal s'est équilibré au préalable avec des roches riches en magnésium. Le rapport anomal de Fe/Mg fait des roches variolitiques un site idéal pour la minéralisation disséminée de sulfures et d'or. De plus, leur tendance à se fracturer permet au fluide de pénétrer la roche en profondeur, améliorant ainsi le potentiel à se minéraliser.

Les roches variolitiques peuvent servir d'outil dans l'exploration de gisements d'or épigénétiques. Par leur composition, elles ont un excellent potentiel à être le site de gisements disséminés de sulfures et d'or, lorsque associées à des zones de cisaillement ou des failles ayant procuré des conduits aux fluides aurifères.

Table of Contents

List of Tables

Table **page**

List of Figures

Figure **page**

Figure **page**

List of Maps

Map **page**

List of Plates

Plate **page**

Mineral Abbreviations

The following mineral abbreviations have been used in the text, figures, etc., in the course of the thesis (Kretz, 1983):

cpy - chalcopyrite
gal - galena
qtz - quartz
cb - carbonate
hem - hematite
py - pyrite
amp - amphibole
mag - magnetite
tnt - titanite
chl - chlorite
ser - sericite
tur - tourmaline
rt - rutile
lxcn - leucoxene
cpx - Ca clinopyroxene

1. Introduction

1.01 Prelude

Variolites are mafic volcanic rocks containing centimetre sized, globular domains, termed varioles. Varioles may occur as distinct individuals, or as coalesced masses in variolitic rocks (Plate 1.1.1). Microscopic examination of varioles normally shows that they are composed of one or more spherulites (Plate 1.1.2), radiating fibres of plagioclase which have grown from a nucleus, resulting from disequilibrium crystallization (Fowler *et al*, 1987). Plagioclase spherulites, particularly open spherulites, may also be found in the groundmass of massive parts of variolitic flows, where varioles may not be distinguishable. Varioles also contain other minerals, notably amphibole (after pyroxene) and Fe-Ti oxides, in dendritic and branching forms also resulting from disequilibrium crystallization. Variolites are commonly high iron mafic to intermediate members of tholeiitic suites. They are characterized by higher SiO_2, P_2O_5, Zr, and REE contents, and higher Fe/Mg ratios in comparison to typical Archean tholeiitic basalts. Similar to spinifex textured komatiites, variolite occurance is for the most part restricted to Archean rocks.

It is well documented that Au mineralization occurs in most Archean rock types (Hodgson and M^{ac}Geehan, 1982; Colvine *et al*, 1988). However, it remains possible that rocks possessing particular chemical characteristics common to variolites may be preferential hosts to gold mineralization (Phillips *et al*, 1983; Neall and Phillips, 1987; Bohlke, 1988). Variolites have been previously recognized as being preferred hosts, or guides, to Au mineralization (Pirie, 1981; Thurston, 1985), likely due to their high iron content (Phillips and Grove, 1987). The possible importance of the characteristic texture and geochemistry of variolites was recognized by geologists working for Newmont Exploration of Canada Ltd. in Timmins, Ontario. This observation forms the basis for the thesis and the participation of Newmont Mining Ltd.

1.1 Objectives

Variolitic volcanic rocks host, or are proximal to, many epigenetic Au deposits in the

Plate 1.1.1: Variolitic pillow basalt examples, Abitibi Greenstone belt: a) upper Kinojevis Group, Elliot Township, Ontario (scale shown is in centimetres), b) Key Flow, Dome Mine, Timmins, Ontario.

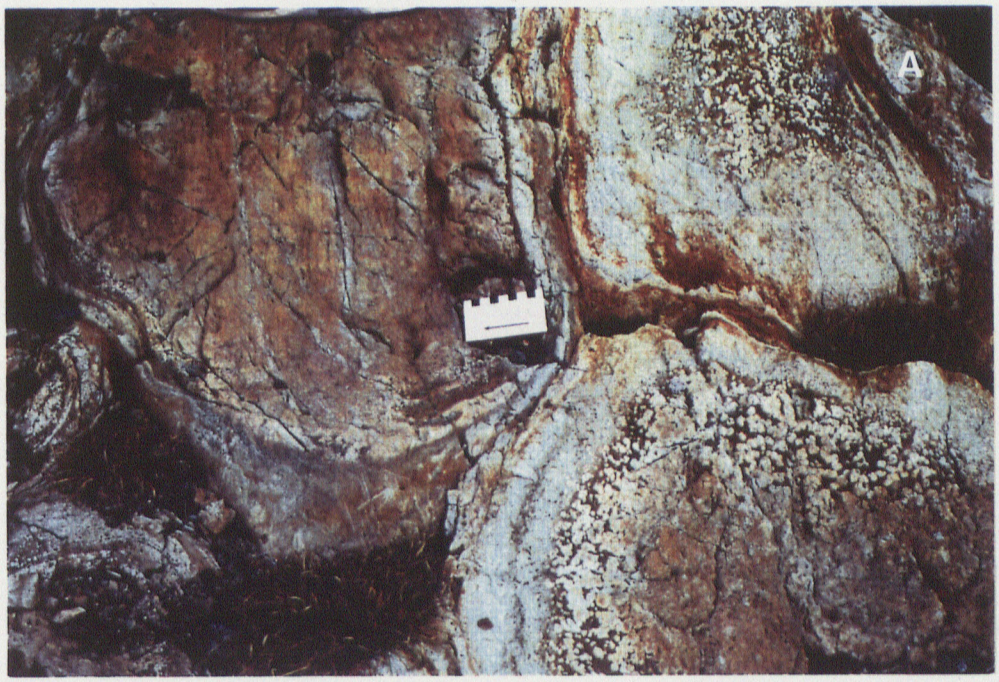
A


B

Plate 1.1.2: Photomicrograph of variole in pillow basalt (plain polarized light (PPL) and crossed nicols (X-nicols) views). Variole is composed of plagioclase spherulites with minor mafic minerals. Field of view is 4 mm.

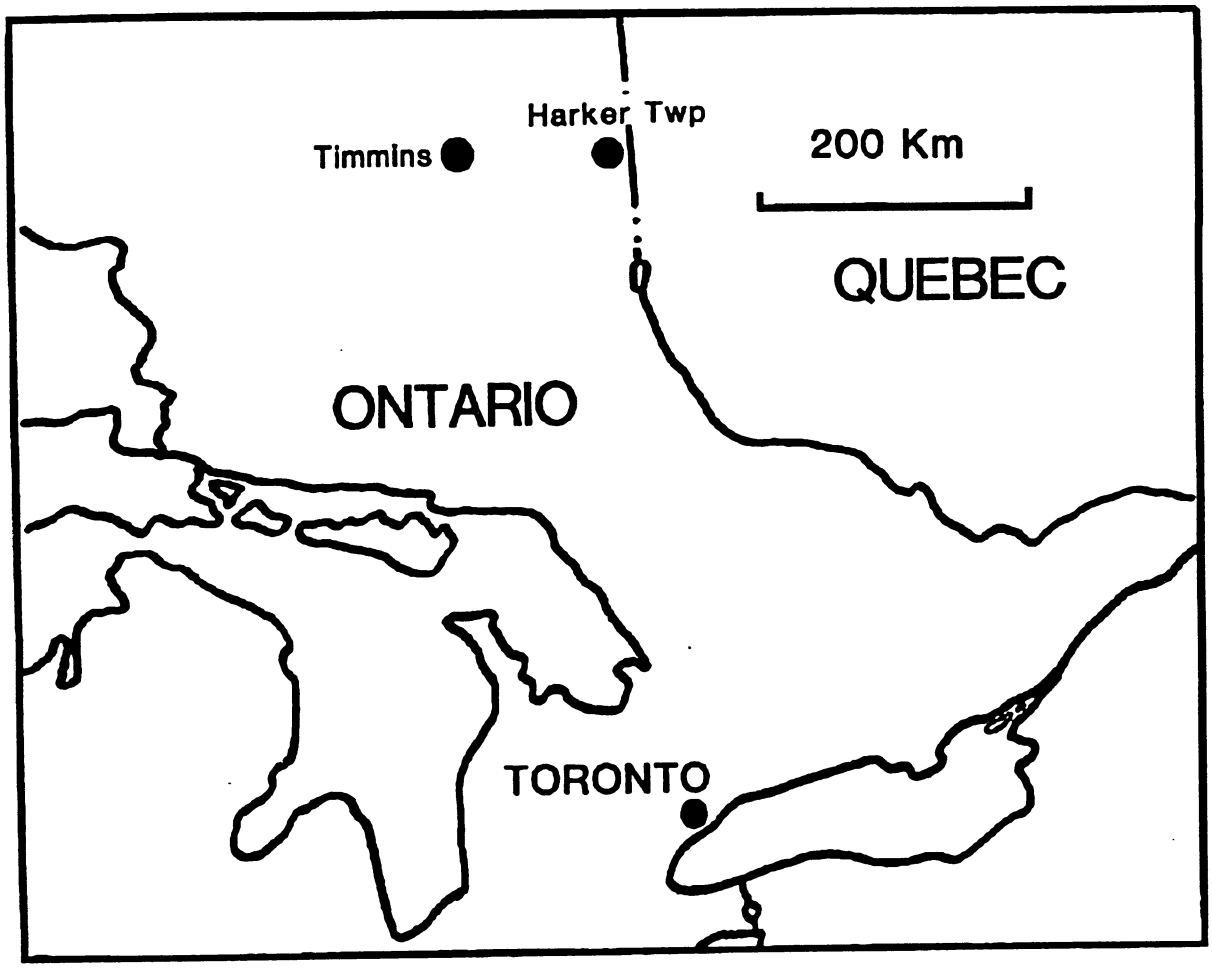

Map 1.2.1: Location of study areas, both within the Abitibi Greenstone Belt of northeastern Ontario.

Archean Abitibi Greenstone Belt (e.g.- Dome, Hollinger, Kerr Addison). The objectives of the research project are to test the observed spatial relationship between Archean epigenetic Au deposits and variolitic basalts in terms of a possible genetic link. A further objective is to better understand the alteration of variolitic basalts. The problem is approached by a detailed and comparative study of the petrology and geochemistry of variolitic rocks. Sample suites reflecting a spectrum of alteration intensities were collected from relatively unaltered terranes through to mineral deposits. As a result, the physical and chemical conditions of the alteration and mineralization associated with gold deposits in Archean terranes will be better defined.

1.1.1 Approach

The research involved comparing and contrasting variolitic and non-variolitic rocks within and between stratigraphic sequences to represent different styles of alteration and record the primary geochemical characteristics. Once the primary characteristics were established, the alteration and element mobility associated with gold mineralization was examined. Finally, the results were interpreted in order to determine the geochemical characteristics of variolitic volcanic rocks important to gold mineralization.

1.2 **Location**

This thesis project involves three different study areas within the Abitibi Greenstone Belt in Northeastern Ontario (Map 1.2.1). One area lies just east of Harker Lake, located in east-central Harker Township, 50 km east of Matheson, Ontario and 40 km north-northeast of Kirkland Lake, Ontario. It is on a group of mining claims, presently held by the estate of Mr. Don Hurd of Kirkland Lake, Ontario. The section is within undeformed tholeiitic rocks of the Kinojevis Group, aproximately 2.5 km south of Highway 101E. Road access is excellent with numerous logging roads in the immediate vicinity which connect to Highway 672 to the west (Map 1.2.2). The region has been the subject of extensive mineral exploration activity. Recently, American Barrick Resources opened the Holt-M^{c}Dermott Mine 4 km northeast of the study area.

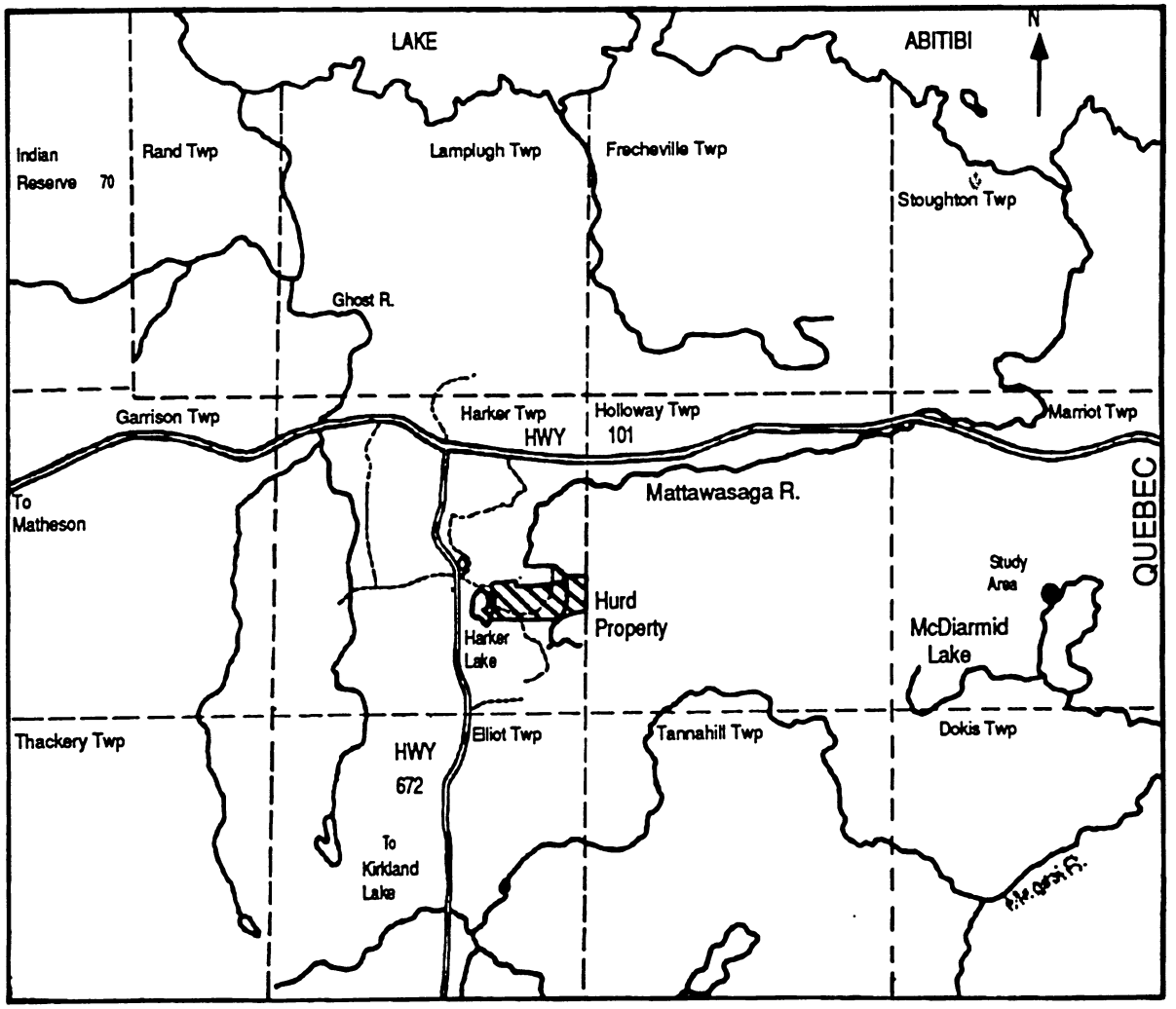

Map 1.2.2: Location and access map for the Harker Lake (Hurd Property) and McDiarmid Lake study areas, northeastern Ontario. For scale, the townships shown are 9.0 kilometres in width.

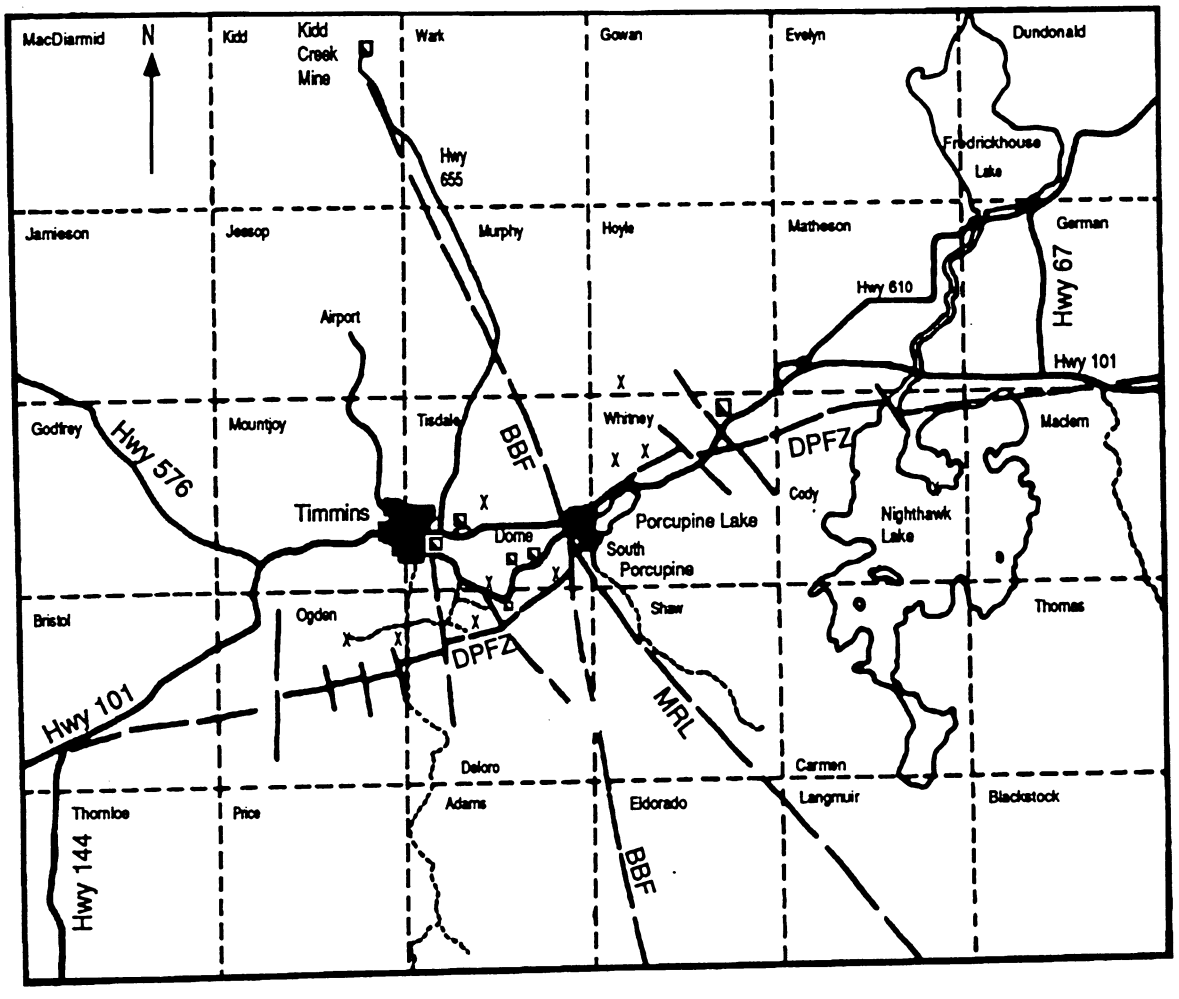

Map 1.2.3: Location and access map for the Timmins area. Townships are approximately 9 kilometres wide. Main faults in the area are included: DPFZ, Destor-Porcupine Fault Zone; BBF, Burrows-Benedict Fault; MRL, Montreal River Lineament. X indicates minor Au producing deposits.

The second area studied is in the Porcupine Mining Camp, Timmins, Ontario. Work was concentrated within the Vipond Subgroup of the Tisdale Group volcanic rocks (Pyke, 1982), in and around the Dome and Porcupine Paymaster Mines (Map 1.2.3) of southeastern Tisdale Township. Access was obtained to the Dome Mine through the cooperation of Placer Dome Inc. Complete sampling of the Vipond sequence and various mineralized zones was done on five different levels in the mine. The Porcupine Paymaster property provides a complete section of the Vipond rocks in a well known surface exposure just east of the mine headframe.

Slightly altered variolites were sampled in the Kinojevis Group volcanic rocks, very near their upper contact with the Blake River Group along the northwest shore of M^{c}Diarmid Lake in central Marriott Township, Ontario (Map 1.2.2). Access was attained by float plane service from nearby Perry Lake.

1.3 Methodology

1.3.1 -Sampling

Since most rocks in the vicinity of epigenetic gold deposits are altered, establishing the primary geochemical signature of variolitic rocks in a mine environment is difficult. The approach has been to obtain samples representing as broad a spectrum as possible of altered variolitic volcanic rocks. Complete sections were sampled, including variolitic and non-variolitic flows. Data has been recorded regarding important parameters such as fracturing, brecciation, vesicularity and other textural and structural features. Sampling was restricted as much as possible to massive, homogeneous parts of flows. Textural and stratigraphic evidence has been noted to correlate units and samples.

Sampling in 1989 was carried out in the three locations described above. These areas were chosen based on field work in 1987 and 1988 which proved that a spectrum of relatively fresh to altered and mineralized variolites were present. In Marriott Township prehnite-pumpellyite facies rocks are exposed in several flows on the shores of M^{c}Diarmid Lake. These rocks have extremely well preserved hyaloclastite and spherulite textures as well as pillow forms and flow contacts. They may represent lesser altered equivalents to some of the

textures observed in the other sample areas. Fourteen samples were collected here.

A 700 metre section of well preserved, low grade metamorphosed volcanic rocks is exposed in Harker Township, including two narrow (2 to 10m) altered and mineralized zones (Maps 2.1.1, 2.1.2). The larger of the two zones, known locally as the the Cryderman Zone, occurs in the middle of the section. Surface stripping during exploration of this zone has provided excellent exposure of the surrounding volcanic succession. The section sampled consists of Fe-rich basalts and includes several variolitic units and at least two intermediate units. A total of 57 samples have been collected. The data base was augmented by samples from diamond drill holes and mapping in the area.

In Timmins, work was concentrated on the Vipond Subgroup, a very well known and well documented variolitic sequence extending throughout most of the Porcupine Camp (Ferguson, 1968). Sampling of variolites at the Dome Mine and near the Porcupine Paymaster Mine was done, but unaltered examples similar to those of Marriott or even Harker Township are not present. To ensure the complete Vipond section was represented, sampling was extended into the upper unit of the underlying Central Subgroup and the lower unit of the overlying Gold Centre Subgroup.

Twenty rocks were collected from the well exposed, moderately altered section of the Vipond Subgroup near the Porcupine Paymaster Mine. Correlative samples from the Dome Mine represent the highly altered end members of this suite (Ferguson, 1968; Brisbin and Mason, 1988). Sixty-one moderately to intensely altered samples were taken on 5 mine levels in order to characterize the Vipond section in the mine as thoroughly as possible. Samples have been taken at and away from ore zones to monitor elemental changes in wall rock alteration.

1.3.2 Study and Analysis

Detailed petrography has been done on all samples collected, thus the metamorphic mineral assemblages as well as the alteration assemblages, where appropriate, have been documented. Determination of immobile and mobile elements with respect to original variolite chemistry has been done using interpretive techniques (Grant, 1986). Approximate chemical reactions were written for the prograde metamorphic and alteration assemblages from the

synthesis of the geochemical and petrographic data. Interpretation of the mineralogical and geochemical progression from least altered to most altered equivalents gives an estimate the primary igneous characteristics of the metamorphosed variolitic suite. By comparing the formation of variolites from different areas, insight into the peculiar nature of variolites with respect to other volcanic rocks is possible. With this insight, the effect of initial variolite chemistry on the localization of gold mineralization can be applied generally to variolitic rocks.

1.3.3 Relation to Au Mineralization

It has been observed that variolites occur dominantly in tholeiitic mafic volcanic rocks, especially those of highly evolved, Fe enriched suites. This is significant because these volcanic rocks may have provided the iron necessary for reactions responsible for the deposition of gold (Fryer *et al*, 1979; Neall and Phillips, 1987). Variolites are enriched in high field strength (HFS) elements, rare earth elements (REE) and silica relative to Fe tholeiites in general (Gélinas *et al*, 1976; Davies *et al*, 1979) providing further evidence of differentiation. Studies show that the favourable host rocks for Au mineralization are more competent, less mafic (but high iron) rocks (Phillips *et al*, 1983; Macdonald and Fyon, 1986; Houstoun, 1987) possessing anomalous Fe/Mg ratios relative to their surrounding terrane (Bolke, 1988; 1989). Variolitic volcanic rocks fit these attributes quite well making them good potential hosts for gold mineralization.

1.4 **Previous Work**

1.4.1 Variolites

Variolites are mafic volcanic rocks containing centimetre-sized, commonly spherical domains, termed varioles, which are dominantly composed of plagioclase spherulites. Variolites also contain other textures characteristic of rocks which have crystallized under conditions of extreme disequilibrium. These include skeletal, dendritic and plumose forms. Variolitic volcanic rocks are found dominantly within tholeiitic successions in Archean terranes. In particular, they are common in the upper portions of Fe tholeiitic suites, although

they are found throughout these sequences. Even when found outside tholeiitic successions, variolitic rocks are usually seen to be tholeiitic interlayers in sequences of other affinities (e.g. the calc-alkaline Blake River Group, Gélinas *et al*, 1976).

There are several theories as to the mechanism of formation of Archean varioles, including:

- disequilibrium crystallization resulting from diffusion limited growth brought on by supercooling of the liquid (Hughes, 1977; Philpotts, 1977; Fowler *et al*, 1987; Fowler *et al*, 1989)

- immiscible splitting of a magma of tholeiitic composition into two liquids, one of low K rhyolitic, and one of basaltic composition (Gélinas *et al*, 1976).

- devitrification texture

Pirie (1981) and Fowler *et al* (1987) noted the fact that although the varioles have more acid composition, partitioning of trace elements between the variole and matrix portions of variolites was inconsistent with the liquid immiscibility theory of Gélinas *et al* (1976). Neither the REE's or trace elements and the oxide P_2O_5 show distributions consistent with the separation of a felsic liquid from a basaltic liquid. Gélinas *et al* (1976) noted a type of variolite having no significant difference between the variole and matrix compositions (Kinojevis type) and attribute no liquid splitting in this case. The observed partitioning of these trace elements is more representative of rapid crystallization of the variole material from an homogeneous melt. Disequilibrium textures support the idea of rapid crystallization.

Thurston (1985, 1986) found that variolites commonly cap Fe enrichment mini-cycles of high alumina tholeiitic sequences in the Uchi subprovince of the Superior Province, and that these units have andesitic bulk composition. Thurston *et al* (1986) envisage the development of these low Fe basalt through high Fe andesite cycles by fractional crystallization of, progressively, olivine, plagioclase and lesser clinopyroxene. Fowler and Jensen (1989) have modelled a similar mechanism for the developement of tholeiitic basalt through rhyolite sequences in the Kinojevis Group volcanic rocks, which include abundant variolitic sections, in the Abitibi subprovince.

Evidence of the differentiated nature of variolite sequences is given by Davies *et al* (1979). They found that the flows of the dominantly variolitic Vipond Subgroup are richer

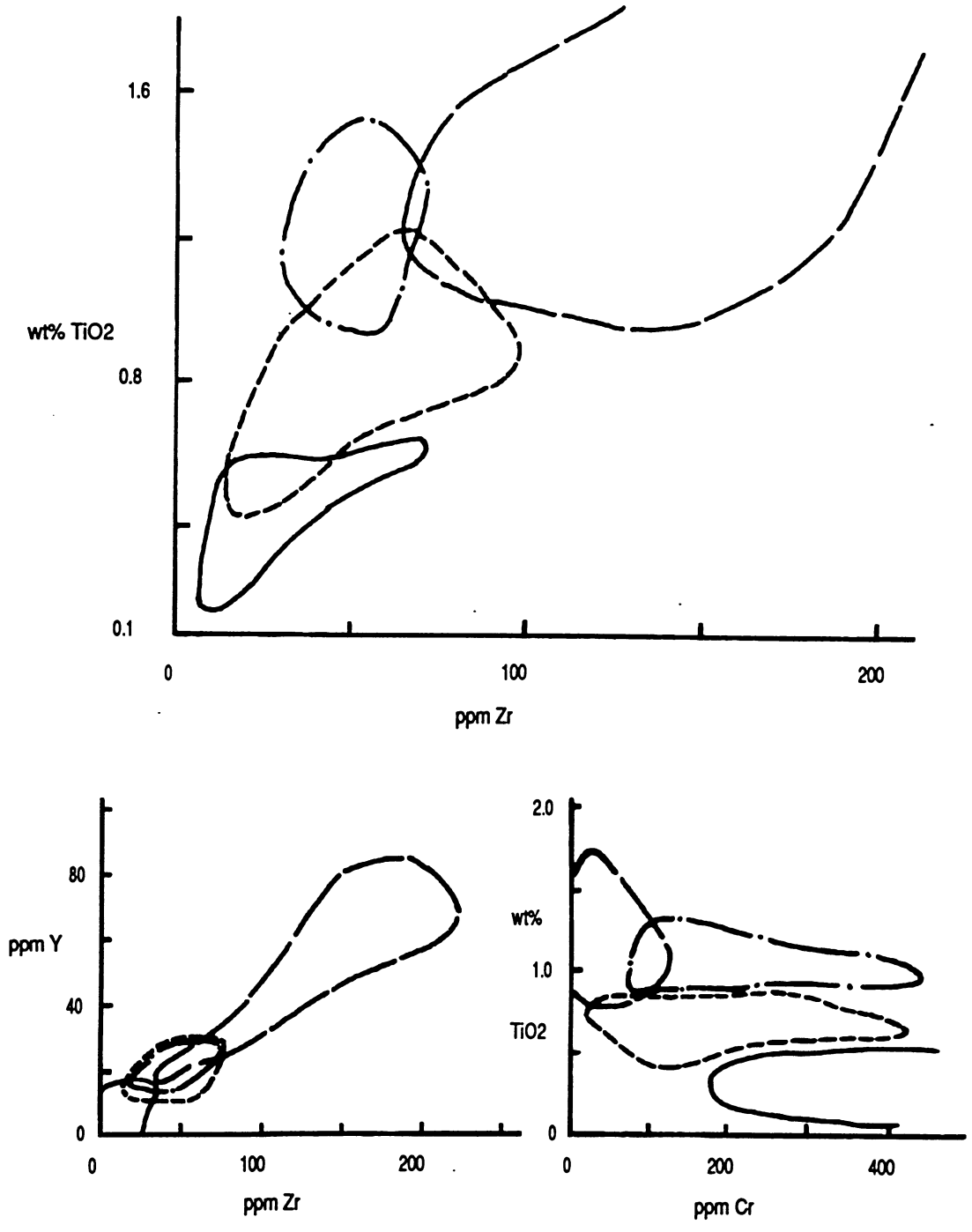

Figure 1.4.1: Diagrams using immobile trace elements, showing the relationship of the Vipond Subgroup to the other subgroups of the Tisdale Group, in the Timmins area. In all diagrams, the Vipond lies in the most differentiated position of any subgroup (Davies et al, 1979; Davies and Whitehead, 1980). Legend: long dashes define the field of the Vipond Subgroup; short dashes, Central Subgroup; dots and dashes, Gold Centre Subgroup; and solid line, Northern subgroup.

in Zr, Y, TiO_2 and poorer in Cr than those of the Central and Gold Centre Subgroups (Figure 1.4.1). This was also demonstrated by Gélinas *et al* (1976). They studied a series of variolitic samples (including matrix-variole separates) that define a silica dependent, Fe enrichment trend on the AFM diagram (Irvine and Baragar, 1971). Some samples have combined iron oxide concentrations greater than 20%. They compare the trend to that of the Skaergaard intrusion, generally considered to be a classic example of progressive differentiation due to fractional crystallization (Wager and Brown, 1967). Gélinas *et al* (1976) also noted that the bulk composition of variolites ranges from basalt to andesite.

It should be stated that although the majority of variolitic volcanic rocks identified in the literature (e.g. Gélinas *et al*, 1976; Pirie, 1981; Thurston, 1985; Fowler *et al*, 1987) are of Fe tholeiitic composition, Pirie (1981) has described a variole-matrix pair in the Red Lake area which give Mg tholeiite-basaltic komatiite compositions respectively (presumably Mg tholeiite bulk composition). Jensen (1978) noted varioles in flows of basaltic komatiite composition in the Stoughton-Roquemare Group.

1.4.2 Variolites and Gold

The association of variolites with Au mineralization has been noted in the past. Hutchinson (1987) documented the regional spatial association of variolite-bearing lower volcanic successions (komatiitic to tholeiitic affinities) with major Au camps in the Archean. In the Timmins camp, Ferguson (1968) made note of the importance of variolites both as hosts for Au mineralization and as marker horizons key to the understanding of structure in the Porcupine Camp. Pirie (1981) noted variolites as an important ore host in the Campbell-Red Lake gold mine of the Red Lake camp, northwestern Ontario, and suggested that the high-iron upper tholeiitic portions of the lower volcanic (komatiitic to tholeiitic) sequences were important in locating Au deposits. Thurston (1985, 1986) has described variolites and associated Au mineralization commonly capping tholeiitic Fe enrichment cycles in the Confederation Lakes area, Ontario. A hiatus in volcanic activity, with deposition of Fe-rich chemical sediments, and related Au enrichment, is commonly found at the top of these cycles. Thurston *et al* (1985) concluded that variolites may help focus exploration activities in unknown greenstone terranes.

1.4.4 Gold Deposits; Geochemistry and Alteration

In the past decade many studies of Archean gold deposits have been undertaken to advance our knowledge of their geological, geochemical, and structural characteristics as well as the nature of the fluid, or fluids, which are involved in their formation. This work has led to several models for the genesis of Archean gold deposits (Kerrich, 1983; Hutchinson and Burlington, 1984; Mason and Melnik, 1986; Wood *et al*, 1986; Phillips and Groves, 1987; Colvine *et al*, 1988), but more importantly, it has led to the careful study of many gold deposits and as a result detailed documentation of their characteristics.

Archean lode gold deposits commonly show evidence of formation at depth, associated with deep deformation zones and, generally, regional scale processes. The characteristic metamorphic assemblage in mafic volcanic host rocks includes actinolite/uralite-chlorite-epidote-albite-quartz. Alteration associated with gold deposits has been summarized as several zones (Fyon and Crockett, 1983; Phillips, 1986; Roberts, 1987). Surrounding the deposits, on a broad mine or camp scale, is a zone of pervasive chloritization (especially of mafic rocks) and carbonatization, generally calcite. This progresses to a proximal zone of more intense carbonatization characterized by Fe carbonates rather than calcite. Finally, an intensely altered, commonly bleached, inner zone which contains K-rich silicates or albite, ankerite-dolomite, quartz and Fe-sulphides is usually found adjacent to the mineralized vein. The centre of these alteration systems is usually focused on a deformation zone and the abundance, hence, importance of quartz veining depends on the style of deformation present (ie. brittle or ductile). The majority of the gold is found in pyrite disseminated in the altered host rocks of the veins.

This alteration assemblage is primarily due to hydrolysis and carbonatization of primary or metamorphic Fe-Mg silicates and oxides, the abundance of which plays an important role in determining the extent of alteration present in any rock (Roberts, 1987). Mass balance calculations in these altered rocks have demonstrated significant additions of CO_2, K or Na, S, and H_2O, along with reduction of the iron present, relative to unaltered equivalent rocks (Kerrich, 1983). The addition of silica is commonly reflected in the intensity of quartz veining present. Kerrich (1983) distinguished two general styles of metasomatism associated with lode gold veins in the Abitibi greenstone belt; 1) potassic reductive and, 2)

sodic reductive. Although mineralogy indicative of oxidative regimes is found in some deposits (usually hematite and sulphates, e.g. the Ross Mine, Ont. (Cameron and Hattori, 1987)), it is not considered to be related to large gold deposits (Kerrich, 1983; Colvine *et al*, 1988). Commonly the following trace elements are enriched in Archean lode gold deposits; Ag, As, B, Rb, Sb, W, Ba, Mo and minor base metals (Roberts, 1987; Phillips and Groves, 1987). With the exception of extremely altered areas, most major and trace elements were immobile with respect to gold mineralization, especially in comparison to metasomatism associated with base-metal deposits (Phillips and Groves, 1987).

Fluid inclusion work and studies of fluid-wall rock reactions provide evidence of the type of fluid involved in Archean lode gold deposits (Kerrich and Fryer, 1979; Phillips and Groves, 1983; Kerrich, 1983; Brown and Lamb, 1986; Cameron and Hattori, 1987; Colvine *et al*, 1988). In general, the typical fluid associated with Archean lode gold deposits is relatively reduced, H_2O(75 mole%)-CO_2(25 mole%) rich, has low salinity and density, and is neutral to alkaline. The composition of the fluid is affected by many factors as it passes through the crust. The temperature of formation for most vein deposits is in the 300-480°C range at pressures up to about 0.5 GPa. At present, most evidence points to thio-complexes, or bisulphide complexes, as the main gold ligand in the fluids (Seward, 1984), although there is a lack of experimental data for the upper end of the range of formation temperatures for these deposits. Much more is known about chloride complexes at these higher temperatures, and in fact, chloride complexes are very efficient carriers of Au at elevated temperatures (Seward, 1984; Bohlke, 1988). However, the Au-only nature of most Archean deposits and the low salinity of their fluid inclusions seems to preclude chloride complexes from having been significant Au-complexing agents under the conditions of formation of the deposits (Seward, 1984). Deposition of gold is due to destabilization of the bisulphide complexes by various mechanisms, such as; 1) formation of pyrite by reaction of sulphur in the fluid with iron in the wall rock, thereby oversaturating Au with respect to the solution; 2) oxidation or reduction of the fluid by redox reactions with the wall rock; 3) reducing sulphur concentration by boiling off H_2S as a result of sudden decrease in geostatic pressure; 4) cooling the solution; 5) change in the pH from neutral conditions. The reactions leading to the emplacement of gold mineralization are entirely dependent on the progressive evolution of

the auriferous fluid as it ascends towards the surface and the nature of the wall rocks.

1.5 Regional Geology

1.5.1 Abitibi Greenstone Belt

The Archean Abitibi greenstone belt of the Superior Province of the Canadian Shield, is the largest greenstone belt in the world, measuring approximately 800 km by 240 km, stretching from Chibougamau in the northeast to the Kapuskasing High, and possibly Wawa, in the south west. Although all rocks have been metamorphosed, the belt is one of the best preserved of the world's Archean terranes as the rocks are, in general, less than upper greenschist facies. It is a composite package of komatiitic through tholeiitic and calc-alkalic to alkalic volcanic rocks (cycles?), with associated intrusive, and sedimentary rocks, both coeval and later than the volcanic successions. The dominant fold axis trends are east-west and northeast-southwest, and these trends are shared by the major deformation zones which traverse the belt. The rocks appear to young progressively to the south, with the oldest volcanic rocks occurring in the Chibougamau region, dated at 2802 +/-3 Ma (Mortenson, 1987). The supposed youngest volcanic rocks in the belt are the alkalic Timiskaming Group, recently dated as being as young as 2677 +/-2 Ma (Corfu *et al*, 1991). The Timiskaming Group is stratigraphically higher than the upper members of the calc-alkaline Blake River Group which have been dated at 2701 +/-2 Ma (Corfu *et al*, 1989). The intrusive rocks show a progression in precise U-Pb age dates (Corfu *et al*, 1989) from older dioritic and trondjhemitic synvolcanic bodies to granodioritic batholiths and smaller porphyries, such as in the Timmins area (approximately 2690 Ma) to a later group of granitic, syenitic and alkalic intrusions, dated between 2681 and 2676 Ma. Albitite dykes, which crosscut the porphyries but not gold mineralization in the Timmins area, give a precise U-Pb zircon date of 2673 +6/-2 Ma (Corfu *et al*, 1989). Lamprophyre dykes are probably the youngest of the known Archean intrusions. Over 100 million ounces of gold have been produced from the Abitibi making it the most productive greenstone belt in the world.

In the southwest Abitibi, rough time-stratigraphic correlations have been made between the volcanic stratigraphy in the Timmins and Harker-Holloway areas (Table 1.5.1).

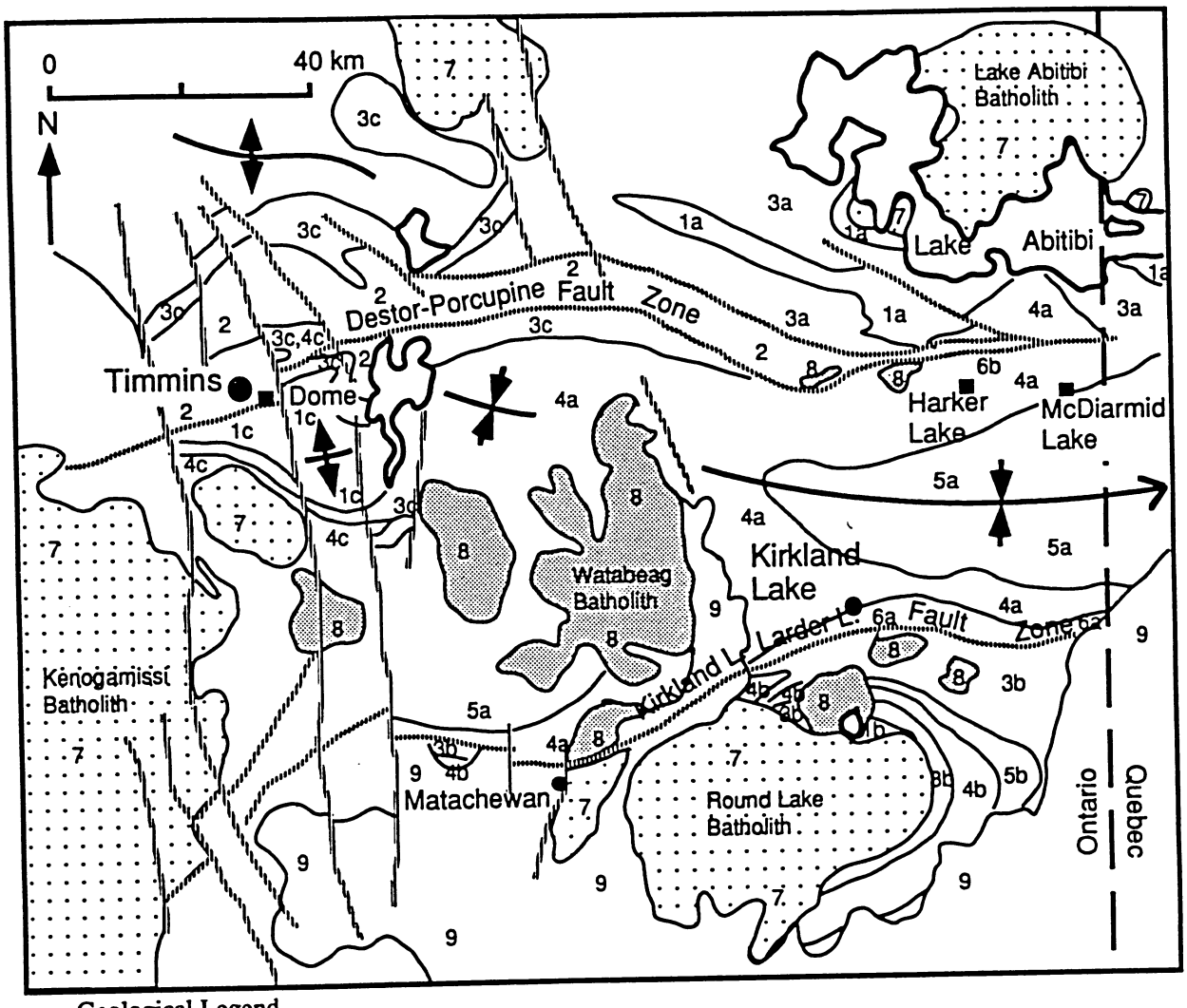

Geological Legend
Proterozoic
9 - Cobalt Group, sediments
Archean
8 - Intrusives, granodiorite, monzonite, quartz monzonite, syenite
7 - massive to gneissic quartz diorite, tonalite, trondjhemite
6 - a) Timiskaming Group, b) Destor-Porcupine Complex
5 - a) Blake River Group, b)Skead Group, c) Upper Member, Tisdale Group
4 - a) Kinojevis Group, b) Catherine Group, c) Middle Member, Tisdale Group
3 - a) Stoughton-Roquemare Group, b) Wabewawa Group, c) Lower Member, Tisdale Group
2 - Porcupine Group, sediments
1 - a) Hunter Mine Group, b)Pacaud Tuff, c) Upper Deloro Group

Map 1.5.1: Geological map of the southwest Abitibi Greenstone Belt, Timmins-Kirkland lake area (after Jensen, 1983). Study areas are marked by squares and labelled.

Table 1.5.1.- Stratigraphic subdivisions in the Timmins and Harker-Holloway areas, including precise age dates (modified from Corfu et al, 1989).

	Timmins Area (Pyke, 1982)	Harker-Holloway Area (Jensen & Langford, 1985)
		Timiskaming Gp.*
	Porcupine Gp.	
	Upper Tisdale Fm (C.A.) (2698+/-4 Ma)	Blake River Gp. (C.A.) (2701+/-2 Ma)
Supergroup III	Middle Tisdale Fm (Thol)	Kinojevis Gp (Thol)
	Lower Tisdale Fm (Kom-Thol)	Stoughton-Roquemare Gp. (Kom-Thol) (2714 +/- 2 Ma)
	Kidd Creek Rhyl-2717 Ma	
	Upper Deloro Fm (C.A.) (2727 +/- 1.5 Ma)	Hunter Mine Gp. (C.A.) 1.(2713+/-2 Ma) 2.(2730+/-1.5 Ma)
Supergroup II	Middle Deloro Fm (Thol)	
	Lower Deloro Fm (Kom-Thol)	
		Pacaud Gp. (C.A.) (2747+/-2 Ma)
Supergroup I		

* Timiskaming Group as young as 2677 +/- 2 Ma (Jackson and Corfu, 1991).

The calc-alkaline upper member of the Deloro Group in Timmins, and the felsic volcanics in the Kidd Creek area have been correlated tentatively with the lower and upper portions of the calc-alkaline Hunter Mine Group in the Harker-Holloway area. The lower komatiitic to tholeiitic, middle tholeiitic, and upper calc-alkaline members of the Tisdale Group in Timmins are roughly time correlative with, respectively, the komatiitic to tholeiitic Stoughton-Roquemare Group, the tholeiitic Kinojevis Group, and the calc-alkaline Blake River Group in the Harker-Holloway area (Map 1.5.1). Both komatiite through calc-alkaline suites were produced between about 2717 and 2698 Ma (Nunes and Jensen, 1980; Barrie, 1989; Corfu *et al*, 1989).

1.5.2 Kinojevis Group

The study area in Harker Township lies within the Kinojevis Group volcanics (Satterly, 1951; Jensen and Langford, 1985). These form part of the north limb of a very large regional feature, the Blake River Syncline (Map 1.5.2). The north limb section consists of a volcanic "supercycle" (Jensen and Langford, 1985) from the basal komatiitic to tholeiitic Stoughton-Roquemare Group through the tholeiitic Kinojevis Group to the upper calc-alkaline Blake River Group. The section was formed between about 2714 +/-2 Ma and 2701 +/-2 Ma (Nunes and Jensen, 1980; Corfu *et al*, 1989), age dates from the base of the Stoughton-Roquemare Group and the top of the Blake River Group respectively.

The Kinojevis Group in Harker Township is an approximately 10 km wide section of south-facing, southwest-northeast trending, alternating Mg and Fe tholeiitic basalt successions which are locally differentiated to intermediate and minor rhyolite flows. Interflow sediments are rare. Commonly, flows of Fe tholeiitic affinity are moderately to very magnetic and are easily distinguished from the Mg tholeiities on regional airborne magnetic survey maps. The units of the Kinojevis can be very thick and laterally appear to be unusually continuous often extending 10's of kilometres. Individual flow morphology commonly progresses from brecciated and hyaloclastitic flow tops to pillowed and fine grained, vesicular (and often variolitic) parts to gradually more coarse grained massive parts (gabbroic textured in places) to a well defined chill margin at the base. It appears that the Kinojevis Group was produced completely in a submarine environment as there is no evidence of subaerial volcanism. The

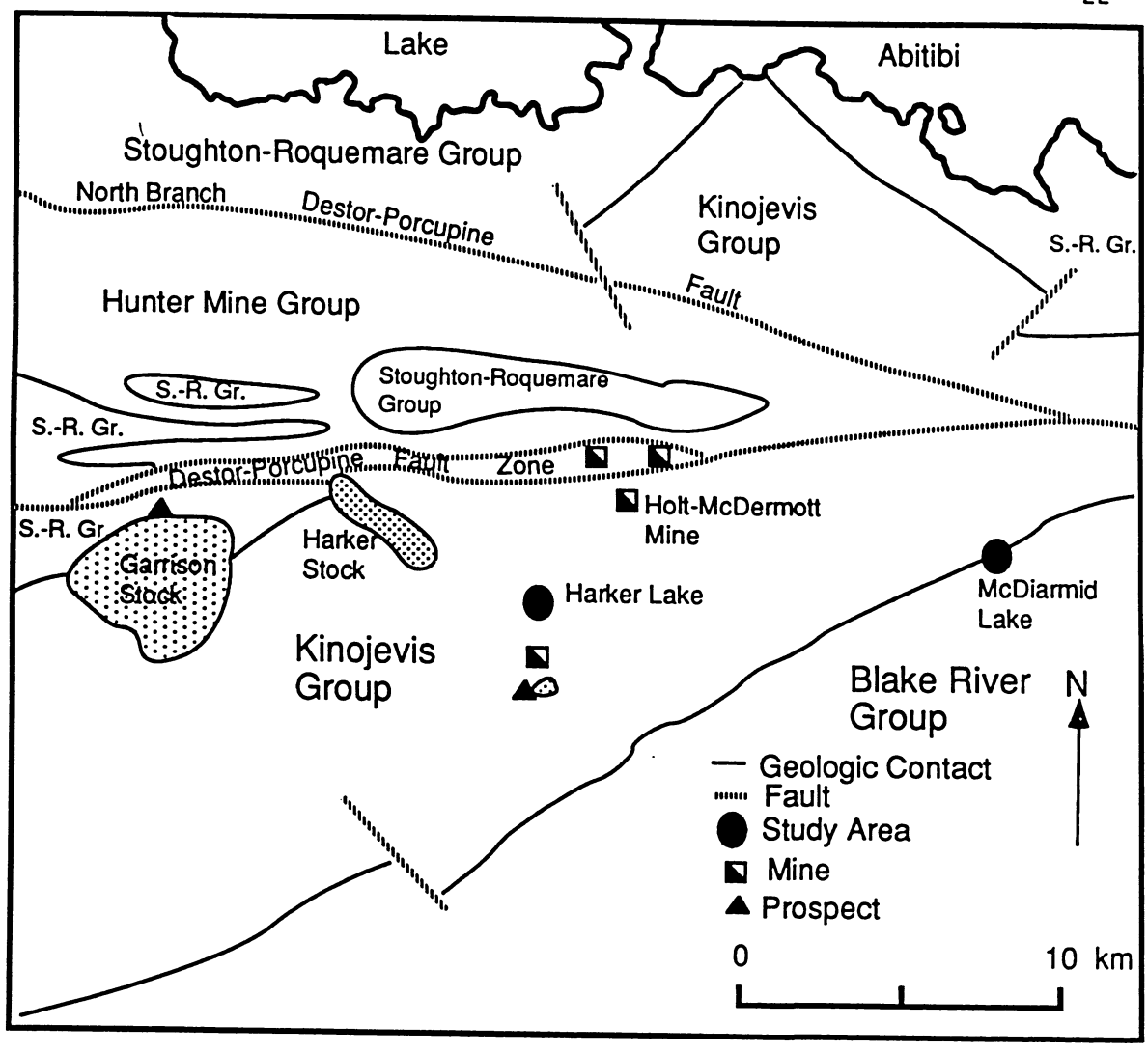

Map 1.5.2: Geology of the Harker-Holloway area, Ontario (modified after Jensen, 1982). The Harker Lake and McDiarmid Lake study areas are shown. The regional Archean volcanic stratigraphy is as follows, from bottom to top: calc-alkaline Hunter Mine Group, komatiitic Stoughton- Roquemare Group, tholeiitic Kinojevis Group, and calc-alkaline Blake River Group. The local felsic intrusions (indicated by the stipple pattern) are later. The Destor-Porcupine Fault Zone consists of fault slices of the various volcanic rocks and asociated sediments, as well as, sediments of the later Timiskaming group. The Quebec border marks the east margin of the map.

preservation of primary textures in the Kinojevis Group is quite remarkable owing to the low grade of metamorphism and lack of deformation. The thickness of the Kinojevis Group has been interpreted to be due to simple stacking of voluminous flows (Jensen and Langford, 1985). However, there may be significant stratigraphic repetition if thrust faults are present as proposed recently by Jackson and Harrap (1989) for the Catherine Group south of Kirkland Lake, Ontario.

There are several intrusive bodies of rock in the region. The largest of the nearby intrusions is the Harker "syenite" stock located in the northeastern quadrant of Harker Township. As described by Satterly (1951), this is a oblong shaped (long axis northwest-southeast), magnetic body composed of pink to red syenite of variable grain size (up to pegmatitic), and commonly containing finely disseminated specular hematite. In the southeast corner of the township, there is a small stock of coarsely porphyritic syenite, which contains epigenetic gold mineralization. Both of these intrusions are characterized by high Na_2O content. A large gabbroic intrusion is found in the north central part of the township, with a smaller outlier to the east. Numerous lamprophyre and feldspar porphyry dykes occur throughout the region, especially in areas of shearing and alteration.

Metamorphic grade in the Kinojevis Group is generally quite low for Archean rocks. Facies range from prehnite-pumpellyite to lower greenschist. Characteristically the rocks of the Kinojevis Group are medium to dark green, to almost black, due to the prevalence of chlorite and actinolite-uralite in the lower greenschist facies assemblage. Typically, the darker the colour the more Fe-rich the rock. Overall, prehnite-pumpellyite facies rocks are a lighter shade of green (ie: M^{c}Diarmid Lake area). Plagioclase is commonly light green due to alteration to albite, epidote, calcite and minor chlorite. Epidote also occurs in fractures and tiny veinlets and their corresponding envelopes. Spilitization of the flows was probably widespread and most plagioclase is albite. Minor contact metamorphic effects can be found in proximity to the larger intrusions in the area.

In general, the Kinojevis Group is a homoclinal sequence with only minor warping of the units along strike (due to minor offset on crossing faults). Local folding of the volcanic strata is evident, as interpreted from the airborne magnetic data, in the vicinity of intrusions. Foliation is present only locally and it is weak where it is observed. Discrete faults are

present throughout the section, generally occurring as narrow zones of brecciation and fracturing of the host rocks with some foliation developed. These faults are subparallel to the stratigraphy, commonly following flowtops and other more easily deformed portions of the flows. Structures oriented close to north-south are common, generally offsetting stratigraphy a few metres to several hundred metres at most. The Destor-Porcupine Fault Zone (DPFZ) crosses the north half of Harker Township in an east-west manner. Close to this deformation zone the rocks of the Kinojevis Group exhibit more complex structure with some folding and overturning of the stratigraphy.

Several gold deposits occur in the vicinity of the study area in Harker Township. The region has been known as a centre of gold mineralization since the early 1900's. Many of these early discoveries were described in a report by Knight (1924). Satterly (1951) also described these showings, as well as later discoveries, in his report on Harker Township. More recently, mining companies have rediscovered the Harker-Holloway area leading to new developments in the 1980's, such as the Holt-McDermott Au Mine of American Barrick Resources. This deposit is situated on a fault zone, subparallel to volcanic stratigraphy within the Kinojevis Group (Workman, 1986). The fault zone appears to be a splay from the DPFZ. The Holt McDermott deposit consists of a narrow but very extensive tabular body of brecciation, alteration and mineralization containing ore bodies over several kilometres of strike length. The wall rock alteration associated with ore is characterized by albitization, hematization, and pyritization. This is similar to other deposits of note in the area including the presently developing Lightning zone, which is just north of the Holt-McDermott Mine within the DPFZ. The Golden Harker deposit (Satterly, 1951), in southeastern Harker Township, and several other small prospects in the area also have similar characteristics.

1.5.3 Timmins Area

Due to its stature as a major gold producing camp, the Timmins area (Porcupine Mining Camp) has been studied extensively through its history. Ferguson (1968) and Pyke (1982) have provided comprehensive syntheses of the regional geology, while Davies *et al* (1979), Davies and Whitehead (1980), Mason and Brisbin (1987) and Piroshco and Kettles (1988) and have dealt with volcanic geochemistry, stratigraphy, and structural history

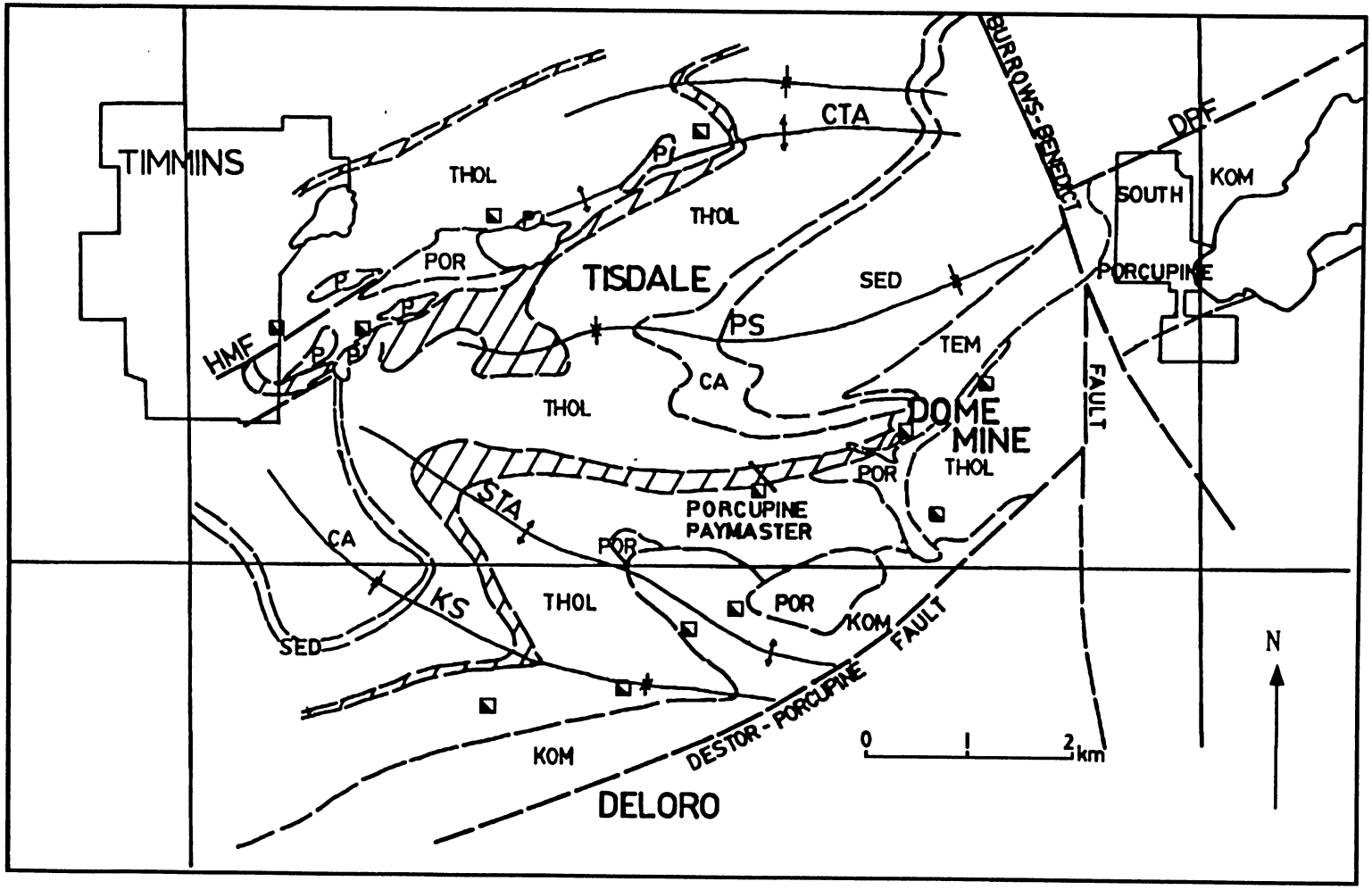

Map 1.5.3: General geology of the Timmins area. Volcanic stratigraphy is labelled according to its chemical affinity i.e. KOM = komatiitic, THOL = tholeiitic, CA = calc alkaline, and the felsic porphyries are labelled, POR, or P. Major structures are also included: HMF = Hollinger Main Fault, DPF = Destor-Porcupine Fault, CTA = Central Tisdale Anticline, PS = Porcupine Syncline, STA = South Tisdale Anticline, KS = Kayorum Syncline. The variolitic Vipond Subgroup is shown as a hachured area.

respectively. Hodgson (1983b) has reviewed the structural and geological aspects of the development of the camp. Other studies have focused on the ore deposits and their relations to the history of the camp (Wood *et al*, 1986; Mason and Melnik, 1986; Burrows and Spooner, 1986).

All bedrock in the Timmins area is of Archean age except for north-south or northeast-southwest trending Proterozoic diabase dykes (Map 1.5.3). Volcanic rocks are divided into two groups, the lower Deloro Group and upper Tisdale Group (Pyke, 1982). These two groups have been subdivided into three formations each. The Tisdale Group is the dominant formation in the Porcupine Camp. It consists of a lower komatiitic through tholeiitic member, a middle tholeiitic member, and an upper calc-alkaline member. The lower formation of the Tisdale group consists of peridotitic and basaltic komatiites at the base grading upwards into magnesium and, finally, iron tholeiites. The tholeiitic portion of this lowermost member corresponds to the Northern and Central subgroups of Ferguson (1968; see also Mason and Brisbin, 1987) as outlined in Table 1.5.2. The middle formation is dominantly made up of flows of iron-rich tholeiitic basalts. Variolitic basalts form a significant portion of the lower to middle parts of this member corresponding to the Vipond subgroup of previous workers (Ferguson, 1968). The uppermost member of the Tisdale consists of felsic calc-alkaline pyroclastic rocks, referred to as the Krist Fragmental by Ferguson (1968). Continuity of some of the units of the Tisdale Group is quite remarkable. In particular, the variolitic units of the Vipond subgroup have been traced over 30 km of strike length through the Porcupine Camp (D. Brisbin, pers. com.). Total thickness of the Tisdale Group as exposed in the Timmins area is about 5000 metres. Sediments, time equivalent to most of the volcanic sequences, form the up to 300 metre thick Porcupine Group. Younger, Timiskaming-style sediments unconformably overly the Porcupine sediments and the upper members of the Tisdale Group volcanics. These are generally conglomerates grading to thin and thick bedded greywackes and argillites (Ferguson, 1968). The locations of the small felsic intrusions in the area are apparently related to the major structural features. The intrusions are of various types, dominanted by quartz-feldspar and feldspar porphyries (Ferguson, 1968). Feldspar phenocrysts are albite or oligoclase. The intrusions are normally grey coloured on fresh surface, pink to reddish where altered and weathered. Generally they

Table 1.5.2: Archean volcanic and sedimentary stratigraphic nomenclature in the Timmins area as designated by Ferguson (1968) and Pyke (1982).

Ferguson	Pyke	
Younger Sediments	Timiskaming Sediments	
Unconformity		
Porcupine Group Sedments	Porcupine Group Sediments	
Transitional and Lateral Facies Contact		
Krist Fragmental	Upper Volcanic (C.A.) Fm	Tisdale Group
Gold Centre Subgroup	Middle Volcanic (Thol.) Fm	
Vipond Subgroup		
99 Flow	99 Flow	
Central Subgroup	Lower Volcanic (Kom. to Thol.) Fm	
Northern Subgroup		
	Upper Volcanic (C.A) Fm	Deloro Group
	Middle Volc. (Thol.) Fm	
	Lower Volcanic (Kom. to Thol.) Fm	

are quite altered, to sericite and quartz, and have evidence of recrystallization and, perhaps, tectonic brecciation during their development. Albitite dykes occur in association with the porphyries of the M^{c}Intyre-Hollinger complex. They are later than the porphyries and are quite important to the understanding of age relationships in the mines as they are crosscut by mineralized veins (Ferguson, 1968). Age dates, summarized by Corfu *et al* (1989), constrain the formation of the Tisdale group volcanics previous to 2698 +/-4 Ma. The albitite dykes, which are the latest intrusive rocks predating mineralization, give a precise date of 2673 +6/-2 Ma (Corfu *et al*, 1989).

The volcanic rocks in the Timmins area have been metamorphosed to greenschist facies (Ferguson, 1968): plagioclase has been altered to albite, chlorite, calcite, and epidote; mafic minerals converted to amphibole with associated chlorite and epidote; and oxides changed to leucoxene. In addition, Ferguson (1968) has noted a widespread carbonatization of the volcanic rocks. The presence of calcite or dolomite is commonly associated with penetrative deformation. These zones of carbonatization have linear traces (stratabound?) and are developed around prominent structures (Karvinen, 1981; Fyon and Crockett, 1983). The more altered rocks weather a dark rusty brown presumably due to the breakdown of Fe-rich

dolomites.

The structure in the Timmins area is more complex than in the Harker-Holloway area and is described by various authors (Hodgson, 1983; Piroshco and Kettles, 1988). Early geologists started to unravel the structural history of the camp when they recognized that the variolitic units were important and continuous marker horizons (see Mason and Brisbin, 1987). One of the earliest events in the history of the Porcupine Camp was the development of large northeast trending structures such as the Porcupine Syncline and the North Tisdale Anticline. These are truncated by the unconformity at the base of the Younger sediments. They are also truncated by early, large faults such as the Dome and Hollinger Faults (Piroshco and Kettles, 1988). Porphyry bodies were emplaced along these early faults and related splays. Later folding along northwest-southeast trending axes resulted in an axial foliation and, locally, extensional vein development. These folds are best represented today by the South Tisdale Anticline and the Kayorum Syncline. The associated foliation crosscuts earlier features such as the Dome Fault and the porphry bodies which also appear to be folded along this northwest-southeast axis. Locally, strong stretching lineations, developed at the intersection of foliations and other structural components, play an important role in the Camp. For instance, in southern Tisdale township, prominent 40-60°, northeast to east plunging lineations match the orientation and distribution of orebodies at the Dome Mine.

The trace of the regional Destor-Porcupine Fault Zone (DPFZ) crosses the area (Map 1.2.3). From the east, it bends south at Porcupine Lake, around the Dome and Buffalo Ankerite mines, and west again past the Delnite and Kennilworth mines south of the city of Timmins and on to Bristol Township, southwest of the city. A wide zone of deformation is associated with this fault. The Burrows-Benedict Fault crosses eastern Tisdale Township striking 160-180°, just east of the Dome Mine, offsetting the local geology significantly in a sinistral fashion (Ferguson, 1968). There may be some rotational movement on this fault and vertical offset is unclear. This fault forms part of the regional Montreal River Lineament. Other northwest-southeast trending structures are found which are an important control on mineralization at the Pamour No. 1 Mine in the east part of the Camp.

The report of Ferguson (1968) contains detailed descriptions, written by the mine geologists, of all of the more important deposits of the Porcupine Camp. Most ore is

restricted to the section of the Tisdale Group volcanics between the 95 Flow (upper portion of the Central subgroup) and the top of the Vipond subgroup. This corresponds generally to the high iron (and variolitic) tholeiitic section of the Tisdale Group volcanics. Most deposits are classified as vein deposits in that the ore is contained within, or intimately related to, veining. Veining is most common in shear zones related to faulting. Vein morphology and distribution is normally controlled by the response of the host rock to stress. This is especially true at the contact of variably competent lithologies within shear zones (e.g. vein formation in pressure shadows at the apices of the felsic porphyry bodies within ductile shear zones). Alteration zones are observed around individual veins indicating reaction between fluids and wall rock. The mafic rocks have been carbonatized, sericitized (commonly with minor chlorite), and pyritized. Disseminated pyritic Au mineralization is common in the altered wall rock surrounding veins. Minor ore has been recovered as sulphide bodies, or pyritized zones, usually disseminated mineralization (up to 15% pyrite) in basalts. These bodies are vein related but may extend up to 30 m from the vein contact (Ferguson, 1968). Vein mineralogy is dominated by two types; 1) quartz-ankerite, which are the most productive and have generally intense alteration haloes, and 2) quartz-calcite, which are generally non-productive, showing minor associated alteration. Other minerals include albite, scheelite, tourmaline, sulphates, sulphides, tellurides and gold. Most gold is not visible and is contained in pyrite.

1.6 **Acknowledgements**

First of all, I must thank my supervisor, Dr. Anthony D. Fowler, of the University of Ottawa, for his constant guidance, support, openness to ideas, and for teaching me many things about igneous petrology and research. His positive attitude, friendship, and confidence in my abilities were strong assets for my studies. I would also like to give credit and thanks to Drs. Jim Franklin and Eion Cameron, both scientists with the Geological Survey of Canada and adjunct professors, at Carleton University and the University of Ottawa respectively, for generously contributing their advice and considerable expertise to my work.

This project was originally supported by Newmont Mining Corporation, Denver, Co., under the Newmont Education Leave Assistance Program (granted to M. Jones) and the

National Science and Engineering Research Council of Canada (grant to Dr. A.D. Fowler), and subsequently by a grant under the NSERC University/Industry Cooperative Research program (grant to Dr. A.D. Fowler). Special thanks go out to Dr. Hugh Squair and Mike White, both formerly of Newmont of Canada Exploration Ltd., to Eric Kallio, chief geologist, and Dan Gagnon, geologist, at the Dome Mine (Placer Dome Inc.), and to the late Don Hurd, owner of the Hurd property in Harker Township.

I am also grateful to the following technicians, scientists, and friends for the time and encouragement they have provided: Dan Brisbin, Hélène De Gouffe, Sylvie Downing, Richard Ernst, Ron Hartree, Dr. Keiko Hattori, Julie Hayes, Edward Hearn, Dr. Don Hogarth, Ron Labelle, John Loop, Dr. Moira M^{c}Kinnon, Sue Meunier, Jean-François Tardiff, and, in particular, my office-mates, Dave Lentz, Robert Thériault and Don Watanabe.

Finally, and most importantly, I would like to thank my children, Louise, Véronique, and Evan, for the sacrifices required when your father is a student, and my wife, Chantal, for her support, both moral and financial, and love, without which nothing would have been possible.

2. Local Geology

2.1 Harker Lake Area

2.1.1 Geology of the Harker Lake Area

The study area in Harker Township was explored by Newmont Exploration of Canada in 1985. Overburden stripping has produced excellent exposure of a section of mafic flows. A grid which was established for exploration purposes has been used as a base for this study (Figure 2.1.1). The grid was constructed from a baseline, called BL 10+00N, located just south of the Cryderman Zone and bearing 065°. Perpendicular lines, bearing 335°, were surveyed from this baseline every 50 metres both north and south. Both the baseline and grid lines were measured from a zero point and labelled with increasing distance to the east and north relative to the orientation of the grid. Labelling of the grid lines is such that Line 14+50E is 1450 metres east from the zero point of the grid. Distances along the lines are labelled such that 10+45N is a point 1045 metres north of the zero point, or 45 metres north of the 10+00N baseline. In this manner it is possible to easily reference and locate any point in the map areas.

The geology of a volcanic sequence containing variolitic flows was examined in two successive sections (Figure 2.1.1, see also Figures 2.1.2 and 2.1.3). The north part, or base of the stratigraphic section, is exposed in trenches along Line 14+50E, north of Baseline 10+00N (Map 2.1.1). About 1 km to the east, the south part of the sequence is variably exposed in outcrop and trenches from Line 24+50E to Line 30+00E, south of Baseline 10+00N to about 7+00N (Map 2.1.2). The western and eastern trench areas combined give excellent exposure of a 700 metre section. The lava flows form a steeply south-dipping and facing, homoclinal sequence striking consistently between 065° and 070°. These flows are continuous along strike, the larger ones correlative over at least 3.5 km. The flows have brecciated, pillowed and massive forms and range in thickness from a few metres to 50-60 metres. A contact exists just south of the study area between Fe and Mg tholeiite sequences (Figure 2.1.1). The study area is located in the upper portion of the Fe tholeiite sequence, just

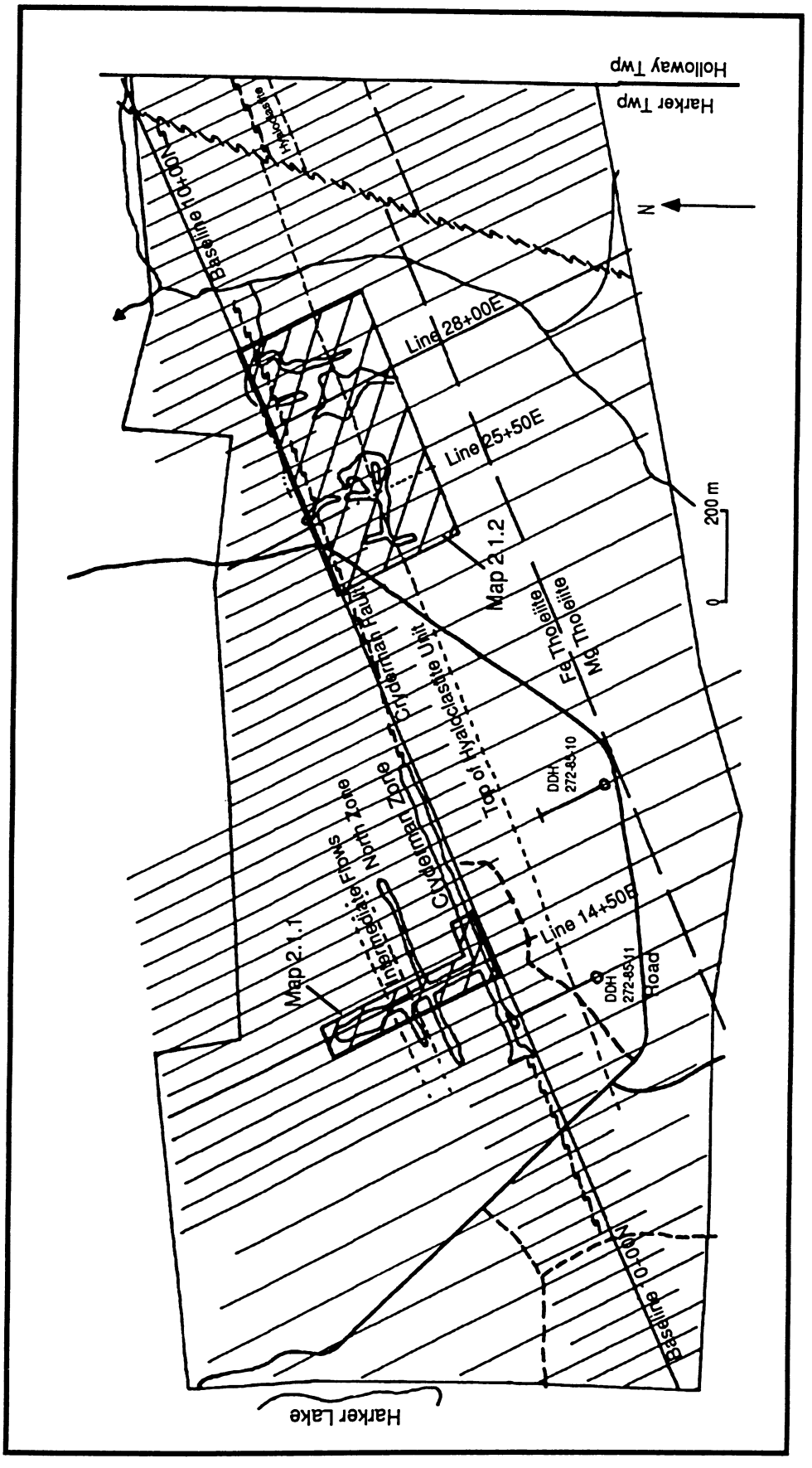

Figure 2.1.1: General geology of the Hurd property, with exploration grid which was used as a base for mapping. Trench areas which were mapped in this study are indicated by hachured areas.

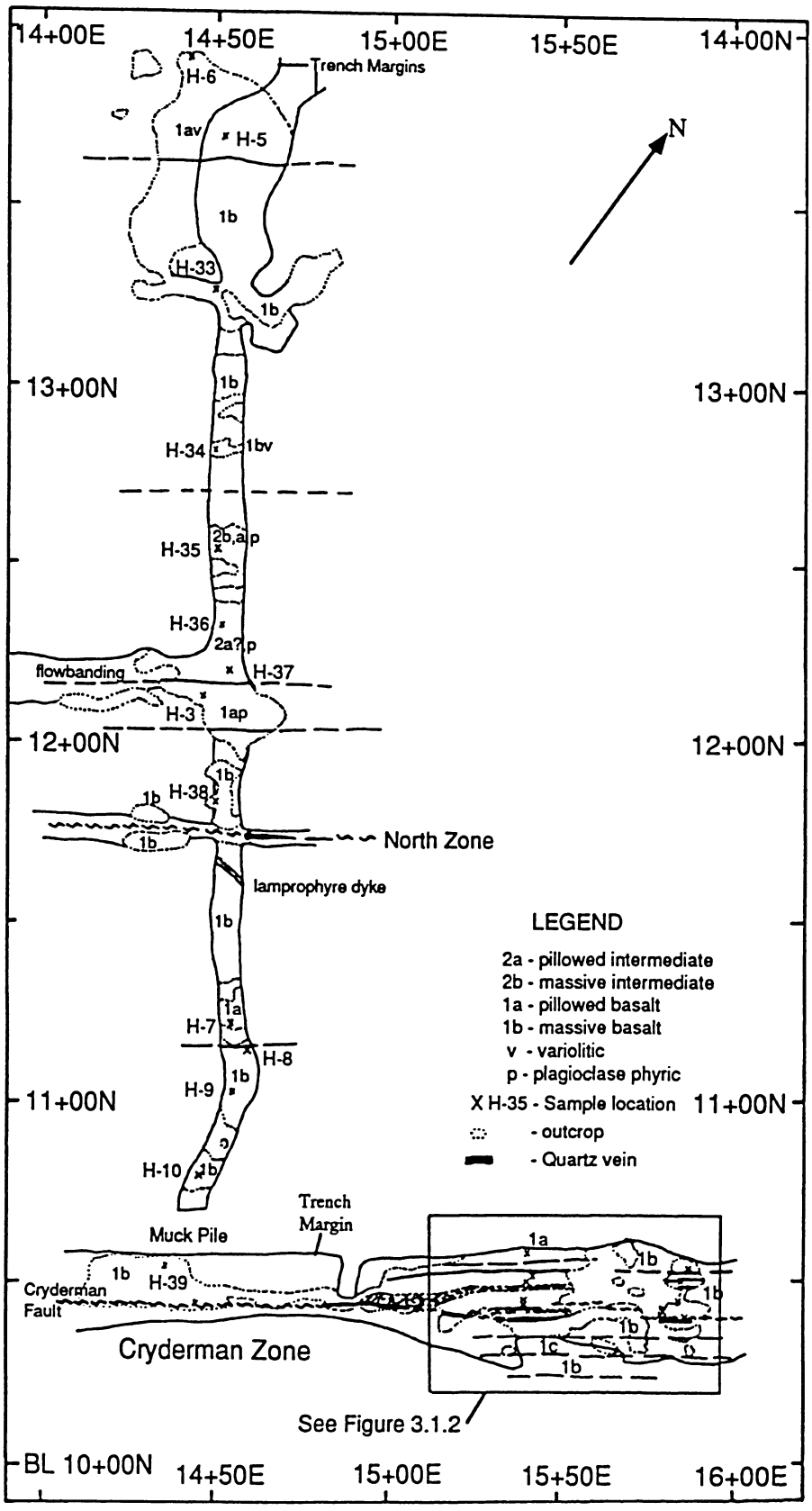

Map 2.1.1: Geology of the Line 14+50E trench, Harker Lake area. This section represents the lower half of the section of stratigraphy examined in the Harker Lake area (see also Figure 2.1.2). The grid lines, marked, are 50 metres apart.

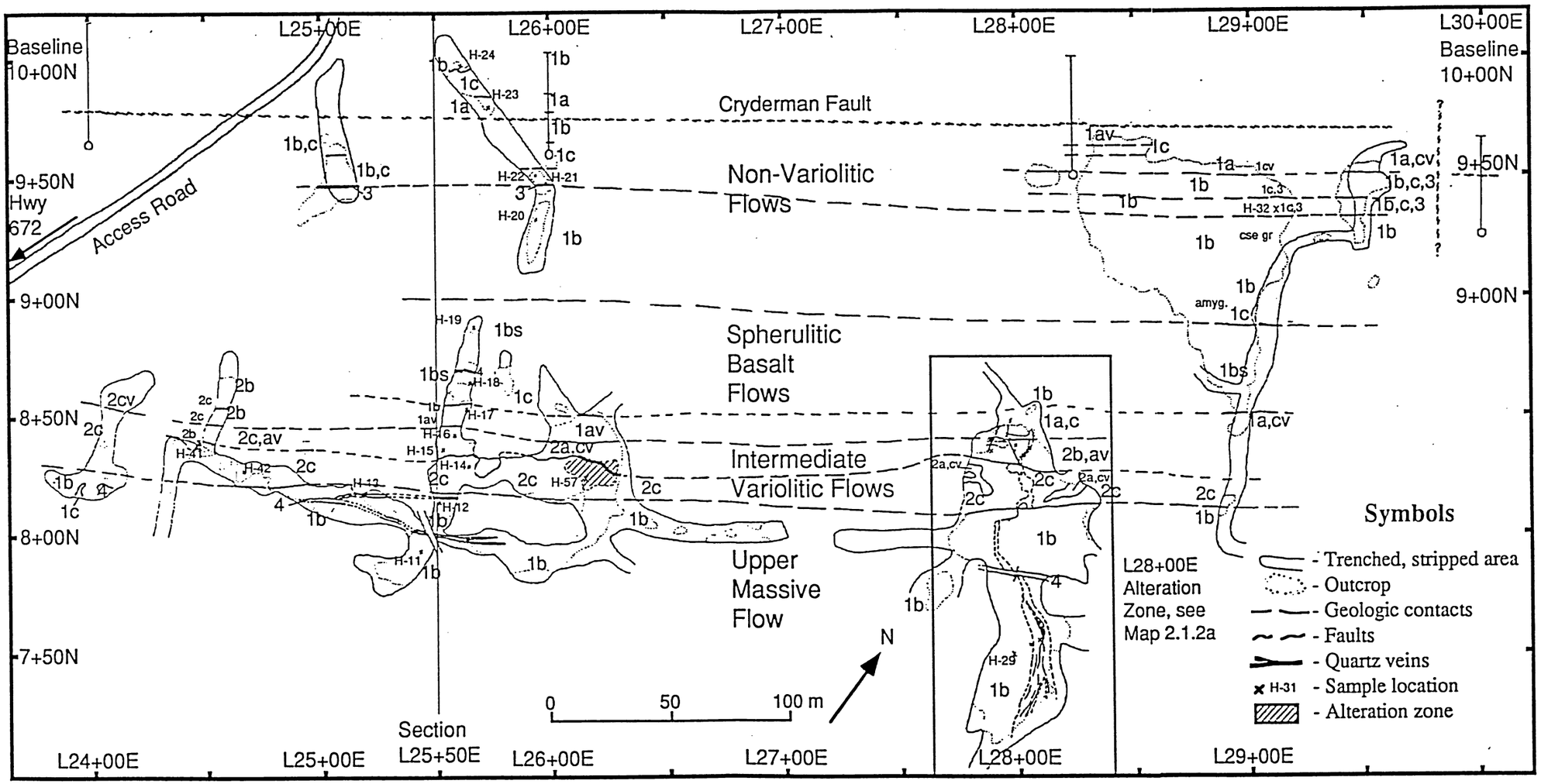

Geologic Legend

Volcanic Rocks

1 - Basalt -
- 1a, pillow basalt
- 1b, massive basalt
- 1c, flow top breccia, hyaloclastite

2 - Intermediate
- 2a, intermediate pillowed flow
- 2b, intermediate massive flow
- 2c, flow top breccia, hyaloclastite

- v, variolitic texture
- s, spherulites in massive flow

Other Rocks

3 - Chert

4 - Lamprophyre-type Dykes

Map 2.1.2: Geology of the Eastern Trench area, Harker Lake section.

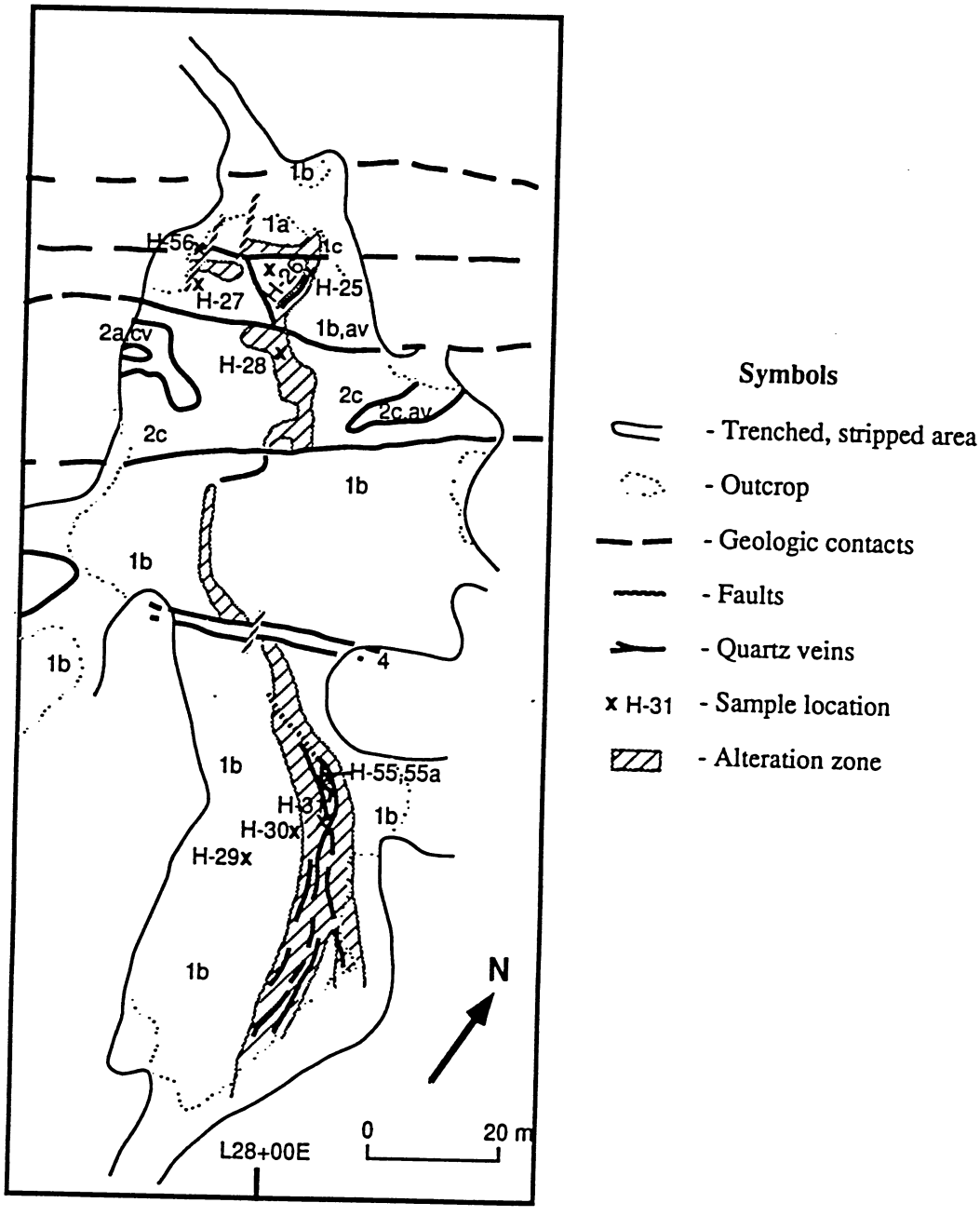

Map 2.1.2a: Inset map of the L28+00E area, from the Eastern map area, Harker Lake section. The alteration zone in the area crosscuts the inset at approximately north-south. The two sample sections used in the alteration studies are shown. Geological legend is on Map 2.1.2.

below the contact with the overlying Mg tholeiites. The flows of both suites are similar, with the exception that no variolites were found in the magnesium-rich section.

14+50E Section (Figure 2.1.2):

The base of this section is at 14+00N on Line 14+50E where a variolitic pillowed basalt is exposed. The pillows have thick (3-10 cm), rusty weathering selvages with abundant hyaloclastite in the interstices. The varioles are light green and spherical, have sharp contacts and are variably distributed within pillows. Overlying this variolitic flow, at 13+60N, is a unit with a thick, coarse-grained massive lower portion. The grain size gradually fines upwards to aphanitic, variolitic material at about 12+80N. The varioles here are not apparently related to any pillow forms or flow contacts but rather form a continuous band across the outcrop surrounding a narrow selvage. They are quite dark in colour and are barely visible in the dark green rock. Above this variolitic band is a short section of aphanitic, vesicular basalt, probably close to a flow top.

Across a short break in outcrop, a section of plagioclase-phyric intermediate rock begins at 12+60N. This is a darkly coloured, weakly magnetic, fine grained rock that is pillowed upsection. The rock is tough and has conchoidal fracture when broken. It has a distinctive bluish-white weathered surface. Massive to pillowed rock gives way, at about 12+30N, to an aphanitic, flow-banded rock still containing plagioclase phenocrysts. In addition, quartz phenocrysts (or amygdules?) are found in this section. The flowbanding is most prevalent at 12+17N near the upper contact with a pillowed unit. The upper pillowed unit also contains plagioclase phenocrysts which occur within the pillow interstices and selvages as well the pillow interiors. This may be a separate unit as the rock is not as tough and there are no quartz eyes present.

A series of three or four flows with thick massive portions starts at 12+03N and continues to the south end of the Line 14+50E section. These flows are quite fresh in appearance, generally darkly coloured with dark green amphibole crystals easily visible in their coarse grained portions. They are also magnetic. They have narrow, 2-8 m wide, pillowed and brecciated flow tops which may have weakly variolitic texture locally. The upper portion of the last flow hosts the Cryderman mineralized zone, and this zone marks the end of exposure on this section at 10+40N.

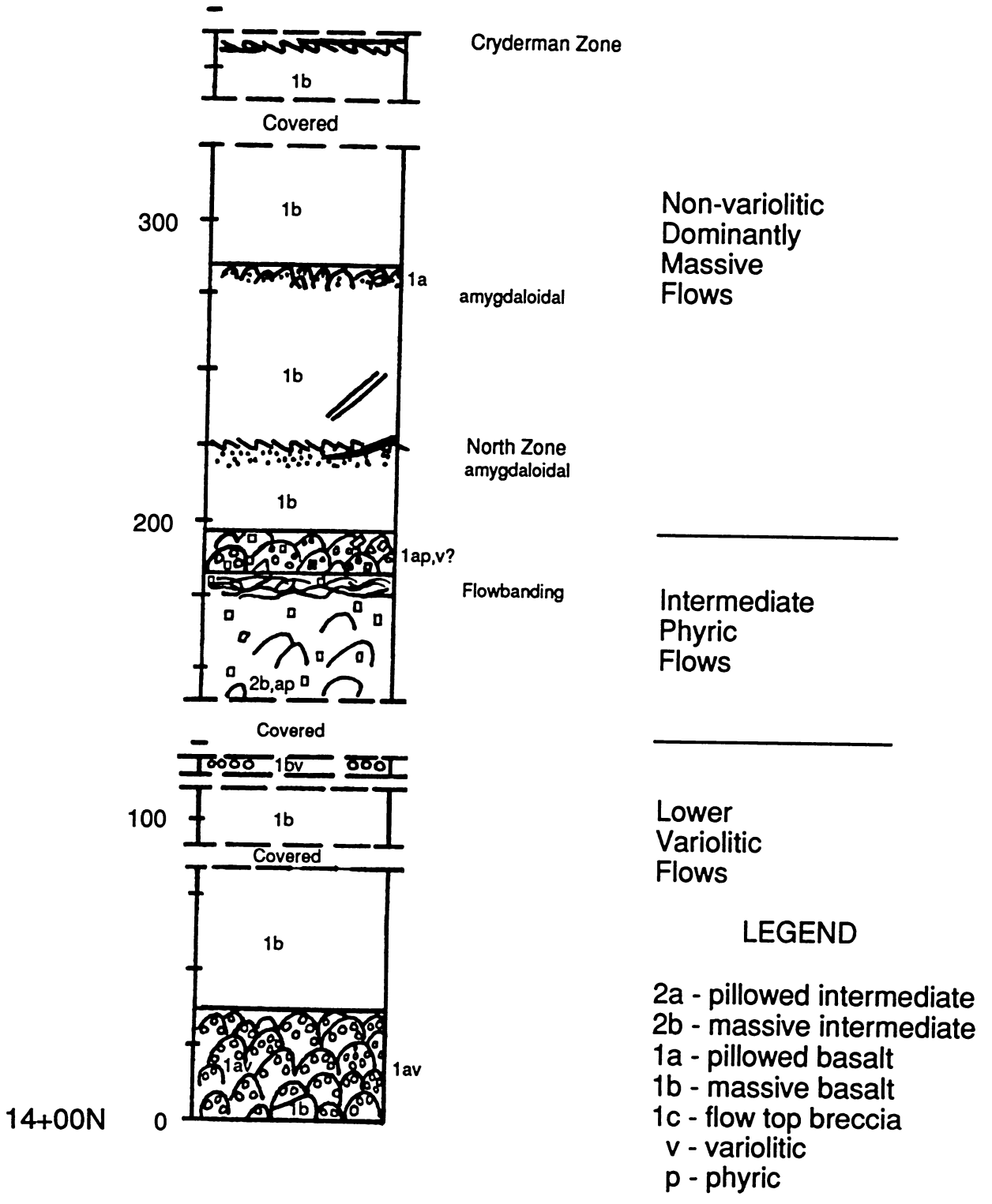

Figure 2.1.2: Stratigraphic Section for Line 14+50E, north of the Cryderman Zone and BL 10+00N. Flows have been divided into three main sections, from bottom to top: the Lower Variolitic, Intermediate Phyric, and Non-variolitic flows.

25+50E Section (Figure 2.1.3):

The volcanic section is exposed on Line 25+50E starting at 10+00N. From here, at least three massive to brecciated, non-variolitic flows constitute about 100 m of stratigraphy. Their massive portions are coarse grained, well jointed, magnetic and appear quite fresh. The upper portions are vesiculated. Brecciated flow tops have highly deformed and unusually shaped clasts with thick, hyaloclastite-rich interstices (Plate 2.1.1a). The uppermost flow of this non-variolitic section is apparently the thickest. Although its top contact is not exposed, it is at least 45 metres wide.

A chert or cherty tuff horizon occurs at the lower contact of the uppermost non-variolitic flow. This horizon is remarkably continuous and can be traced in outcrop over at least 500 m of strike as a discrete band, or as disaggregated pods in the interstices of flow top breccia (Plates 2.1.1b). This horizon extends to Line 14+50E, just south of the Cryderman Zone. Considering the similarity of the non-variolitic flows in the Line 14+50E and Line 25+50E sections, and the continuity of the cherty horizon, one can correlate the rocks between the two areas.

A section of massive to pillowed and brecciated flows overlies this non-variolitic sequence. Spherulitic texture is visible in the massive part of the lowermost flow. Amygdules are common in the fine grained massive portions of the flows just below the flow top. These are filled with chlorite, calcite and to a lesser extent pyrite. Varioles are present in the flow top pillows and breccia material. The flows are magnetic, especially in their massive portions.

The next section of stratigraphy is intermediate in composition. Near the top of the first flow, two bands of varioles, parallel to stratigraphy, are related to a linear selvage-like feature in an otherwise aphanitic to fine grained basalt. This texture is similar to that noted on the 14+50E section at 12+80N. Above this first flow is a section dominated by brecciated and flow banded lava, indicative of its more felsic nature (Plate 2.1.2). The lower part of this section is a blocky breccia, consisting mostly of large blocks of material, up to 3 m in diameter. These are commonly pillow-like in shape, with flow banded spherulitic material, and hyaloclastite in the interstices. In places the blocks have homogeneous, aphanitic interiors. Elsewhere, the blocks are essentially composed of hyaloclastite, similar to the overlying unit. On strike, in the Line 28+00E area, this part of the section is massive to

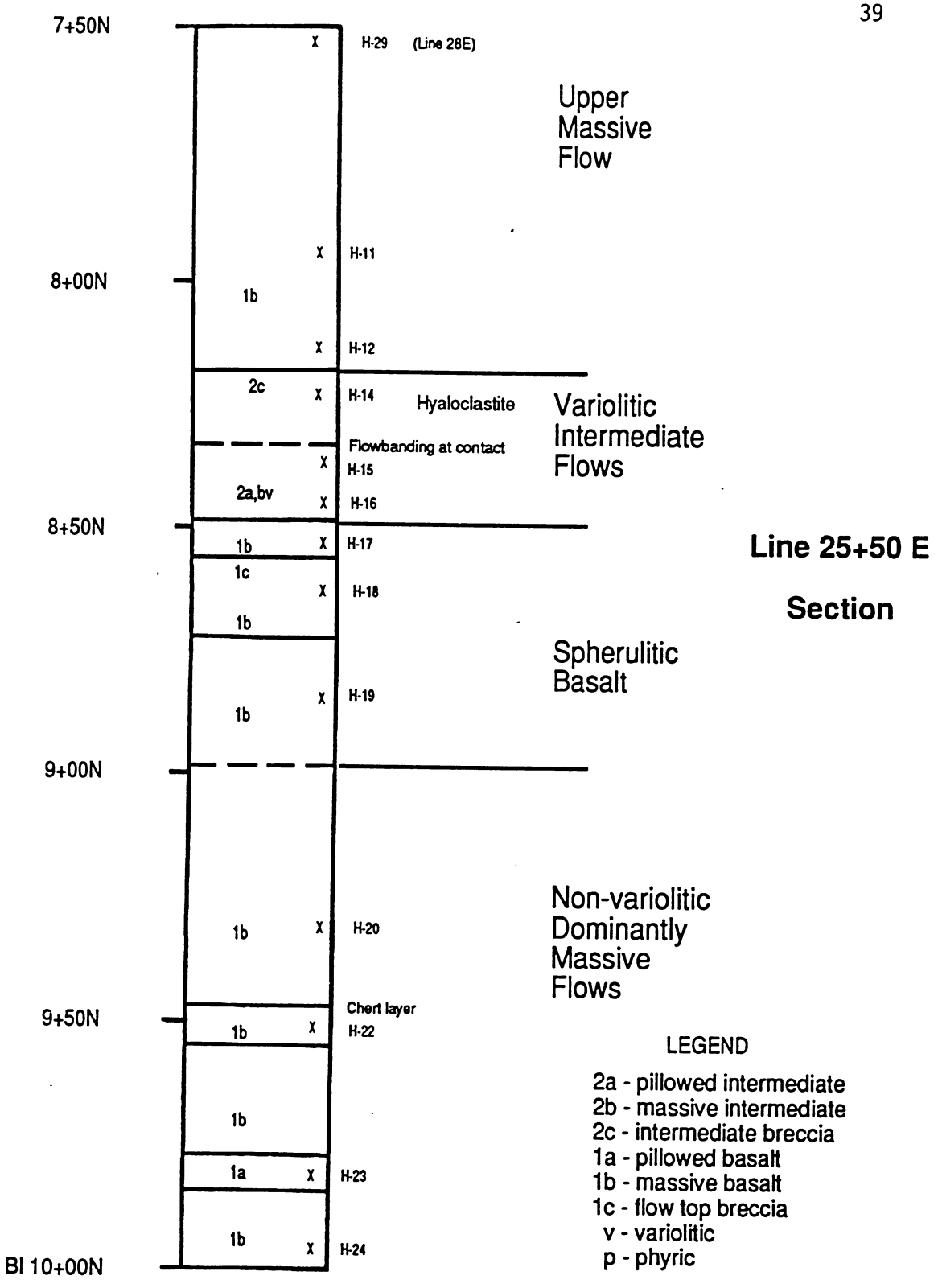

Figure 2.1.3: Stratigraphic column for volcanic flows on Line 25+50 E, Harker Lake area. Sample locations are marked by X, with sample number adjacent.

Plate 2.1.1: Non-variolitic Flows, Harker Lake area: a) Example of hyaloclastite in flow top breccia (near H-24). Field of view is approximately 1 m. b) Cherty material occurring in flow top breccia and at upper contact of flow (L 29+50E). Arrow on scale indicates the flow top.

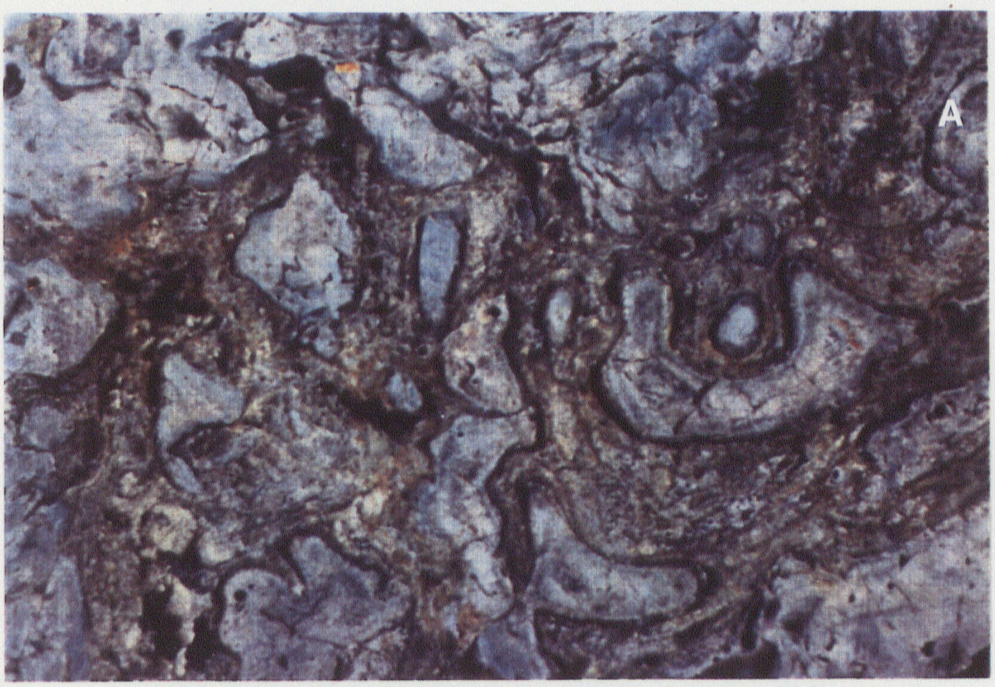
A

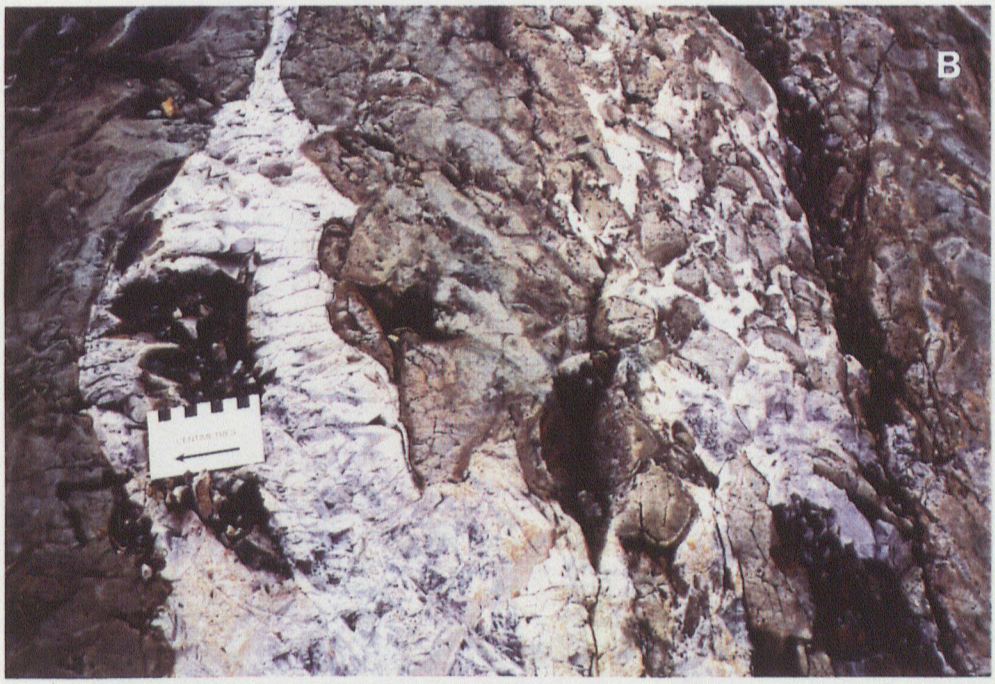
B

Plate 2.1.2: Flowbanding in the blocky, variolitic breccia, Intermediate Variolitic Flows, L25+50E section. Flowbanding is common in the blocks and their interstices.

Plate 2.1.3: Convoluted flowbanding at the contact between the blocky breccia and the overlying hyaloclastite unit (L 25+50E section). Tops are toward the bottom of the photo.


CENTIMETRES

pillowed, similar to the first flow. The upper contact of this lower section is extremely convoluted, having thin flow-banded layers of felsic, spherulitic material (Plate 2.1.3). Tongues (5-7 m wide), consisting mostly of large varioles, extend from the blocky breccia into the overlying hyaloclastite breccia.

The upper portion of the intermediate section is a thick, magnetic, hyaloclastite breccia (Plate 2.1.4a) of remarkable continuity, traceable the entire 500 m across the eastern map area. The hyaloclastite is between 10 and 20 metres thick and is characterized by fragments of layered rock ranging in size from a few centimetres to a couple metres (Plate 2.1.5). These fragments are highly convoluted and commonly show wispy or ragged borders. The layers are composed of dark, magnetite-rich, and light coloured, plagioclase spherulite-rich bands. The fragments are supported by a matrix of tiny glassy shards altered to chlorite and magnetite with resistant glassy margins. Locally, near the upper contact of this hyaloclastite unit, the alteration surrounding cooling cracks forms a distinctive interconnected pattern (Plate 2.1.6a). The upper contact is extremely flat over large distances (Plate 2.1.4b). The upper 50 cm is a lighter grey colour than the rest of the flow and has a subtle foliation (Plate 2.1.6b). This is interpreted to be due to weathering and subsequent compaction due to the overlying flow.

Near Line 24+50E, at 8+40N, trenching has exposed a small occurrence of massive rock within the hyaloclastite flow. This rock is dark grey to black, amygdaloidal, and quite tough. It has conchoidal fracture, and contorted grey and black laminations are visible. The rock is magnetic especially in proximity to the dark laminations. It is interpreted to be a massive equivalent to the hyaloclastite breccia described above.

Only the massive basal portion of the uppermost flow on this section is exposed, from 8+18N to 7+80N on Line 25+50E and between 8+10N and 7+10N on Line 28+00E. The rock is homogeneous, dark green, medium to coarse grained with prominent jointing and is quite magnetic. This flow must be very thick as 100 metres are exposed with no indication of an upper contact. Because the upper contact is covered, the unit could be interpreted to be a large sill. However, the perfectly conformable nature of the lower contact, and the lack of other sills in the vicinity, indicate it is most likely a flow.

Within the chill margin at the base of the upper massive flow a weak foliation, or

Plate 2.1.4: Hyaloclastite breccia unit: a) General texture, pock-marked appearance is due to the weathering of hyaloclastite clasts with resistant, glassy rims. b) Upper contact is quite smooth, possibly due to compaction (L28+00E area). The geology marked on the photo is: 2c, intermediate hyaloclastite breccia, 1b, massive basalt flow. Tops are to the left.

Plate 2.1.5: Layered fragments in the hyaloclastite breccia unit. Dark layers are very magnetic, composed dominantly of magnetite. Convoluted appearance is a primary feature.


A
CENTIMETRES


B
B
1-b
2c

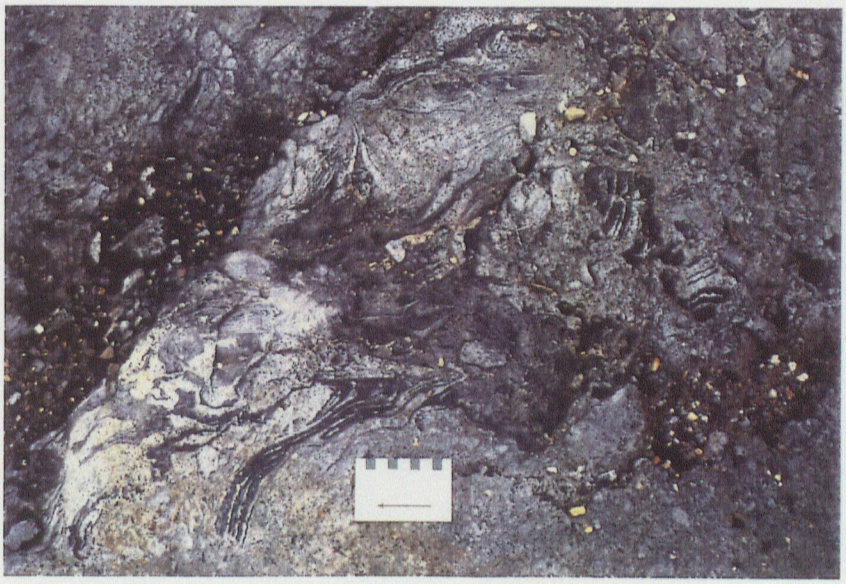

Plate 2.1.6: Textures characteristic of the top of the hyaloclastite breccia unit: a) Interconnected pattern, formed by alteration along cooling cracks(?). Scale marks the top of the flow. b) Alignment of fragments (weathered-out spots) at upper contact, possibly caused by compaction. Upper contact of the flow is at the base of the hammer handle.


A


B

layering, is developed possibly due to mineral alignment. Although this is most easily noticed in the base of this flow, it is present in other flows near the top of the section (e.g. sample H-56, Map 2.1.2a).

2.1.2 Structure

The rocks in the study area are not deformed. There is no evidence of penetrative deformation or large-scale folding. Some bands in the more felsic rocks are convoluted, however, this is due to flow. All flows have tops to the south.

Faults are common in the area. In particular, there are numerous northwest-southeast, vertical faults with minor associated offset. Generally, these faults have no more than a few metres horizontal movement and the sense of displacement is dextral in most instances. Other steep to vertical faults, subparallel to the strike of the volcanic rocks, are related to regional scale structures of the Kinojevis Group. These are associated with mineralization and alteration and host late felsic and lamprophyre dykes.

A minor fault was found in the stripped area on Line 28+00E. It cuts the section at a high but somewhat irregular angle, striking approximately 170° and dipping between 20° and 50° to the east. It has no apparent offset and is interpreted to be a splay of the mineralized fault set.

2.1.3 Metamorphism

The rocks in the vicinity of Harker Lake are metamorphosed to the lower greenschist facies. Epidote is a common alteration mineral and occurs in patches and envelopes related to fractures, or veins, or both. Characteristic minerals visible in hand specimen include chlorite and amphibole, albitic plagioclase, and calcite. Calcite occurs in amygdules and veinlets.

2.1.4 Mineralization and Alteration

The main mineralized zone in the study area is known as the Cryderman zone (Satterly, 1951). It crosses about half way through the composite section and marks the south end of the 14+50E trench (Map 2.1.1). This zone was discovered in the early 1920's and has

undergone sporadic exploration ever since. Initial descriptions of the zone called it a mineralized rhyolite due to its apparent siliceous nature (conchoidal fracture, light colour, hardness). The zone is centred on a structure, the Cryderman Fault, which is subparallel to the volcanic stratigraphy, striking across the area at 067°. The Cryderman zone is best developed between Lines 13+00E and 20+00E, coinciding with the area of best exposure due to extensive trenching. True thickness of the zone as measured in drill sections, ranges between 7 and 15 metres. Alteration and mineralization declines substantially outside the section between Lines 13+00E and 20+00E, although the zone is continuous as a weakly altered fault.

In the main section of the Cryderman Zone, most alteration and mineralization is in the footwall to the fault. The host rocks to the zone are typical non-variolitic Fe tholeiites of the study area. The alteration halo is marked by intense fracturing of the host rocks up to 15 metres from the fault which coincides with a colour change from dark green to dark purplish grey. The colour change is due to pervasive calcite and fine grained, hematite alteration. Quartz-calcite veinlets fill the fractures. Further in, towards the core of the zone, specular hematite-quartz veinlets become more prevalent and calcite diminishes in abundance with respect to other carbonate minerals. Bleached patches of rock with associated pyritization (up to 20%) and gold mineralization are quite common. Quartz veins and stockworks occur at the edges of, and in the central fault. Only at the very core of this zone is there any indication of foliation associated with the faulting. Hematite, quartz and pyrite are common in the fault breccia. Large, discontinuous, milky quartz veins found throughout the alteration zone seem to be later features and are sparsely mineralized with chalcopyrite, galena and pyrite with very little gold (Plate 2.1.7).

Gold mineralization within the Cryderman zone is commonly of ore grade concentration, however, it is also quite sporadic and as a result significant tonnages have not been outlined. Nonetheless, values up to 37 g/T over a metre are found in surface sampling of the zone.

Another small zone, similar to the Cryderman zone, is located about 125 m north within the study area. The intensity of alteration and gold content is considerably less here, although the zone appears no less continuous. A hornblende porphyry intrusive, which is

Plate 2.1.7: Large, late, milky quartz veins, usually containing chalcopyrite and galena, common in the Cryderman Zone (looking southwest from about 16+00E). Dashed line marks Section I (see Fig. 3.1.2), and is about 15 m long. White lines are the late, milky quartz veins. The main mineralized zone is the gossanous part, to the right of the large quartz vein on the left end of the dashed line.

Plate 2.1.8: Cross-section, looking east, through the alteration zone in the upper massive flow, Line 28+00E area. Zone is dipping away at about 25°. Dark green, unaltered rock is visible in the foreground (e.g. sample H-29). The core of anastomosing quartz veins is visible in the upper part of the photograph (e.g. sample H-55). Notebook is approximately 20 cm long.

variably altered and locally mineralized, is found within this zone.

The large stripped area on Line 28+00E contains a small mineralized structure which appears to be a splay from the Cryderman zone (Map 2.1.2). This zone has the alteration and mineralization characteristics of the Cryderman zone but to a much lesser degree. It crosses the variolitic intermediate and upper massive flows at a high angle, striking about 170° overall. Veining and fracturing follow two main orientations (170°/20-50°E; 130°/25°NE) in the zone. Alteration is variable, spreading out in more permeable rocks such as flow top breccias. This is especially noticeable where it crosses the hyaloclastite unit. In the uppermost flow, south of the hyaloclastite, the zone branches out into an anastomosing network of quartz veins (Plate 2.1.8). The true thickness of the zone reaches about 8 metres and the intensity of alteration and pyritization also approaches that in the Cryderman zone in this area.

2.2 Dome Mine Area

2.2.1 Geology of the Vipond Subgroup

The rocks in the vicinity of the Dome Mine, are composed of a relatively homoclinal section extending from the Deloro Group in the south, across the Destor-Porcupine Fault Zone, through all the members of the Tisdale Group to the Porcupine Group sediments (Fig. 2.2.1). The Younger Sediments (Timiskaming-style) are also included in this section. This north-facing section forms the north limb of the South Tisdale Anticline or, alternatively, the south limb of the Porcupine Syncline. The volcanic stratigrapic nomemclature is complex in this area. Figure 2.2.2 compares and correlates the subdivisions of the volcanic flows and the various names given to them. In the Dome Mine, the Greenstone Nose is a section of volcanic stratigraphy, bounded on the east by an unconformity (Figure 2.2.1). Flows, striking slightly north of east, encounter this termination with no evidence of folding or facies change. The section of stratigraphy found in the Greenstone Nose is marked on Figure 2.2.2 and has its own distinctive nomenclature which is used at the mine. The upper contact of the lavas in the mine sequence is marked by a 10 m thick section of sheared carbonaceous sediments. The "Sedimentary Trough" contacts the Greenstone Nose to the south and, at shallow depths, to the west. Recent work (Pirshco and Kettles, 1988) indicates this is an intrusive breccia

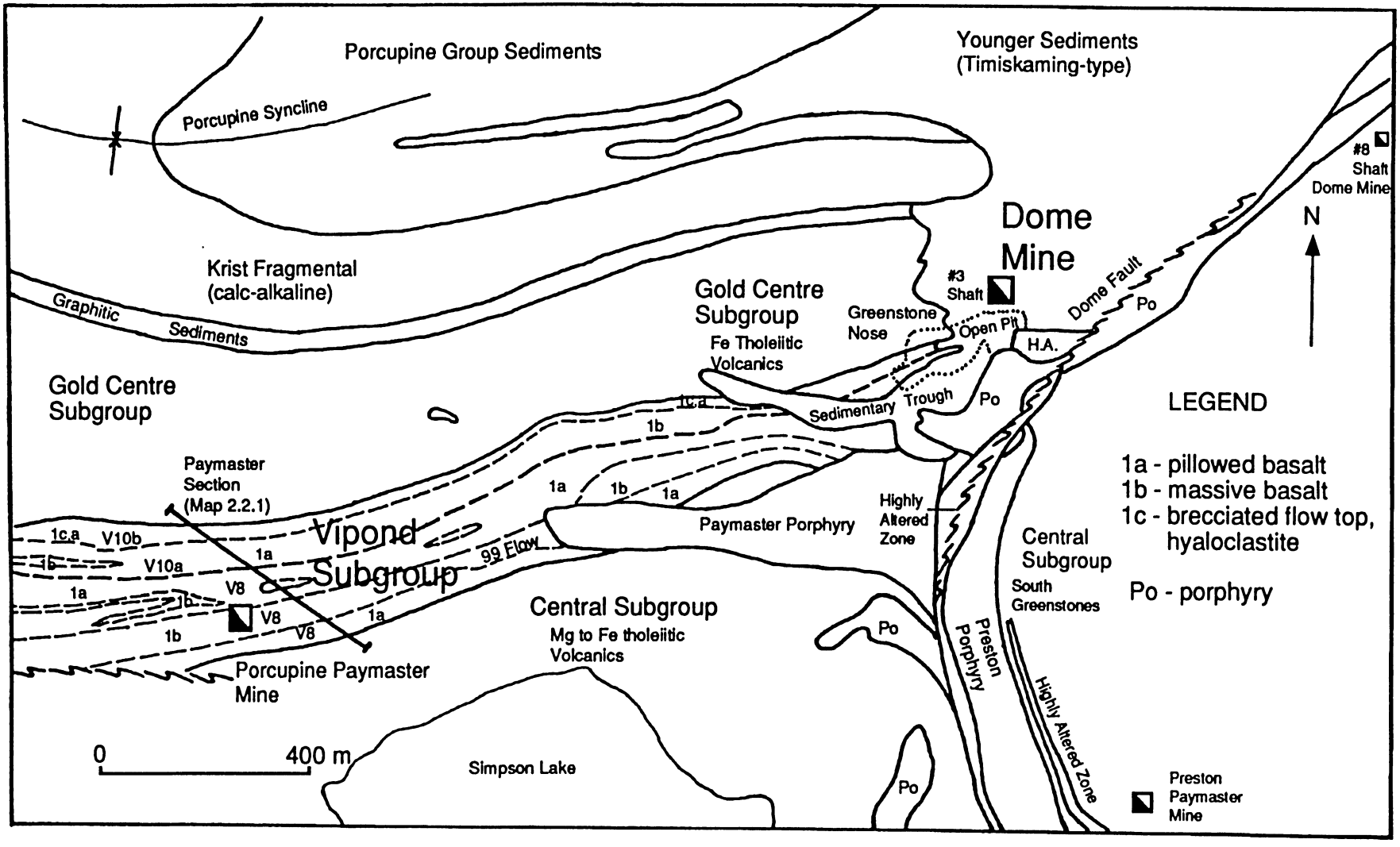

Figure 2.2.1: Geology of the Dome Mine area, Timmins, Ontario (modified after Ferguson, 1968).

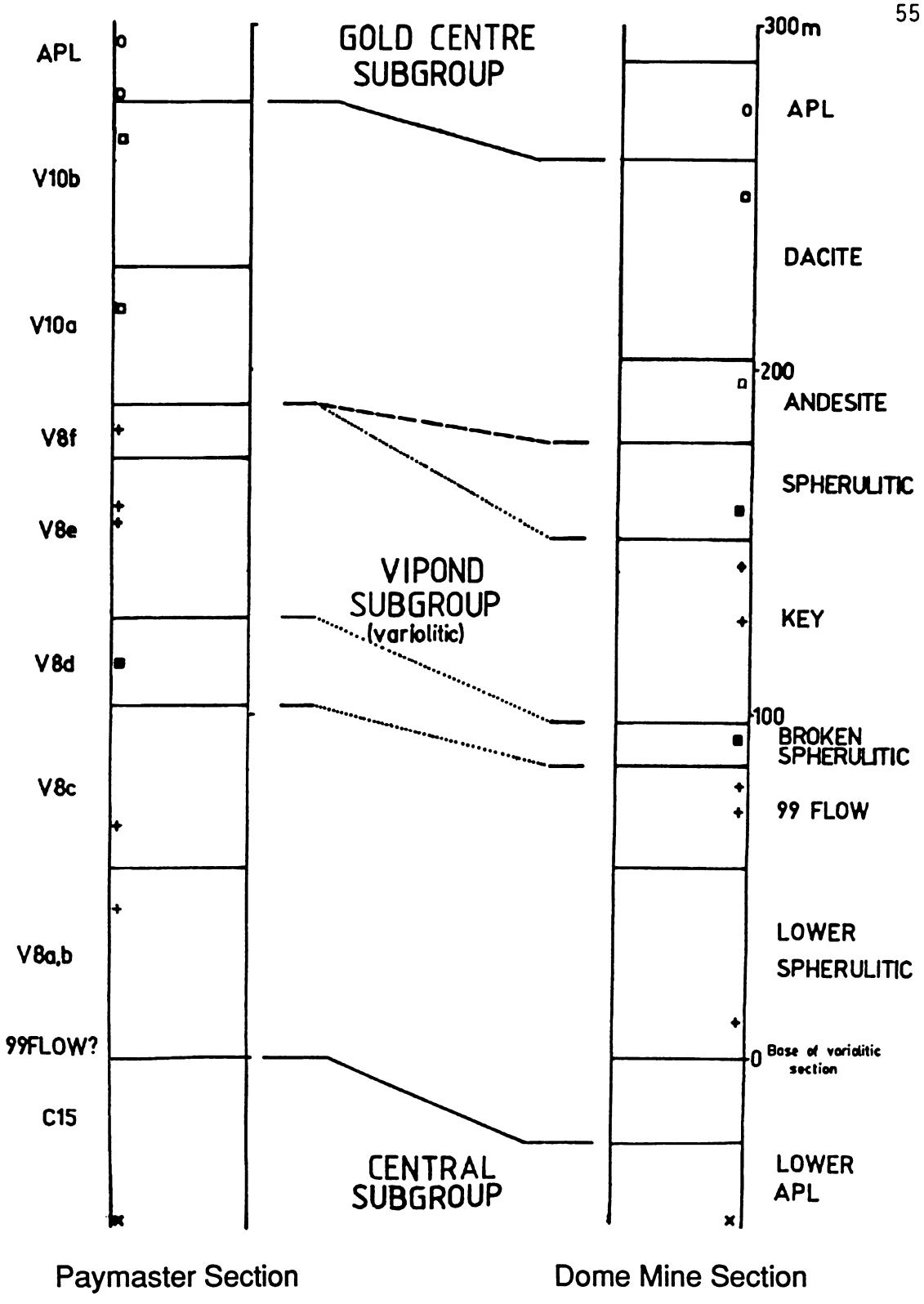

Figure 2.2.2: Stratigraphic columns correlating units from the Dome Mine and Porcupine Paymaster sections. Symbols represent locations of samples used for geochemical plotting (Chapter 4).

rather than a structurally confined sedimentary basin. Intrusive porphyry bodies are present in the area as well. They are spatially related to the Dome Fault, the main structural break in the vicinity. Associated with the Dome Fault and porphyry rocks are a group of highly altered and carbonatized, ultramafic rocks. Another group of tholeiitic volcanics, termed the South Greenstones, are located south and east of the fault. These flows represent the Mg-rich section of the Central Subgroup. The South Greenstones are bounded to south by the Destor-Porcupine Fault Zone.

Broad scale mapping of the local geology and the units of the Dome Mine was not done since the geology is very well known from earlier work. The geological descriptions which follow are based on the sections which were directly examined in the field and at the Dome Mine and as such are quite restricted in their scope. They are not intended to represent all the characteristics of the variolitic suite in the Timmins area.

2.2.1a Porcupine Paymaster Section

The Porcupine Paymaster section (Map 2.2.1) begins on the south side of the back road between Timmins and South Porcupine, about 1.4 km west southwest of the No. 3 shaft of the Dome Mine. North of the road the section follows a hydroline clearcut northeast for approximately 500 m. Several Timmins area field trip guides include this location for its excellent exposure of the Vipond Subgroup with its well known variolitic marker horizons (Pyke, 1978). The rocks are moderately foliated and pervasively carbonatized. A steep easterly plunge is present along the intersection of foliations, especially noticeable by elongation of varioles throughout the section.

On the south side of the road there are several outcrops of the uppermost flows of the Central subgroup. They are pillowed, dark green, non-magnetic basalt with tiny (1 mm or less) chlorite-filled amygdules and fine specks of leucoxene. Crossing the road to the powerline, the first outcrop encountered is a variolitic pillowed unit. This is presumably stratigraphically above the massive 99 Flow (not exposed, or not present here) which generally marks the lower contact of the Vipond section (and Pyke's middle Tisdale member) as well as the V8 subunit of the Vipond. The pillowed unit is approximately 40 metres wide in plan. The rock is strongly foliated though relict fibro-radial texture is still visible in some

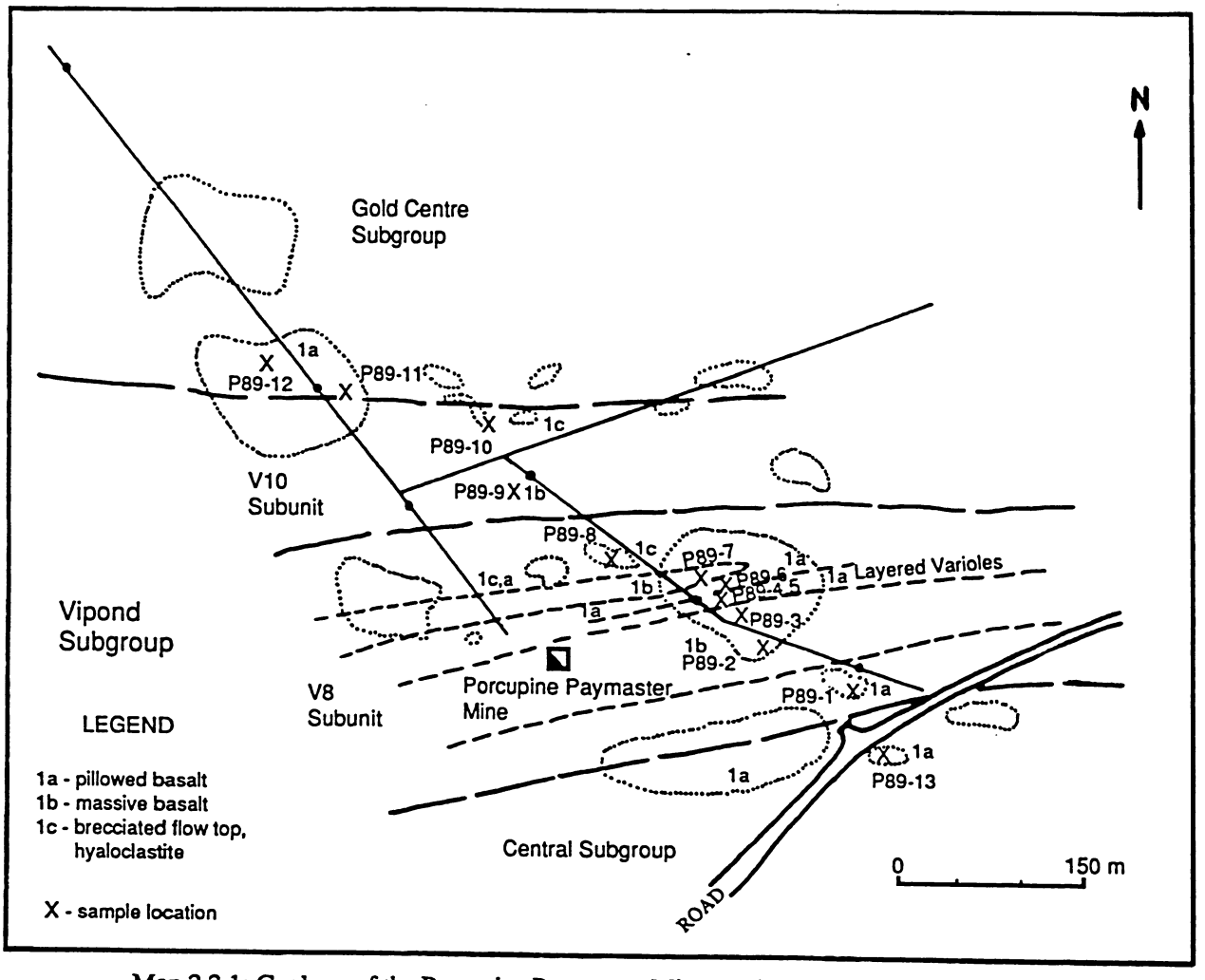

Map 2.2.1: Geology of the Porcupine Paymaster Mine section (after, Pyke, 1978).

varioles. Varioles tend to be concentrated around the margins of pillows which have dark green, aphanitic interiors. Generally, the unit is non-magnetic. Above this pillowed unit is a massive flow, about 50 m wide, with a vesicular upper portion and a hyaloclastitic flow top. This unit is magnetic and calcite occurs as distinctive speckles throughout the rock. The flow top is also distinguished by a narrow discontinuous cherty layer.

The next unit is a variolitic pillowed basalt which is characterized by large pillows (up to several metres in length) with coalesced, layers of varioles near their margins. Commonly the varioles also coalesce towards the core of the pillows. The varioles appear siliceous and have a purplish caste, rather than a creamy white colour. Overlying this unit is another variolitic pillowed section which is characterized by more evenly distributed and less prominent varioles (Plate 2.2.1). They are light grey to green and may have ragged borders. The matrix to the variole material in this flow is magnetic whereas the previous flow is non-magnetic. Overall, these two pillowed units cover about 30 metres of section.

At the top of the pillowed section is a sharp contact with massive lava which continues to the end of the outcrop. Across a roadfill the outcrop is again variolitic pillowed rock with a brecciated, hyaloclastitic flow top. The upper contact of this unit marks the upper limit of the V8 subunit.

The V10 subunit outcrops 20 to 30 metres north. It consists of massive to variolitic, brecciated flows approximately 90 metres thick. The lower part is a massive basaltic or intermediate rock, non-magnetic, quite fine grained and homogeneous in appearance. This is overlain by a fairly wide section of pillowed and brecciated material, characterized by broken varioles. The upper contact of the variolitic section is usually marked by a characteristic texture, called "ropy texture" (Plate 2.2.2), which is very similar to that noted at the top of the hyaloclastite unit in the Harker section described previously.

Sampling on this section was extended into the lowermost flow of the overlying Gold Centre Subgroup. This unit is a massive to pillowed unit of amydaloidal lava, generally dark green, aphanitic and non-magnetic. The amygdules consist dominantly of chlorite.

Plate 2.2.1: Scattered varioles in pillow basalt, V8 subunit of the Vipond Subgroup, Porcupine Paymaster Section (near P89-06).

Plate 2.2.2: Characteristic "ropy texture" at the uppermost contact of the V10 subunit, Vipond Subgroup, from the Porcupine Paymaster section (near P89-10). Note similarity to texture in Plate 2.1.6a.

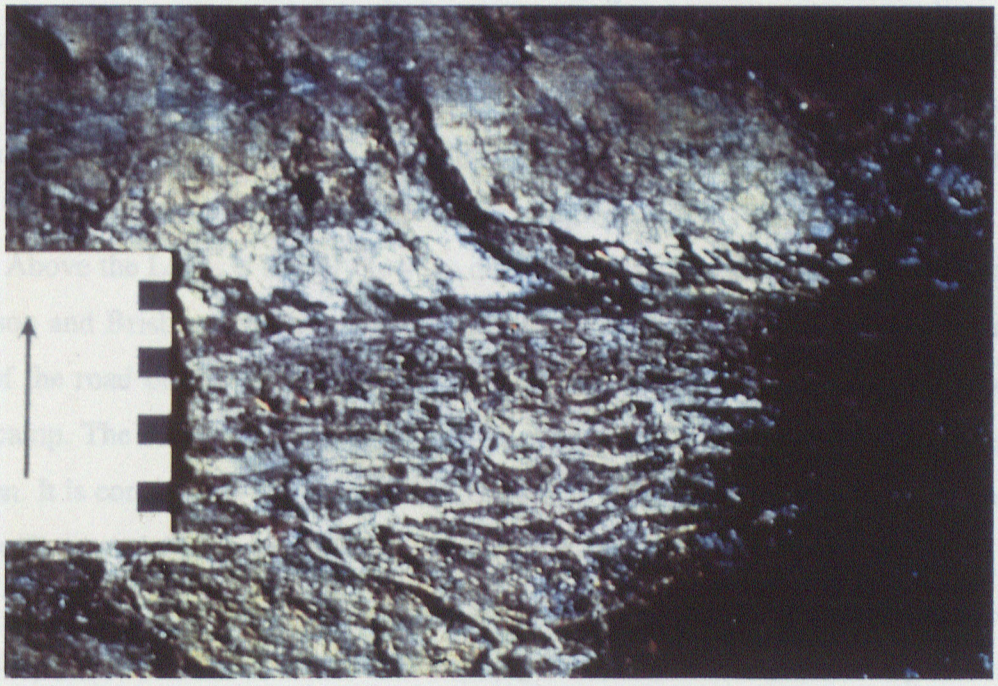

2.2.1b Dome Mine Section

Rocks at the Dome Mine were sampled on 5 different levels and within the Greenstone Nose only (Maps 2.2.2 to 2.2.6). The South Greenstones are not part of the variolitic section. The sampled section includes rocks of the upper Central Subgroup through to the Gold Centre Subgroup, similar to the Paymaster section. Terminology used for the mine stratigraphy is very different and some minor stratigraphic differences exist between the two sections, as seen in Figure 2.2.2, but overall they are easily correlated. Throughout the Dome Mine the intensity of deformation and alteration is quite high except in a few minor enclaves of relatively undeformed rock such as at sample D89-21 in the 99 Flow (Map 2.2.5).

The lowermost unit sampled in the Dome is the Lower Amygdaloidal Pillow Lava (LAPL). This flow is similar in stratigraphic position and description to the upper flow of the Central Subgroup as sampled on the Paymaster section. The unit is massive to pillowed, greyish to buff coloured due to carbonatization and, generally, contains carbonate-quartz amygdules and tan coloured leucoxene. The southern limit of the LAPL is usually cut off at the "sedimentary trough" so true thickness is difficult to determine.

The Lower Spherulitic Flow (LSPL) occurs immediately above the LAPL and is the lowest variolitic unit in the mine sequence. According to Mason and Brisbin (1987) there is a massive flow base to the LSPL which may correlate with the 99 Flow as designated elsewhere in the camp (Figure 2.2.2). The LSPL is generally about 45-60 metres thick, containing variolitic pillowed lava with the varioles commonly coalesced. Massive portions of this flow, such as on 2900 Level, are quite magnetic.

Above the LSPL is the 99 Flow, as designated by the mine geologists. As pointed out by Mason and Brisbin (1987), this unit seems to correlate better with the first massive flow north of the road on the Paymaster section than with the 99 Flow as recognized elsewhere in the camp. The 99 Flow in the Dome Mine is generally massive, with a coarse grain size common. It is consistently in the range of 25-40 metres thick and is magnetic. There are tiny, chloritic(?) amygdules present locally in the upper portion of the flow.

The Broken Spherulitic flow is usually found above the 99 Flow at the Dome Mine. It is between 15 and 25 metres thick, normally pillowed, and characterized by varioles which have apparently been brecciated. Leucoxene is commonly visible in the foliated matrix to the

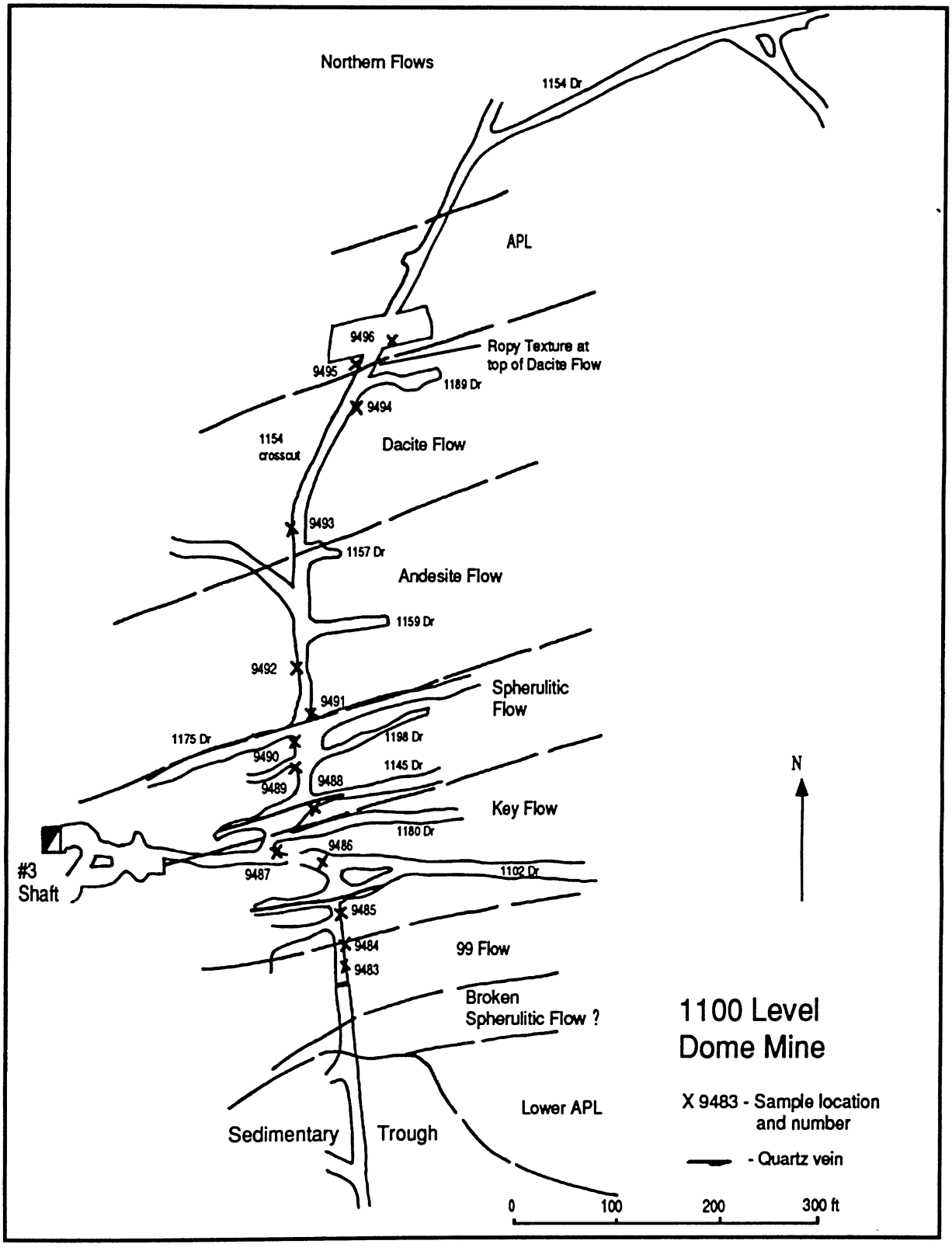

Map 2.2.2 Geological section through the Vipond Subgroup in the 1154 crosscut, 1100 Level, Dome Mine. Mine units are labelled and sample locations are shown.

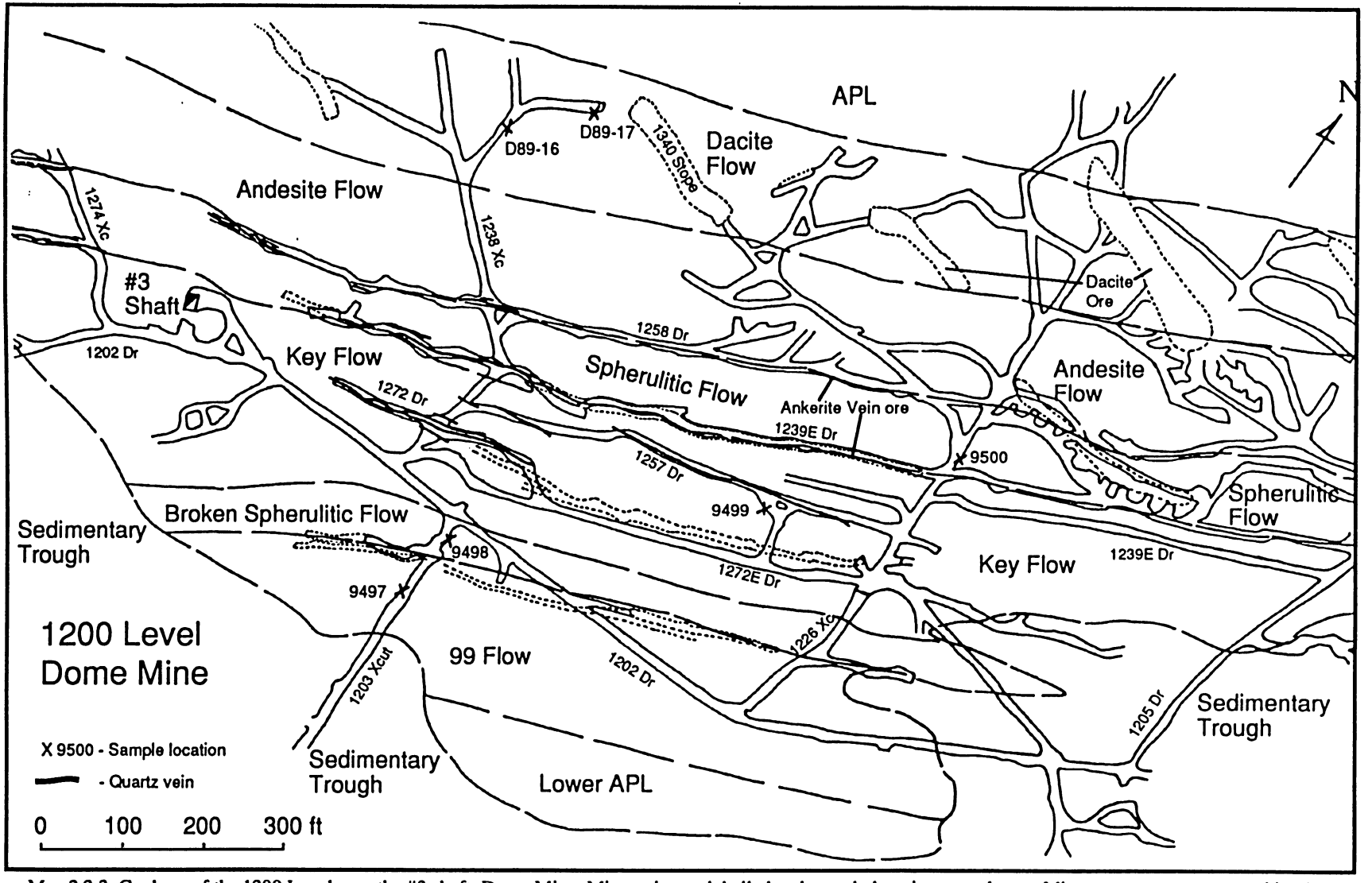

Map 2.2.3: Geology of the 1200 Level near the #3 shaft, Dome Mine. Mine units are labelled and sample locations are shown. Mine stopes are represented by the dotted outlines.

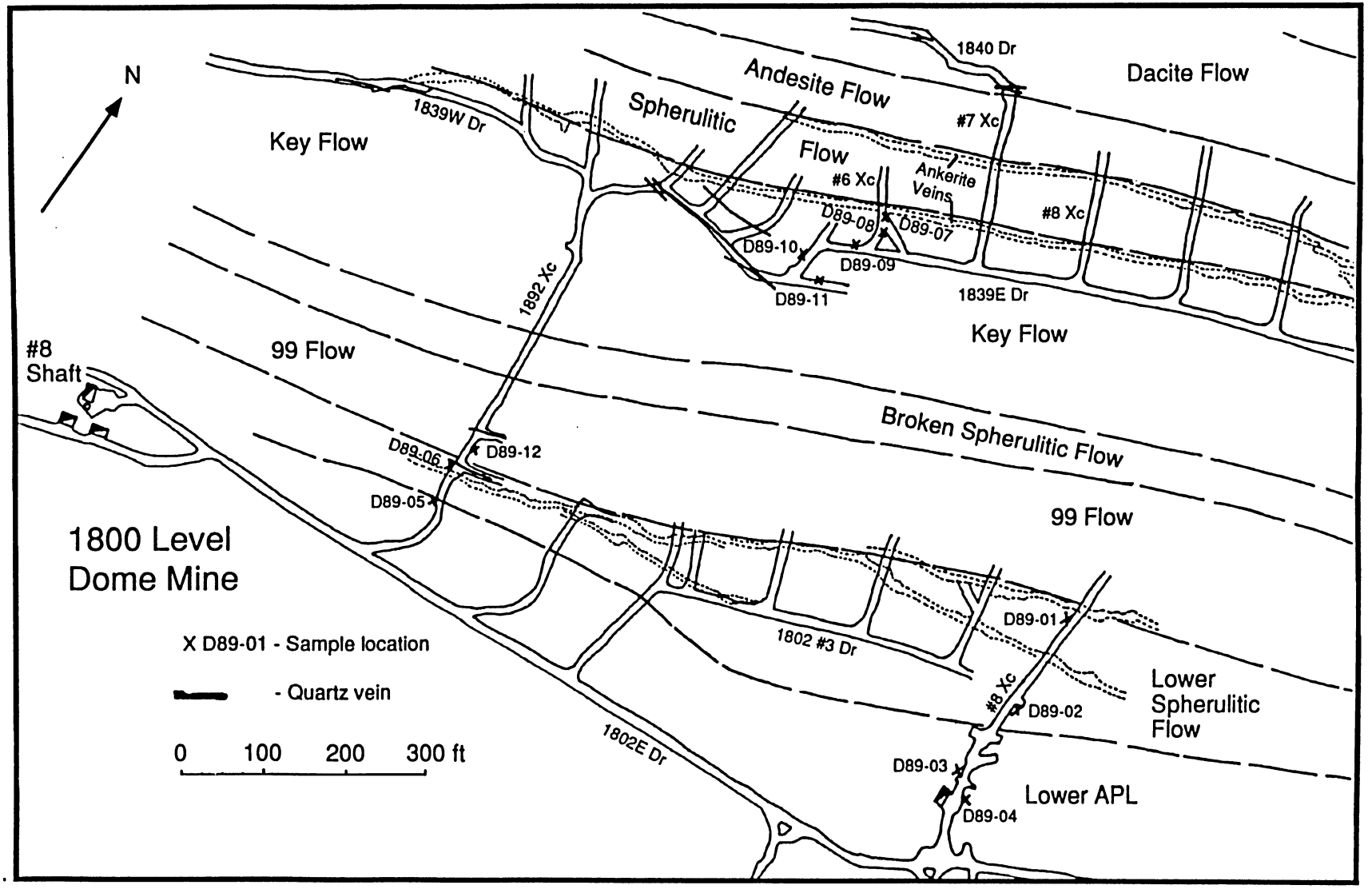

Map 2.2.4: Geology of the Vipond Subgroup in the vicinity of the #8 Shaft, 1800 Level, Dome Mine. Mine units are labelled and sample locations are shown. Mine stopes are shown by dotted outlines.

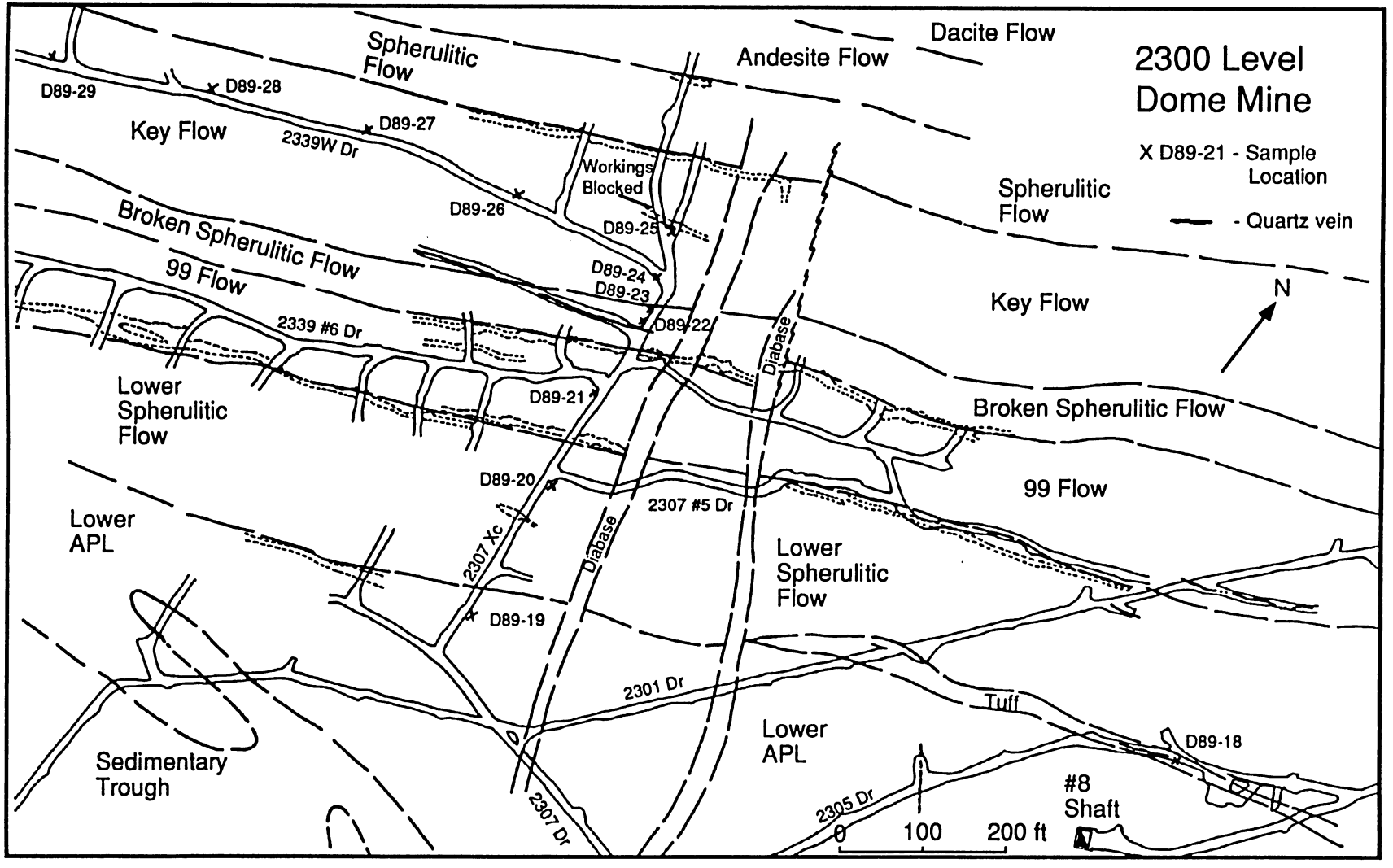

Map 2.2.5: Geology of part of the 2300 Level near the #8 Shaft, Dome Mine. Mine stopes are indicated by the dotted outlines.

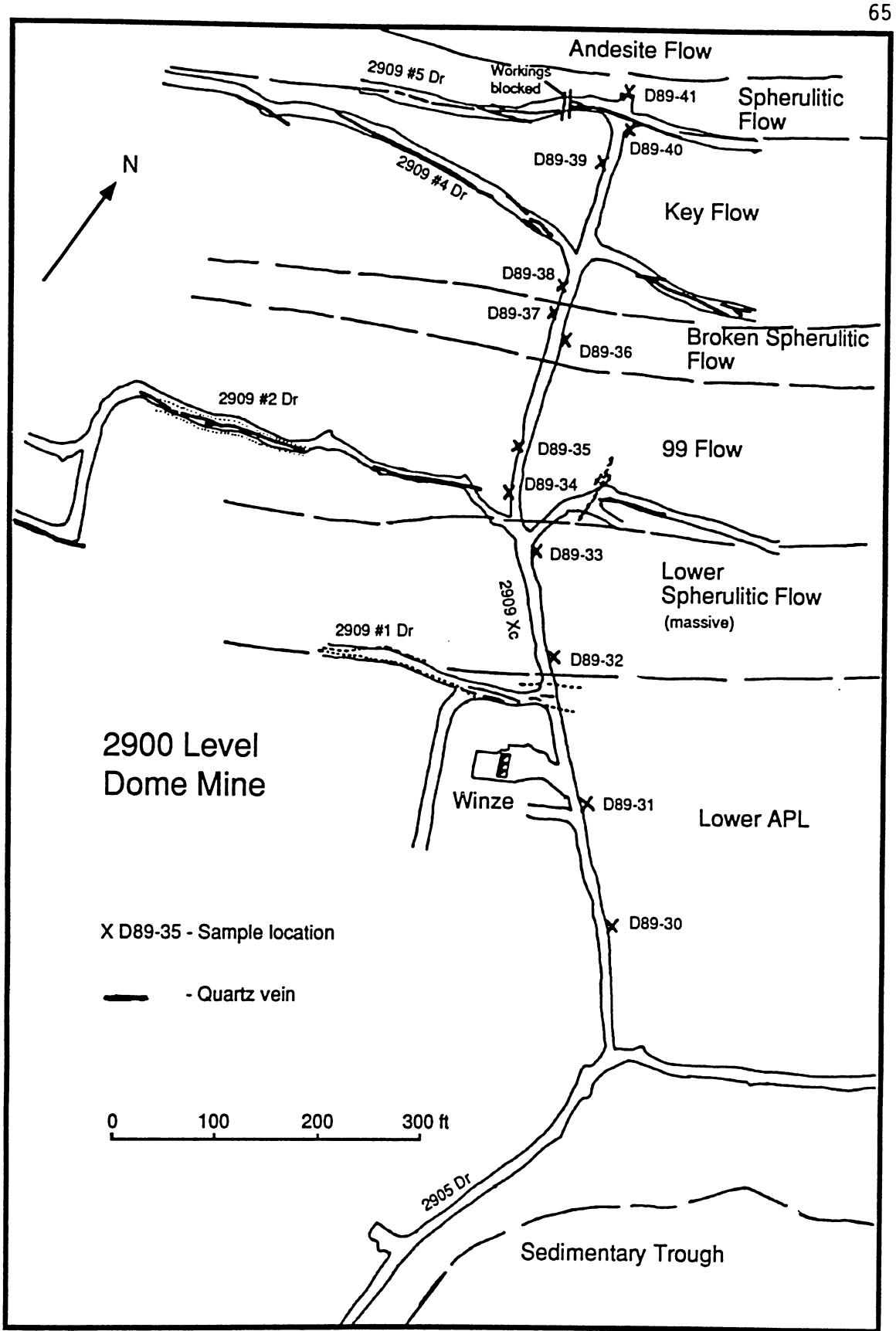

Map 2.2.6: Geological section through lower Vipond Subgroup in the 2909 crosscut, 2900 Level, Dome Mine. Mine stopes are indicated by dotted outlines. Mine units are labelled on the map.

varioles. The stratigraphic position of the Broken Spherulitic Flow is not always consistent, at least as it has been mapped. On most levels in the mine it is found immediately overlying the 99 Flow, however, on the 1200 Level it is below the 99 Flow. Also, in places it may be indistinguishable from the overlying Key Flow. Discontinuous units and anastomosing flows, common in lava piles, may be the cause of the confusion.

The Key Flow is a 50-70 metre wide section of dominantly pillowed variolitic lavas. The pillows are commonly quite large. The varioles are large, cream to grey in colour and variably distributed. Above the Key is the Spherulitic Flow which is both pillowed and brecciated. It is between 25 and 30 metres thick and marks the upper contact of the V8 subunit within the Dome Mine stratigraphy. The Spherulitic Flow is characterized by "flowy texture", a mine term used to described lightly coloured, lensy siliceous material, which is possibly flow banded. A narrow, white coloured band of rock commonly occurs at the base of the unit (Ferguson, 1968).

The V10 subunit is defined at the Dome by two main units; the Andesite and the Dacite Flows. Both of these units are massive to pillowed, and usually variolitic. The upper contact of the Dacite has the characteristic "ropey" texture noted at the top of the V10 section at the Porcupine Paymaster Mine and elsewhere in the Camp. Each of these units ranges from 30 to 50 metres in thickness. Massive portions of the flows are generally fine grained and homogeneous in appearance. They may be weakly magnetic.

The uppermost unit sampled at the Dome is the lowermost flow of the Gold Centre Subgroup, which is termed the Amygdaloidal Pillow Lava (APL) at the Dome Mine. This flow marks the start of the Northern series of volcanics in the mine which are less important as ore hosts. The APL is characterized by carbonate, chlorite, and pyrite filled amygdules. The rock is light grey to buff in colour due to alteration of its aphanitic groundmass. There is no evidence of any unconformity or other discontinuity separating the rocks of the Vipond and Gold Centre Subgroups.

2.2.2 Structural Geology

The geology in the vicinity of the Dome Mine is characterized by a homoclinal sequence of volcanic rocks cut by porphyritic intrusions and faults (Ferguson, 1968).

Structural elements include foliation and stretching lineation imparted by regional folding events. The structural setting of the Porcupine Paymaster and Dome Mines is very important to the localization of ore (Roberts 1987). The attitude and morphology of the Greenstone Nose and its associated altered and mineralized rocks are related to these regional structural constraints (Figure 2.2.3). Also, mineralization is commonly associated with shearing related to local splays from the Dome Fault.

The Dome Fault, a major northeast-southwest trending fault, passes through the mine. The fault zone hosts the Highly Altered and Carbonatized rock units of the mine. In the vicinity of the Greenstone Nose this fault is subparallel to the Destor-Porcupine Fault, however, it joins the DPFZ to the south of the mine area. The abundant alteration and mineralization present in this fault zone suggests that it was formed previous to the mineralizing event. Mineralization at the Dome Mine is associated with splays from this fault. The Burrows-Benedict Fault is encountered on the eastern flank of the deposit, near 3900 feet in depth. Numerous late faults, having offsets up to 50 or 60 metres, and various orientations, are present in the area.

2.2.3 Metamorphism

The general metamorphic assemblage in the Dome Mine area consists of chlorite-amphibole-plagioclase-carbonate-epidote-oxides and is characteristic of greenschist facies rocks. The carbonate is a product of the alteration associated with the development of the regional foliation. Chloritization is also associated with this regional event. Details of the assemblages and alteration are discussed in Chapters Three and Five.

2.2.4 Gold Deposits

One million, two hundred thousand ounces of gold were produced from the Porcupine Paymaster Mine, chiefly from the No. 5 shaft area located in the northwest part of the property immediately west of the sampled section (Figure 2.2.1). The ore at the Porcupine Paymaster is concentrated in veins in dilatent zones near the Paymaster porphyry and along structures subparallel to the volcanic stratigraphy (Ferguson, 1968). Large, continuous veins are in the massive portions of flows, whereas anastomosing stockworks are in the less

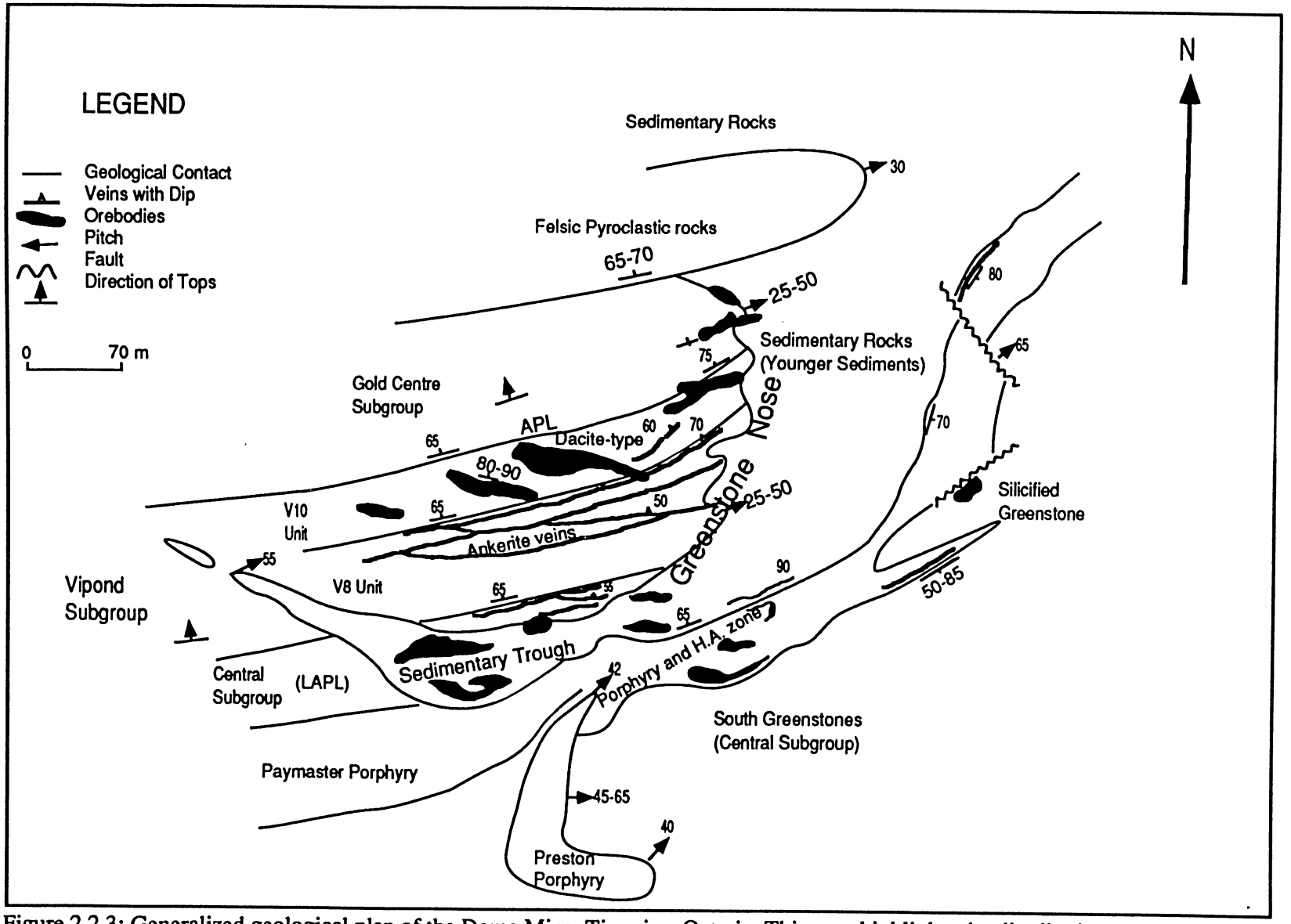

Figure 2.2.3: Generalized geological plan of the Dome Mine, Timmins, Ontario. This map highlights the distribution and morphology of the main orebodies at the mine. The difference in the morphology of orebodies in the V10 unit (Dacite-type) and the V8 (ankerite vein-type) is quite obvious.

competent flow tops. Most of the ore is in the upper Central to upper Vipond subgroups, especially the lowermost variolitic and massive flow of the Vipond (LSPL at the Dome Mine). Another important ore host is the upper contact of the V8 subunit with the V10 subunit.

Gold production from the Dome Mine is approaching 12 million ounces. The mine has ore in most every rock type present save the late diabase dykes (Figure 2.2.3). Structural control of the ore is most important. Most ore bodies either have severely strained host rocks (e.g. ankerite veins) or fill voids produced by the response of the host rocks to stress (e.g. dacite ore). The main structures are continuous and crosscut most contacts, including the unconformity at the Greenstone Nose. A great deal of the ore at Dome is concentrated in an area near the outline of the Greenstone Nose. This may in part be due to the chemical contrast between the volcanic rocks of the Nose and the sedimentary and sedimentary-type rocks surrounding it. Production from volcanic rocks is largely restricted to the Vipond sequence of the Greenstone Nose. In particular there are two main styles of mineralization in the Greenstone Nose (Ferguson,1968); the "ankerite veins", generally in the less competent flow tops of the V8 subunit, and, the dacite ore, large lenticular ore bodies consisting of en-echelon quartz veins with well mineralized wall rocks.

Ankerite veins consist of massive ankerite to mixtures of ankerite stringers with altered wall rock. They crosscut flow contacts at acute angles, not more than 20°. Quartz occurs in these zones as ladder veins and is usually associated with higher gold concentrations. These ore bodies contain up to 5% pyrite and/or pyrrhotite and some native gold. Although the ankerite veins cross the greenstone-sediment contact, they die out quickly suggesting that the sediments may inhibit their formation. Narrow, less than 1 m wide, alteration zones of bleached basalt containing disseminated Fe sulphides usually surround the ankerite veins. The en-echelon dacite ore bodies occur within the massive parts of the V10 subunit. Quartz veining makes up about 20% of these ore bodies. They are surrounded by large, commonly coalesced, alteration haloes containing fine grained, disseminated sulphides, generally about 3% pyrite and pyrrhotite.

Native gold and tellurides occur in the quartz veins. Gold is always associated with Fe sulphides, however, the converse is not always true. Other sulphides, such as, chalcopyrite,

sphalerite and galena are also present in minor quantites and commonly indicate higher gold concentrations.

Wall rock alteration associated with mineralization in the mafic volcanics chiefly involved the breakdown of ferromagnesian minerals, Fe-Ti oxides and plagioclase combined with the addition of CO_2, K and S. This combination resulted in the formation of carbonates, sericite and Fe sulphides which comprise the most common metasomatic minerals. In addition there is evidence of reduction of the oxidation state of iron towards the mineralized zones (Fryer *et al*, 1979). Tourmaline is a common component of both the veins and altered wall rocks at the Dome.

2.3 M^{c}Diarmid Lake Area

2.3.1 Stratigraphy of Sampled Section

In Marriot Township, a section of variolitic flows representing the least altered rocks of the study were examined and sampled. This section is on the northwest shore of M^{c}Diarmid Lake very near the upper contact of the tholeiitic Kinojevis Group with the overlying calc-alkaline Blake River Group (Jensen, 1978). These flows are exposed over an area of about 60 m by 50 m and form an undeformed, southfacing succession striking about 060° and dipping steeply north. There is no evidence of any strong structural influence in this area, such as penetrative foliation or folding. Delicate textures, and even volcanic glass, are well preserved at this locality.

The section sampled at M^{c}Diarmid Lake includes parts of at least three flows. None of the flows are magnetic and all are a light to medium green colour. The upper part of the lowermost flow is variolitic and pillowed. These pillows are quite large (up to 1.5 m diameter) with the varioles in layers near the pillow rims and apparently coalesced towards the centres. Hyaloclastite is abundant in the pillow interstices but not so at the flow top, which is quite narrow. The next flow is mostly massive with variolites visible at the contact between the massive portion and a fairly wide hyaloclastitic flow top. The massive portion contains ample spherulites, which are distinguishable on the weathered surface. The spherulites are visible mostly near the top of the massive portion. The top of this unit occurs

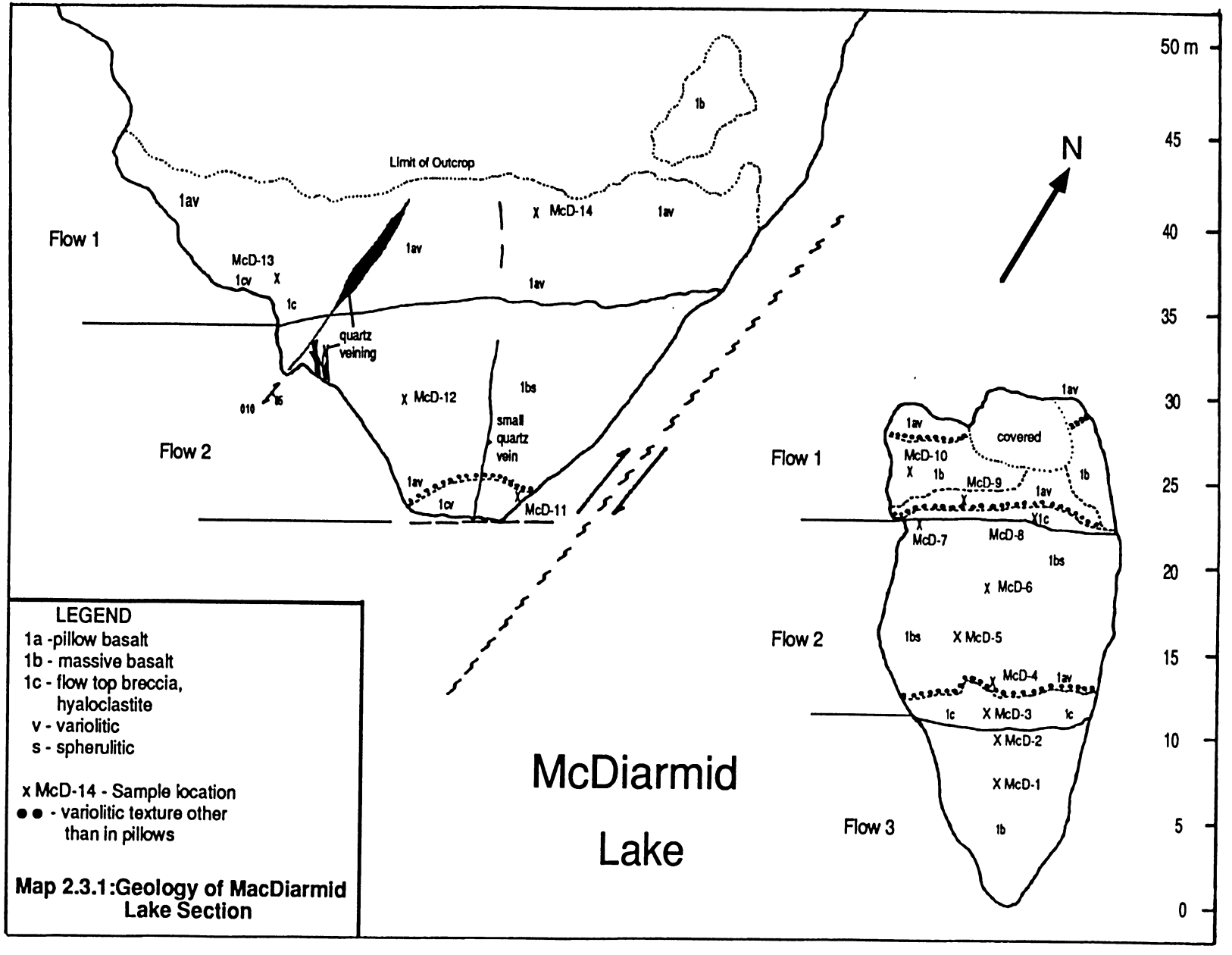

Map 2.3.1:Geology of MacDiarmid Lake Section

at the edge of the lake and the section is continued about 25 m east on a small island.

On the island, the northernmost flow is a repeat of the extreme upper section of the first flow on the mainland. The next flow is also repeated. Here a better view of the extent of spherulites with depth in the flow is found. It appears that the spherulites are well developed only about 3/4 the way through the flow (6.0 m from the hyaloclastite contact). Only the lower part of the uppermost flow on the island is exposed. The exposed section is strictly massive with no other textures noted other than a basal chill margin.

2.3.2 Metamorphism and Alteration

The metamorphic grade appears to be quite low in these outcrops judging by the well preserved original textures. The prevalence of epidote over chlorite suggests that this area may belong to the lower greenschist facies. There is apparent silicification of the matrix of the hyaloclastite breccias which may be due to seafloor alteration. The preservation of this feature could indicate an even lower grade than lower greenschist facies.

3. Petrography

3.1 Harker Lake Area

3.1.1 Petrography of the Harker Lake Section

The mineral assemblage of the Harker Lake area is characteristic of lower greenschist grade and consists mostly of uralite and plagioclase. Also common are chlorite, magnetite, sphene, epidote (and/or clinozoisite), and quartz. Up to 15% quartz and accessory apatite and zircon(?) are present in the more felsic flows of the section.

Uralite is a product of the alteration of pyroxene and is ubiquitous in the Harker Lake section, comprising between 35-50% of any sample. It occurs as large, acicular crystals or irregular masses in the coarse grained parts of flows and stubby, prismatic crystals in the finer grained parts. The uralite is a blue or emerald green to greenish yellow, Fe-rich amphibole. It has low birefringence and, generally, shows no cleavage. Uralite commonly pseudomorphs primary pyroxene textures (Plate 3.1.1).

Plagioclase generally occurs as small laths and locally skeletal or subhedral twinned grains. Its present composition is albite. It is turbid and contains inclusions of chlorite, epidote, quartz and carbonate. Plagioclase spherulites are common in the groundmass of many flows and are essential components of varioles.

Rocks of the Harker Lake section contain up to 10-15% Fe and Ti-rich oxides and leucoxene. These minerals form euhedral, and locally skeletal, crystals in some of the more coarse grained samples and small disseminated blebs in fine grained samples. Rutile is present in some samples, as very narrow, acicular crystals. Ti-rich oxides have been variously altered to leucoxene, along internal lamellae and grain boundaries. Microprobe analyses show that the products of this alteration are very pure magnetite and sphene (Appendix 3.1c).

Chlorite is formed as a result of retrograde metamorphism of uralite and plagioclase. It comprises up to 30% of a rock depending on the extent of alteration. It does not pseudomorph the amphibole but rather forms mottled patches which are generally interstitial to plagioclase, quartz and other groundmass minerals. Epidote occurs disseminated throughout the rocks and in association with fractures and small veins. It rarely makes up more than 3-

Plate 3.1.1: Uralite pseudomorphs of primary mafic minerals, probably pyroxene:
a) hollow, skeletal, acicular grains (sample H-19, PPL, Long side of view is approximately 2x mm),

b) banching and acicular crystals, grown in coalesced varioles (H-5c, PPL, 2 mm),

c) partially or completely enclosing sub-hedral to euhedral plagioclase crystals, sub-ophitic texture (H-9, PPL, 2 mm).


A

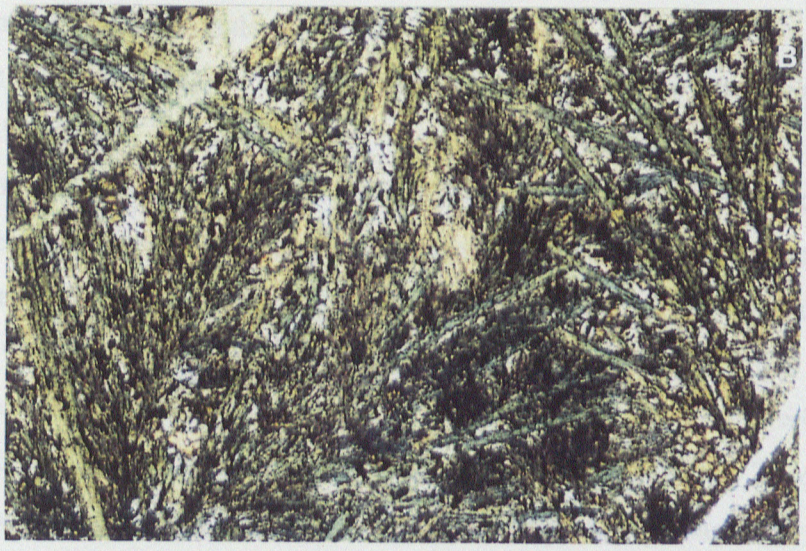
B

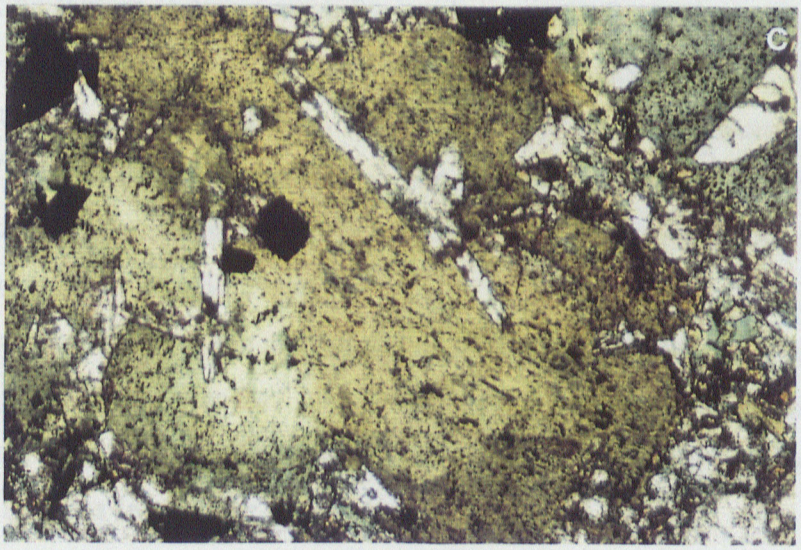
C

5% of the rocks. Quartz is present as scattered grains in most samples, generally as an alteration product of plagioclase. In more felsic flows, some quartz is likely a remnant of the primary mineralogy.

Accessory minerals, apatite and zircon(?), are found in flows of more acidic composition. Apatite occurs as thin, jointed fibres and small prismatic crystals, which are most easily distinguished in large grains of plagioclase or quartz where they stand out due to their high relief. Zircon occurs as small, highly birefringent crystals with high relief can be detected in chlorite where they have a characteristic dark pleochroic halo. These are tentatively identified as zircons although they may be other similar minerals, such as monazite or xenotime (Schandl and Gorton, 1990). The term zircon(?) is used throughout the thesis in reference to these crystals.

The massive parts of flows are homogeneous, dominated by interlocking plagioclase laths and acicular uralite. Plagioclase fan spherulites are common in the groundmass of massive sections of the upper flows. Varioles are characterized by a combination of plagioclase spherulites, dendritic oxides, and acicular or radiating uralite crystals (Plate 3.1.2). The amphibole and oxides are more common in areas of coalesced varioles, such as the cores of pillows. The varioles have sharp boundaries with only minor metamorphic smudging. The matrix to the varioles is generally composed of felted chlorite and uralite with fine grained disseminated oxides. The upper part of many flows contain amygdules. These are filled by chlorite, carbonate, epidote, quartz, pyrite and albite in varying amounts.

Myrmekitic texture is common in this section, especially in the coarser grained parts of flows (Plate 3.1.3). The texture consists of vermicular intergrowths of albite and quartz associated with altered plagioclase grains, with a clear "cap" of quartz commonly present. The development of this texture is interpreted as part of the degradation of plagioclase during metamorphism and not a primary igneous feature such as similar intergrowths between k-spar and quartz common in more acidic rocks.

Small veins observed in the section are usually composed of, in order of abundance, quartz, epidote, calcite and chlorite. Along with some fractures, they commonly have a narrow (1-2 mm), bleached envelope associated with them, formed by the breakdown of uralite and Fe-Ti oxides in the host rock.

Plate 3.1.2: Variole textures:
a) plagioclase spherulites, outlined by fine grained chlorite and leucoxene (H-5a, X-nicols, 2 mm),

b) rectilinear patterns, formed by oxides and, commonly, acicular uralite (H-16, PPL, 2 mm),

c) fern-like uralite, after pyroxene (H-5c, PPL, 1.6 mm).

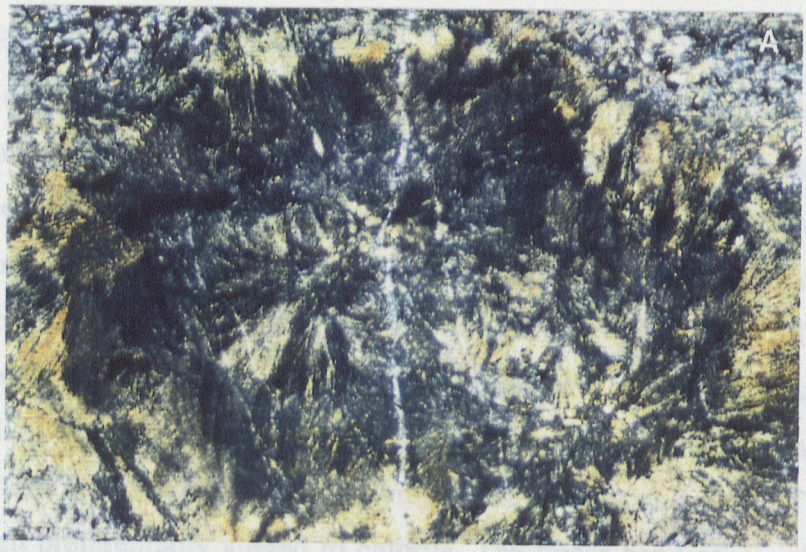
A

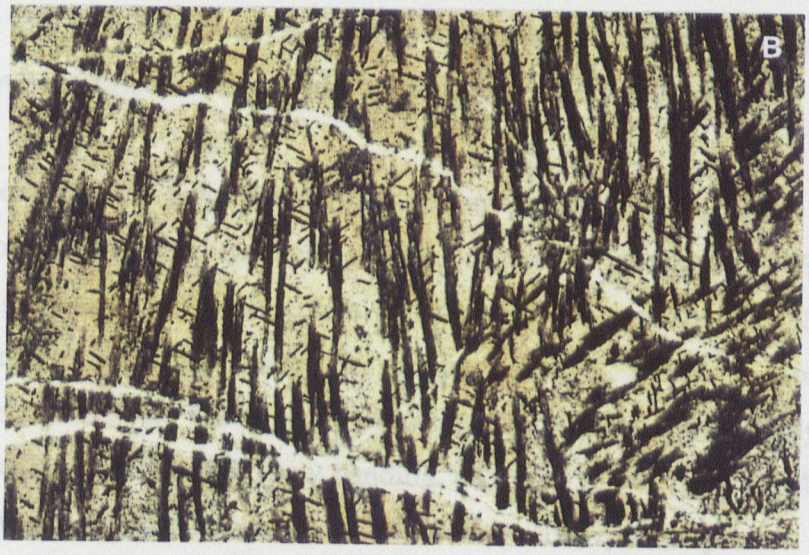
B


C

14+50E Section:

There is a variolitic pillowed flow at the base of the section on Line 14+50E (Map 2.1.1). This flow was sampled in both its pillowed and massive portions (samples H-5 and H-6). The pillowed section of the flow was examined in a series of three thin sections progressing from the margin of a pillow to its core. Near the margin are scattered varioles which increase in concentration and coalesce towards the pillow core. The varioles are dominantly plagioclase near the margin of the pillow and contain several crystal forms including axiolitic and fan spherulites. Towards the coalesced core, they are a mixture of uralite, plagioclase and oxides. In the overlying massive flow, the cores of acicular uralite grains have been preferentially altered to chlorite. The linear band of varioles found in the upper part of this flow (or overlying flow?) is similar in mineralogy and texture to the variolitic pillows described above. This portion of the flow also contains rare plagioclase phenocrysts.

The rock samples from the phyric section (samples H-35, H-36, H-37, H-3) are characterized by plagioclase phenocrysts and the presence of greater than 10% quartz (except in H-3), indicative of their intermediate composition. Commonly, the phenocrysts have formed small clusters, although there does not appear to be, overall, a glomeroporphyritic texture. Quartz phenocrysts found in this section are rounded and partially to completely recrystallized and contain apatite. Flow banding, observed in the field, involved shearing as indicated by rotation of, and deflection of foliation around, quartz eyes.

The three non-variolitic flows at the southern end of the 14+50E trench (samples H-38, H-7, H-8, H-9, and H-10) are relatively coarse grained and have very good preservation of primary subophitic textures (Plate 3.1.1c). Oxides, dominantly Ti-rich magnetite, are abundant, generally comprising 5 to 15% of the rock. There is no evidence of varioles in thin section which is consistent with field observations.

The Cryderman zone occurs at the termination of the 14+50E section. The mineralized zone occupies the upper part of the host flow, so representative samples are from the lower massive part (samples H-39, H-47 and 45722, from DDH 272-85-16). Overall, this flow is very similar to the other non-variolitic flows in this part of the Harker Lake section. No foliation is evident in any of these relatively unaltered samples, despite being less than 10

Plate 3.1.3: Myrmekitic texture, intergrowths of albite and quartz, especially common in coarser grained, more evolved flows (H-12, X-nicols, 2 mm).

Plate 3.1.4: Open plagioclase spherulites in the groundmass of massive basalt, from the Spherulitic Basalt Flows of the Harker Lake section (H-19, X-nicols, 2 mm). These spherulites are not associated with obvious varioles, as are the ones in Plate 3.1.2a, and occur in a relatively coarse grained rock.

Plate 3.1.5: Acicular uralite crystals with variable orientations due to growth of the crystals from scattered nuclei in coalesced varioles (H-16, PPL, 2 mm).

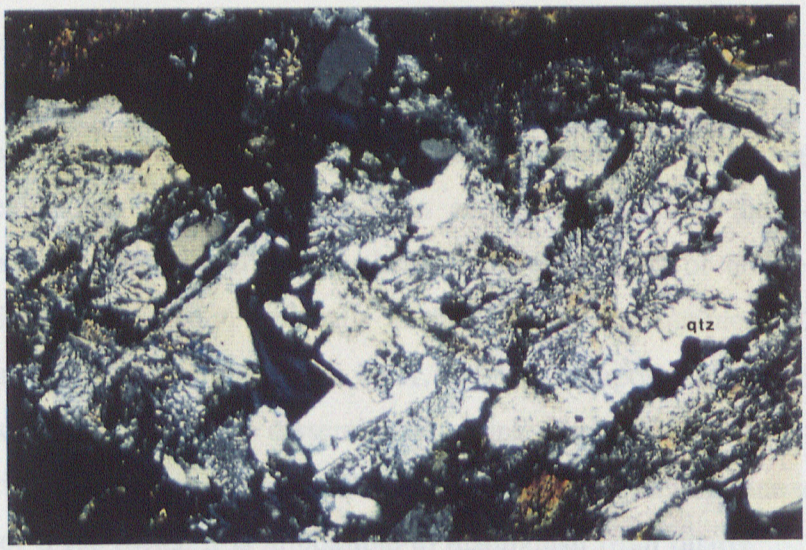
qtz

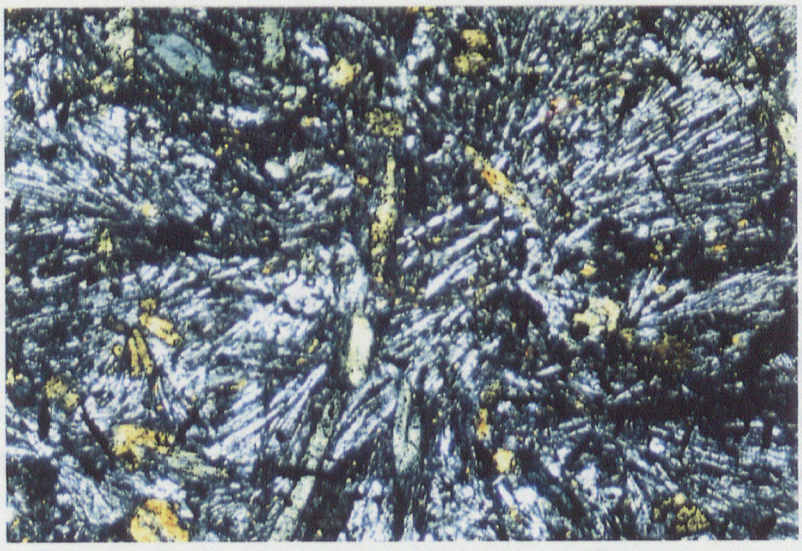

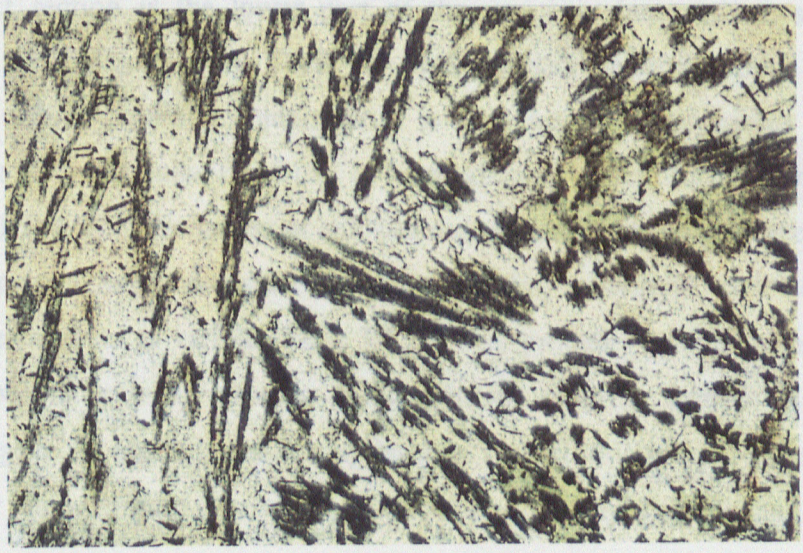

metres from the Cryderman fault.

25+50E Section:

The non-variolitic flows on the 25+50E section (samples H-20 through 24, Map 2.2) have similar textures to their equivalent flows at the south end of the 14+50E section. Overall, these samples are slightly more altered with conversion of uralite and oxides to chlorite and sphene respectively, especially in the upper flows (samples H-22, H-20). The narrow chert, or cherty tuff, unit (samples H-21, H-32) is composed mostly of quartz (about 70%) but includes 20% chlorite as disseminated grains. There is 5-8% of a mineral having some of the optical properties of sphene. Plagioclase may be present but due to the extremely fine grain size of these rocks, it is impossible to distinguish from quartz.

The overlying section of spherulitic basalt is represented, in stratigraphic order, by samples H-19, H-18, and H-17. The first flow has a groundmass that is dominated by open fan spherulites of plagioclase (Plate 3.1.4). Uralite occurs as acicular crystals with epidote-chlorite altered cores (originally hollow?, Plate 3.1.1a). In addition, uralite occurs, with oxides, as fine branching crystals in the matrix and interstices of the plagioclase spherulites. In the massive lower portion of the second flow, plagioclase occurs as randomly oriented laths rather than spherulites. The laths are commonly skeletal, have curved outlines, and occur in a very fine grained groundmass made up of altered glass(?), chlorite, sphene, opaques and minor quartz. This texture is very similar to samples H-27 and H-26 from the Line 28+00E area.

The next section is the lower part of the variolitic intermediate series of flows (samples H-16, H-15, and H-40). These are fine grained, heterogeneous, brecciated and variolitic rocks which generally contain close to 20% quartz. The varioles are commonly coalesced and contain a peculiar dendritic, or herringboned, pattern formed by the uralite and oxides (Plate 3.1.2b). The orientation of acicular rods of uralite in the coalesced parts is quite striking. The crystals have consistent orientation within individual varioles but different orientations from variole to variole (Plate 3.1.5). This probably relates to the formation of these disequilibrium crystals, growing from scattered centres. Sample H-15 is from a relatively homogeneous block in the blocky breccia. Overall this sample has a darker colour due to a greater concentration of uralite and chlorite and finely disseminated magnetite and

Plate 3.1.6: Hyaloclastite unit. a) Perlitic fracture in breccia fragments is well preserved (H-42, PPL, 3 mm). b) Banded fragment, consisting of magnetite (dark) and altered plagioclase (light) layers. Relict spherulites are visible in plagioclase layers (H-14, X-nicols, 3 mm).


A

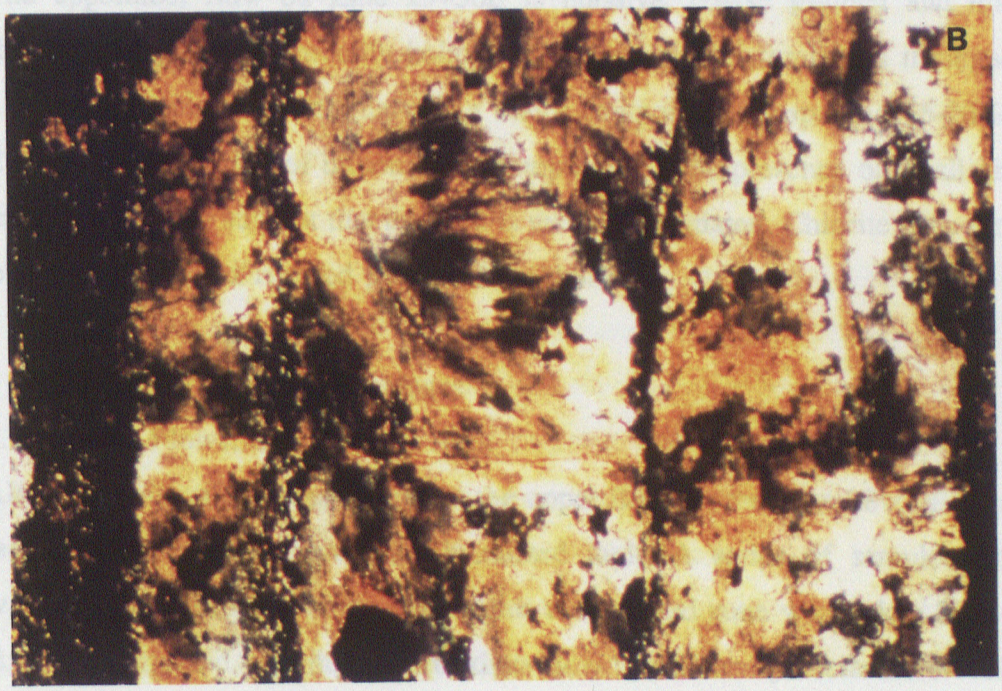
B

sphene. The sample has a very similar overall texture to the coalesced varioles described above. The flowbanded, spherulitic material from the interstices of the blocky breccia (sample H-40), is similar to the coalesced varioles as well.

The hyaloclastite flow is heterogeneous in thin section and most original textures are well preserved. The breccia clasts have an altered glassy margin composed of plagioclase, quartz and carbonate and perlitic factures are common (Plate 3.1.6a). The clast interiors are dominantly fine grained, felted chlorite and randomly oriented needles of magnetite. The breccia matrix is composed of extremely fine grained quartz, albite and minor carbonate and abundant shards of altered glass. The larger banded fragments which characterize the hyaloclastite on the outcrop scale are composed of alternating layers of magnetite and altered plagioclase. Relict spherulites are evident throughout the plagioclase-rich layers (Plate 3.1.6b). The massive portion of the hyaloclastite flow (sample H-41) has flowband laminations visible in the hand specimen. Similar layering is found in the chilled base of flows in this part of the section (e.g. H-56). These bands are due to variable concentrations of magnetite which is disseminated throughout imparting a dark colour Quartz is a major component of the rock (20%). Carbonate occurs in the groundmass of this rock especially in certain layers, though no particular reason for this preference was determined.

The uppermost flow on Line 25+50E is massive, coarse grained and magnetic. Euhedral magnetite grains, commonly hollow or skeletal, are disseminated throughout the rock. As in the hyaloclastite unit, quartz is a major component, comprising 15-20% of the rock and suggesting that it is of intermediate composition. The presence of small grains of apatite and zircon(?) also suggest that the rock is well differentiated. Chlorite is an important component, forming quartz rimmed patches throughout.

3.1.2 Alteration Assemblages

1. Variolitic Flows, Line 28+00E Area

Alteration mineralogy was studied in the upper flows in the Line 28+00E area (Map 2.1.2) associated with a crosscutting, mineralized fault. A series of samples from the relatively unaltered host rock into the core of this mineralized zone were taken from two of the flows; the fine grained, variolitic intermediate flow below the hyaloclastite breccia, and,

Table 3.1.1: Modal mineralogy (as estimated volume percent) associated with alteration in the Variolitic Intermediate Flow, L28+00E area, Harker Lake section.

	H-27 (least alt'd)	H-26 (mod. alt'd)	H-25 (most alt'd)
uralite	10		
chlorite	30	25	tr
plagioclase	35	45	45
quartz	10	10	30
sphene/leucoxene	tr	3-5	2-3
epidote	1-2		
carbonate	5	3	5-8
magnetite	5	8-10	8-10
hematite			1-2
pyrite		1-2	1-2
apatite			2
Mg riebeckite			tr
talc			2-3

the thick, medium to coarse grained, massive intermediate flow which overlies the hyaloclastite. There is no evidence of foliation in any of the rocks in the study area.

Within the fine grained, variolitic intermediate flow three samples were taken. These are, in order of least to most altered, samples H-27, H-26, and H-25. Sample H-27 (13 m from the altered zone) represents the least altered sample typical of the local metamorphic facies (Table 3.1.1). There is more chlorite than uralite and about 5% carbonate present indicating some minor alteration related to a small splay from the mineralized zone which passes near (3 m) the sample location. Sample H-27 also contains 2-3% amygdules, something not found in the other samples in this alteration profile. There is no visible difference between samples H-26 and H-27 in hand sample. In thin section, however, sample H-26 (5 m from the zone) is obviously a lighter colour due to the elimination of the amphibole and some chlorite component and the paler green colour of the chlorite present. There is a slight increase in albite content contributing to the lighter colouration. As a result of further alteration, sample H-25, in the core of the zone, has an insignificant mafic component and would be colourless in thin section if not for oxide minerals which are more common than in the previous sample. Whereas the only significant opaque mineral in sample

H-27 is magnetite, the opaque mineralogy in H-25 consists of mostly magnetite with lesser hematite and pyrite. There has been significant increase in quartz and carbonate as well as the appearance of apatite, Na amphibole and talc in sample H-25.

Texturally, the rock has changed with progressive alteration from a very fine grained mix of interstitial chlorite, branching uralite and plagioclase laths to a medium grained, recrystallized mixture of myrmekitic albite and quartz, large turbid and commonly twinned albite grains, plus carbonate and opaques. Several generations of tiny quartz-carbonate veins cut the section. These usually have pyrite and Fe-oxides associated.

Four samples were studied in the upper massive flow where the crosscutting mineralized zone is widest and most intense (Map 2.1.2, Table 3.1.2, Plates 3.1.7 and 3.1.8). These samples range from the least altered H-29, to H-30 at the edge of the visually altered area, to H-31 in obviously altered and mineralized but relatively homogeneous rock, to H-55 which was taken near the core of the altered zone within a highly mineralized quartz stockwork. Sample H-55 was studied in three parts (Figure 3.1.1); the altered and mineralized wall rock, the intensely altered narrow (1 cm) envelope to the veins, and, the stockwork vein material itself.

Sample H-29 is a medium grained, homogeneous mixture of weakly altered acicular uralite, myrmekitic albite and quartz, altered plagioclase, magnetite/sphene, and minor amounts of epidote, carbonate and sphene. Magnetite grains are commonly associated with uralite, outlining the acicular crystals. In H-30, the uralite is largely replaced by chlorite and sphene whereas magnetite grains still outline the relict crystals. Alteration of plagioclase to chlorite and carbonate is more pronounced. Chlorite is lighter green and shows anomalous purple birefringent colours indicating a less Fe-rich composition than in H-29 (p. 133, Shelley, 1979). Epidote is absent whereas the amount of carbonate (calcite) has increased.

The most noticeable change between H-30 and H-31 is the elimination of almost all mafic minerals within the alteration zone. About 10% chlorite remains which is very lightly coloured indicating further depletion of iron. This is corroborated by the presence of anomalous brown birefringent colours in some of the chlorite, especially in association with oxides or pyrite. Magnetite content has also been reduced slightly to 8-10%. Trace hematite and 1-2% pyrite are present. Myrmekitic texture is more prevalent in H-31, with a coincident

Plate 3.1.7: Progressively altered samples from the alteration study in the upper massive flow. Modal mineralogy for the samples is summarized in Table 3.1.2.
a) Least altered sample, H-29, (PPL, X-nicols, Long axis of photo, 2 mm).

b) Strongly altered sample, H-31 (PPL, X-nicols, reflected light (RL), 2 mm). Only minor carbonate (high birefringence) is present.

c) Vein envelope, H-55a (PPL, X-nicols, RL, 2 mm). Rock is silicified and recrystallized resulting in the elimination of myrmekitic texture. Carbonate is present in only trace amounts.

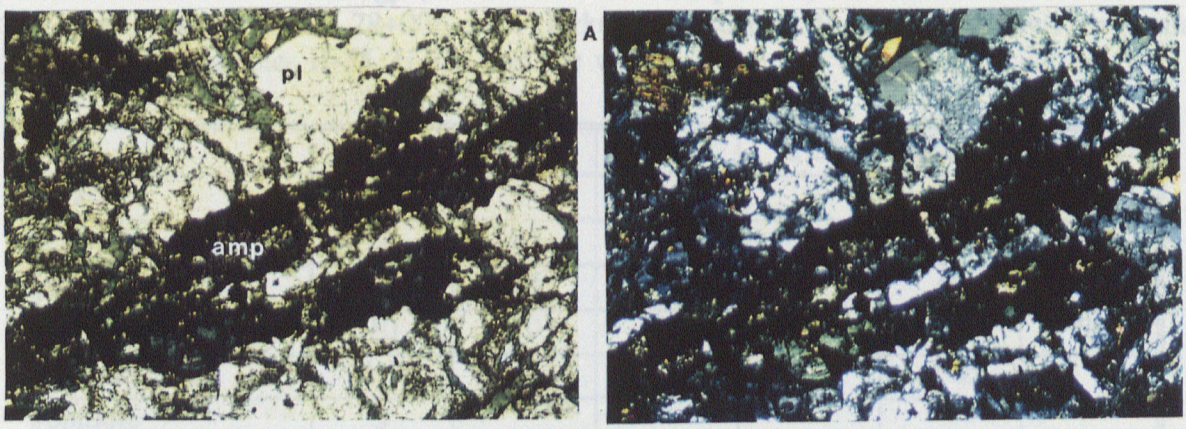
A
pl
amp

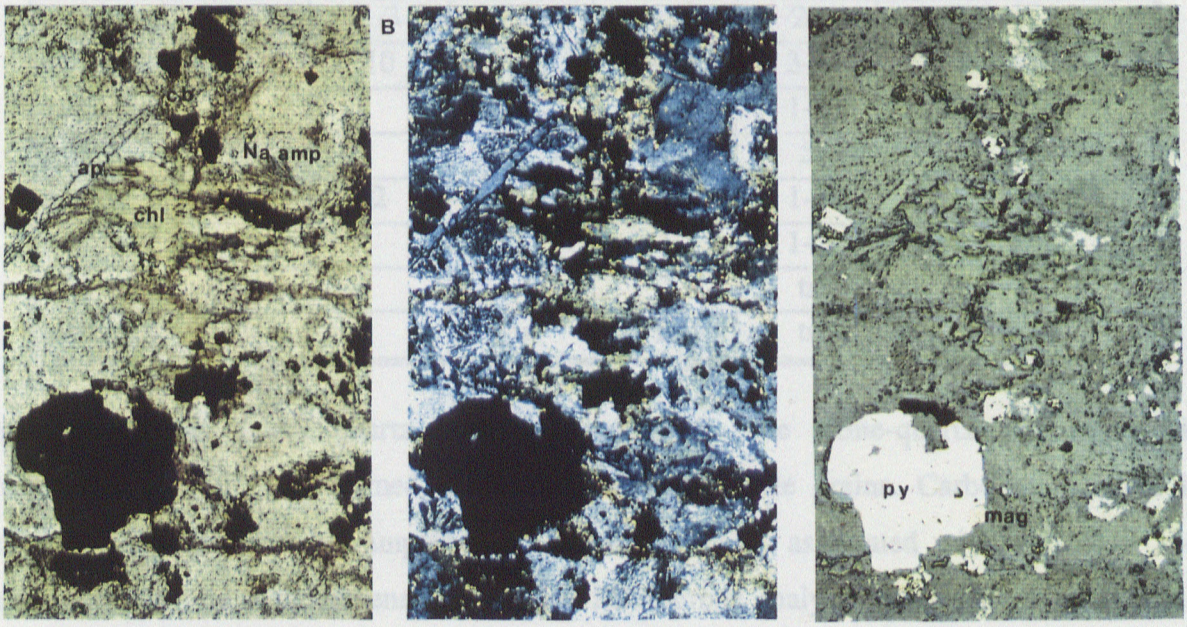
B
ap
Na amp
chl
py
mag

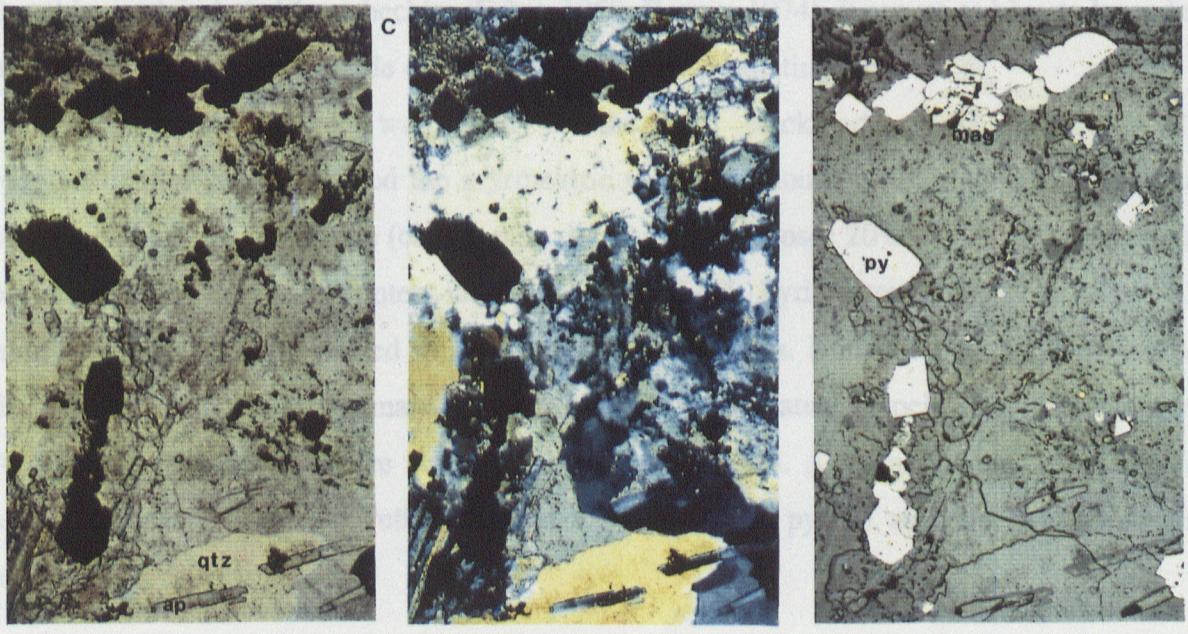
C
qtz
ap
mag
py

Table 3.1.2: Modal mineralogy (as estimated volume percent) associated with alteration of the Upper Massive Flow, L28+00E area, Harker Lake section. Figure 3.1.1 shows the spatial relationship of samples H-55, H-55a and the vein.

	H-29	H-30	H-31	H-55	H-55a	Vein
uralite	15	5				2-3 ?
chlorite	20	25	10	5	tr	1-2
plagioclase	35	45	45	45	40	
quartz	10	10	15	15	30	65
sphene/lcxn	1-3	2	1	1-2	1-2	
epidote	3					
carbonate	1-3	5	15	20	10	10
magnetite	10	8	8-10	3-5	5-8	2-3
hematite			tr	1-2	2	3-5
pyrite			1-2	5	5-8	10
apatite	2	tr-1	1-2	1-2	2-3	
Mg riebeckite			1	1-2	tr-1	
talc				tr		2-3
zircon(?)		tr	tr	tr		

increase in the modal quartz content from H-30. The albite-quartz groundmass is recrystallized with well formed, commonly twinned albite grains. Carbonate content is substantially increased. Na amphibole is present in H-31, associated with carbonate, and apparently formed at the expense of chlorite. Microprobe analyses (Appendix 3.1a) indicate that this amphibole is Mg-riebeckite (Ernst, 1960; Brown, 1974). It occurs as blue to lavender pleochroic grains with a single cleavage or as fibrous, radiating sheaves.

Within the altered wall rock of the core stockwork (H-55, Figure 3.1.1) recrystallization has eliminated the myrmekitic texture, although twinning is still visible in some albite grains. Carbonate (calcite plus dolomite?) composes 20% of the rock and pyrite 5% whereas the magnetite content has decreased to 3-5%. Pyrite occurs mostly as large (1-3 mm) crystals and blebs related to fractures and small veins. It also occurs as fine grained disseminations in the groundmass. In places, pyrite is intimately associated with magnetite. Apatite and Na amphibole are common accessory minerals. A minor amount of very pale chlorite is present. Traces of rutile, talc (usually surrounding pyrite), and zircon(?) have been identified in this sample.

Plate 3.1.8: Sample H-55, from the core of the alteration zone in the Upper Massive Flow, L28+00E area. See sketch below for details.

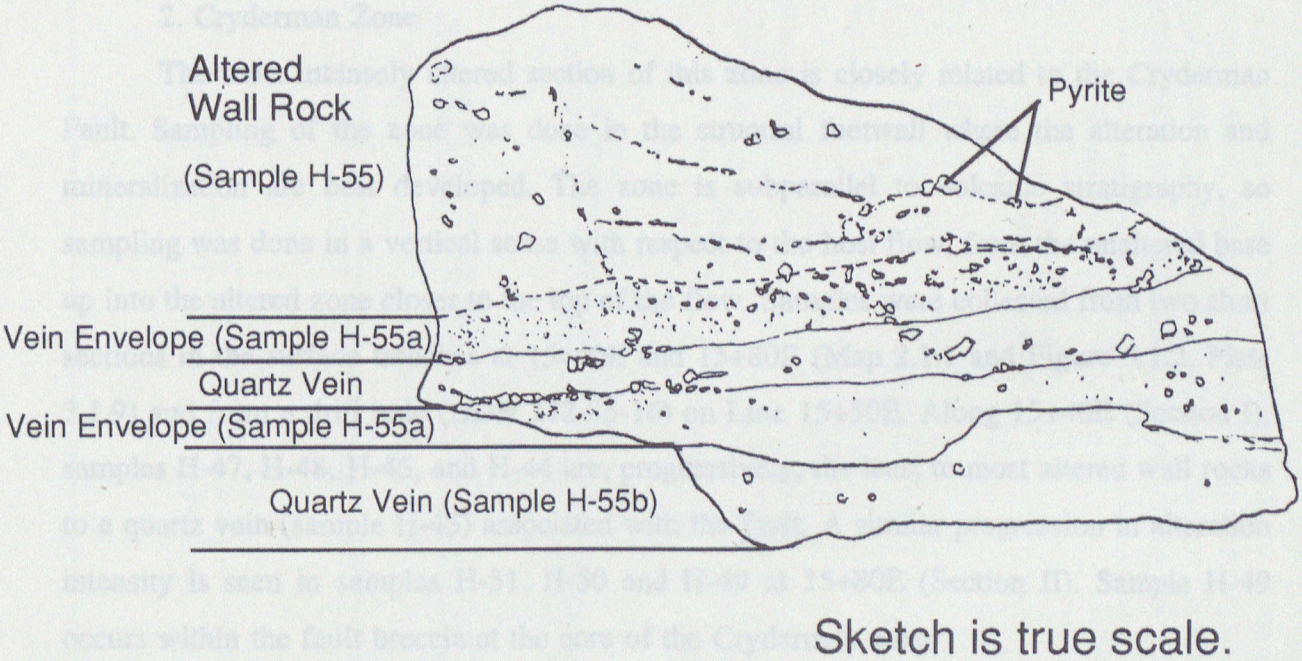

Figure 3.1.1: Sample H-55 from the core stockwork area of the alteration zone in the Line 28+00E area (see also Plate 3.1.x). Sample includes stockwork veins, the altered envelope to the veins, and the highly altered wall rock . Pyrite distribution (speckles) changes from the altered wall rock to the vein envelope to the vein. Mineralogy of the zones is summarized in Table 3.1.2.

A sharp boundary exists between the altered wall rock and the envelope to the vein in sample H-55. The envelope is distinguished from the wall rock by its lighter colour and the fact that pyrite occurs mostly as disseminated blebs. The quartz-albite groundmass is further recrystallized evident by the sutured nature of most grain boundaries, especially those of plagioclase and quartz. Considerably more quartz and less carbonate are present. Apatite is more common (2-3%) in the envelope than the wall rock whereas there is less Na amphibole. Magnetite and pyrite account for about 15% of the rock. Their complex intergrowths, and the fact that either mineral can be found enclosed in the other, make any interpretation of their paragenetic relationship questionable. A minor amount of hematite is present as anhedral disseminations.

The vein consists dominantly of quartz (65%) which has numerous minute inclusions, frequently in a zonal patterns. Pyrite is an important component of the vein, occurring mostly along the margins. Carbonate is scattered throughout the vein, interstitial to the quartz. Minor amounts of chlorite, magnetite, actinolite and white mica are also present. Late specular hematite occurs as large blebs and in fractures. Pyrite and magnetite occur together, in places rimmed by sphene. Pyrite is also rimmed by white mica in parts of the vein.

2. Cryderman Zone

The most intensely altered section of this zone is closely related to the Cryderman Fault. Sampling of the zone was done in the structral footwall where the alteration and mineralization are best developed. The zone is subparallel to volcanic stratigraphy, so sampling was done in a vertical sense with respect to the host flow, from the unaltered base up into the altered zone closer to the top of the flow. Samples were collected from two short sections in the surface trenches at 15+40E and 15+80E (Map 2.1.1 and Figure 3.1.2, Plate 3.1.9) and from a drill hole (DDH 272-85-16) on Line 15+50E. Along 15+40E (Section I), samples H-47, H-48, H-45, and H-44 are, progressively, the least to most altered wall rocks to a quartz vein (sample H-43) associated with the fault. A similar progression in alteration intensity is seen in samples H-51, H-50 and H-49 at 15+80E (Section II). Sample H-49 occurs within the fault breccia at the core of the Cryderman zone.

The unaltered flow base has been described above (section 3.1.1) and is represented by samples H-39, H-47 and 45722. The mineral modes are summarized in Table 3.1.3.

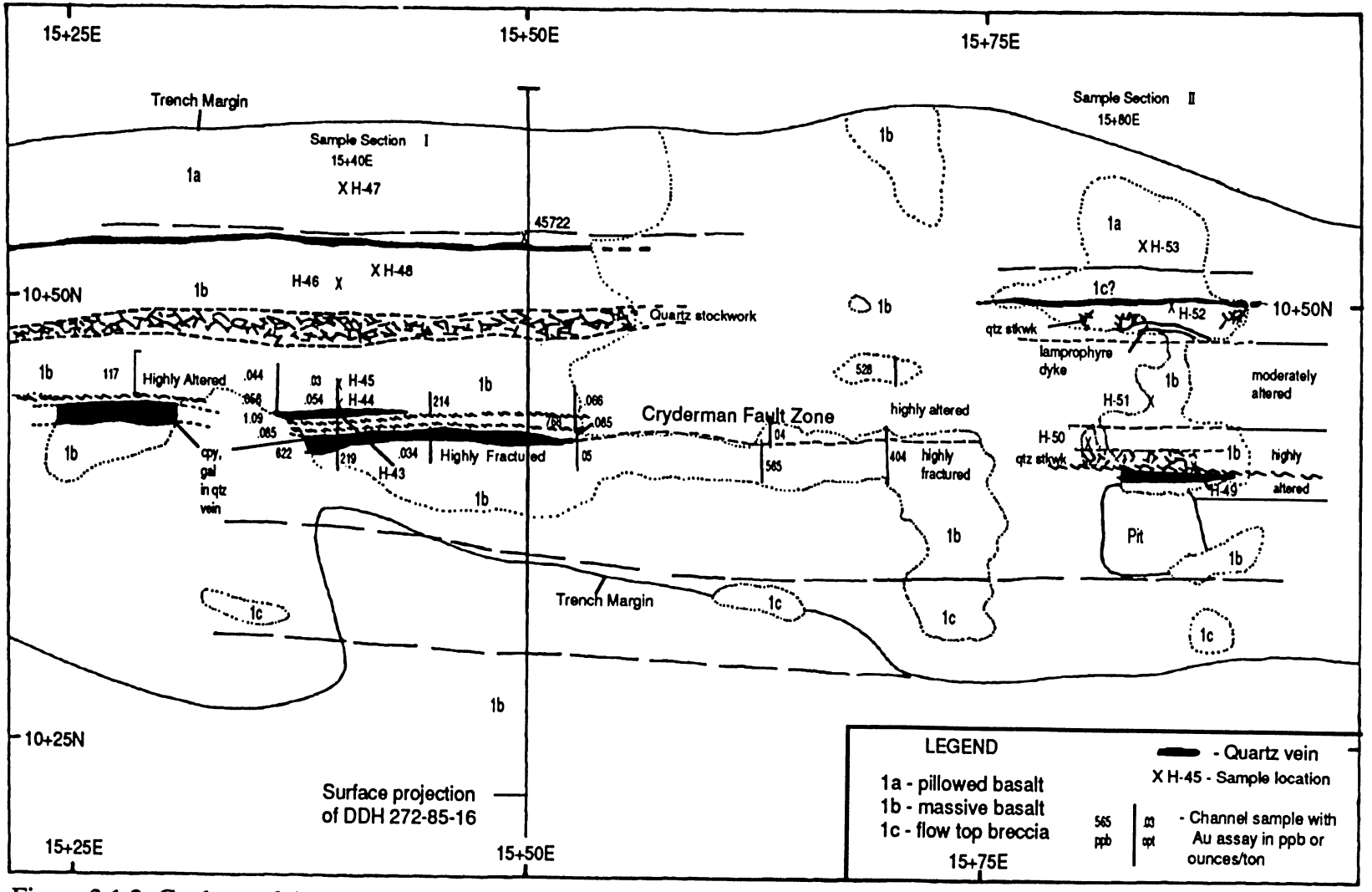

Figure 3.1.2: Geology of the Cryderman Zone in the vicinity of the sample sections used for the alteration study. Figure contains assay results from previous exploration work which give an indication of the intensity of mineralization and the spatial relationship of the samples to alteration and mineralizaion. The large quartz veins dominate the core of the zone, although these are generally unmineralized with respect to Au, especially those which contain chalcopyrite and galena. Grid markings (at border of figure) are 25 metres apart. Grid north is 335°.

Table 3.1.3: Modal mineralogy (as estimated volume percent) associated with the alteration of Non-variolitic Flows in the Cryderman Zone, Harker Lake section. Alteration increases toward the vein (H-43).

	45722	H-48	H-51	H-45	H-44	H-49	H-43
uralite	40	40	10				
chlorite	2-3	5	20			1	tr
plagioclase	40	40	40	30	25-30	25	
quartz			2	5	5-10	15	90
sphene/lcxn	5	5	5	2-3	tr		tr
carbonate	1-2		5-8	35	30-40	35	2-3
epidote		1					
magnetite	5-8	5-6	5-8	2	3-5		
hematite		2-3	5-8	18	15-20	15	2-3
pyrite		tr-1	1	3	3-5	5	1
chalcopyrite				tr	tr	1-2	tr
galena						1	

Generally, the host flow is a relatively homogeneous mixture of plagioclase and amphibole, or chlorite, and 5-10% disseminated Ti-rich magnetite. Initial alteration resulted in the breakdown of amphibole to chlorite and magnetite to sphene, as well as the formation of hematite and carbonate (e.g. sample H-51). Both hematite and magnetite occur as disseminated grains. The hematite is smaller and anhedral and also rims magnetite in veinlets and in the groundmass. There is less than 1% pyrite and it is mostly associated with veinlets, but also occurs as disseminations. The birefringent colour of chlorite is dominantly brown at this stage, indicating that it is relatively more Mg than Fe-rich.

Moderate to strong alteration is represented by samples 45721 and H-45 (Table 3.1.3). Primary textures, such as plagioclase spherulites, are still visible in the rocks. All amphibole has been eliminated although chlorite is still a major component. The abundance of hematite in these samples seems to be inversely related to the chlorite content of the rock. Hematite content reaches 20%, in sample H-45. This concentration is observed to the core of the mineralized zone. Significant reduction of plagioclase abundance is coincident with a large increase in the carbonate content to 25-30%. Up to 3% pyrite occurs as fine disseminations and as blebs in veinlets. Magnetite is disseminated in the groundmass and commonly

Plate 3.1.9: Sample sequence from least to most altered in the Cryderman Zone (see Figure 3.1.2). Modal mineralogy is summarized in Table 3.1.3a and 3.1.3b.
a) Least altered sample, 45722, from DDH 272-85-16 (PPL, X-nicols, 2 mm). Opaques are dominantly magnetite.

b) Strongly altered sample, H-45 (PPL, X-nicols, RL, 2 mm). Open plagioclase spherulites are visible despite the intensity of alteration. Opaques are dominantly hematite.

c) Highly altered and mineralized sample, H-44, including late carbonate-quartz vein, at the edge of the central fault/vein zone (PPL, X-nicols, RL, 2 mm). Note the relative lack of hematite in the rock's groundmass near concentrations of pyrite.
d) Over page.

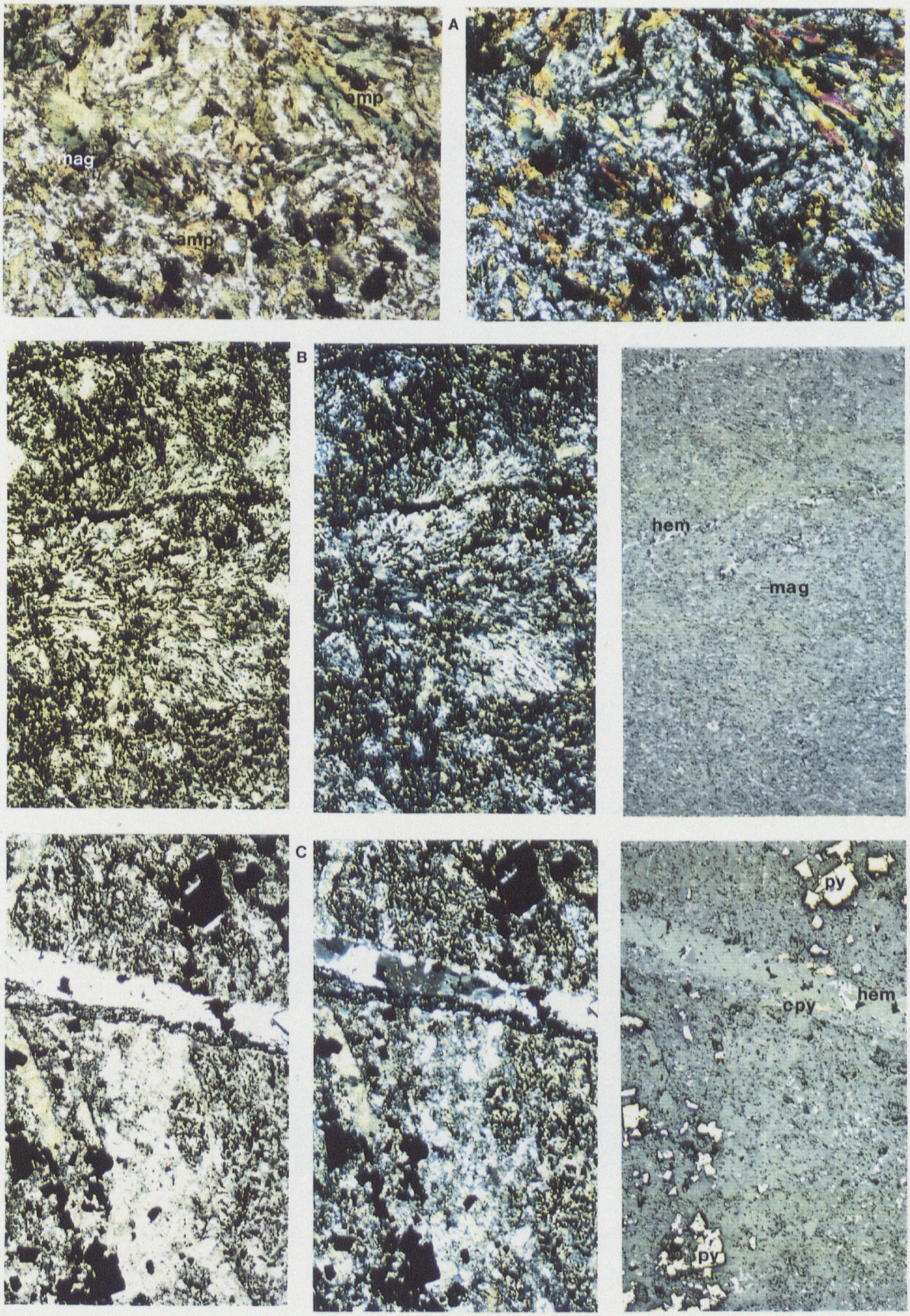
A
amp
mag
amp
B
hem
mag
C
py
cpy
hem
py

Plate 3.1.9, con't: Sample sequence from least to most altered in the Cryderman Zone (see Figure 3.1.2). Modal mineralogy is summarized in Table 3.1.3a and 3.1.3b.
d) Brecciated sample, H-49, from the central fault zone (PPL, X-nicol, RL, 2 mm). Opaques consist mostly of specular hematite and pyrite.

Plate 3.1.10: Chalcopyrite and galena in quartz-rich part (vein material?) of breccia matrix in H-49 (RL, 2 mm).

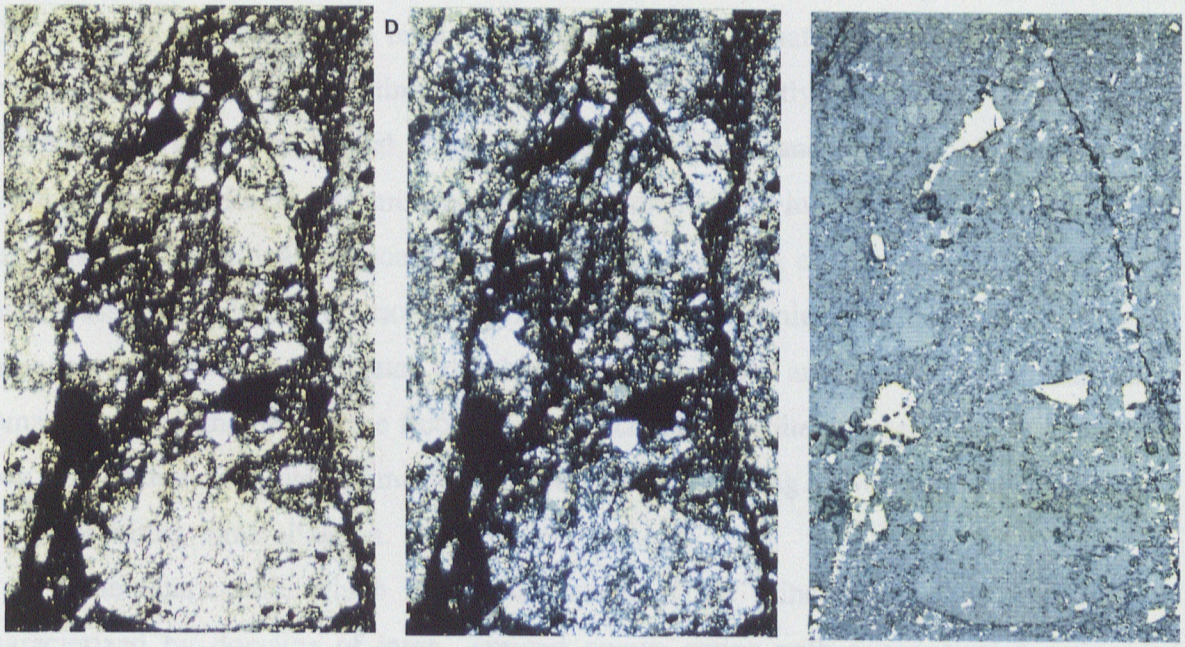
D

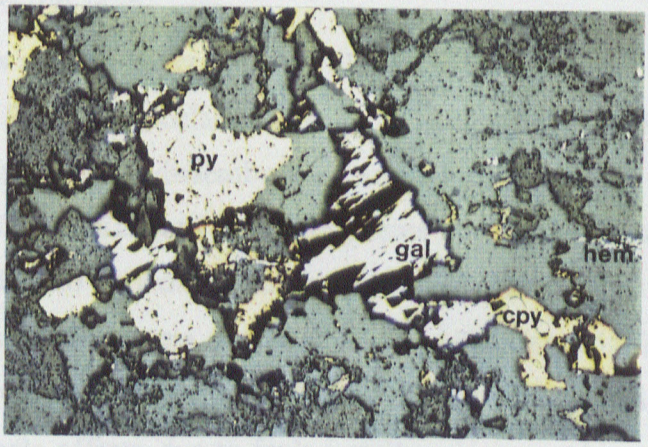
py
gal
hem.
cpy

associated with pyrite. Locally, hematite replaces both pyrite and magnetite. Trace amount of chalcopyrite is present, as tiny (0.1 mm) blebs in small crosscutting veinlets and fractures.

On the border of the central quartz vein, alteration is quite strong (samples H-44, H-50). Here, all the chlorite has been eliminated leaving no mafic minerals and the primary textures of the rock are indistinguishable. The rock is mostly composed of a mixture of carbonate and albite. In general, it has about 20% hematite and 5% each of magnetite and pyrite. Hematite is finely disseminated throughout the rock giving it a dark colour. Up to 10% quartz is found mostly as crosscutting veinlets also containing carbonate. Pyrite is present as small masses or pods, and is associated with fractures and veinlets. Pyrite masses and quartz-carbonate veinlets have associated bleached envelopes which are the result of breakdown of hematite and magnetite and the flooding of quartz and/or albite and carbonate into the wall rock. Brecciation of pyrite and magnetite is common, indicating movement on the Cryderman Fault postdating mineralization.

The quartz vein which marks the centre of the mineralized zone at 15+40E is characterized by domains of large, strained quartz grains with tiny inclusion trains and fractures, separated by highly brecciated, fine grained sections. The fine grained material shows signs of recrystallization such as sutured grain boundaries. The vein also contains minor interstitial carbonate and chlorite. Pyrite, and trace chalcopyrite, are found as extremely fine grained disseminations throughout the rock but especially in the brecciated sections. Minor amounts of specular hematite is found in fractures throughout the vein. In addition, there are traces of zircon(?) in the vein.

Sample H-49 is a highly brecciated and altered rock, the matrix consisting largely of quartz and hematite. Relict plagioclase laths are distinguishable in some of the altered fragments. Pyrite occurs as both disseminations and large, brecciated masses. Hematite is present as fine grained disseminations in the fragments and as aggregates and smears in the breccia matrix. There is also very minor chalcopyrite and galena interstitial to quartz grains in quartz-rich domains of the breccia matrix (Plate 3.1.10). Magnetite is not present in this rock. There is ample evidence of brecciation, several sections of "milled" (fine grained) rock and numerous small scale offsets, due to fault activity which postdates mineralization.

Several large milky quartz veins are found within the Cryderman Zone. These veins

appear to be quite late, are not necessarily related to the strongest alteration or mineralization in the zone and do not have significant gold mineralization. Sample H-43b is from a vein within the hanging wall of the Cryderman Fault at 15+40E. It is composed of 80% quartz with minor carbonate and chlorite. It contains about 5% combined chalcopyrite, specular hematite, lesser amounts of galena and trace magnetite and pyrite. The chalcopyrite and galena occur interstitially to the quartz and chalcopyrite is replaced locally by hematite and malachite.

3.2 Dome Mine Area

3.2.1 Petrography of the Vipond Subgroup

The mineral assemblage in the Dome Mine area reflects stronger regional retrograde alteration of the original greenschist metamorphic facies mineralogy than at Harker Lake. In general, the assemblage consists of plagioclase, chlorite, carbonate, quartz, magnetite/sphene, and epidote. The extreme prevalence of chlorite over amphibole and the presence of significant carbonate are typical of the mineral assemblages. Otherwise, the mineral assemblages are similar to those at Harker Lake. Penetrative foliation is present in most areas, and is generally more pronounced at the Dome Mine.

Plagioclase is the most important component of the lesser altered rocks in the Dome Mine area. It is invariably altered to a combination of albite, carbonate, chlorite, epidote and quartz giving it a turbid appearance. Original textures are usually not preserved and twinning is not commonly observed. The next most common mineral is chlorite. The chlorite does not pseudomorph the the amphibole from which it is dominantly derived, but rather occurs interstitial to plagioclase-quartz-carbonate domains. It is commonly wispy in appearance, due to the penetrative foliation in these rocks (Plate 3.2.1a). The third important mineral in the Dome Mine area assemblages is carbonate, normally calcite. However, close to mineralized zones (including most samples examined from the Dome Mine) dolomite dominates over calcite. Carbonate normally occurs as small grains scattered throughout the rocks but may also be closely associated with small crosscutting veins. Ti-rich magnetite, which is especially noticeable in coarse grained samples, occurs in concentrations up to 10%. In general, this

Plate 3.2.1: Mineral textures in the Dome Mine area. a) Highly foliated chlorite wrapping around varioles in the Lower Spherulitic Flow (D89-01, PPL, 2 mm).
b) Tourmaline grains in groundmass of the Broken Spherulitic Flow, pleochroic colours indicate the Fe-rich variety, schorl (D89-37, PPL, 0.5 mm). c) Altered exsolution lamellae of Ti-rich oxide in magnetite grains, from the 99 Flow (D89-21, PPL photomicrograph, 2 mm; RL photomicrograph of area in dashed box in previous picture, 0.5 mm).

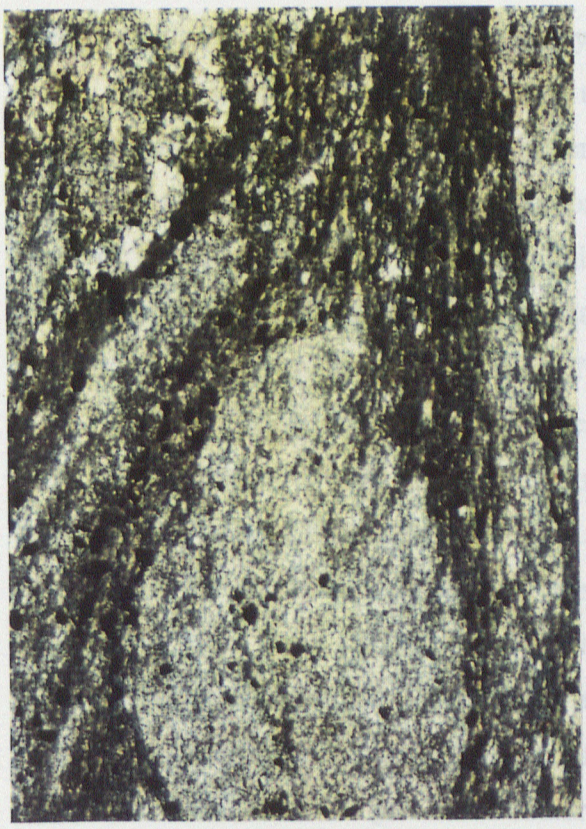
A


B

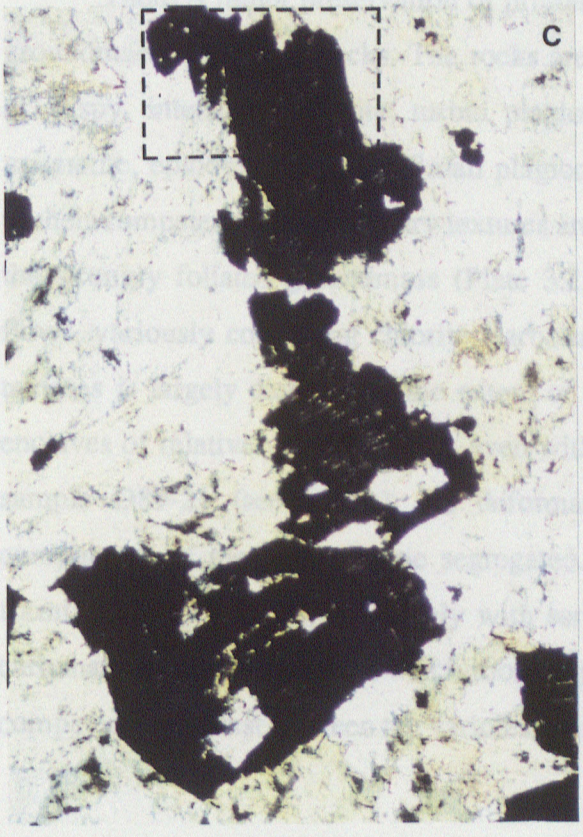
C

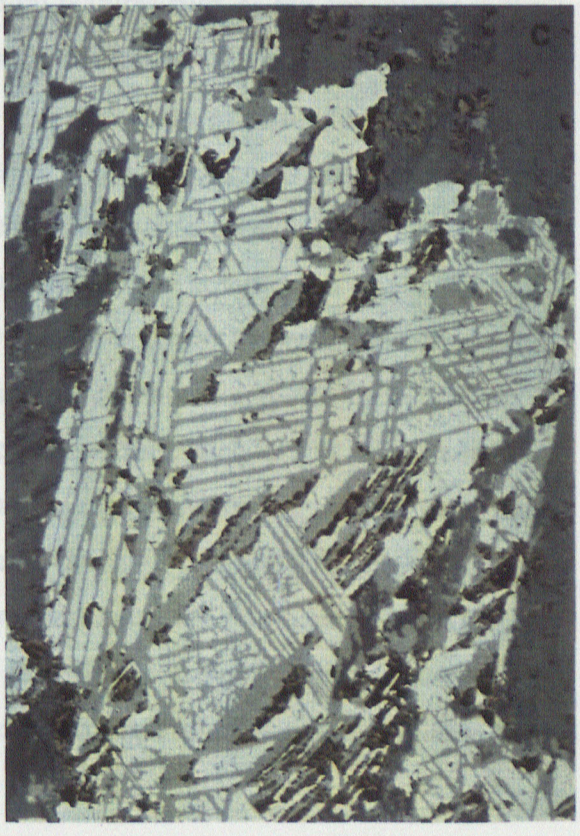
C

mineral has undergone retrograde alteration, resulting in development of pure magnetite and sphene which pseudomorph the original crystal (Plate 3.2.1c).

Quartz is present in most rocks of the volcanic sequences in the Dome Mine area. Generally, the quartz occurs as small, scattered grains in the groundmass of rocks, apparently as an alteration product. It is a major component, occurring as large clear grains, in the upper flows of individual volcanic cycles, including the Lower Spherulitic Flow (LSPL) and the V10 subunit, and in the intermediate interlayers of the V8 subunit. These quartz rich units also contain accesssory apatite and zircon(?).

Epidote is more common in the Porcupine Paymaster section than in the Dome Mine. It occurs as scattered grains, in concentrations up to 2-5%, especially common in flow tops and vesicular parts of flows. Tourmaline is another fairly common mineral in the section. It is especially noticeable in rocks of the Dome Mine where it is associated with metasomatized rocks rather than those affected by regional metamorphism alone. Tourmaline commonly occurs as large prismatic grains with blue-green to pink pleochroism, indicative of the Fe-rich variety, schorl (Plate 3.2.1b). This was confirmed by microprobe analysis (sample D89-25, Appendix 3.1e). Sericite is present in minor amounts in some weakly metasomatized rocks.

There is minor preservation of primary textural features such as fan spherulites in the groundmass of massive rocks. The rocks are normally composed of a homogeneous pattern of wispy, interstitial chlorite, turbid plagioclase, and carbonate grains with disseminated magnetite, epidote and quartz. Small plagioclase laths in the groundmass are common. Due to their competent nature, primary textures are more commonly preserved within varioles than the strongly foliated groundmass (Plate 3.2.2). Amygdules are common in upper parts of flows, variously containing chlorite, carbonate, pyrite and epidote. Preservation of primary textures is largely dictated by the extent of deformation present in a rock. There are small enclaves of relatively pristine rock, even within the Dome Mine, such as that represented by sample D89-21 (see below). As deformation and alteration increase in intensity the components of the rock become segregated. Chlorite becomes progressively more foliated forming wispy partings, commonly with sericite, around lensoidal domains of plagioclase-carbonate-quartz. Foliation is much more apparent in variolitic samples, possibly due to the competency contrast between the varioles, composed of plagioclase, carbonate and quartz, and

Plate 3.2.2: Textures common to the varioles in the Vipond Subgroup. a) Skeletal plagioclase grains, particularly well preserved in this example from the Porcupine Paymaster section (9831, PPL, 1.6 mm). b) Dendritic oxide crystals, commonly altered to leucoxene as in this example, in the groundmass of a variole, Key Flow, Dome Mine (D89-08, PPL, 0.5 mm). c) Plagioclase spherulites, in this case centred on a skeletal plagioclase grain, also from the Porcupine Paymaster section (9831, PPl and X-nicols, 1 mm).

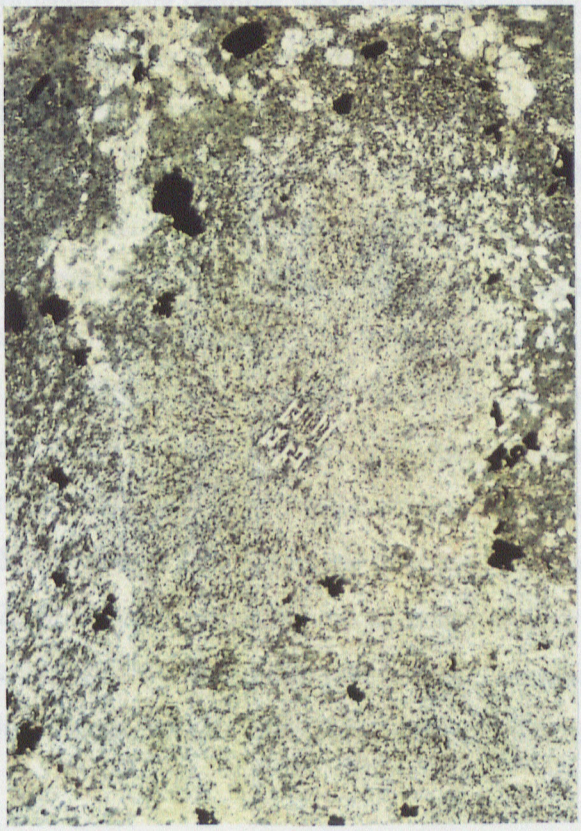

C

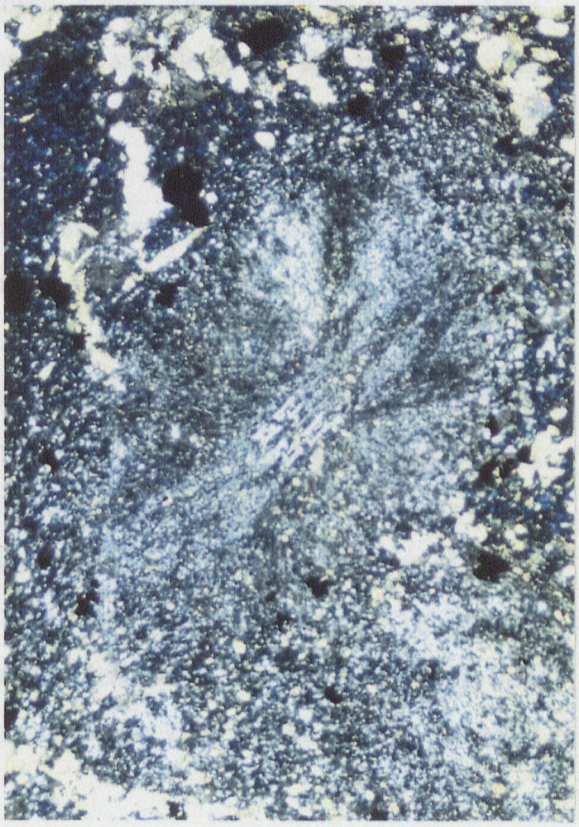

their chlorite and/or sericite dominated matrix. The varioles may be brecciated in strongly sheared rocks, the matrix filled by quartz, carbonate and tourmaline.

Myrmekite is a common texture of the volcanic suite in the Dome Mine area just as it is in the Harker Lake area. Again, it is more common in the coarser grained parts of flows, formed by intergrowth of albite and quartz with clear quartz "caps". Myrmekite is more prevalent in the upper flows of the volcanic cycles in the Dome Mine area, such as the V10 subunit.

Sample locations in the Dome Mine area can be found on Map 2.2.1 for the Paymaster section and Maps 2.2.2 to 2.2.6 corresponding to the levels examined at the Dome Mine. These maps also provide the general geology and stratigraphic relationships of the rocks examined in the study.

3.2.1a Porcupine Paymaster Section

The Porcupine Paymaster section begins with a pillowed unit at the top of the Central Subgroup (sample P89-13). This unit consists of 50% well foliated, relatively Mg-rich chlorite in a very fine grained matrix of plagioclase and carbonate. Moving to the lowermost exposure of the V8 subunit of the Vipond Subgroup, a sample from a massive part of the variolitic pillowed lava (sample 9832), contains quartz as discrete grains, comprising up to 15% of the unit. Chlorite in this sample is more Fe-rich than the sample from the upper Central Subgroup. Varioles from pillowed samples in this unit (P89-2, 9831) have many delicate, skeletal plagioclase crystals preserved within the varioles (Plate 3.2.2a). The overlying massive flow contains slightly more quartz than the previous variolitic flow, up to 15-20% (sample P89-02). Although the flow is magnetic most of the oxides have been converted to sphene. A trace tourmaline is present in this flow.

Four samples were taken from the next flow, whose pillows are characterized by coalesced, layered varioles; one sample from the massive central portion of a large (3.0 m diameter) pillow (P89-4), the others from sections of the layered and coalesced varioles (P89-5, P87-3 and 3a). The cores of these pillows are fine grained and homogeneous with about 25% chlorite interstitial to a recrystallized mass of plagioclase and quartz. The layered varioles have abundant spherulites, commonly emphasized by alignment of chlorite and leucoxene in their interstitial spaces. Quartz comprises about 20% of the variole material

compared to 10% in the massive sample. This is explained by the fact that quartz is a product of the alteration of plagioclase which is the prime component of varioles. The interstices of these pillows do have remnant glassy features including, possibly, perlitic fractures.

The next flow, also pillowed, has evenly scattered varioles and up to 10% epidote present as disseminated grains throughout the samples (P89-6, P87-2). Chlorite in this flow usually has anomalous brown birefringence, indicating a slightly more Mg than Fe-rich character. The varioles appear ragged in places and are quite altered with all primary textures eliminated. As a result, plagioclase is difficult to distinguish. There is abundant leucoxene (sphene?) scattered throughout the rock, about 10% in total, giving the sample a very murky appearance in thin section.

The next flows (samples P89-7, P87-1 and P89-8) represent the upper part of the V8 subunit of the Vipond. Along with Fe-rich chlorite and altered plagioclase, the massive flow overlying the pillowed units just described contains about 20% carbonate, 10% leucoxene and minor epidote. The brecciated and pillowed, variolitic flow at the top of the V8 contains abundant hyaloclastite. Epidote is the main mineral component occuring primarily as a replacement of altered glass in the breccia. Aproximately 20% chlorite is present, mostly in the matrix to the breccia fragments.

The V10 subunit is represented by two samples taken from the massive lower part (P89-9) and the spherulitic, brecciated upper part (P89-10). The massive part is characterized by a feldspathic groundmass with abundant myrmekitic texture. The chlorite has birefringent colours indicative of an Fe-rich composition. Trace apatite is seen primarily as narrow, segmented needles in plagioclase. The upper spherulitic portion is quite altered with breccia fragments containing apparent remnant altered glassy material. Most of the matrix to these fragments is large lumps or wisps of chlorite and extremely fine grained plagioclase and quartz. This brecciated flow top represents the uppermost part of the Vipond Subgroup.

The lowermost flow of the overlying Gold Centre Subgroup was sampled in two locations; 3 m (P89-11) and 30 m (P89-12) above the upper V10 contact. The rock is composed mainly of plagioclase and chlorite with carbonate, leucoxene and minor epidote and quartz. The altered plagioclase has a skeletal appearance, possibly due differential replacement of zoned phenocrysts (Plate 3.2.3). Myrmekitic texture is very common in this

Plate 3.2.3: Altered zoned plagioclase phenocryst, in the non-variolitic Amygdaloidal Pillow Lava (APL), Gold Centre Subgroup, Porcupine Paymaster section (P89-12, X-nicols, 2 mm).

Plate 3.2.4: Uralite (green) enclosing sub-hedral plagioclase (white) grains (sub-ophitic texture), from sample D89-21, 99 Flow, Dome Mine. Uralite is not preserved in any other sample recovered in this study from the Dome Mine area (PPL, 2 mm).

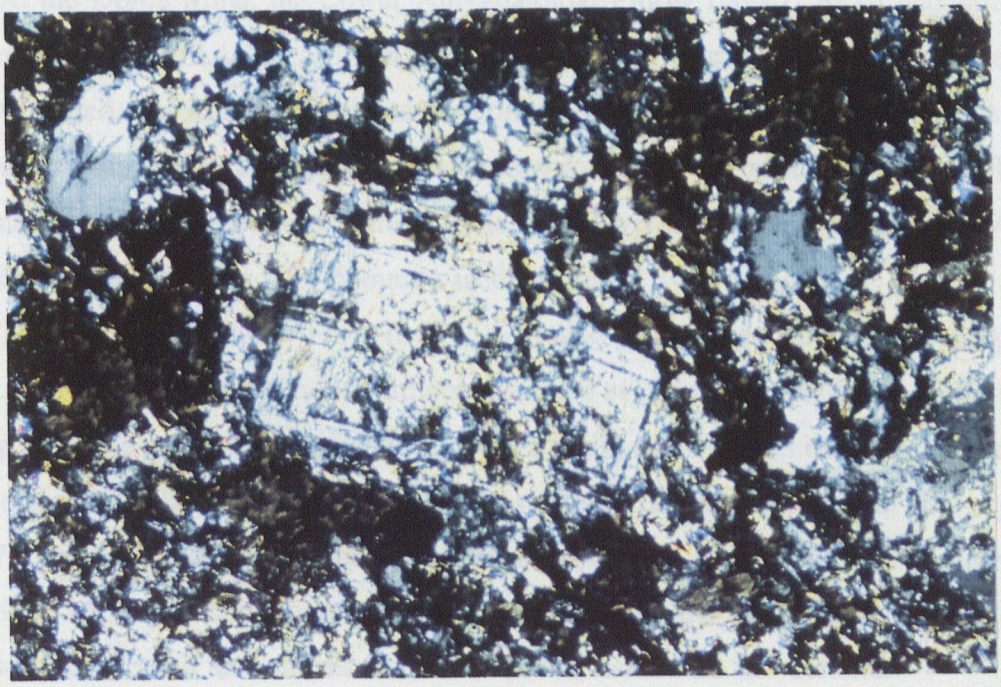

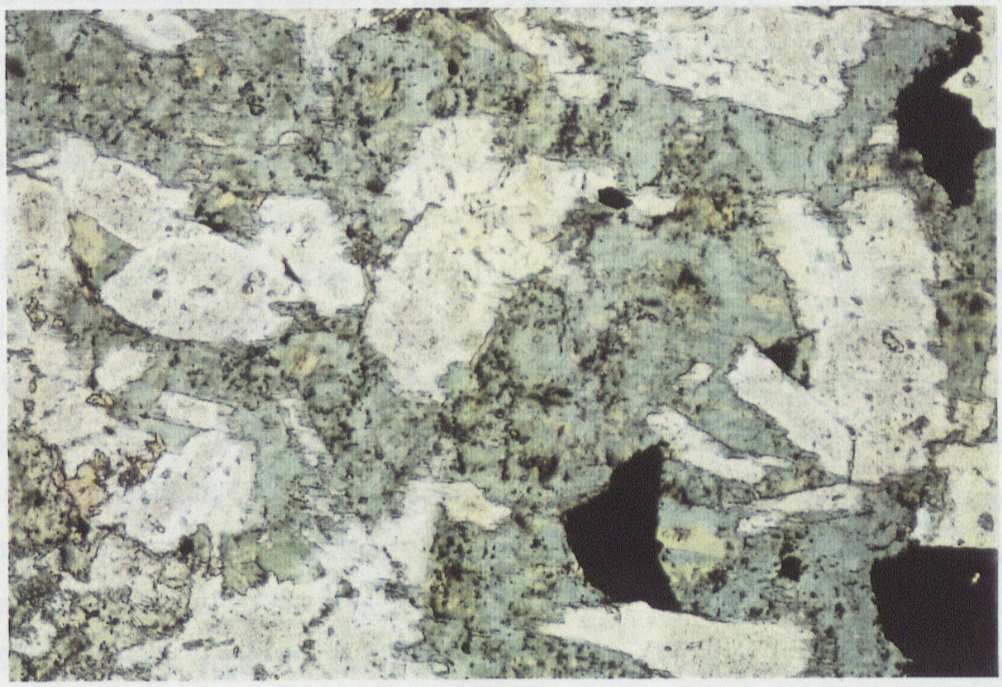

flow.

3.2.1b Dome Mine Section

At the Dome Mine, the Lower Amygdaloidal Pillow Lava (LAPL) was sampled on three levels (Maps 2.2.4, 2.2.5, 2.2.6). The least altered example (D89-19) of the unit is strongly foliated, consisting of carbonate-chlorite-sericite wrapping around domains of very fine grained plagioclase and quartz. Scattered throughout are relict, skeletal Fe-Ti oxide grains, now altered to leucoxene, with chlorite rims. Overall, the chlorite is a relatively Mg-rich variety. Tourmaline is very common in this sample.

The Lower Spherulitic Flow (LSPL) was also sampled on three levels (Maps 2.2.4, 2.2.5, 2.2.6). In general, the samples are not as altered as those from the LAPL. Still, foliation is strong in all the samples except D89-32 from a thick, massive part of the unit. Overall, the rock contains 10-15% quartz. Pleochroic haloes in chlorite mark the sites of tiny crystals of zircon(?). Tourmaline is found in trace quantities in the more altered samples. Samples D89-1 and D89-20 are both examples of the variolitic pillowed parts of the unit. Varioles in these samples are brecciated and altered to mostly quartz, carbonate and sericite.

The 99 Flow in the Dome Mine stratigraphy is always massive and generally coarse grained although there are fine grained vesicular portions near its upper contact. A remarkably unaltered and undeformed example of the 99 Flow was located on the 2300 Level (sample D89-21, Map 2.2.5, Plate 3.2.4). This sample is the only one taken in the Dome Mine area containing uralite. The uralite is quite massive in appearance with extremely ragged edges. There is minor retrograde alteration of the amphibole, to Fe-rich chlorite. The primary sub-ophitic texture of the rock is preserved with well formed rectangular plagioclase grains enclosed by uralite. Twinning is common in plagioclase grains and best estimates of composition are at most An_8, or almost pure albite. Large euhedral to skeletal grains of magnetite, with lamellae altered to sphene are scattered throughout the section (microprobe data, Appendix 3.1d). There is 5-8% epidote present in this sample. Sample D89-21 is remarkable in that there is almost no carbonate present. Other samples taken from the 99 Flow are not similarly well preserved and have a chlorite-plagioclase-carbonate dominated assemblage more typical of the mine area.

Samples taken from the Broken Spherulitic Flow are quite altered. Samples were

collected on three levels (Maps 2.2.3, 2.2.5, 2.2.6) and contain a large proportion of varioles in all cases. The varioles tend to coalesce to form a blotchy appearance in hand samples. Chlorite and sericite wrap around the varioles which are locally brecciated. Quartz and carbonate as well as Fe-rich tourmaline fill veinlets and the matrix of brecciated varioles. Wispy trails of leucoxene are found in the foliated groundmass of these rocks.

The Key Flow unit of the Dome Mine stratigraphy consists of several flows with massive, pillowed and brecciated portions. The Key Flow has been sampled on all five levels of the Dome Mine for a total of 19 samples. Interestingly, even samples presumed to be extremely altered due to proximity to an ore horizon, such as D89-7 (Map 2.2.4), still retained some distinguishable spherulitic textures within varioles. Pillowed examples of the Key Flow unit are invariably variolitic. There seems to be two types of varioles identified in the Key Flow in this study. Indistinct, lensy varioles are found in the middle to lower parts of the unit (samples D89-24 and D89-38). These varioles tend to be a mass of fan spherulites without other distinguishing features (Plate 3.2.5a). The other type (e.g. samples D89-27, D89-39), found in the upper parts, is characterized by distinct varioles, commonly quite small (Plate 3.2.5b), with well defined axiolitic and bow-tie spherulites, as well as other disequilibrium textures such as dendritic oxides and skeletal grains (Plate 3.2.2b). Tourmaline is also commonly found in veinlets and at the borders of varioles.

Overlying the Key Flow is the Spherulitic Flow which has been sampled on three levels (Maps 2.2.2, 2.2.3, 2.2.6). Brecciated samples contain hyaloclastite material and the outlines of altered glass shards are still visible. The matrix of the breccia is composed of quartz, chlorite or sericite, carbonate and plagioclase. Samples of typical, "flowy" textured rock have coalesced, lense-like varioles in a very fine grained matrix of plagioclase, quartz, carbonate and sericite. The varioles contain scattered, large grains of ragged, inclusion-filled quartz or plagioclase in a fine grained groundmass made up mostly of quartz, plagioclase and sericite. Spherulites, especially fan type, are found in the lense-like varioles but they are not common, having been mostly obliterated by alteration. Strongly foliated chlorite and sericite occur in the matrix, wrapping around the lenses. Tourmaline and zircon(?) are also present in this matrix.

The Andesite Flow is the lower of the two units which define the V10 subunit of the

Plate 3.2.5: There appears to be two distinct types of varioles in the Key Flow: a) lensy varioles composed of masses of plagioclase fan spherulites (D89-24, X-nicols, 2 mm), b) distinct varioles, consisting of individual or grouped plagioclase spherulites (D89-39, X-nicols, 2 mm).

Plate 3.2.6: V10 subunit. a) Generally homogeneous texture, characterized by large, clear quartz grains, acicular apatite, and pale coloured chlorite (D89-16, PPL, 2 mm). b) Tiny crystals of zircon(?), easily detected by their pleochroic halo, are especially common in this unit (D89-16, PPL, 0.5 mm).

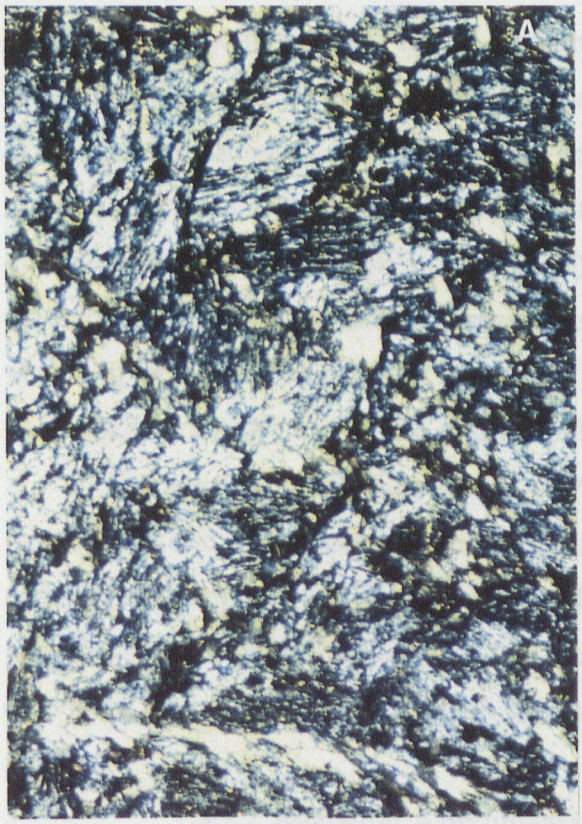
A

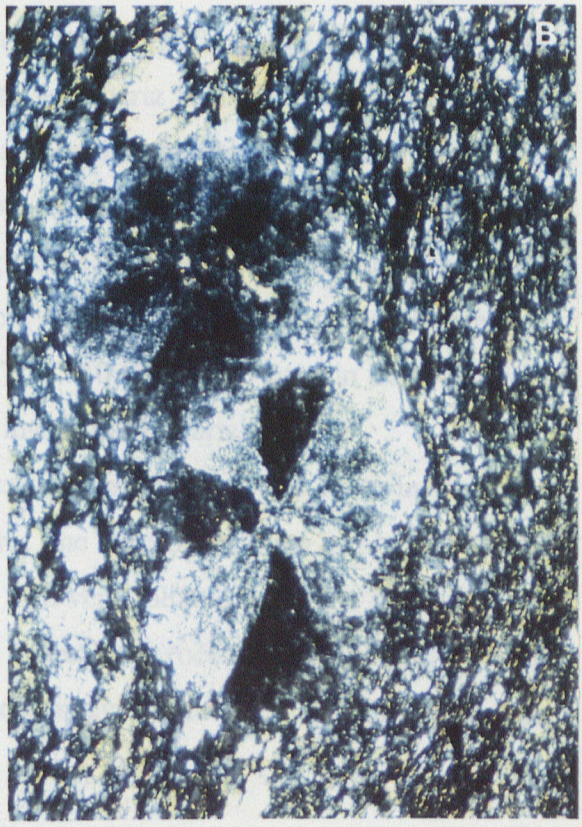
B

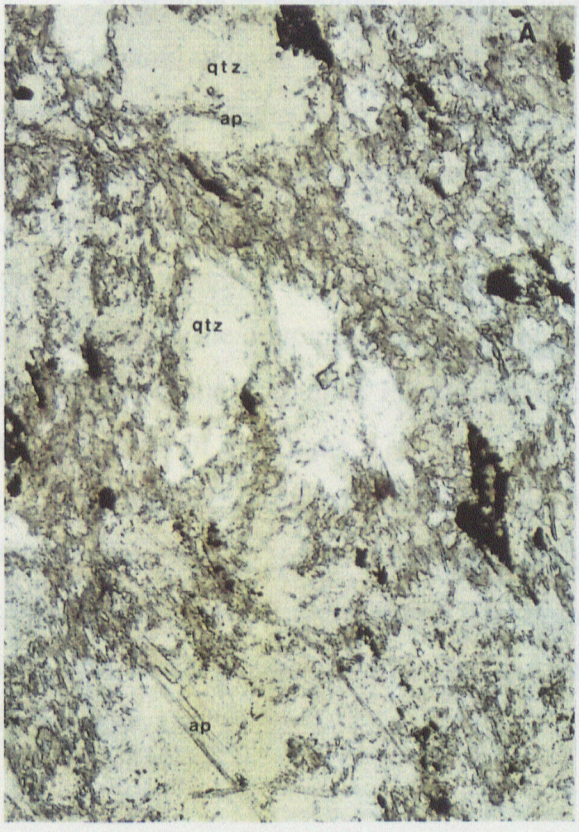
A
qtz
ap
qtz
ap

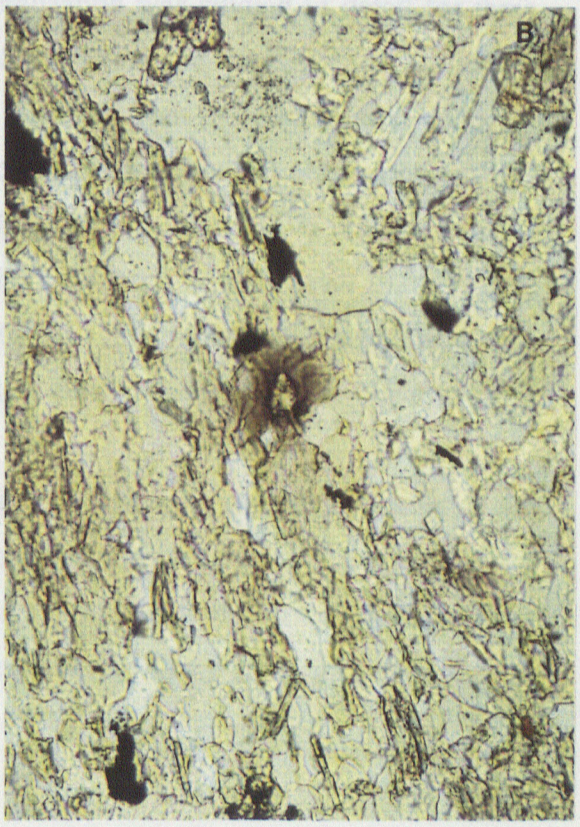
B

Vipond Subgroup at the Dome Mine. Massive segments of the Andesite Flow (sample 9491, Map 2.2.2) are homogeneous, fine to medium grained, with 20-25% quartz occurring as large grains in a matrix of plagioclase, chlorite, carbonate and quartz (Plate 3.2.6a). Small needles of apatite are common, and mostly seen in the large quartz grains. The Dacite Flow, the upper unit of the V10 section, also contains about 20-25% quartz in relatively unaltered massive portions (sample 9493, Map 2.2.2). Plagioclase laths are common and frequently quite long. There are abundant tiny crystals of zircon(?) (Plate 3.2.6b) with pleochroic haloes, visible in the chloritic patches of both these units. The V10 flows also contain trace amounts of toumaline, usually in the fine grained chloritic interstitial material.

The Amygdaloidal Pillow Lava (APL) was only sampled on one level in the mine (Map 2.2.2) due to accessibilty problems elsewhere. The base of the flow is highly sheared and altered (sample 9495). Further up, the flow is still very foliated but some relict primary textures, such as plagioclase laths, can be found. In general, the rock is very fine grained with carbonate prevalent. Chlorite is pale yellow in colour and occurs only in small vein-like features.

3.2.2 Alteration Assemblages

Alteration mineralogy associated with mineralization was studied in detail for three of the Vipond units in the Dome Mine sequence; the 99 Flow and the Key Flow of the V8 subunit and the Dacite Flow from the V10 subunit. Samples from these units were collected on various levels in the mine to provide the most complete spectrum of alteration possible. Although the samples come from widespread localities within the mine, it is expected that they are quite similar in nature, as correlation of the units from level to level is fairly well established by the ongoing geological compilation by the mine geologists. Comparison with samples from the Porcupine Paymaster section is less certain because of the distance from the ore zones of the Dome.

Sampling of alteration zones in the V8 subunit was done in a similar manner to the Cryderman Zone in Harker Township, that is perpendicular to flow contacts since most ore zones are sub-parallel to the flows. The ore zones in the V10 section crosscut the flow units obliquely which allows sampling into the alteration halo from along strike at the same level in the flow.

Table 3.2.1: Modal mineralogy (as estimated volume percent) associated with alteration of the 99 Flow, V8 subunit, Dome Mine, Timmins, Ontario.

	D89-21	D89-35	D89-34
amphibole	30		
chlorite	5	35	
plagioclase	50	35	
quartz	1-2	10	25
carbonate	2-3	10	50
magnetite	5	5	
sphene/lcxn	1	3	3
pyrite			1
epidote	5-8	2	
sericite			20
apatite	tr		
tourmaline			tr

99 Flow, V8 subunit:

The alteration study for the 99 Flow was focused on three samples (Table 3.2.1, Plate 3.2.7). Sample D89-21 from the 2300 Level (Map 2.2.5) is probably the most mineralogically pristine sample and undeformed rock recovered from the Dome Mine and represents the least altered end member of the alteration suite. Samples D89-35 and D89-34 were both taken from the 2900 Level (Map 2.2.6) stepping out from an ore zone. The moderately altered sample, D89-35, was taken aproximately 14 metres up flow from D89-34. Sample D89-35 is a finer grained sample than D89-21 which may in part be due to the foliation in the moderately altered rock. Sample D89-34 was taken at the core of a highly sheared and altered zone which contains "ankerite vein" ore less than 10 metres away on strike. There is a direct relationship between the amount of alteration apparent in these rocks and the intensity of deformation. This suggests a strong structural control on the passage of mineralizing metasomatic fluids.

Uralite, common in D89-21, is completely replaced by the relatively modest alteration present in D89-35. The resulting chlorite is strongly foliated. It has birefringent colours indicative of a more Mg than Fe-rich composition. Epidote has also been diminished in this moderately altered sample but not as completely as the amphibole. D89-35 contains a

Plate 3.2.7: Progressively altered samples from the 99 Flow alteration study. Modal mineralogy is summarized in Table 3.2.1.
a) Least altered sample, D89-21 (PPL and X-nicols, 6.5 mm). Coarse grained rock consists mostly of plagioclase and uralite and has no distinguishable foliation.

b) Moderately altered sample, D89-35 (PPL and X-nicols, 6.5 mm). More fine grained example of the 99 Flow, foliation is readily apparent.

c) Most altered sample, D89-34 (PPL and X-nicols, 6.5 mm). This highly altered rock consists dominantly of carbonate, quartz, and sericite. Lenses of carbonate suggest a large volume gain associated with alteration.

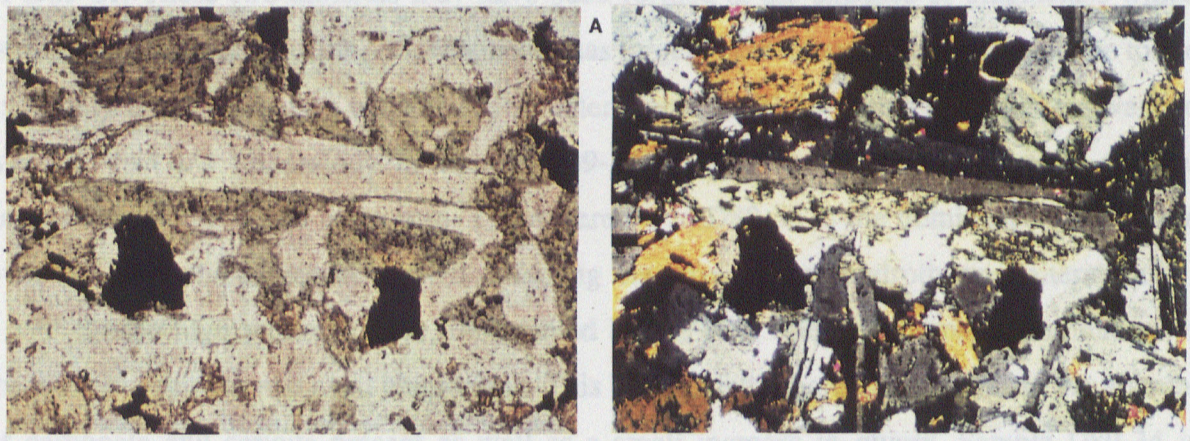

A

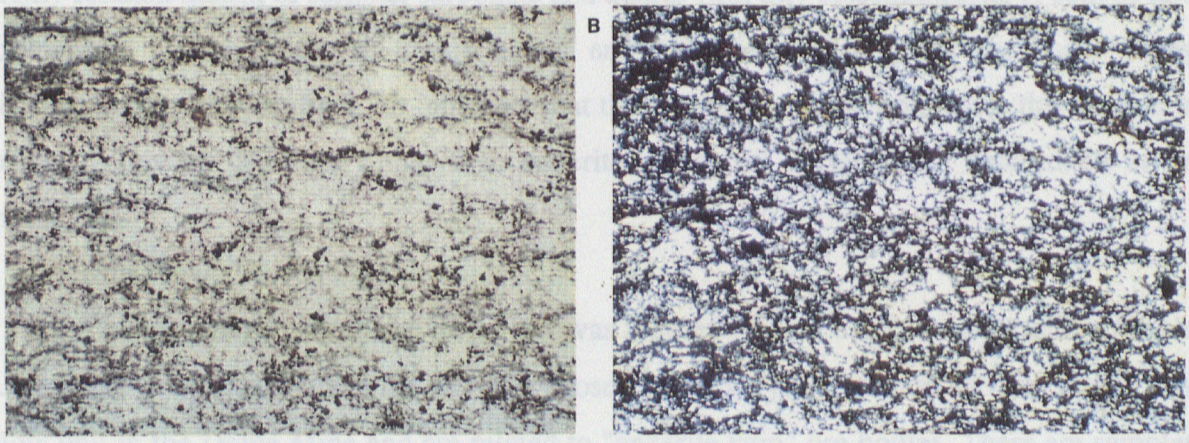

B

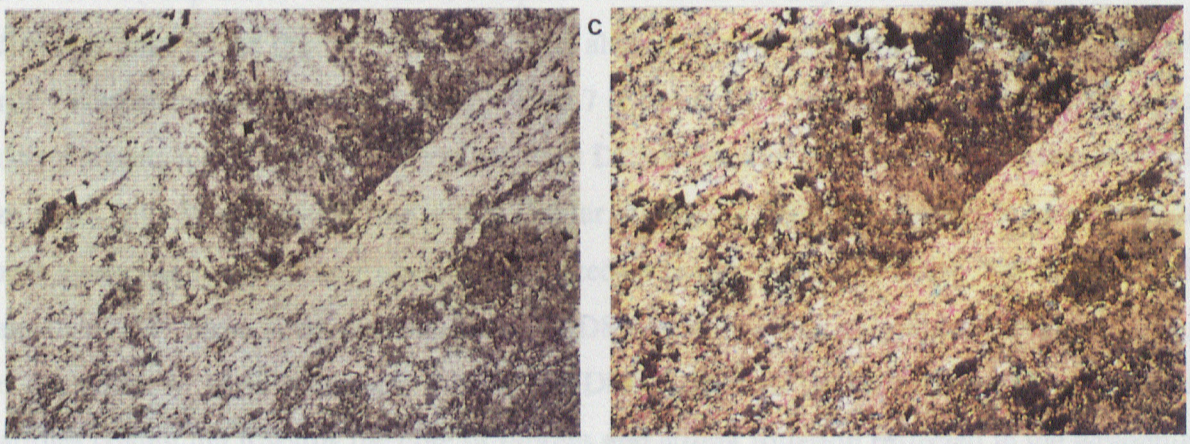

C

significant percentage of carbonate and quartz (10% each) which are only minor components of D89-21. These two minerals may have been formed at the expense of plagioclase which is much less abundant in D89-35. Magnetite has largely been converted to sphene. Due to the extremely unaltered nature of D89-21, the alteration in D89-35 seems to be quite advanced when in fact the mineralogy in sample D89-35 is representative of the general mineral assemblage in the Dome Mine area. The difference in D89-35 is the dominance of dolomite over calcite as the carbonate present reflecting the proximity of hydrothermal alteration.

In the highly altered zone, represented by D89-34, there is complete elimination of the chlorite, epidote and even plagioclase. This is reflected by a large increase in the amount of carbonate and sericite present as well as a small increase in quartz. Sample D89-34 is characterized by large, brecciated lenses of carbonate, quartz and sericite in a fine grained and highly foliated matrix of sericite, carbonate and quartz with tiny disseminations of sphene and tourmaline. Pyrite occurs as small grains and aggregates throughout the rock. X-ray diffraction data (Appendix 3.2c) indicates that the carbonate which dominates this sample is primarily ferroan dolomite rather than ankerite. Also, the sericite was determined to be muscovite.

Key Flow, V8 subunit:

The alteration study of the Key Flow was focused on four samples in particular (Table 3.2.2, Plate 3.2.8). All four of the samples chosen occur very near the upper limit of the Key Flow unit in the Dome Mine and are related to "ankerite vein" ore bodies. These are samples D89-7 and D89-8 on the 1800 Level (Map 2.2.4) and samples D89-39 and D89-40 on the 2900 Level (Map 2.2.6). None of the samples collected in the Key Flow have the preservation of sample D89-21 of the 99 Flow. The least altered sample of this study is D89-8, located only 7 metres from an ore zone. Sample D89-7 is located 1.5 metres from the same ore zone and represents a strongly altered equivalent to D89-8. On the 2900 Level, 15 metres from an ore zone, D89-39 was taken from a very similar setting to D89-8 but appears to be somewhat more altered and represents a moderately altered example of the Key Flow. The most altered sample of Key Flow in this detailed study is D89-40 which was only about 1.5 metres from an ore zone. In hand specimen, D89-8 and D89-7 seem to be very similar with rounded varioles coalescing towards the core of pillows and strong foliation reflected in the wrapping

Plate 3.2.8: Progressively altered samples from the Key Flow alteration study. Modal mineralogy is summarized in Table 3.2.2.
a) Least altered sample, D89-08. The chloritic matrix wraps around altered variole (PPL and X-nicols, 2 mm).

b) Moderately altered sample, D89-07. Chlorite and sericite form a foliated matrix to varioles which contain weakly preserved spherulites (PPL and X-nicols, 2 mm).

c) Moderately altered sample, D89-39, similar in alteration intensity to D89-07 (PPL and X-nicols, 2 mm). This sample is characterized by small varioles with well preserved spherulites. Foliation is clearly seen in the micaceous matrix.

d) Most altered sample, D89-40. This sample differs from the others in being relatively homogeneous and having no varioles (PPL and X-nicols, 2 mm).

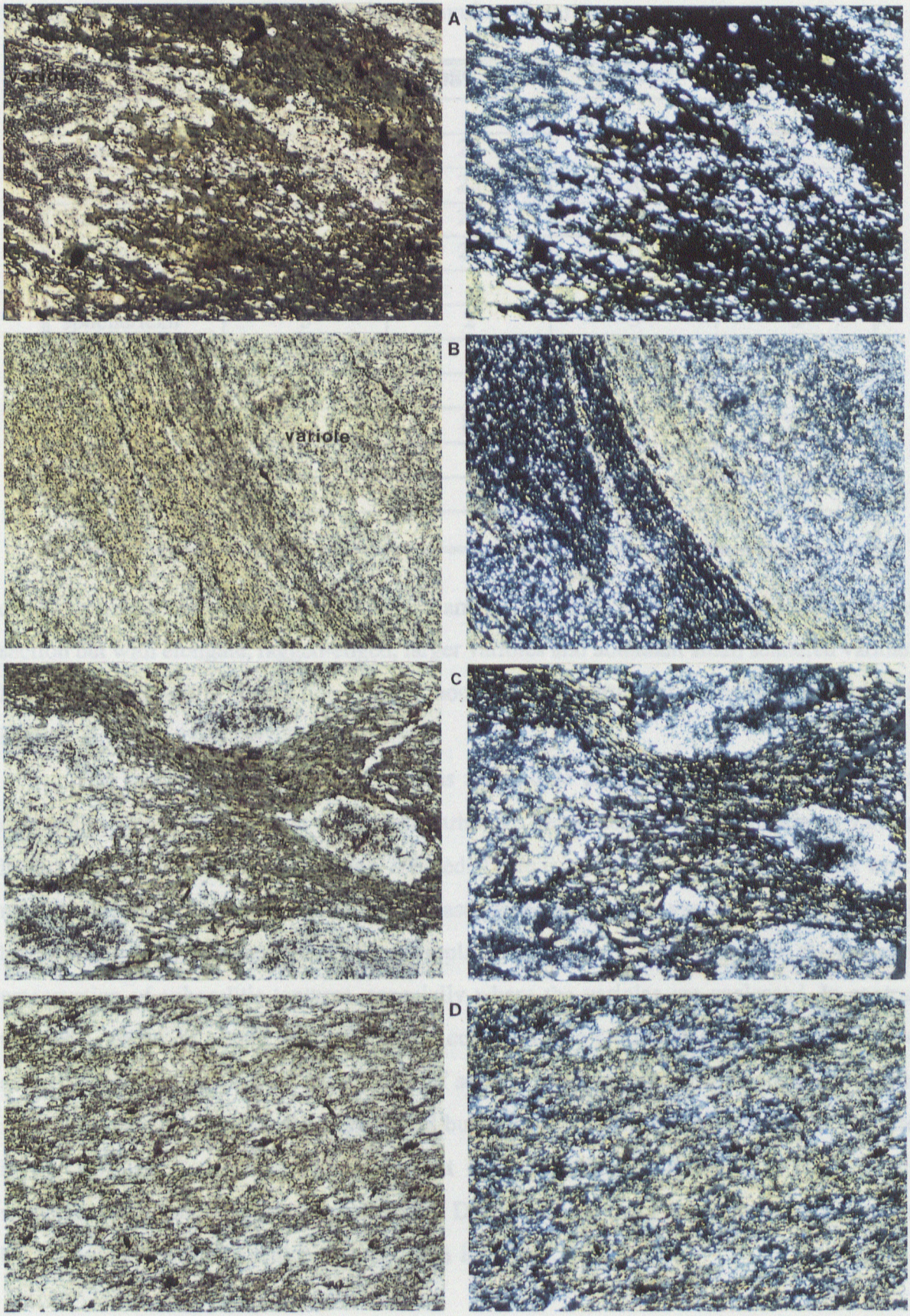
A
variole
B
variole
C
D

Table 3.2.2: Modal mineralogy (as estimated volume percent) associated with alteration of the Key Flow, V8 subunit, Dome Mine, Timmins, Ontario.

	D89-08	D89-39	D89-07	D89-40
amphibole				
chlorite	25	20	15	5
plagioclase	35	25	30	25
quartz	20	20	15	20
carbonate	15	20	25	40
magnetite				
sphene/lcxn	5	2	3	3
pyrite	tr-1		1	tr
epidote				
sericite		10	10	5-8
apatite				
tourmaline			1	1
zircon(?)	tr			

of micaeous minerals around the varioles. Sample D89-39 is also from a variolitic pillowed section but with elongate, ragged-edged, larger varioles and abundant small scattered varioles. In contrast, D89-40 is from a fine grained, non-variolitic portion of the same flow. Foliation is quite strong in both D89-39 and D89-40.

The least altered sample, D89-8, has no epidote present. Only a minor amount of calcite is found in this sample with most carbonate being dolomite. The matrix to varioles is dark green chlorite which is strongly foliated. There is a high concentration of quartz which may be related to the alteration of plagioclase, especially in the varioles. The varioles are brecciated, by shearing, and there is some replacement by carbonate. However, there is good preservation of spherulitic textures, especially where the varioles are coalesced. In contrast to D89-8, D89-7 is a light yellowish green colour in thin section due to the elimination of some chlorite and subsequent appearance of sericite in the matrix of the varioles. Dolomite is more abundant in this sample than D89-8 but there is still some calcite present in fractures in the varioles. Tourmaline is also present in the matrix of the varioles. Pyrite occurs scattered throughout the rock as small grains. Deformation is more prevalent in D89-7 evident by flattening of varioles which was not seen in D89-8.

Sample D89-39 is more altered than D89-8 but not as strongly as D89-7. There is less chlorite and plagioclase and more carbonate and sericite relative to D89-8 and the thin section has a light green colour overall. Dolomite is the dominant carbonate present. The larger varioles are quite altered and have very little preservation of original textures whereas the small scattered varioles contained in this sample have remarkable preservation of spherulite textures (Plate 3.2.5b). D89-40 is not variolitic and is quite fine grained indicating proximity to the upper contact of the flow, the site of an ankerite vein. The sample is well foliated reflecting the shearing related to the nearby ore zone. Dolomite makes up almost half the rock volume. The rock is a light tan colour in part due to the elimination of almost all chlorite. Tourmaline is present as widely scattered subhedral, prismatic grains. About 1% pyrite is found filling tiny veinlets.

Dacite Flow, V10 subunit:

Samples of the Dacite Flow (Table 3.2.3, Plate 3.2.9) were taken on the 1100 and 1200 Levels in the Dome Mine (Maps 2.2.2 and 2.2.3). The extent of alteration is moderately advanced in all these samples so a sample from the Porcupine Paymaster section (P89-9, Map 2.2.1) was included in this study as the least altered equivalent. Initial sampling in the Dacite unit did not come up with a sample immediately adjacent to one of the ore bodies. Unfortunately, due to a protracted strike at the Dome Mine, follow up work was not possible and so the intensity of alteration in the most altered Dacite Flow samples may not be as strong as possible. Foliation is not as strong in the rocks associated with the Dacite ore bodies. The ore is associated with dilatent zones formed as a response to shearing which is apparently concentrated at the margins of the unit.

Sample P89-9 was used because correlation between the Paymaster and the Dome sections is good since the V10 subunit is relatively narrow and quite distinctive (Figure 2.2.1). The weakly foliated sample is made up of plagioclase, chlorite and quartz and contains weak pervasive calcite alteration consistent with local metamorphism and alteration. Chlorite has anomalous birefringent colours which indicate that it is Fe-rich. Trace amounts of apatite and zircon(?) are found in this unit. Magnetite is still relatively fresh with only minor alteration to sphene.

At the Dome Mine, samples 9493 and 9494 of the Dacite Flow on the 1100 Level,

Plate 3.2.9: Progressively altered samples from the Dacite Flow/V10 subunit alteration study. Modal mineralogy is summarized in Table 3.2.3.

a) Least altered sample, P89-09, from the Porcupine Paymaster section (PPL and X-nicols, 2 mm).

b) Most altered sample, D89-16. This is the same rock as in Plate 3.2.6a. (PPL and X-nicols, 2 mm). Carbonate alteration is not as strong as in the other units studied.

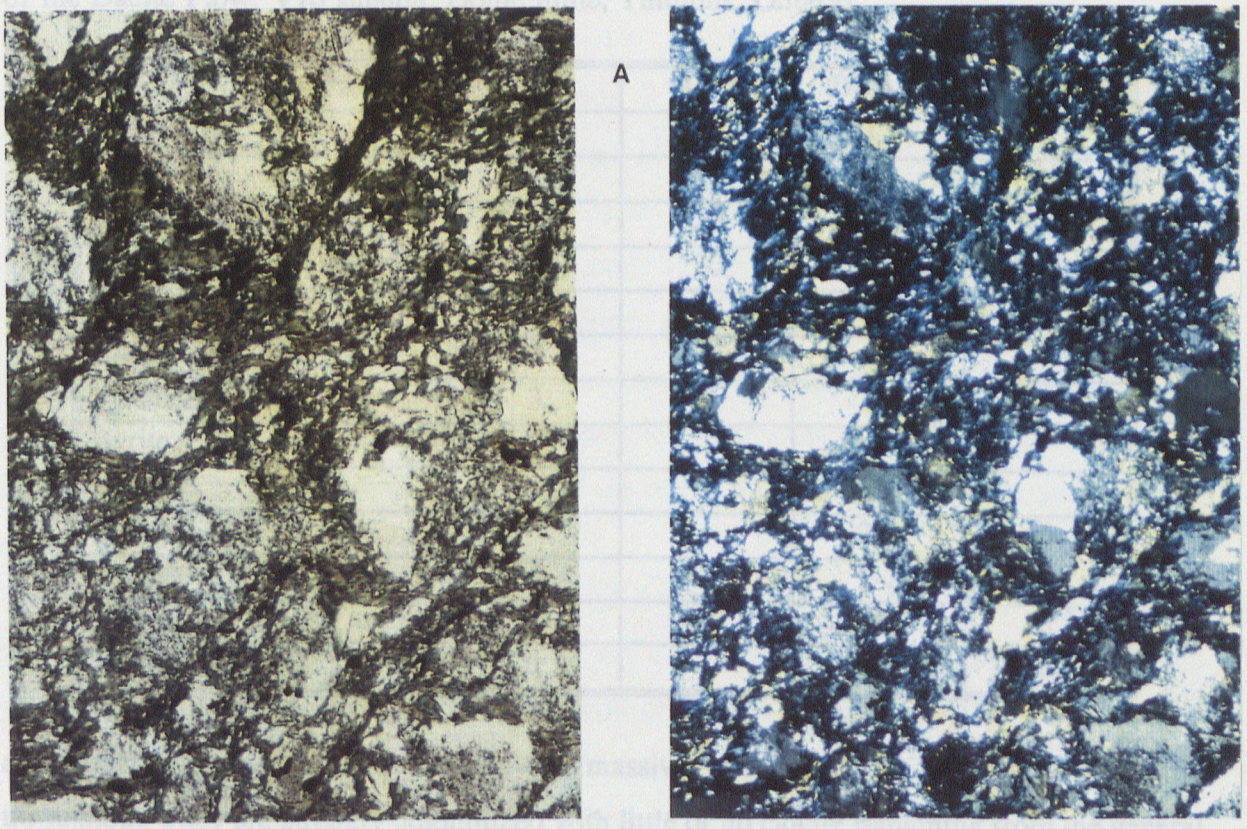
A

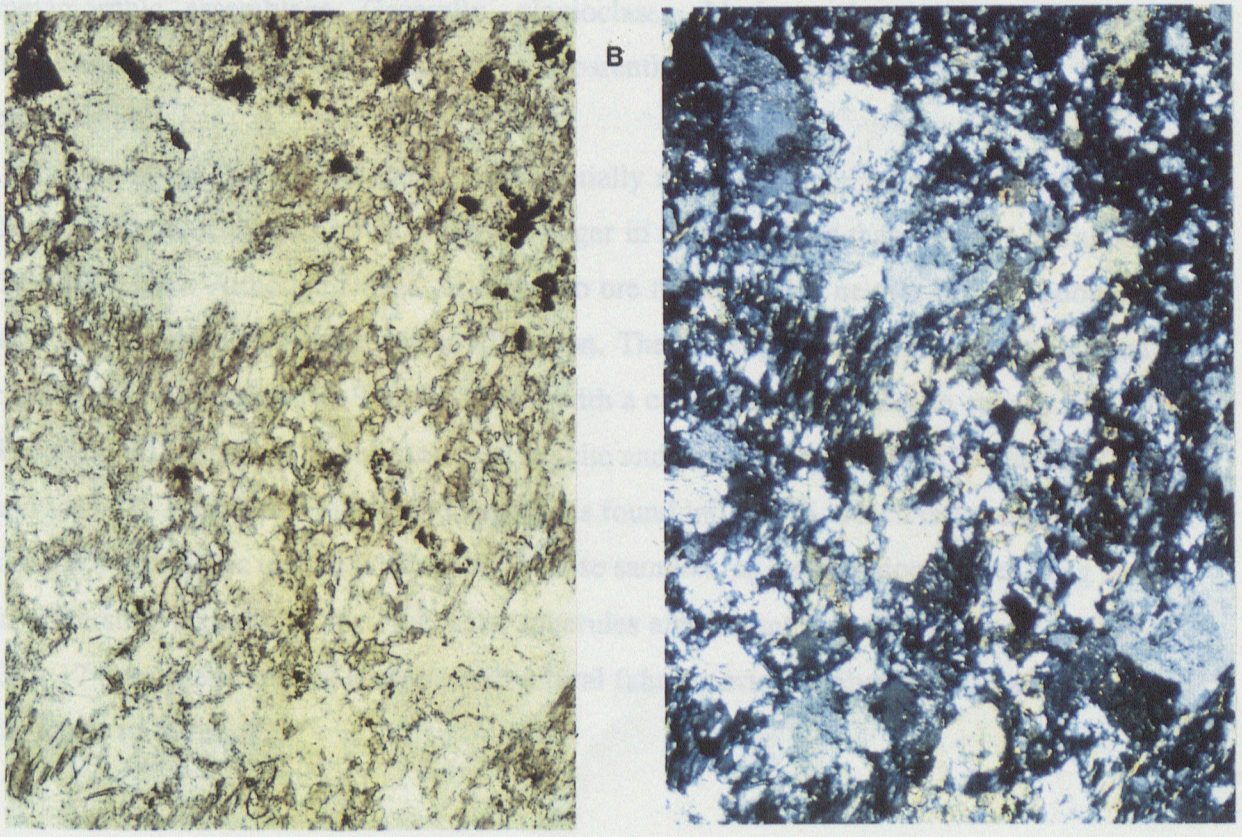
B

Table 3.2.3: Modal mineralogy (as estimated volume percent) associated with the alteration of the Dacite Flow, V10 subunit, Dome mine, Timmins, Ontario.

	P89-09	9494	9493	D89-16	D89-17
amphibole					
chlorite	30	30	25	20	30
plagioclase	35-40	25	25	30	25
quartz	10-15	20	20	20	15
carbonate	15	20	25	15	15
magnetite	2-3	2	1		
sphene/lcxn	1	3	3	5	5
pyrite				1	
epidote					
sericite				2-3	5
apatite	tr-1		1	1-2	
zircon(?)	tr	tr	tr-1	tr	tr
tourmaline		tr		tr	tr

are moderately altered. Both samples are massive with relatively homogeneous texture throughout. They are strongly dolomitized with little or no calcite remaining from the general metamorphic assemblage. Generally, plagioclase, chlorite and magnetite contents are diminished relative to P89-9. Chlorite is apparently still Fe-rich. Foliation is not strong in either sample.

Samples D89-16 and D89-17 are spatially related to a dacite ore body on the 1200 Level. Alteration appears to be slightly stronger in these samples than the two samples from the 1100 Level. Although D89-17 is closer to ore than D89-16, neither is close enough to a vein to distinguish a progression in alteration. These samples have less carbonate (and no calcite) and magnetite than 9493 and 9494 with a concomitant increase in sphene and rutile. The main difference is the occurrence of sericite and a trace of tourmaline in samples D89-16 and D89-17. A noticeable increase in apatite is found in D89-16, which is the coarser grained sample. Myrmekitic texture is observed in these samples, as deformation is not strong enough to erase such textures. In fact, relict fan spherules are present in the groundmass of D89-16. D89-17 does seem to have a stronger structural fabric, perhaps enhanced by the fine grained character of the rock.

3.3 M^{c}Diarmid Lake Area

3.3.1 Petrography of the Section

The general metamorphic assemblage in the M^{c}Diarmid Lake area consists of plagioclase-uralite-quartz-leucoxene(sphene) plus minor chlorite, epidote and carbonate. Leucoxene is presumably an alteration product of Ti-rich oxides although there is very little of these original minerals remaining. The chlorite appears to be mostly an alteration product of uralite. Plagioclase is altered to epidote, chlorite and carbonate. Epidote is present in all samples up to about 3%, commonly as pseudomorphs of other minerals. Quartz occurs as small scattered grains in the groundmass of the rocks. Myrmekitic texture is seen in more coarse grained parts of the flows.

In the lowermost flow, a variolitic pillowed lava (samples M^{c}D-10 and 14), fine grained, homogeneous cores of the pillows are characterized by well defined plagioclase spherulites and acicular and branching amphibole crystals. In some places, the plagioclase and amphibole form "bundles" of fibres, rather than spherulitic or branching features, and these bundles are reminiscent of spinifex texture. There is very good preservation of these textures, even on the scale of individual mineral fibres.

The overlying flow is the only one on this section which is exposed from the bottom to the top. It provides an excellent view of the distribution of spherulites with depth in a flow (Plate 3.3.1). The flow is mostly massive with a narrow rim of varioles occurring at the contact between the lower massive part of the flow and the hyaloclastitic flow top. This border region of the flow (sample M^{c}D-4) has a mixture of acicular and branching amphibole with plagioclase spherulites, giving way to a section dominated by very well formed plagioclase spherulites towards the massive part of the flow. Approximately 2.8 m below M^{c}D-4, sample M^{c}D-5 was taken from a massive part of the flow where spherulites were easily distinguished on the weathered surface of the rock. The thin section of this sample has abundant, still very well formed spherulites but they are not as concentrated as in M^{c}D-4. Branching amphibole crystals are also not as common. At 6.0 m from the top of the massive part of the flow (sample M^{c}D-6) there is only scattered fan spherulites in the groundmass of the rock. Well formed spherulites are no longer found. Amphibole crystals appear stubby and

Plate 3.3.1: The morphology of plagioclase spherulites with depth in the massive part of Flow 2 (see Map 2.3.1):

a) from sample M^{c}D-04, near upper contact, fine spherulite (PPL and X-nicols, 2 mm),

b) from sample M^{c}D-06, lower down in the flow, coarser spherulite with branching uralite (PPL and X-nicols, 2 mm).

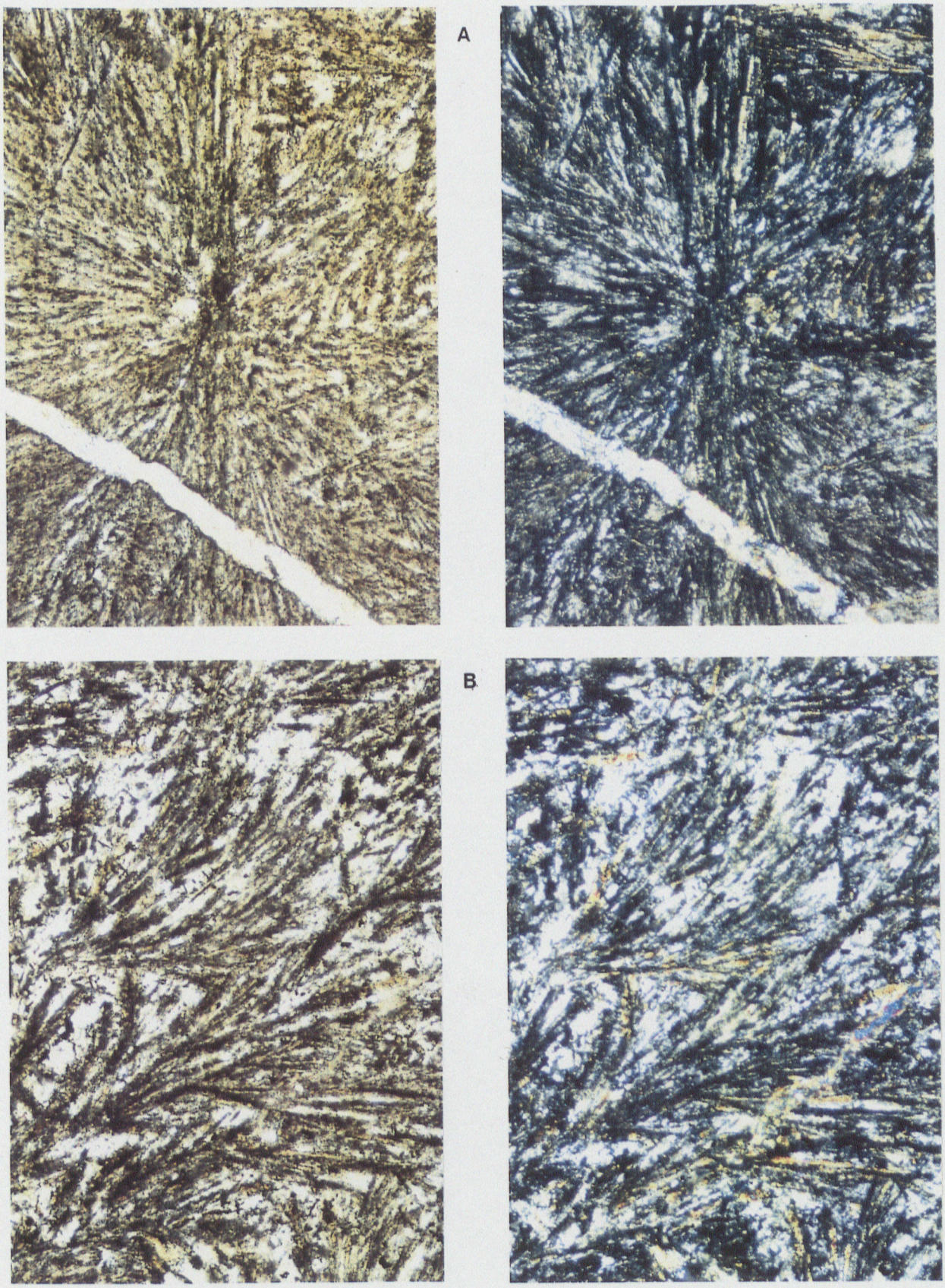
A
B

Plate 3.3.2: Skeletal grains of plagioclase, now altered to mostly epidote, in Flow 2 (sample M^{c}D-12, PPL and X-nicols, 2 mm).

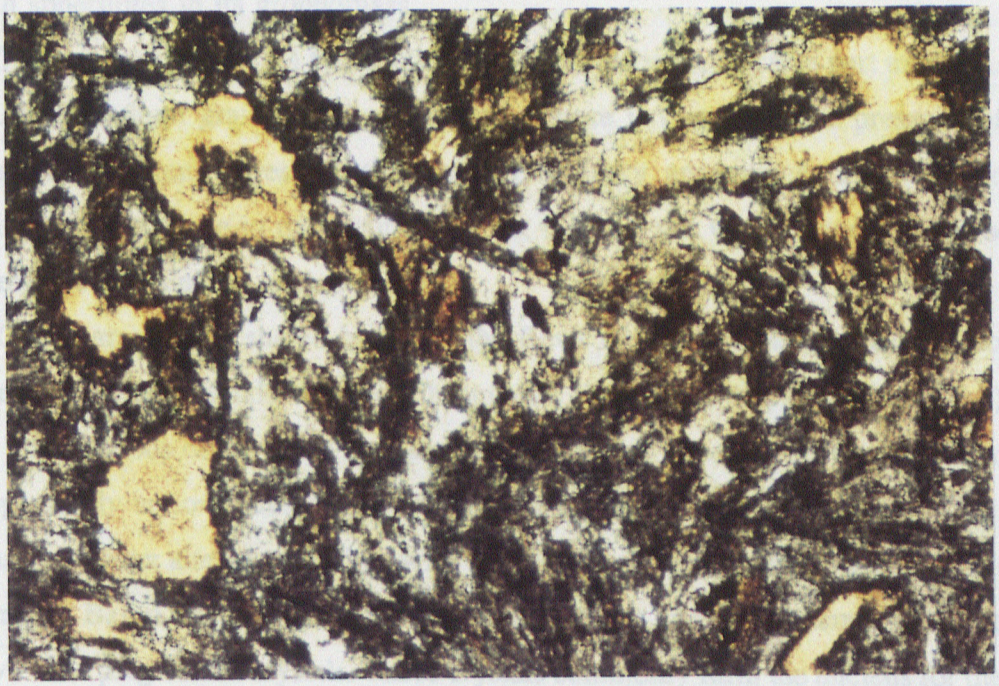

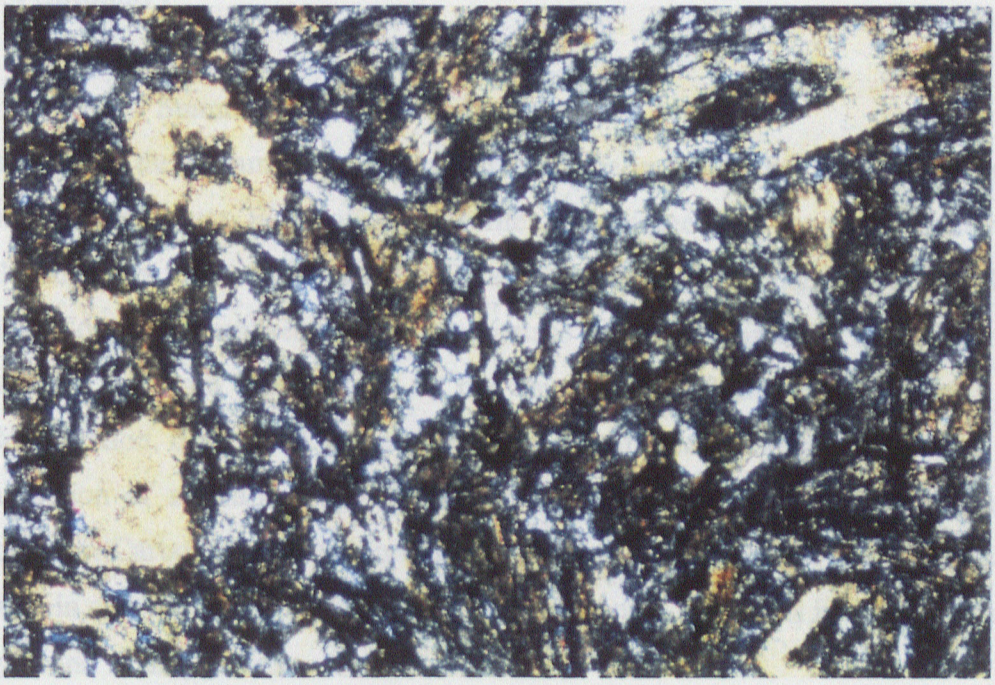

more prismatic than acicular. This sample is definitely more coarse grained than the previous two samples. McD-12, 5.0 m from the hyaloclastite contact, is similar to McD-6 except it has more fan spherulites in its groundmass.

The uppermost flow on this section has only its lower, massive part exposed (sample McD-1). It is medium grained and myrmekitic texture is common. The presence of 5-10% fine grained leucoxene gives the thin section a murky appearance. There are some fan spherulites of plagioclase in the groundmass but they are not well formed. Uralite occurs as ragged masses and slender acicular crystals.

One characteristic shared by all of the flows on the McDiarmid Lake section is the presence of skeletal crystals scattered throughout their massive parts (Plate 3.3.2). These crystals have various outlines but are usually subhedral to euhedral, rectangular forms. They were appparently hollow, subsequently filled by epidote, chlorite and carbonate. The mineral itself has since been altered to epidote with chlorite rims. The original mineralogy is difficult to determine. Based on their generally rectangular shape and their alteration products, they may have been plagioclase crystals. These crystals commonly form the nucleus for the growth of spherulites in the rocks.

3.4 Summary

3.4.1 Summary of Harker Lake Area

In general, the metamorphic mineral assemblage in the Harker Lake area consists of uralite, plagioclase, quartz, Fe-Ti oxides, chlorite, and epidote. The non-variolitic flows tend to have slightly more mafic minerals (amphibole plus chlorite) than plagioclase. Variolitic and intermediate flows commonly have more plagioclase than mafic minerals. Significant quartz, apatite and zircon(?) are present only in the upper flows of the volcanic cycles. Minor retrograde alteration, not related to metasomatism, has affected most samples and is evident by the alteration of amphibole to chlorite and Fe-Ti oxides to sphene and magnetite in varying degrees. Carbonate is a very minor component of the unaltered Harker rocks, and is rarely found in concentrations as high as 5%. The carbonate mineral is invariably calcite and is usually found in amygdules.

Variolitic flows in the Harker Lake area have both massive and pillowed sections. In general, the varioles which are seen in outcrop are in pillows or near the borders of flow tops. Spherulites are ubiquitous in varioles but are not always present in the non-pillowed parts of flows. Spherulites are more commonly found in massive parts of flows near the top of variolite-bearing suites, such as the flows immediately below the intermediate units on Line 25+50E (Map 2.2). They occur as well defined, often open spherulites in the groundmass of the flow, usually decreasing in concentration towards the base of the flow. Spherulites in the lower part of variolitic suites are usually found only in varioles. Varioles throughout the suite commonly contain dendritic forms of amphibole and oxides. The matrix to these varioles is aphanitic, locally glassy, and quite mafic. The massive parts of the lower variolitic flows are quite similar in texture to the non-variolitic flows with plagioclase laths and large grains of acicular uralite dominating the rock. The phyric intermediate flow(s) on Line 14+50E do not contain any spherulitic textures. Myrmekitic texture is most common in the upper flows of the suite.

Hydrothermal alteration related to gold mineralization results in significant changes to the general metamorphic assemblage. The style of alteration also varies somewhat depending on the unit being metasomatized. In the Line 28+00E area, rocks of the upper flows undergo progressive alteration from plagioclase, uralite and magnetite assemblages to albite, quartz, carbonate and pyrite rich rocks containing minor Mg riebeckite and hematite. The more mafic, non-variolitic host rocks of the Cryderman Zone have a most altered wall rock assemblage characterized by carbonate, plagioclase and hematite with significant amounts of quartz and pyrite. Progressing towards the most altered areas within the mineralized zones the pyrite concentration increases whereas the iron oxide mineral concentrations decrease. Chlorite changes from relatively Fe-rich to relatively Mg-rich composition near the margin of the zone. Calcite is present at the fringes of the altered zones and is gradually replaced by dolomite and ankerite as alteration intensifies.

There are several differences between the two studied alteration zones in the Harker Lake area (Table 3.4.1). The Cryderman Zone is obviously larger and stronger in comparison to the small crosscutting zone in the Line 28+00E area. Whereas both areas have had significant formation of carbonate, quartz and pyrite, the Cryderman Zone has a greater

abundance of all three minerals. Also, the elimination of mafic minerals, such as amphibole and chlorite, and magnetite is more complete in the Cryderman Zone. The Cryderman zone is characterized by a large content of hematite (up to 20%) whereas hematite is only a minor component of the Line 28+00E zone. Plagioclase content is significantly less in the altered rocks of the Cryderman zone, in contrast to the altered variolitic flows on Line 28+00E. Finally, the two altered flows on Line 28+00E contain small amounts of both soda-rich amphibole and talc not observed in the larger Cryderman Zone. Notably, Mg riebeckite is not as common in the narrow envelope to the stockwork veins (i.e. in the most intensely altered zone).

Table 3.4.1. Mineral transformations between host rock and most altered rock in the two mineralized zones examined in the Harker Lake area.

-significant positive changes in mode:	
Cryderman Zone	-cb(35%), hem(18%), qtz(8%), py(5%)
L28+00E Area	-cb(20%), pl(5-10%), qtz(5%), py(5%), hem(2%)
-significant negative changes in mode:	
Cryderman Zone	-amp(40%), pl(10%), mag(4%), chl(3%), tnt(2%)
L28+00E Area	-amp(15%), chl(15%), mag(5%), ep(3%),

3.4.2 Summary of Dome Mine Area

Overall, samples from this area have been deformed and altered, obscuring regional metamorphic mineral assemblages. As a result of this alteration, which has imprinted a retrograde assemblage on most of the rocks of the Dome Mine area, it can be quite difficult to establish a typical metamorphic facies assemblage. Using the least altered sample from this area, D89-21, as a guide, the regional metamorphic assemblage is albitic plagioclase, uralite, epidote, magnetite plus or minus chlorite. This indicates that these rocks have undergone middle greenschist facies metamorphism at most (Winkler, 1979).

The retrograde assemblage is characterized by turbid albitic plagioclase, chlorite, and carbonate (predominantly calcite). Less abundant but still common are sphene/magnetite

grains and epidote. Quartz is present in all samples, as an alteration product, but it was probably a primary component in the V10 subunit and the more felsic interlayers in the V8 subunit. In addition, zircon(?) is found in the flows with higher quartz content. Apatite is only commonly seen in the V10 and LSPL (lowermost variolitic flow at the Porcupine Paymaster).

The retrograde effects are more advanced at the Dome Mine indicating more substantial hydrothermal activity. Whereas the Porcupine Paymaster rocks have between 10-20% carbonate, dominantly calcite, the rocks of the Dome have 15-25% carbonate, with dolomite dominant over calcite. Quartz is more prevalent due to advanced alteration, and this is amplified in rocks where it was a primary component. The Fe-Ti oxides, ilmenite and magnetite are usually almost completely converted to sphene at the Dome Mine. Finally, epidote is a far less common mineral in the rocks of the Dome Mine, occurring mostly in the best preserved examples. It is interesting to note that the least altered rock of all the samples is from the 99 Flow in the Dome Mine (sample D89-21). This illustrates the potential for pristine enclaves within deformed and altered terranes.

Several flows have more intermediate composition, indicated by their elevated quartz content (up to 20%). These include the LSPL and the Spherulitic and Broken Spherulitic Flows at the Dome Mine, and their stratigraphic equivalents on the Porcupine Paymaster section (the lowermost variolitic flow and the layered-varioles pillowed flow), as well as the units of the V10 subunit in both areas. The presence of apatite and zircon(?) in these flows also indicates a more felsic composition. Significantly these flows have anomalous textures associated with them, such as the broken varioles in the Broken Spherulitic Flow, the "flowy" texture in the Spherulitic Flow, and the "ropy" flow top of the V10 subunit. As well, they have higher concentrations of varioles.

In general, the variolitic flows in this section are similar in appearance, commonly containing textures representative of disequilibrium crystallization, such as distinctive, delicate, skeletal plagioclase crystals and dendritic oxides. The Key Flow has two styles of varioles; lensy varioles made up of many fan spherulites, and distinct varioles with well formed spherulites. There are varying degrees of preservation of the spherulitic textures. Massive parts do contain spherulites, commonly fan type, in their groundmass. This is more pronounced in the more felsic flows, such as the V10 subunit and the LSPL. Within

individual units, spherulites are more common in the finer grained parts near the top of flows.

Non-variolitic flows in the sampled sections include the 99 Flow, the uppermost flow of the Central Subgroup and the lowermost flow of the Gold Centre Subgroup. The 99 Flow has its primary sub-ophitic texture well preserved in coarse grained sections. It also has a very narrow flow top. The other two flows, though not rich in quartz, have well developed myrmekitic texture in their massive parts. Non-variolitic flows do not contain disequilibrium textures such as the spherulites and skeletal grains noted in the variolitic Vipond flows.

The mineral asemblages of the most altered samples of the units at the Dome Mine depend to a certain extent on the unit examined (Table 3.4.2).

Table 3.4.2 Mineralogy characteristic of the most altered assemblage of the Dome Mine stratigraphic units.

Unit	**Mineral Assemblage**
V10/Dac:	pl-chl-qtz-cb-ser-tnt-tur-py +rutile?
V8/Spher:	qtz-chl-ser-cb-tnt-py-tur
V8/Key:	cb-pl-qtz-ser-chl-tnt-tur-py
V8/99 Flow:	cb-qtz-ser-tnt-py-tur

The mineral compositions show some trends with respect to the intensity of alteration. The carbonate minerals observed progress from calcite, which is quite widespread in the Dome Mine area, to ferroan dolomite, which is concentrated near the core of the main alteration zones, especially associated with ore bodies. Chlorite composition, as indicated by anomalous birefringent colours, shows a distinct progression in only one suite of rocks, those from the 99 Flow. In this case, the well preserved sample D89-21 contains chlorite with relatively more iron than magnesium. With only moderate alteration, such as in D89-35, chlorite has become relatively Mg-rich. The highly altered D89-34 does not contain any chlorite for comparison. Other sample suites did not provide definitive estimations of any chlorite composition shifts towards ore. A progressive change in tourmaline composition was also not

evident. All tourmaline observed had blue-green to pink pleochroic colours indicating an Fe-rich composition, typical of schorl.

3.4.3 Comparisons and Conclusions

One of the objectives of this study is to look for evidence in the study areas to show similarity in the development of variolitic suites. An obvious characteristic is that all suites have varioles. The varioles are dominantly plagioclase spherulites although they may contain other textures indicative of disequilibrium crystal growth such as skeletal, dendritic and branching crystals. Some textural differences between the areas may have to do with the level of preservation. While uralite pseudomorphs of branching crystals can be found in the Harker Lake and M^{c}Diarmid Lake areas, almost all amphibole is altered to chlorite in the Dome Mine area. The chlorite tends to form patches rather than pseudomorphs and the deformation in the Dome Mine area is taken up primarily by the chlorite resulting in foliated masses unrelated to primary forms. Myrmekitic texture is common in both areas, in both variolitic and non-variolitic flows, but more commonly in the upper, evolved flows, such as the V10 subunit in the Dome Mine area.

The restricted extent of the section at M^{c}Diarmid Lake does not allow comparisons with the general progressions observed in the larger sections in the Harker Lake and Dome Mine areas. Massive portions of variolitic flows contain spherulitic textures in all suites and consistently this is most common in the upper part of the Harker and Dome sections. In addition, spherulites are most common in the upper, fine grained parts of the massive sections of variolitic flows, displayed particularly well by the flows in the M^{c}Diarmid Lake area. The upper parts of the variolitic suite in both areas have several characteristics more typical of felsic flows. This includes flow banded fragments in breccias, flowbanding in the flows and the characteristic texture at the top of the most felsic flows, called "ropy" in Timmins. Mineralogically, the upper parts of variolitic sections are more felsic, containing up to 20% quartz as well as minor apatite and zircon(?).

The development of plagioclase spherulites and other disequilibrium textures in the variolites could be indicative of crystallization from an undercooled melt. The combination of undercooling plus high viscosity in the more evolved flows explains the preponderance of

varioles in the upper parts of the variolitic suites. Crystal growth would be stabilized by the reduced elemental diffusivity in the more felsic liquids resulting from the extensive polymerization of silica tetrahedra in the melt. Textural variations, such as the change from small, closed spherulites in varioles near cooling surfaces to larger, more open spherulites toward the centre of the flow (e.g. M^{c}Diarmid Lake) reflect various degrees of undercooling at the point of crystallization (e.g. Lofgren, 1974).

Alteration studies show that the metasomatic changes in the rocks from the Harker Lake and Dome Mine areas are not similar. This may be a result of the fluid composition that altered the rocks, the size or intensity of the hydrothermal system, or the cumulative effects of the local lithology on the fluid composition. Deformation is more intense at the Dome Mine which results in more lensoid shapes, intense foliation, significant quartz vein emplacement in dilatencies, and more pathways for metasomatic fluids resulting in wider zones of alteration on the mine scale. In the Harker Lake area there is almost no penetrative deformation, resulting in narrow alteration zones characterized by brittle fracturing with very little significant vein development. Most of the alteration is *in situ* re-crystallization as a result of fluid-rock interaction in permeable zones of either primary origin (brecciated flow tops) or resulting from brittle fracture.

The altered zones in both areas have had strong addition of carbonate minerals, quartz and pyrite combined with the breakdown of mafic minerals and Fe-Ti oxides. Other characteristics are different. At the Dome Mine, alteration includes the formation of sericite, and tourmaline and the breakdown of sodic plagioclase. The alteration assemblage at Harker Lake includes formation of hematite and Na amphibole as well as stabilization of albite.

It is interesting to note that in both areas the alteration assemblages depend to a certain extent on the unit which is being metasomatized. The assemblages for the alteration suites studied are given below (minerals are listed in order of abundance and those which have their first letter capitalized comprise greater than an estimated 5% of the rock):

Harker Lake Area

Line 28+00E, Variolitic Flow:

Albite-Quartz-Magnetite-Carbonate-talc-sphene-apatite-hematite-pyrite

Line 28+00E, Massive Flow:

Albite-Carbonate-Quartz-Pyrite-chlorite-magnetite-sphene-hematite-apatite-Mg riebeckite

Cryderman Zone:

Carbonate-Albite-Hematite-Quartz-pyrite-magnetite

Dome Mine Area

99 Flow (V8):

Carbonate-Quartz-Sericite-sphene-pyrite-tourmaline

Key Flow (V8):

Carbonate-Plagioclase-Quartz-Sericite-chlorite-sphene-tourmaline-pyrite

Dacite Flow (V10):

Plagioclase-Chlorite-Quartz-Carbonate-sericite-sphene-pyrite-tourmaline-apatite-zircon

Overall, the assemblages shown are indicative of the progressive alteration in these various units. The differences can in part be explained by the level of alteration represented by the most altered samples in the various units studied. However, flow composition plays an important role in determining the alteration mineral assemblage.

4. Geochemistry of Variolitic Suites

4.1 Scope

This chapter documents the primary geochemical characteristics of variolites and variolitic suites in the study areas. Analysis of the trends of elemental changes in the rocks has led to a model of their development. All samples examined in this study have been affected by regional metamorphism and, in some cases, metasomatism. Samples discussed in this chapter represent the least altered examples available from the various areas. These include a fairly wide spectrum of alteration, especially in the Dome Mine area. In consideration of the alteration present, effort has been made to interpret those elements capable of discriminating primary magmatic trends and least affected by the metamorphism (see section 4.3 below).

In this work, techniques useful for mafic to felsic suites and relatively insensitive to low grade alteration effects have been used. One example is the Jensen Cation plot (Jensen, 1976), a ternary diagram which distinguishes rocks of komatiitic, tholeiitic and calc-alkaline affinity, as well as, giving rock type classification. The apices of the diagram are oxides, which are not normally affected by low grade metamorphism; total Fe oxides plus TiO_2, MgO, and Al_2O_3 expressed as molecular percentages. Interpretation of the diagram also relies upon field descriptions (e.g. colour) of the rocks which are commonly neglected factors in other plotting techniques. The AFM diagram (Irvine and Baragar, 1971) is also included for comparative purposes because of its extremely common usage. However, care must be exercised in its interpretation due to the mobile nature of the alkalis. Trace elements have been used to test for differentiation as well as to identify and separate individual units. REE plots are also quite useful as they are sensitive indicators of magma evolution in the same manner as incompatible elements such as Zr. Quantitative techniques, specifically the Pearce Element Ratio plots (Pearce, 1968) and trace element plots of Allégre *et al* (1978), were used to model petrogenesis of the variolitic suites using the geochemical data.

4.2 Analytical Methods

The samples chosen for this study have been analysed for major and trace elements by X-ray fluorescence (XRF) analysis, FeO and Fe_2O_3 by cold acid digestion (Wilson, 1955), rare earth elements (REE) plus Ta, Th, and U by instrumental neutron acitivation analysis (INAA) and volatile content (CO_2/H_2O, S, LOI) by various dispersion techniques. Hand specimens were split in two prior to analysis, one half having been kept for petrographic work. The other half was cleaned of all weathered material, veinlets and obvious contamination and crushed in a steel jaw crusher. The crushed material was then split several times to obtain a 50 to 80 g portion. This amount was pulverized in a tungsten carbide ring mill using a shatterbox apparatus and stored in sealed plastic bags. The ring mill was cleaned between samples and then pre-contaminated with a small amount of the next sample before the full sample was pulverized.

XRF:

All major oxides (reported as wt%) including P_2O_5 plus the trace elements Ba, Cr, Zr, Sr, Rb, Y, Nb, Zn, Ni, and V (reported as ppm) were determined by R. Hartree in the University of Ottawa laboratories by XRF analysis on fused glass discs using a Phillips 1410 x-ray fluorescence spectrometer. The discs are prepared by mixing a 1.3 g aliquot of powdered, homogenized whole rock material with 3.3 g lithium tetraborate and 0.433 g lithium carbonate and melting the mixture in a Pt crucible. This mixture results in a homogeneous, glass medium for analysis with sufficient and evenly distributed sample materials.

The sample is exposed to X-ray irradiation and the resultant fluorescence measured to determine specific element concentrations by ratioing the counts obtained to calibrated standards. A Rh α tube is used to produce X-rays because it results in better precision than the commonly used Cr α tube for determinations of the heavier elements (Cr and up) and is just as good for the lighter elements. The Rh α tube has low sensitivity for elements in the vicinity of the Ba peak (Ti, V included) but fortunately the rocks being studied have generally high concentrations of these elements. Internal checks were included by the lab at intervals of 3 or 4 analyses to monitor instrumental drift. Overlap of the fluorescence spectrum of

various elements present in the sample may add some error to analyses, in particular to the determination of V (overlap by Ti α and Cr ß peaks) and Zr (Sr ß peak) but the rocks studied have concentrations of these elements well above levels where detection and accuracy problems occur.

The laboratory reports less than 5% error relative to the oxide concentration present for most major elements. The lighter elements, in particular Na_2O, MgO and Al_2O_3, may have relative error as high as 10% for very low concentrations (< 2.0 wt%). The dectection limit for trace elements is 10 ppm and values reported less than this limit are suspect. Trace element concentrations reported are accurate to within 50% of the concentration present between 10 and 30 ppm (10 to 50 ppm for Ba), and to within 10% for concentrations greater than 30 ppm (50 ppm for Ba) (R. Hartree, pers. com.).

Duplicate analyses were routinely obtained for aproximately every tenth sample in this study. Analytical error has been estimated (as a percentage of concentration present) from these duplicates and is reported in Table 4.2.1. As a rule, analytical error estimated from the duplicate samples is much less than the labratory estimates.

INAA:

Analyses of the REE, Ta, Th and U were obtained by instrumental neutron-activation analysis at L'Institut de Génie Nucleaire, Ecole Polytechnique, Université de Montréal using the general technique of Gordon *et al* (1968). The analytical spectra have been corrected for interferences by U (Kennedy and Fowler, 1983), Th and other interfering elements. The analyses were performed on aproximately 2.0 g samples taken from the powdered, homogenized whole rock material. Analytical error for the LREE, Ta and Th is estimated by the labratory to be 5% based on replicate analyses of USGS standard rock powders. The estimated error for the HREE is higher, generally less than 10%, because of the lower abundance of these elements. Errors determined from a limited number of duplicate sample analyses (3) in this study generally fall well below these estimates (Table 4.2.1)

Fe Titration:

The method of Wilson (1955) enables the determination of the ferrous iron content in HF soluble silicate, carbonate and oxide minerals. Digestion of whole rock powders in cold HF releases Fe^{2+} to solution which is subsequently oxidized by a known amount of

Table 4.2.1: Average relative error in analyses of elements as estimated from duplicate analyses.

Element	n	Coefficient of Variation (%)	Method of Analysis	Element	n	Coefficient of Variation (%)	Method of Analysis
SiO_2	11	0.37	XRF	Zn	11	7.11	XRF
TiO_2	11	0.52	XRF	Ni	10	10.49	XRF
Al_2O_3	11	0.40	XRF	V	8	1.80	XRF
Fe_2O_3	85	5.72	Titration	La	3	1.14	INAA
FeO	85	1.25	Titration	Ce	3	1.45	"
Fe_{Total}	10	0.34	XRF	Nd	3	1.12	"
MnO	11	0.00	"	Sm	3	2.30	"
MgO	11	1.81	"	Eu	3	2.30	"
CaO	11	0.40	"	Tb	3	3.91	"
Na_2O	11	5.09	"	Dy	3	4.52	"
K_2O	10	0.52	"	Ho	3	1.46	"
P_2O_5	11	2.22	"	Yb	3	1.21	"
Ba	11	29.51	"	Lu	3	0.50	"
Cr	11	6.36	"	Ta	3	4.46	"
Zr	11	1.55	"	Th	3	2.20	"
Sr	11	1.17	"	U	3	2.17	INAA
Rb	7	6.66	"				
Y	11	2.43	"				
Nb	7	13.51	"				

ammonium metavanadate. The excess V^{5+} resulting from the oxidation reaction is then reduced by titration against potassium dichromate in conjunction with a standard amount of ferrous ammonium sulphate. The amount of ferrous iron in the rock can be calculated by the titration results. Fe_2O_3 is calculated by subtracting FeO determined in the titration (and expressed as Fe_2O_3) from the total iron measured by XRF analysis (expressed as Fe_2O_3). All samples were run in duplicate, some in quadruplicate, to determine error. The variations in the replicate analyses depend on the amount of Fe in a sample, with error generally rising for smaller FeO concentrations (especially less than 5%). Generally the relative error for FeO is 1.25% of the concentration present. Because Fe_2O_3 is normally present in small amounts, the corresponding relative error is significantly higher, averaging 5.7%.

Problems in precision arise in samples where there is abundant S present for the following reasons; 1) S may oxidize during the fusing process for the XRF analyses giving erroneous results due to weight gain in fused disc, 2) Pyrite, the prime host of S in these rocks, is not digested in the cold HF digestion and so does not contribute to the Fe^{2+} in solution (Studemeister, 1983). This results in Fe_2O_3 values for the sample which are too high, consequently resulting in misleading Fe^{3+}/Fe^{2+} values. Commonly, as a result of oxidation during fusion, the sum of all iron components is too large, making determination of overall oxidation state of the Fe difficult to establish. This problem is mostly encountered in samples from mineralized zones.

CO_2 and H_2O:

Mineral-bound CO_2 and H_2O concentrations in powdered samples of whole rock material were determined at the laboratories of the Geological Survey of Canada, in Ottawa using combustion to disperse the volatile phases in the sample which are then collected and measured by infrared detection. For these measurements, the lab reports plus or minus 0.1 ppm absolute error for both compounds and, for H_2O and CO_2 respectively, 5% and 3% error relative to the concentration present.

S:

Sulphur content of the whole rock samples was determined at Bondar-Clegg Laboratories, Ottawa, Ontario by a similar combustion/infrared detection method to the CO_2/H_2O measurements at the GSC. Absolute error in these measurements is plus or minus 0.01%, whereas relative error is 5% of the concentration present (at GSC).

Loss On Ignition (LOI):

LOI was determined for samples where volatiles were not analysed and also to provide checks on some volatile analysis totals. Samples of whole rock powders were heated to 1100°C for 1.5 to 2.0 hours to drive off volatile materials. The difference in weight before and after heating, giving loss on ignition, is expressed as a percentage of the initial weight. Problems in this process include oxidation of various elements (in particular Fe^{2+}) during the heating which results in added weight (oxygen) and low values for the LOI.

4.3 Effects of Low Grade Metamorphism on Element Mobility

The rocks of this study have all been altered to various degrees. They are all submarine units and likely to have been subjected to low grade alteration by circulating geothermal brines. In addition, they have experienced greenschist facies metamorphism. The effects of these processes on whole rock geochemistry are complex and must be considered from the point of view of primary and secondary mineralogy, initial rock permeability, subsequent deformation, volume changes and retrograde effects. This includes a survey of major and trace element mobility during seafloor metamorphism (and/or spilitization), regional metamorphism and deformation.

In order to avoid excessively altered rocks, sampling for this part of the study was concentrated where circulating fluids would have the least effect on the rocks. The massive central part of flows and pillow cores are commonly less affected by alteration although they must be examined carefully. Where possible samples were taken in these locations. Volcanic glass, common in flow breccias and pillow rims, is especially susceptible to alteration by circulating fluids (palagonitization) and was not sampled. Flows containing phenocrysts are not common in the sampled sections and where they do occur, the phenocryst phases are not a large proportion of the rock. Amygdules are more commonly present in the flows and in places it was not possible to avoid sampling amygdaloidal rock. Samples which contain phenocrysts or amygdules have been noted and avoided, if possible, when interpreting the volcanic suites.

The primary composition of submarine volcanic units is modified almost from the moment of extrusion. As burial takes place beneath the sea, one of the major effects is spilitization of mafic rocks. As described by Hughes (1973), spilitization is essentially low temperature metasomatism of basalts by infiltration of seawater. Spilitization changes the mineral assemblage of basalts, especially plagioclase and Ca-poor pyroxenes resulting in albitization of plagioclase and chloritization (Mg fixation). Ca is usually leached from the rock unless it is incorporated in epidote. Staudigal and Hart (1983) suggest the overall chemical mass balance of oceanic rocks is maintained by redeposition of leached elements into local vugs, veins and secondary mineralogy rather than disturbed by long distance

transport. The mineralogy of the rocks in this study (high proportion of albite, chlorite, epidote) indicate that spilitization was involved early in their metamorphic history.

Gélinas *et al* (1982) studied the heterogeneities of chemical modification in variously altered pillow basalts of the Abitibi, very similar to the rocks in this study. They found that samples having the largest number of mineral phases are most likely to have primary geochemical characteristics. This reflects the fact that the mineral assemblage of rocks becomes progressively simpler with increasing alteration due to leaching and chemical substitution by infiltrating fluids. In this respect, the fluid/rock mass ratio is the controlling factor in alteration of submarine volcanics (Ludden and Thompson, 1979; Michard *et al*, 1983). Gélinas *et al* (1982) found three general types of metamorphic assemblages in their study: 1) chlorite-epidote-actinolite, 2) chlorite-epidote, and 3) chlorite ± sericite. Only in the first type were the major elements considered to have been entirely immobile. Based on variation coefficients of the major oxides in the types 1) and 2), they found that essentially immobile oxides included P_2O_5, SiO_2, Al_2O_3, and TiO_2, moderately mobile oxides included MgO, FeO, Na_2O, and CaO, and highly mobile oxides included Fe_2O_3, S, H_2O, K_2O, and CO_2. In the third type of alteration, which included examples with silicification, all the elements had enhanced mobility, in particular MgO and FeO, but most "immobile" elements still had very minor variation. In general, the apparent "mobility" of the iron oxides is a result of changes in the redox state of the original iron due to reaction with the invading fluid. Gélinas *et al* (1982) note that the total iron content does not change drastically, especially in alteration types 1) and 2), as reflected in the consistent Fe/Mg ratios observed.

Condie *et al* (1977), reached similar conclusions regarding element mobility in Archean flows of the Barberton Greenstone Belt. They found that the chemical composition of least altered flows compare favourably with modern, unaltered flows. The study considered epidote and carbonate-chlorite alteration of Archean tholeiites: epidotization (up to 60% epidote) results in oxidation of iron, increase in Ca, depletion in H_2O, Na, Mg, K, Si, Ti, P, Zr, while carbonatization (up to 10% carbonate minerals) results in reduction of Fe, significant increase in CO_2 and H_2O, and depletion of Na, Ca, and Mn. Apparently, Condie *et al* (1977) did not allow for volume and specific gravity changes which may have been significant considering the influx/removal of volatiles indicated by the data. These changes

may give the impression of element mobility when they are simply being concentrated or diluted. It is possible that mobility of some of the major elements occurs only at the most elevated levels of alteration. In a study in the Abitibi Greenstone Belt, Jolly (1980) concluded that total Fe, TiO_2, MnO, Al_2O_3, and SiO_2, plus MgO to a lesser extent, provide reliable estimates of the primary abundances of metamorphosed Archean lavas. Based on results of these studies, it is possible to carefully use most major oxides for rock classification as long as the mineralogy of the samples is still relatively complex indicating low levels of alteration. Fewer oxides (e.g. TiO_2, Al_2O_3, P_2O_5) may also be studied in a restricted manner for samples with moderate to strong alteration.

Considerable work has been done using the "immobile trace elements" to establish the original affinity of altered or metamorphosed igneous rocks. Generally, the immobile elements are thought to be those of high field strength (HFS) which are difficult to complex and require considerable energy to carry in solution. These include the transition group elements, such as Ti, Zr, Y, Nb and P, and the rare earth elements. Menzies and Seyfried (1979) found no significant change in the distribution of these trace elements at greenschist facies and similar results were found at higher grades as well (Nicollet and Adriambololona, 1980). However, these ideas have been challenged by evidence suggesting that even these relatively insoluble elements may be moved under certain conditions (Hellman and Henderson, 1977; Hynes, 1980; Murphy and Hynes, 1986).

In terms of the REE, seafloor metamorphism does not seem to disturb the abundances and patterns of REE distribution in the vast majority of ocean floor basalts (Michard *et al*, 1983; Staudigal and Hart, 1983) due to relatively low water/rock ratio. In contrast, in palagonatized material, indicative of high water/rock ratios, the REE patterns and abundances may be very altered on a small scale of observation (Ludden and Thompson, 1979). Actinolite (or hornblende) and sphene are thought to be most responsible for maintaining balance (buffering) of REE at greenschist facies conditions beneath the ocean floor (Ludden *et al*, 1982; Michard *et al*, 1983), while plagioclase is not thought critical on the basis of strong Eu and Sr anomalies measured in ascending hydrothermal plumes. Other minerals which may affect the distribution of REE's at greenschist facies metamorphism include chlorite and clays (Humphris *et al*, 1978) and epidote (Ludden *et al*, 1982) as well as

accessory mineral phases such as apatite, zircon, monazite and xenotime (Grauch, 1989).

Ludden *et al* (1982) studied the samples of Gélinas *et al* (1982) in order to describe the mobility of some trace elements and the REE in Archean volcanic flows. They found that for lower grade metamorphism the HFS elements and the REE were immobile. In addition, they concluded that even under conditions of strong carbonate and potassium metasomatism the relative abundances of the HFS elements and REE remain unchanged although their absolute abundances were diluted by trace element-poor mineral phases such as calcite. Condie *et al* (1977) concluded that formation of up to 60% epidote and 10% carbonate (with chlorite) of metamorphic mineral assemblages did not affect the magmatic trends of the immobile trace elements identified in their study. This evidence seems to contradict other studies (Hynes,1980; Murphy and Hynes, 1986) which demonstrated variable mobility of the HFS elements and REE's involving carbonate-rich solutions in a regional metamorphic context. This contradiction may be due to two types of alteration associated with carbonate-rich fluids Ludden *et al* (1982): one which is essentially in equilibrium with the metavolcanic pile, and another which is enriched in certain trace elements and is characteristic of intensely altered, commonly mineralized, systems (Kerrich and Fryer, 1979).

There are several important factors to be considered when evaluating the extent of modification of an altered rock's primary composition. This includes the permeability and porosity of the rock, the original mineral phases and the composition of the invading fluid. One main point, as outlined by Humphris *et al* (1978) and Humphris (1984), is that whole rock major, trace element and REE mobility really depends on their abundance in the minerals being broken down and their distribution coefficients for the secondary minerals being formed. Thus the mobility of elements can be inferred through petrography and knowledge of the chemistry of mineral phases being destroyed. The breakdown of a mineral may point to changes in the whole rock abundances of elements known to be concentrated in that mineral. Coherence of behaviour of chemically similar elements during alteration is an important phenomenon and may provide additional evidence to support conclusions about the nature of the alteration process (Grant, 1986).

Most petrographic and geochemical studies of deformation zones indicate reactions involving the addition of volatiles, especially H_2O and CO_2 (Kerrich *et al*, 1977; Beach, 1980;

Brodie, 1980). Commonly there is also the addition of other components such as K, Ba, and Rb and depletion of SiO_2 and Na_2O (or K_2O) in the shear zone relative to undeformed equivalents (O'Hara, 1988). Volume changes are common in deformed rocks and they are important when calculating mass balance. Beach (1980) states that although local transport of chemical components in shear zones is common, overall, the shear zone behaves as a closed system and alteration is isochemical. The result of local transport is a homogenization of mineral compositions and elemental ratios throughout the deformation zone.

Metasomatic or metamorphic reactions commonly proceed at the same time as stress is being applied to the rocks. This usually results in a self-propogating process where the increased internal energy imparted by the applied stress enhances the reaction process, and the recrystallization enhances deformation (called strain softening) by decreasing the grain size of the minerals (Brodie, 1980) and producing phyllosilicates (O'Hara, 1988). These complex reactions between the fluid and rock during stress can create compositional layering and mobilize some components (notably silica and soda). This process is known as pressure solution (Kerrich *et al*, 1977). Mobilized components are usually redeposited nearby in dilatent features also caused by the deformation process. As the reactions wane, grain size will increase causing deformation to switch to dominantly dislocation creep (Beach, 1980). Kerrich *et al* (1977) indicate that pressure solution dominates in lower grade metamorphic regimes, such as greenschist facies, whereas isochemical dislocation creep is more common in higher grade terranes. They also postulate that the degree of chemical modification of the host rock is directly related to the amount of finite strain although O'Hara (1988) has documented that most chemical change associated with a thrust-related mylonite occurs in the early stages of deformation. Finally, Kerrich *et al* (1977) have shown that the specific gravity of rocks decreases with increasing deformation.

Ludden *et al* (1982) and Gélinas *et al* (1982) recommend restricting conclusions regarding the primary composition of Archean metavolcanic rocks to those characterized by either chlorite-actinolite-epidote, or at most, chlorite-epidote mineral assemblages. The secondary mineral assemblage is important as it determines which elements may remain in the altered rock and whether or not the alteration can be isochemical. In general, spilitization and other processes render Na and Ca highly unreliable for petrogenetic work. As well, the

mobility of the alkalis and alkaline earths, K, Rb, Sr, and Ba make them difficult to interpret. The nature of the altering fluids is important when estimations of element mobility are made (Hynes, 1980; Murphy and Hynes, 1986). In any case, interpretations of the geochemical composition of any metavolcanic rock must first consider the potential for extensive changes from the primary rock chemistry.

4.4 Geochemistry of the Harker Lake Area

4.4.1 Major Element Geochemistry of Units

For the discussion of the major element oxide patterns of the variolitic suite in the Harker Lake area, the whole rock data has been grouped and averaged according to the geological divisions described previously. Sample locations can be found on Maps 2.1.1 and 2.1.2. The major element data are presented in Table 4.4.1. Within units, and individual flows, variance in oxide concentrations sample to sample can be high, especially for elements of low concentration. Interpretations are restricted to oxides having the lowest variance.

Three cycles of volcanic activity are outlined by the major element data (Figure 4.4.1). These are represented by enrichment of oxides, such as SiO_2 and P_2O_5, and depletion of TiO_2, MgO, CaO and total Fe. In addition, the ratio of total Fe (as FeO) to MgO varies in a cyclical manner, increasing towards the top of each cycle. On the other hand, Al_2O_3 and P_2O_5 concentrations decrease and increase respectively quite smoothly throughout the section, apparently being much less affected by the individual cycles than the other oxides. The absolute change in concentration of these two oxides is not as great as some others. Fortunately, these two oxides do not have very much variability between samples from the same unit (less than 1.5% for aluminum and 10% for phosphorous) which adds significance to the observed trends.

The first cycle ends at the top of the phyric unit on Line 14+50E, and includes the underlying lower variolitic units. Oxides which increase through the cycle include SiO_2 (54 to 62 wt%), MnO (0.21 to 0.25 wt%), and P_2O_5 (0.22 to 0.32 wt%) whereas those that decrease include TiO_2 (1.81 to 0.97 wt%), Al_2O_3 (13.1 to 12.6 wt%), MgO (5.2 to 1.3 wt%), and CaO (8.2 to 5.5 wt%). Changes in other oxide abundances can not be distinguished from

Table 4.4.1a: Whole rock geochemistry, Lower Variolitic Flows, Harker Lake section.

	H-06	H-33	H-34	Mean	Std.Dev.	Co.Var.%
SiO_2	53.17	54.74	52.94	53.62	0.80	1.49
TiO_2	2.03	1.69	1.70	1.81	0.16	8.74
Al_2O_3	12.78	12.98	13.48	13.08	0.29	2.25
Fe_2O_3	4.53	2.6	3.04	3.39	0.83	24.36
FeO	9.41	9.63	10.53	9.86	0.48	4.92
MnO	0.22	0.18	0.22	0.21	0.02	9.12
MgO	4.50	5.13	5.82	5.15	0.54	10.47
CaO	8.86	7.71	7.94	8.17	0.50	6.08
Na_2O	3.37	3.02	3.12	3.17	0.15	4.64
K_2O	0.23	0.35	0.55	0.38	0.13	35.04
P_2O_5	0.23	0.21	0.21	0.22	0.01	4.35
H_2O^+						
S						
CO_2						
LOI	0.6	1.19	1.46	1.08	0.36	33.15
TOTAL	99.93	99.43	101.01	100.12	0.66	0.66
Ba ppm	14	40	48	34	14.5	42.69
Cr	59	73	120	84	26.1	31.06
Zr	145	165	116	142	20.1	14.17
Sr	124	110	99	111	10.2	9.22
Rb		7	10	9	1.5	17.65
Y	63	72	51	62	8.6	13.87
Nb	4	4	3	4	0.5	12.86
Zn	70	69	93	77	11.1	14.33
Ni	44	43	66	51	10.6	20.81
V	551	392	435	459	67.2	14.62
La	7.6	8.2	6	7.3	0.9	12.78
Ce	21.7	24.2	18.8	21.6	2.2	10.23
Nd	18.3	21.1	14.7	18.0	2.6	14.53
Sm	6.0	6.7	4.7	5.8	0.8	14.29
Eu	1.84	2.18	1.60	1.87	0.24	12.70
Tb	1.54	1.71	1.24	1.50	0.19	12.98
Dy	8.9	10.3	6.8	8.7	1.4	16.60
Ho	1.90	2.30	1.61	1.94	0.28	14.61
Yb	6.0	6.6	5.3	6.0	0.5	8.90
Lu	1.08	1.16	0.80	1.01	0.15	15.23
Ta	1.01	1.12	0.77	0.97	0.15	15.12
Th	0.64	0.60	0.39	0.54	0.11	20.18
U	0.16	0.13	0.21	0.17	0.03	19.80
Fe_T	13.44	11.94	13.23	12.87	0.66	5.14
Fe/Mg	2.99	2.33	2.27	2.50	0.32	12.96
La/Yb	1.27	1.24	1.13	1.22	0.06	4.81

Table 4.4.1b: Whole rock geochemistry, Phyric Intermediate Flows, Harker Lake section.

	H-35	H-36	H-37	Mean	Std.Dev.	Co.Var.%
SiO_2	63.85	62.25	61.15	62.42	1.11	1.78
TiO_2	0.90	0.98	1.02	0.97	0.05	5.16
Al_2O_3	12.33	12.76	12.62	12.57	0.18	1.42
Fe_2O_3	2.99	2.75	2.80	2.85	0.10	3.63
FeO	8.73	9.20	10.68	9.54	0.83	8.71
MnO	0.23	0.26	0.26	0.25	0.01	5.66
MgO	1.05	1.70	1.25	1.33	0.27	20.39
CaO	5.15	4.93	6.26	5.45	0.58	10.69
Na_2O	4.21	4.58	1.74	3.51	1.26	35.92
K_2O	0.23	0.41	0.84	0.49	0.26	51.87
P_2O_5	0.32	0.30	0.34	0.32	0.02	5.10
H_2O^+						
S						
CO_2						
LOI	0.01	0.31	0.65	0.32	0.26	80.86
TOTAL	100.00	100.43	99.61	100.01	0.33	0.33
Ba ppm	58	93	269	140	92.3	65.95
Cr	30	28	34	31	2.5	8.13
Zr	280	256	258	265	10.9	4.11
Sr	62	74	236	124	79.3	63.99
Rb		6	18	12	6.0	50.00
Y	107	98	105	103	3.9	3.73
Nb	7	7	10	8	1.4	17.68
Zn	48	54	216	106	77.8	73.42
Ni	31	7	14	17	10.1	58.14
V	n.d.	n.d.	n.d.			
La	12.4	11.1	13.6	12.4	1.0	8.26
Ce	39.3	35.3	38.7	37.8	1.8	4.66
Nd	30.8	27.8	30.2	29.6	1.3	4.38
Sm	10.4	9.5	10.2	10.0	0.4	3.85
Eu	2.86	2.78	3.31	2.98	0.23	7.82
Tb	2.68	2.47	2.52	2.56	0.09	3.50
Dy	15.2	13.7	15.0	14.6	0.7	4.54
Ho	3.6	3.5	3.5	3.5	0.0	1.33
Yb	10.7	9.9	10.5	10.4	0.3	3.28
Lu	1.80	1.68	1.71	1.73	0.05	2.95
Ta	2.29	1.77	1.47	1.84	0.34	18.38
Th	1.09	0.92	1.07	1.03	0.08	7.39
U	0.39	0.17	0.24	0.27	0.09	34.41
Fe_T	11.39	11.64	13.17	12.07	0.79	6.51
Fe/Mg	10.85	6.85	10.54	9.05	1.81	20.05
La/Yb	1.16	1.12	1.30	1.19	0.07	6.27

Table 4.4.1c: Whole rock geochemistry, Non-variolitic Flows, Harker Lake section.

	H-38	H-08	H-39	45722	H-24	H-23	H-22	H-20	Mean	Std.Dev.	Co.Var.%
SiO_2	47.45	47.84	50.05	50.88	49.05	52.03	48.01	46.86	49.02	1.60	3.27
TiO_2	2.88	2.59	2.45	2.47	2.46	2.53	2.8	2.32	2.56	0.17	6.50
Al_2O_3	12.14	13.35	12.15	12.17	12.25	12.49	12.52	13	12.51	0.39	3.15
Fe_2O_3	3.47	4.37	4.4	5.34	3.14	1.94	2.57	2.4	3.45	1.03	29.86
FeO	13.12	12.24	11.32	8.23	12.69	11.48	13.29	13.17	11.94	1.48	12.40
MnO	0.32	0.26	0.28	0.2	0.21	0.25	0.2	0.2	0.24	0.04	16.55
MgO	6.54	6.2	5.78	4.39	5.41	4.96	6.42	7.24	5.87	0.81	13.89
CaO	8.72	9.1	7.43	9.92	8.6	7.34	7.42	7.42	8.24	0.86	10.49
Na_2O	2.58	2.2	3.54	2.78	2.27	2.39	2	1.43	2.40	0.54	22.55
K_2O	0.38	0.75	0.67	0.59	0.35	0.44	0.1	0.37	0.46	0.18	40.12
P_2O_5	0.35	0.26	0.29	0.25	0.25	0.27	0.33	0.22	0.28	0.04	13.88
H_2O^+				1.8							
S				0.14							
CO_2				0.5							
LOI	1.75		0.95	2.44	2.80	2.88	3.39	4.06	2.61	0.89	34.12
TOTAL	99.70	99.16	99.31	99.66	99.48	99.00	99.05	98.69	99.26	0.31	0.31
Ba ppm		44	78		34	42		90	58	20.2	35.09
Cr	132	71	55	28	97	56	76	103	77	28.8	37.28
Zr	88	94	111	91	85	114	105	76	96	11.7	12.30
Sr	92	99	197	112	69	79	100	85	104	35.1	33.74
Rb	3	26	22	8	7	7		8	12	7.6	65.37
Y	41	32	40	41	40	44	43	37	40	3.3	8.36
Nb			5		5	4	4		5	0.4	9.94
Zn	91	149	73	108	93	112	112	109	106	19.5	18.40
Ni	101	34	47	36	68	48	45	81	58	20.9	36.32
V	521	570	568	542	540	519	447	478	523	37.6	7.18
La	4.0		4.6		3.9	4.7	5.1	4.0	4.4	0.4	9.40
Ce	12.5		13.9		12.0	14.8	15.3	12.2	13.5	1.2	8.89
Nd	9.9		11.0		10.0	11.2	12.2	9.8	10.7	0.8	7.53
Sm	3.5		3.8		3.3	3.9	4.2	3.1	3.6	0.3	9.50
Eu	1.50		1.52		1.31	1.42	1.66	1.23	1.44	0.13	9.08
Tb	0.90		1.02		0.87	0.98	1.06	0.82	0.94	0.08	8.35
Dy	5.5		6.0		5.2	6.0	5.9	4.8	5.6	0.4	7.48
Ho	1.31		1.25		1.12	1.29	1.36	0.92	1.21	0.14	11.39
Yb	3.5		3.9		3.4	4.1	4.0	3.2	3.7	0.3	8.39
Lu	0.58		0.66		0.60	0.68	0.66	0.53	0.62	0.05	7.94
Ta	0.39		0.67		0.57	0.54	0.43	0.24	0.47	0.13	27.17
Th	0.32		0.38		0.21	0.34	0.44	0.25	0.32	0.07	21.97
U			0.09		0.08	0.11	0.08	0.07	0.09	0.01	14.40
Fe_T	16.20	16.12	15.23	12.98	15.48	13.20	15.57	15.30	15.01	1.09	7.28
Fe/Mg	2.48	2.60	2.64	2.96	2.86	2.66	2.43	2.11	2.56	0.25	9.59
La/Yb	1.14		1.18		1.15	1.15	1.28	1.25	1.19	0.05	4.46

Table 4.4.1d: Whole rock geochemistry, Spherulitic Basalt Flows, Harker Lake section.

	H-19	H-18	H-17	Mean	Std.Dev.	Co.Var.%
SiO_2	55.70	54.48	54.75	54.98	0.52	60.95
TiO_2	2.09	2.24	2.10	2.14	0.07	3.19
Al_2O_3	11.79	12.18	11.75	11.91	0.19	1.63
Fe_2O_3	3.86	3.59	3.78	3.74	0.11	3.02
FeO	10.57	10.26	9.79	10.21	0.32	3.14
MnO	0.20	0.17	0.19	0.19	0.01	6.68
MgO	3.08	4.17	2.67	3.31	0.63	19.14
CaO	6.88	5.88	5.25	6.00	0.67	11.18
Na_2O	2.42	2.87	3.36	2.88	0.38	13.31
K_2O	0.10	0.35	0.11	0.19	0.12	61.91
P_2O_5	0.51	0.42	0.52	0.48	0.04	9.30
H_2O^+						
S						
CO_2						
LOI	1.71	2.47	3.84	2.67	0.88	32.97
TOTAL	98.91	99.08	98.11	98.70	0.42	0.43
Ba ppm		66	6	36	30.0	83.33
Cr	27	30	34	30	2.9	9.45
Zr	267	214	188	223	32.9	14.74
Sr	122	137	84	114	22.3	19.51
Rb		6		6	0.0	0.00
Y	81	66	65	71	7.3	10.36
Nb	9	3	4	5	2.6	49.21
Zn	96	95	98	96	1.2	1.29
Ni	28	26		27	1.0	3.70
V	184	276	3	154	113.4	73.48
La	10.1	9.0	9.0	9.4	0.5	5.54
Ce	29.5	26.8	27.0	27.8	1.2	4.42
Nd	23.3	21.2	20.8	21.8	1.1	5.04
Sm	8.1	7.0	7.1	7.4	0.5	6.71
Eu	2.77	2.41	2.47	2.55	0.16	6.18
Tb	2.07	1.77	1.68	1.84	0.17	9.06
Dy	11.7	10.6	10.2	10.8	0.6	5.85
Ho	2.7	2.4	2.2	2.4	0.2	8.44
Yb	8.0	6.7	6.4	7.0	0.7	9.87
Lu	1.30	1.13	1.11	1.18	0.09	7.22
Ta	0.99	0.86	0.75	0.87	0.10	11.32
Th	0.74	0.68	0.74	0.72	0.03	3.93
U	0.12	0.18	0.18	0.16	0.03	17.68
Fe_T	14.00	13.45	13.15	13.53	0.35	2.60
Fe/Mg	4.55	3.23	4.93	4.09	0.73	17.80
La/Yb	1.26	1.34	1.41	1.33	0.06	4.42

Table 4.4.1e: Whole rock geochemistry, Variolitic Intermediate Flows, Harker Lake section.

	H-16	H-15	H-27	H-40	H-41	Mean	Std.Dev.	Co.Var.%
SiO_2	59.09	61.24	60.82	64.38	62.05	61.52	1.73	2.81
TiO_2	1.69	1.47	1.39	1.42	1.54	1.50	0.11	7.11
Al_2O_3	11.42	11.27	11.14	10.71	11.40	11.19	0.26	2.32
Fe_2O_3	2.49	5.37	3.04	4.51	4.47	3.98	1.05	26.51
FeO	12.31	7.43	10.19	7.60	7.69	9.04	1.92	21.27
MnO	0.25	0.19	0.21	0.16	0.16	0.19	0.03	17.43
MgO	2.73	1.74	2.11	1.31	1.63	1.90	0.49	25.51
CaO	3.73	4.25	3.89	3.76	3.16	3.76	0.35	9.35
Na_2O	2.16	4.44	2.80	3.70	3.98	3.42	0.83	24.16
K_2O	0.08	0.08	0.14	0.09	0.10	0.10	0.02	22.73
P_2O_5	0.68	0.58	0.56	0.60	0.56	0.60	0.04	7.47
H_2O^+		1.50	2.90			2.20	0.70	31.82
S		0.05	0.08			0.07	0.02	23.08
CO_2		0.60	0.80			0.70	0.10	14.29
LOI	2.60	2.15	3.78	1.39	2.41	2.47	0.78	31.44
TOTAL	99.23	100.21	100.07	99.63	99.15	99.66	0.43	0.43
Ba ppm	26	17	57	13	41	31	16.3	52.77
Cr	41	33	30	29	25	32	5.4	16.94
Zr	299	304	312	282	300	299	9.8	3.28
Sr	188	64	69	61	50	86	51.2	59.24
Rb								
Y	83	91	93	84	91	88	4.1	4.61
Nb	5	7	8	5	6	6	1.2	18.81
Zn	148	68	143	80	93	106	32.9	30.95
Ni	8	14	22	5	6	11	6.3	57.50
V								
La	12.0	11.4	12.2	10.5	11.7	11.6	0.6	5.15
Ce	34.9	35.3	39.2	31.9	35.6	35.4	2.3	6.57
Nd	29.1	28.7	29.0	25.7	29.8	28.5	1.4	5.01
Sm	9.1	9.1	9.7	8.0	9.3	9.0	0.6	6.24
Eu	3.03	2.91	2.83	2.85	3.08	2.94	0.10	3.36
Tb	2.26	2.27	2.43	2.04	2.34	2.27	0.13	5.70
Dy	14.2	13.2	13.7	11.8	13.2	13.2	0.8	6.06
Ho	2.8	2.9	3.1	2.7	3.3	3.0	0.2	7.28
Yb	9.0	8.9	9.3	8.2	8.6	8.8	0.4	4.25
Lu	1.54	1.51	1.56	1.38	1.50	1.50	0.06	4.19
Ta	0.80	1.22	1.07	0.93	1.44	1.09	0.22	20.46
Th	0.87	0.95	0.95	0.76	1.00	0.91	0.08	9.28
U	0.26	0.22	0.31	0.17	0.21	0.23	0.05	20.33
Fe_T	14.52	12.20	12.89	11.61	11.66	12.58	1.08	8.56
Fe/Mg	5.32	7.01	6.11	8.86	7.16	6.61	1.19	17.97
La/Yb	1.33	1.28	1.31	1.28	1.36	1.31	0.03	2.35

Table 4.4.1f: Whole rock geochemistry, Upper Massive Flow, Harker Lake section.

	H-11	H-12	H-29	Mean	Std.Dev.	Co.Var.%
SiO_2	58.40	52.23	57.70	56.11	2.76	4.92
TiO_2	1.99	2.51	1.83	2.11	0.29	13.76
Al_2O_3	11.68	12.17	11.17	11.67	0.41	3.50
Fe_2O_3	4.96	4.87	3.62	4.48	0.61	13.64
FeO	9.03	11.48	9.44	9.98	1.07	10.73
MnO	0.19	0.24	0.18	0.20	0.03	12.91
MgO	3.25	4.16	2.86	3.42	0.54	15.91
CaO	5.07	6.15	4.39	5.20	0.72	13.93
Na_2O	3.27	2.56	2.77	2.87	0.30	10.39
K_2O	0.18	0.61	0.18	0.32	0.20	62.69
P_2O_5	0.53	0.37	0.65	0.52	0.11	22.20
H_2O^+	2.5		2.9	2.7	0.2	7.41
S	0.07		0.01	0.04	0.03	75.00
CO_2	0.1		0.4	0.3	0.2	60.00
LOI	2.67	2.25	3.31	2.74	0.44	15.89
TOTAL	101.22	99.60	98.10	99.64	1.27	1.28
Ba ppm	65	142	32	80	46.1	57.85
Cr	50	38	32	40	7.5	18.71
Zr	249	141	273	221	57.4	25.98
Sr	159	139	97	132	25.8	19.62
Rb		14		14	0.0	0.00
Y	69	52	76	66	10.1	15.35
Nb	6	5	4	5	0.8	16.33
Zn	89	111	51	84	24.8	29.62
Ni	24	16	5	15	7.8	51.93
V	42	225	2	90	97.1	108.27
La	8.5	7.1	9.4	8.3	0.9	11.36
Ce	23.5	18.6	30.3	24.1	4.8	19.88
Nd	21.7	15.6	23.7	20.3	3.4	16.94
Sm	6.9	5.1	8.0	6.7	1.2	17.93
Eu	2.58	2.04	3.05	2.56	0.41	16.14
Tb	1.72	1.25	1.89	1.62	0.27	16.71
Dy	9.9	7.8	10.8	9.5	1.3	13.23
Ho	2.3	1.6	2.5	2.1	0.4	18.82
Yb	6.8	5.3	7.6	6.6	1.0	14.52
Lu	1.17	0.85	1.26	1.09	0.18	16.09
Ta	0.98	0.57	0.89	0.81	0.18	21.63
Th	0.61	0.53	0.76	0.63	0.10	15.05
U	0.21	0.13	0.21	0.18	0.04	20.57
Fe_T	13.44	15.81	12.66	13.97	1.34	9.59
Fe/Mg	4.14	3.80	4.43	4.08	0.26	6.26
La/Yb	1.25	1.34	1.24	1.27	0.05	3.60

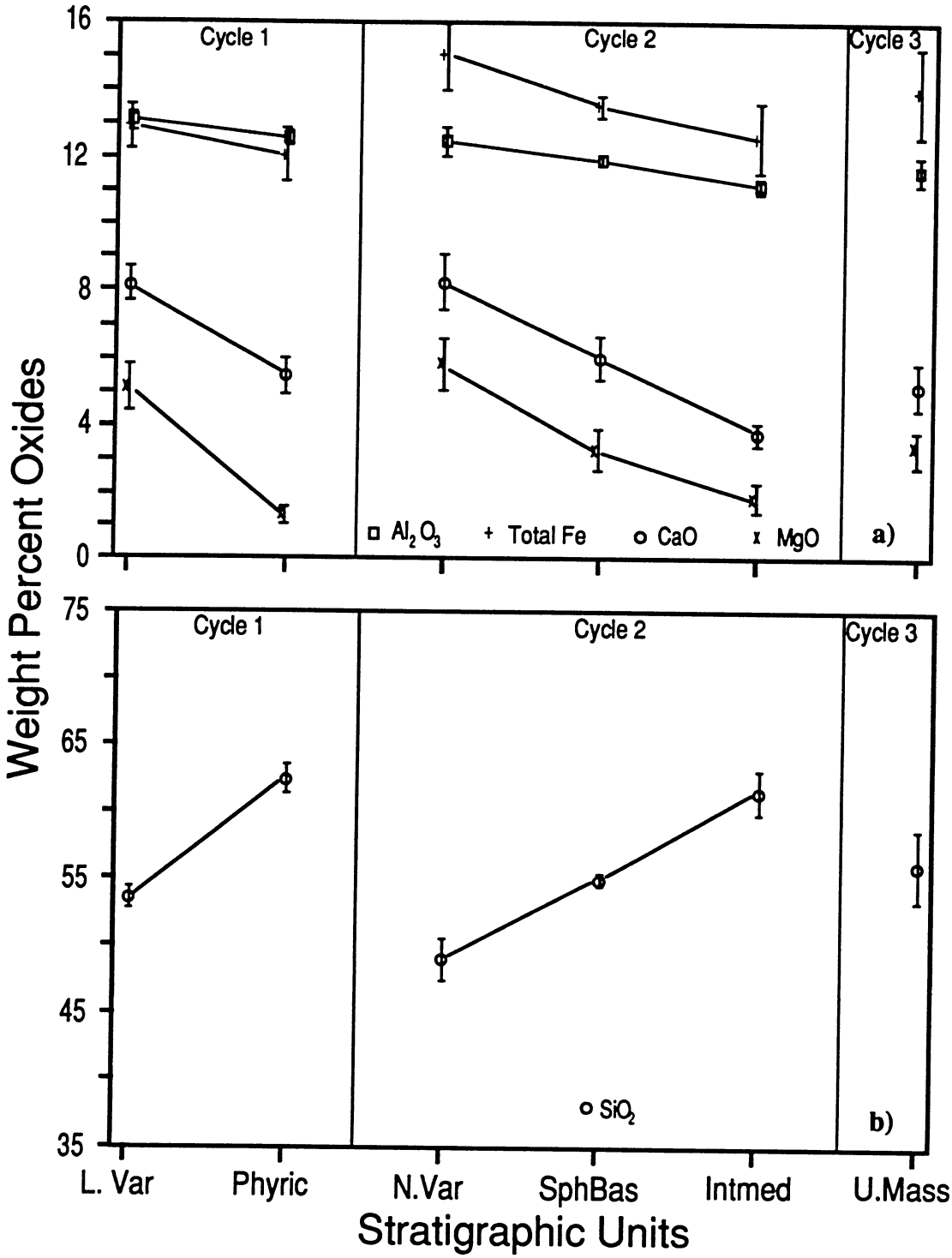

Figure 4.4.1: Averaged major element concentrations for the various subdivisions of the Harker Lake section stratigraphy (from Table 4.4.1). The trends in the concentrations define three volcanic cycles. Error bars represent twice the standard deviation. Unit abbreviations are as follows: L.Var - Lower Variolitic Flows, Phyric - Phyric Intermediate Flows, N.Var - Non-variolitic Flows, SphBas - Spherulitic Basalt, Intermed - Intermediate Variolitic Flows, U.Mass - Upper Massive Flow. a) Oxides of Al, Fe (total as FeO), Ca and Mg. b) Silica concentrations.

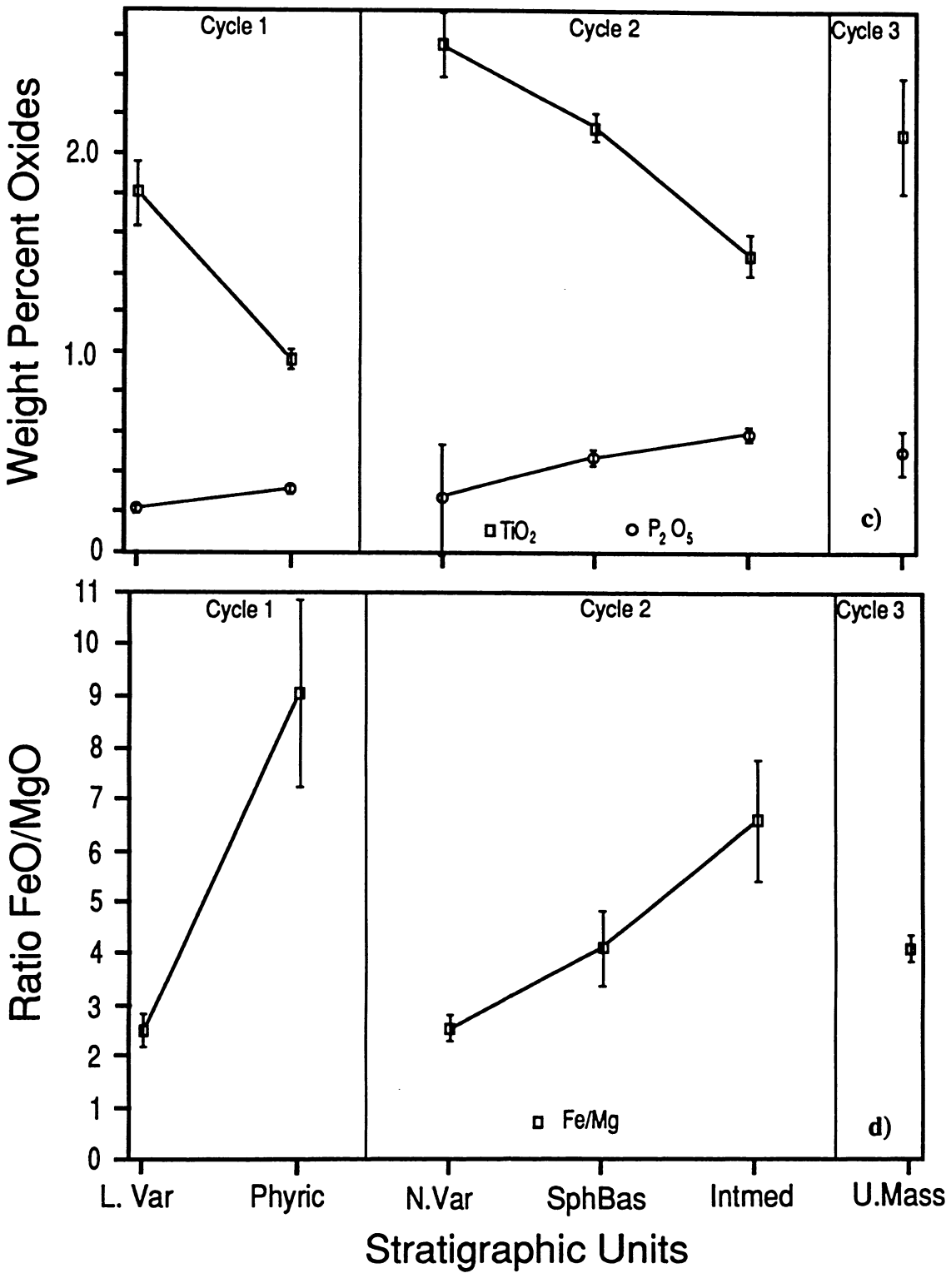

Figure 4.4.1: c) Oxides of Ti and P. d) Ratio of total Fe (as FeO) to Mg

their sample variance.

The second cycle extends from the non-variolitic, dominantly massive flows above the phyric unit to the intermediate, brecciated flows on Line 25+50E. Comparison of the major element data from the non-variolitic flows on Lines 14+50E and 25+50E confirms their geologic correlation (Table 4.4.1c). These flows are the most basic in the section. They are characterized by the lowest SiO_2 (49 wt%) concentration, and highest TiO_2 (2.3-2.9 wt%), total FeO (15 wt%), MgO (6.0 wt%) and CaO (7.7-8.8 wt%) concentrations of all the flows. The overlying spherulitic basalt and intermediate flows, are differentiated and have SiO_2 contents of 55 wt% and 61.5 wt% and TiO_2 contents of 2.14 wt% and 1.54 wt% respectively. MgO and CaO decrease progressively and significantly to an average 1.9 wt% and 3.8 wt% respectively in the intermediate flows. Total Fe decreases progressively, although there is considerable variance in concentration of Fe_2O_3 and FeO, especially in the intermediate flows. This may be a result of variable alteration in these flows which are brecciated. Na_2O increases slightly up section but this trend is obscured by the strong variance in the samples. The intermediate flows represent the most acidic compositions in the Harker Lake section.

The composition of the massive, uppermost flow of the sequence is again more basic, but not as basic as the non-variolitic flows. As there is no exposure of overlying flows on this section, it is not possible to see if there is a progression to more acidic composition up section. However, the samples do indicate some differentiation in the flow itself. Sample H-12, taken very near the base of the flow is quite distinct from samples H-11 and H-29 which were both taken higher up in the flow (Map 2.1.2). H-12 has significantly lower SiO_2 and P_2O_5 and higher TiO_2, Al_2O_3, total Fe, MnO, MgO, CaO, and K_2O than the other two samples. Due to the thickness of this flow, over 100 metres, slower cooling may have allowed differentiation.

The composition of the various variolitic flows of the Harker Lake section changes from bottom to top. The lowermost unit, the pillowed variolitic flow at the north end of Line 14+50E, is significantly more basic than the variolitic section just below the intermediate flows. Differences between the two units reflect the overall progression from mafic to more felsic rock throughout the section. The upper variolites have more SiO_2, and P_2O_5 and less of most other oxides including Al_2O_3, MgO, CaO and total Fe. The trend of the alkalis is less

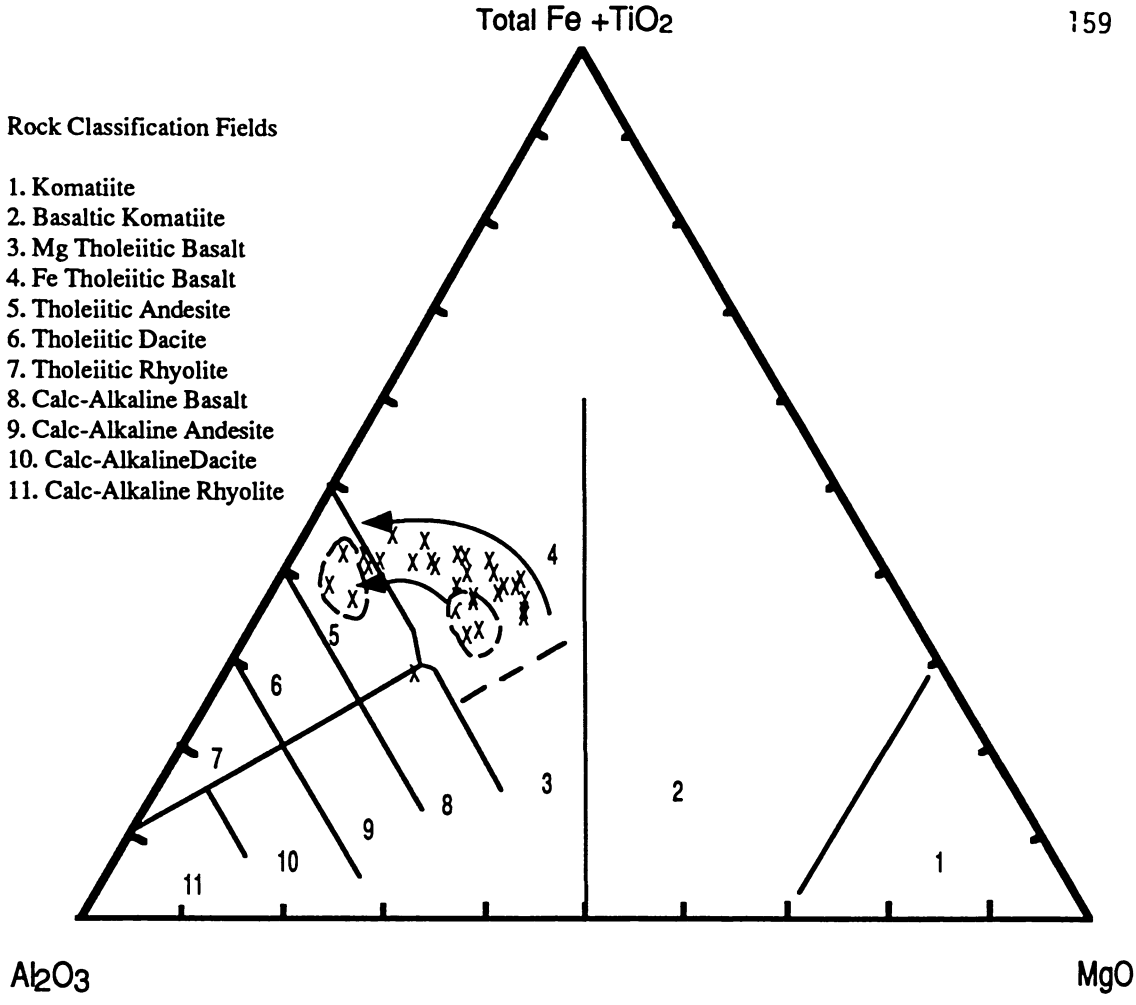

Figure 4.4.2: Jensen Cation plot for Harker Lake section. Samples define typical Fe-enrichment trends progressing to andesitic composition in the upper parts of the cycles. The progressions for the Lower Variolitic to Intermediate Phyric Flows (dashed fields, lower arrow) and the Non-variolitic to Intermediate Flows (upper arrow) are shown.

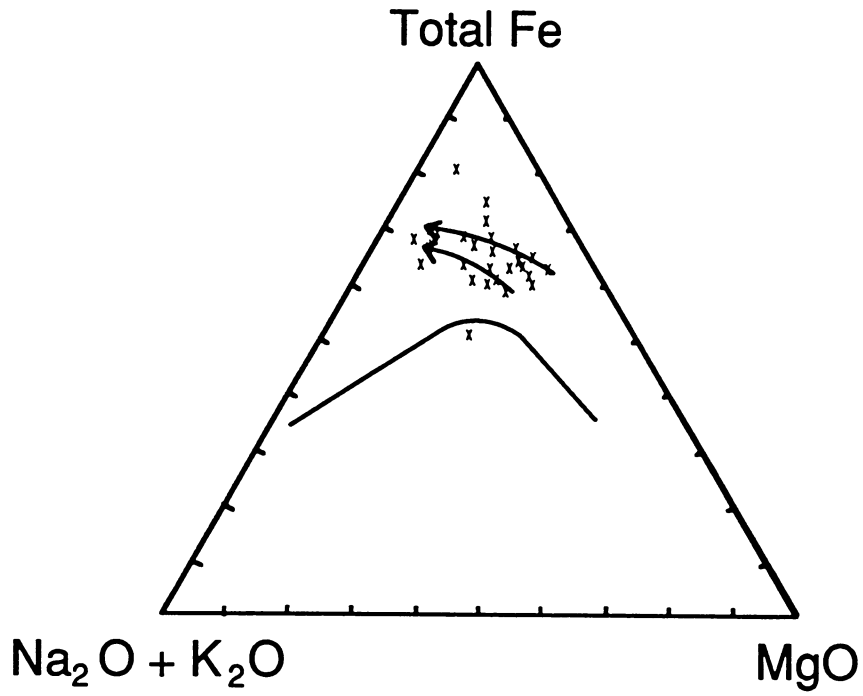

Figure 4.4.3: AFM plot for Harker Lake section, displays similar Fe-enrichment trends toward intermediate composition as noted in Figure 4.2.2. Lower arrow represents the lower cycle (Cycle 1) to the Phyric Flow, whereas the upper arrow represents Cycle 2 to the Intermediate flows on Line 25+50E. Line on diagam divides the tholeiite field (above) from the calc-alkaline field (below).

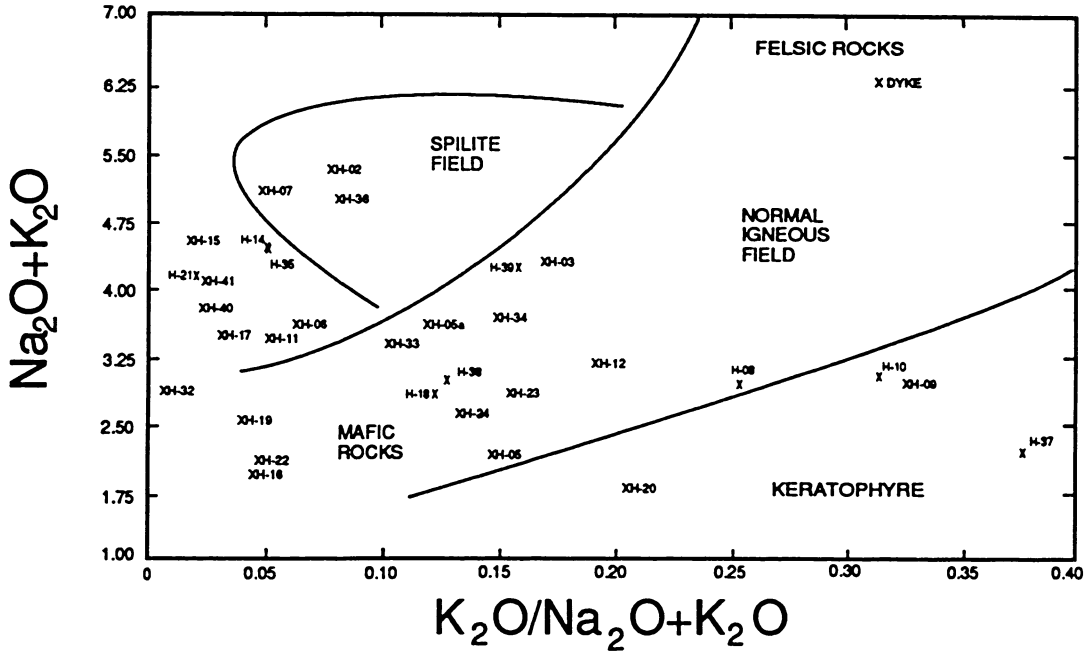

Figure 4.4.4: Diagram from Hughes (1973) to determine samples whose chemical composition indicates that they may have been spilitized. Most samples from the Harker Lake section plot in, or close to, the normal igneous field. Sample numbers are as shown.

definitive because the analytical error and intra-unit sample variance is greater the change in concentration observed. TiO_2 is greater in the upper variolite (2.14 wt%) than in the lower unit (1.81 wt%), possibly because fractionation of Fe-Ti oxides had not occurred. Fractionation of Fe-Ti oxides causes a rapid decrease in the concentration of Ti in particular, since it is generally in much smaller supply than Fe in a magma.

The Jensen cation plot (Jensen, 1976) shows typical tholeiite suite Fe enrichment trends, progressing towards more evolved compositions (Figure 4.4.2). Two trends can be identified; one from the lower variolitic flows to the phyric unit on Line 14+50E, and one for the non-variolitic to intermediate sequence. The second trend has higher associated Fe enrichment and a larger range of compositions. The upper, intermediate flows fall short of the andesite field on this plot. An AFM plot (Irvine and Baragar, 1971) of the Harker data is very similar to the Jensen cation plot (Figure 4.4.3). Most flows have compositions which would be expected in fresh rocks as defined on a diagram plotting total alkalis versus the ratio of K to total alkalis (Figure 4.4.4) (Hughes, 1973). Little emphasis is placed on interpretation of diagrams using the alkalis because of their well known mobility.

4.4.2 Trace Element Geochemistry of Units

The trace elements which have relatively consistent concentrations within flows include Zr, Y, Th, Cr, Ni, V and the REE. Other elements have too much intra-unit variation, such as Ba and Sr, due to alteration effects whereas the concentration of others, such as Nb and Rb, is too near detection limit to be interpreted with confidence. Trace element variation between samples of the same unit is in general more pronounced than the variation in major oxides (see Coefficient of Variation, Table 4.4.1). Consequently, not all the trace element trends are interpreted within the variolitic suite.

Cyclical variations of the compatible and incompatible trace elements are outlined in the diagrams in Figure 4.4.5. In the first volcanic cycle, the lower variolitic section contains much higher concentrations of the compatible elements, such as Cr, than does the phyric section. The difference in V concentrations is particularly large, with an average of 460 ppm in the variolitic flows, whereas it is less than 10 ppm (lower detection limit) in the samples of the phyric section. The incompatible elements Zr, Y and Th increase significantly in the

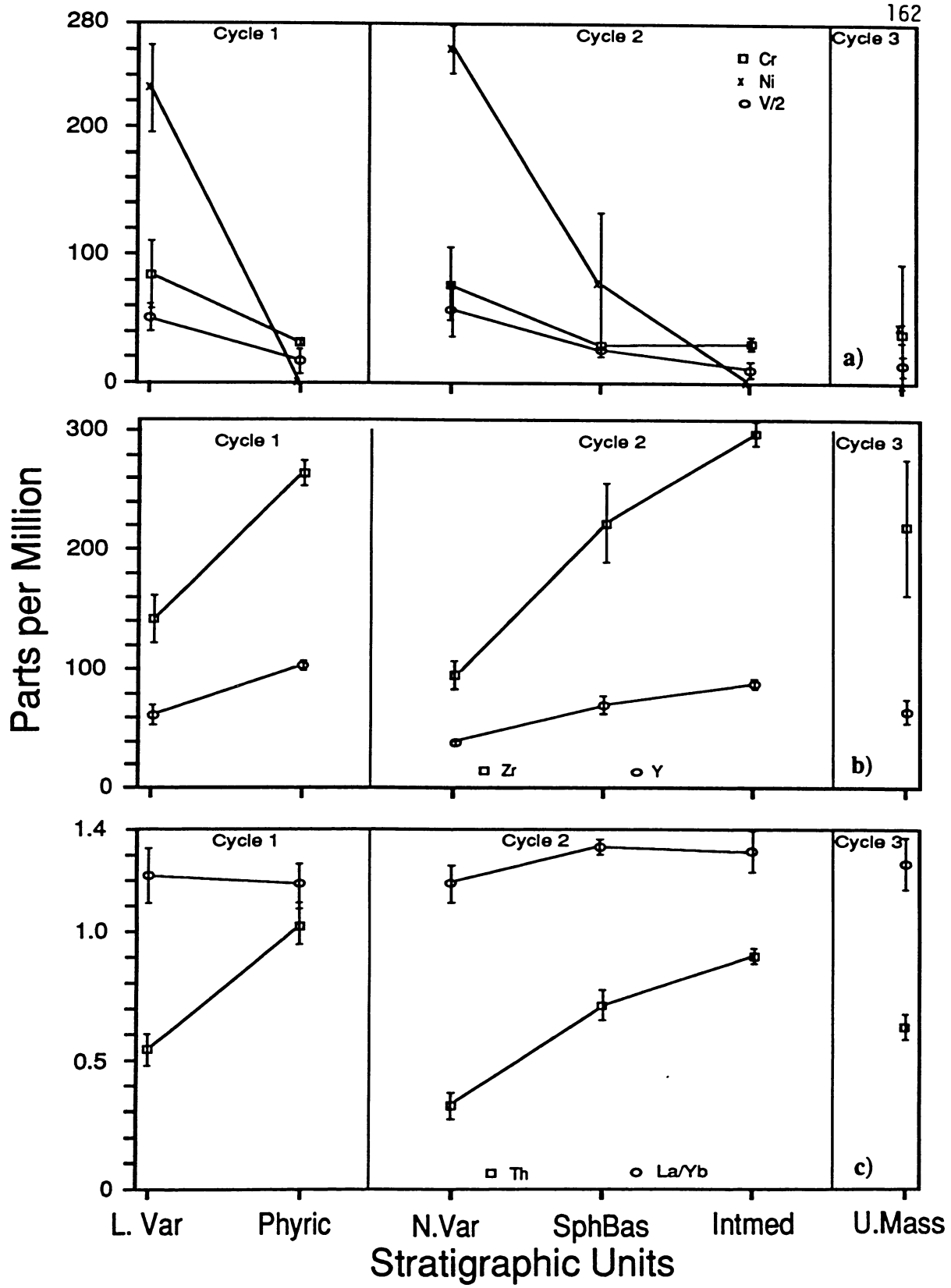

Figure 4.4.5: Averaged trace element concentrations for the various subdivisions of the Harker Lake section stratigraphy (from Table 4.4.1). Trends in the concentrations corroborate the major oxides, indicating three volcanic cycles. Abbreviations for the stratigraphic units are as in Figure 4.4.1. a) compatible elements Cr, Ni, and V. b) incompatible elements Zr and Y. c) incompatible element Th and ratio of La to Yb. Error brackets are equal to twice the standard deviation in all cases.

phyric section relative to the lower variolitic unit. These differences reflect the more acidic composition of the phyric flows. The incompatible REE have much higher concentration in the phyric flows, 35-60 times chondrite values, compared to the variolitic section which is 20-35 times. Consistent with field and petrographic data, sample H-3 (not included in Table 4.4.1b), which has generally more basic composition than the other phyric flows, has REE concentrations very similar to the variolitic samples.

Trace element concentrations in the second volcanic cycle have progressive trends reflecting the differentiation of the units. The compatible elements Cr, Ni and V decrease from average values of 80 ppm, 60 ppm, and 500 ppm, respectively, in the non-variolitic flows to 30 ppm, 20 ppm, and 150 ppm in the variolitic flows, and to 30 ppm, 10 ppm, and less than 10 ppm in the intermediate flows. The incompatible elements have increasing abundances from bottom to top of the cycle. Zr, Y and Th increase from about 95 ppm, 40 ppm and 0.3 ppm in the non-variolitic flows to 220 ppm, 70 ppm and 0.7 ppm in the variolitic flows and to 300 ppm, 90 ppm and 0.9 ppm in the intermediate flows. The REE also increase progressively from about 10-20 times chondrite values at the bottom of the cycle to 33-50 times at the top (Figure 4.4.6).

Throughout the Harker Lake section there is little fractionation of the REE associated with the increase in absolute concentration except for a slight increase in light REE (LREE) relative to heavy REE (HREE) in the upper parts of the cycle (see La/Yb ratios, Table 4.4.1, Figure 4.4.6). The REE patterns of the samples from the Harker section consistently have relatively flat profiles with slight LREE depletion. A significant negative Eu anomaly occurs in the uppermost, or more acidic, parts of the cycles. A similar anomaly also occurs in samples where varioles are concentrated (e.g. H-5, 5a, 6, Appendix 4.1).

Figure 4.4.7 shows the relationship of the Zr content of flows in the Harker Lake area to the Fe# (Fe# = FeO_{Total} / [FeO_{Total}+MgO], FeO_{Total} = FeO + $O.889Fe_2O_3$). A Zr versus Fe# plot monitors the differentiation of the suite using two different scales; the incompatible element Zr, which tends to be concentrated in the residual liquid during fractional crystallization processes, and the Fe#, which tends to increase as magma composition becomes more acidic because the more compatible oxide MgO is depleted early. Both Zr and the Fe/Mg ratio are generally unchanged in weakly to moderately metamorphosed rocks, thus

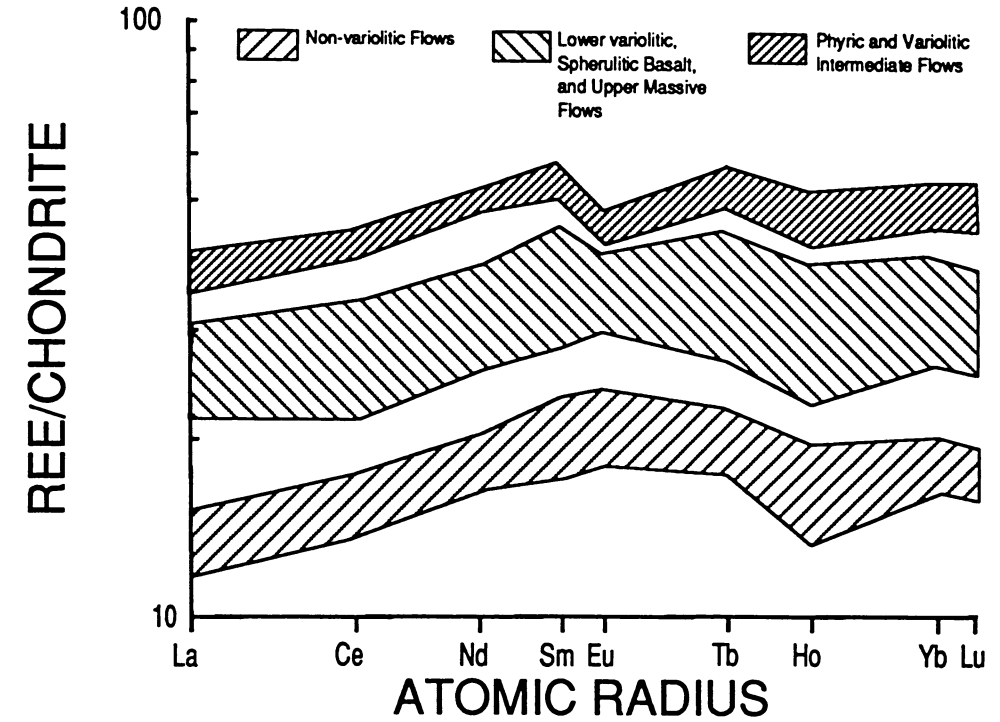

Figure 4.4.6: REE plots for selected samples from the Harker Lake section. Geological subdivisions are correlated with the appropriate profiles. There is some overlap between the three cycles.

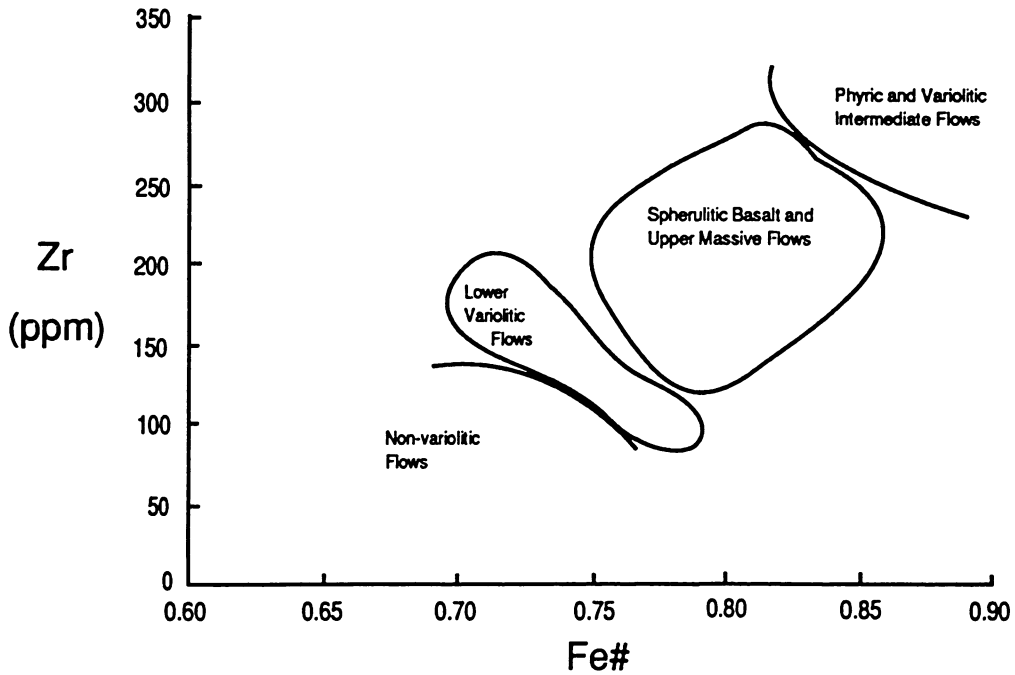

Figure 4.4.7: Zr vs Fe# (see text) plot for Harker Lake section. Geological subdivisions are labelled. This figure illustrates the progressive fractionation within the cycles of the Harker Lake suite.

the diagram closely reflects the primary trends in the volcanic suites. As the plot indicates, there is progressive fractionation of the rocks through each of the cycles described, with progressive increase in the base level of each cycle.

4.5 Geochemistry of the Dome Mine Area

4.5.1 Major Element Geochemistry of Units

The whole rock data for the suite of rocks examined in the Dome Mine area have been grouped according to the stratigraphic subdivisions at the Dome Mine (Table 4.5.1) because the stratigraphy is very well known here. The data are consistent with the mine units. In addition, the samples from the Porcupine Paymaster are easily correlated, by geochemical and geological means, with the Dome Mine units. As the samples from the Dome Mine area are quite altered, the discussion of the whole rock geochemistry is largely restricted to the least altered examples.

Overall, the suite shows a general progression towards more evolved rocks at the top of the Vipond Subgroup (Figure 4.5.1). Within the succession, there is evidence of three mini-cycles of differentiation, similar to, but not as well defined as, those of the Harker Lake section. In addition, flows with anomalous composition occur within the middle cycle (Broken Spherulitic, Spherulitic Flows), a feature not evident at Harker Lake.

The first cycle culminates at the top of the Lower Spherulitic Flow (LSPL) and includes the Lower Amygdaloidal Pillow Lava (LAPL), the uppermost unit of the Central Subgroup underlying the Vipond Subgroup. The lower parts of this cycle were not sampled. The LAPL is an Fe tholeiitic flow, closer to Mg tholeiite composition (Figure 4.5.2) than the Vipond subgroup. On average, the LAPL has an Fe/Mg ratio less than 2.0 compared to an Fe/Mg ratio greater than 4.0 for the LSPL. The value 2.0 is used to distinguish between rocks of Mg and Fe tholeiite affinity (Jensen, 1976). There is a significant increase in TiO_2, total Fe, and P_2O_5 and decrease in MgO and Al_2O_3 concentration in the LSPL versus the LAPL. These data reflect a progression from more Mg-rich to more Fe-rich rocks consistent with differentiation of tholeiitic suites.

The second cycle which includes most of the Vipond Subgroup is the only complete

Table 4.5.1a: Whole rock geochemistry, Lower Amygdaloidal Pillow Lava (LAPL), Central Subgroup, Dome Mine.

	D89-03	D89-19	D89-30	P89-13	Mean	Std.Dev.	Co.Var.%
SiO_2	46.22	48.00	48.94	44.98	47.04	1.54	3.27
TiO_2	0.85	0.86	0.77	0.82	0.83	0.04	4.24
Al_2O_3	12.87	13.05	13.05	13.83	13.20	0.37	2.81
Fe_2O_3	1.08	1.24	0.85	1.40	1.14	0.20	17.79
FeO	10.04	9.28	9.07	9.55	9.49	0.36	3.83
MnO	0.24	0.21	0.25	0.24	0.24	0.02	6.38
MgO	5.52	5.87	5.70	5.61	5.68	0.13	2.28
CaO	8.98	8.55	8.29	9.71	8.88	0.54	6.05
Na_2O	2.75	1.13	2.97	3.10	2.49	0.79	31.91
K_2O	0.02	0.98	0.01	0.08	0.27	0.41	150.22
P_2O_5	0.04	0.04	0.04	0.03	0.04	0.00	11.55
H_2O^+	4.3	4.8	4.1	5.4	4.7	0.5	10.81
S							
CO_2	7.7	6.9	6.3	7.0	7.0	0.5	7.12
LOI	12.0	11.7	10.4	12.4	11.6	0.7	6.45
TOTAL	100.61	100.91	100.34	101.75	100.90	0.53	0.52
Ba ppm	7	93	20	33	38	32.9	86.06
Cr	99	114	86	80	95	13.1	13.79
Zr	43	41	40	42	42	1.1	2.69
Sr	76	54	55	44	57	11.6	20.35
Rb	1	22	0	0	6	9.4	163.32
Y	17	20	19	21	19	1.5	7.68
Nb	1	0	0	0	0	0.4	173.21
Zn	144	190	110	128	143	29.7	20.76
Ni	71	69	57	70	67	5.7	8.50
V	320	303	281	304	302	13.9	4.59
La		2.3	2.1	2.4	2.3	0.1	5.50
Ce		6.4	6.9	6.8	6.7	0.2	3.22
Nd		6.0	5.5	5.7	5.7	0.2	3.58
Sm		1.9	1.7	1.8	1.8	0.1	4.54
Eu		0.63	0.60	0.60	0.61	0.01	2.32
Tb		0.44	0.43	0.52	0.46	0.04	8.69
Dy		2.9	3.2	3.4	3.2	0.2	6.49
Ho		0.68	0.65	0.71	0.68	0.02	3.60
Yb		2.1	1.9	2.3	2.1	0.2	7.78
Lu		0.36	0.35	0.39	0.37	0.02	4.64
Ta		0.67	0.44	0.50	0.54	0.10	18.15
Th		0.24	0.15	0.22	0.20	0.04	18.98
U		0.06	0.06	0.06	0.06		
Fe_T	11.00	10.38	9.83	10.79	10.50	0.45	4.27
Fe/Mg	1.99	1.77	1.72	1.92	1.85	0.11	5.94
La/Yb		1.10	1.11	1.04	1.08	0.03	2.51

Table 4.5.1b: Whole rock geochemistry, Lower Spherulitic Flow (LSPL), Dome Mine.

	D89-20	D89-32	P89-02	Mean	Std.Dev.	Co.Var.%
SiO_2	49.97	52.42	47.89	50.09	1.85	3.70
TiO_2	1.40	1.34	1.49	1.41	0.06	4.37
Al_2O_3	11.11	13.21	12.62	12.31	0.88	7.18
Fe_2O_3	1.44	7.37	3.44	4.08	2.46	60.33
Feo	9.72	6.66	10.61	9.00	1.69	18.80
MnO	0.24	0.20	0.19	0.21	0.02	10.29
MgO	2.38	3.08	3.61	3.02	0.50	16.66
Cao	10.16	6.06	8.41	8.21	1.68	20.46
Na_2O	3.10	3.55	2.63	3.09	0.38	12.14
K_2O	0.05	0.06	0.43	0.18	0.18	98.24
P_2O_5	0.22	0.25	0.12	0.20	0.06	28.26
H_2O^+	3.1	3.2	3.9	3.4	0.4	10.47
S	0					
CO_2	7.1	3.4	6.5	5.7	1.6	28.61
LOI	10.2	6.6	10.4	9.1	1.7	19.26
TOTAL	99.99	100.80	101.84	100.88	0.76	0.75
Ba ppm	0	18	82	33	35.2	105.57
Cr	36	62	70	56	14.5	25.92
Zr	93	105	82	93	9.4	10.06
Sr	127	188	114	143	32.3	22.56
Rb	0	0	3	1	1.4	141.42
Y	41	43	34	39	3.9	9.81
Nb	5	4	2	4	1.2	34.02
Zn	105	92	138	112	19.4	17.34
Ni	4	0	21	8	9.1	109.25
V	96	86	280	154	89.2	57.91
La	7.0	7.4	5.5	6.6	0.8	12.33
Ce	20.7	23.0	16.7	20.1	2.6	12.93
Nd	15.7	16.3	11.4	14.5	2.2	15.08
Sm	4.9	5.3	3.9	4.7	0.6	12.53
Eu	1.54	1.71	1.23	1.49	0.20	13.31
Tb	1.21	1.29	1.10	1.20	0.08	6.49
Dy	6.2	7.3	5.9	6.5	0.6	9.31
Ho	1.55	1.58	1.21	1.45	0.17	11.60
Yb	4.4	4.8	4.1	4.4	0.3	6.47
Lu	0.73	0.81	0.66	0.73	0.06	8.36
Ta	0.73	1.33	0.66	0.91	0.30	33.17
Th	0.65	0.65	0.52	0.61	0.06	10.10
U	0.20	0.20	0.08	0.16	0.06	35.36
Fe_T	11.00	13.21	13.67	12.63	1.17	9.23
Fe/Mg	4.62	4.29	3.79	4.18	0.34	8.23
La/Yb	1.59	1.54	1.34	1.50	0.11	7.21

Table 4.5.1c: Whole rock geochemistry, 99 Flow, Dome Mine.

	D89-12	D89-21	D89-35	9497	Mean	Std.Dev.	Co.Var.%
SiO_2	48.19	51.56	50.17	48.25	49.54	1.41	2.85
TiO_2	1.35	1.45	1.40	1.58	1.45	0.09	5.92
Al_2O_3	13.24	14.06	13.15	13.54	13.50	0.36	2.63
Fe_2O_3	4.96	5.62	4.16		4.91	0.60	12.15
FeO	8.70	8.94	9.56		9.07	0.36	4.00
MnO	0.22	0.20	0.21	0.27	0.23	0.03	11.97
MgO	4.94	5.38	5.39	3.50	4.80	0.77	16.11
CaO	5.68	5.14	5.91	8.11	6.21	1.13	18.23
Na_2O	4.57	5.52	3.06	1.72	3.72	1.45	38.98
K_2O	0.06	0.22	0.02	1.12	0.36	0.45	126.19
P_2O_5	0.13	0.14	0.13	0.16	0.14	0.01	8.75
H_2O^+	3.2	2.5	4.1		3.3	0.7	20.05
S							
CO_2	5.3	0.2	3.1		2.9	2.1	72.86
LOI							
TOTAL	100.54	100.93	100.36		100.61	0.24	0.24
Ba ppm	36	4	7	166	53	66.3	124.48
Cr	107	458	101		222	166.9	75.18
Zr	80	93	76	93	86	7.6	8.93
Sr	174	264	123	109	168	60.7	36.26
Rb	0	0	0		0	0.0	
Y	34	15	35		28	9.2	32.86
Nb	6	26	0		11	11.1	104.21
Zn	67	203	164	330	191	94.3	49.37
Ni	54	182	27		88	67.6	77.12
V	254	548	255		352	138.4	39.27
La		6.0	5.5	5.0	5.5	0.4	7.42
Ce		16.9	17.2	14.1	16.1	1.4	8.69
Nd		13.6	13.2	10.7	12.5	1.3	10.27
Sm		4.1	3.8	3.5	3.8	0.2	6.45
Eu		1.39	1.30	1.17	1.29	0.09	7.02
Tb		0.92	0.85	0.80	0.86	0.05	5.75
Dy		5.8	5.0	5.9	5.6	0.4	7.24
Ho		1.25	1.13	1.21	1.20	0.05	4.17
Yb		3.9	3.5	3.3	3.6	0.2	6.99
Lu		0.64	0.63	0.51	0.59	0.06	9.96
Ta		0.87	1.16	0.28	0.77	0.37	47.55
Th		0.50	0.46	0.46	0.47	0.02	3.98
U		0.17	0.13	0.11	0.14	0.02	18.25
Fe_T	13.10	13.94	13.26	11.55	12.96	0.87	6.74
Fe/Mg	2.65	2.59	2.46	3.30	2.70	0.32	12.03
La/Yb		1.54	1.57	1.52	1.54	0.02	1.50

Table 4.5.1d: Whole rock geochemistry, Broken Spherulitic Flow, Dome Mine.

	9498	D89-23	D89-37	Mean	Std.Dev.	Co.Var.%
SiO_2	59.97	55.93	65.49	60.46	3.92	6.48
TiO_2	0.86	1.01	0.74	0.87	0.11	12.72
Al_2O_3	11.02	15.75	11.20	12.66	2.19	17.29
Fe_2O_3	1.52	1.53	0.60	1.22	0.44	35.84
FeO	7.16	7.77	6.64	7.19	0.46	6.42
MnO	0.16	0.11	0.07	0.11	0.03	31.12
MgO	3.43	2.95	2.11	2.83	0.55	19.28
CaO	4.09	4.27	3.51	3.96	0.32	8.19
Na_2O	0.25	0.82	3.60	1.56	1.46	94.16
K_2O	1.84	2.51	0.13	1.49	1.00	67.08
P_2O_5	0.16	0.17	0.12	0.15	0.02	14.13
H_2O^+		4.1	2.4	3.3	0.9	26.15
S						
CO_2		3.3	2.8	3.1	0.3	8.20
LOI	7.35	7.40	5.20	6.65	1.03	15.42
TOTAL	97.79	100.22	99.41	99.14	1.01	1.02
Ba ppm	88	137	26	84	45.4	54.29
Cr	25	26	22	24	1.7	6.98
Zr	232	369	257	286	59.6	20.83
Sr	44	65	56	55	8.6	15.64
Rb		66	5	36	30.5	85.92
Y	73	139	96	103	27.4	26.64
Nb		12	6	9	3.0	33.33
Zn	80	109	86	92	12.5	13.64
Ni		2	5	4	1.5	42.86
V	110	101	67	93	18.5	19.98
La	10.8	20.4	15.6	15.6	3.9	25.12
Ce	29.2	62.1	46.3	45.9	13.4	29.29
Nd	22.9	47.0	33.3	34.4	9.9	28.69
Sm	7.5	14.6	10.7	10.9	2.9	26.55
Eu	1.87	3.15	2.51	2.51	0.52	20.82
Tb	1.99	3.53	2.64	2.72	0.63	23.21
Dy	14.3	21.9	15.7	17.3	3.3	19.09
Ho	2.70	5.22	3.70	3.87	1.04	26.75
Yb	8.4	15.0	11.1	11.5	2.7	23.56
Lu	1.33	2.53	1.82	1.89	0.49	26.02
Ta	0.59	2.15	1.93	1.56	0.69	44.29
Th	1.16	1.96	1.54	1.55	0.33	21.03
U	0.34	0.55	0.34	0.41	0.10	24.15
Fe_T	8.51	9.13	7.17	8.27	0.82	9.87
Fe/Mg	2.48	3.09	3.40	2.92	0.38	13.07
La/Yb	1.29	1.36	1.41	1.36	0.05	3.64

Table 4.5.1e: Whole rock geochemistry, Key Flow, Dome Mine.

	D89-08	D89-27	D89-39	9499	P89-06	P89-07	Mean	Std.Dev.	Co.Var. %
SiO_2	52.26	49.65	51.43	52.32	53.08	49.84	51.43	1.28	2.50
TiO_2	1.14	1.22	1.12	1.15	1.04	1.00	1.11	0.07	6.54
Al_2O_3	12.74	13.48	12.50	12.07	13.23	12.45	12.75	0.48	3.76
Fe_2O_3	1.22	1.43	1.31	1.40	2.98	2.03	1.73	0.62	35.73
FeO	9.15	9.88	9.27	7.96	8.02	7.55	8.64	0.84	9.72
MnO	0.20	0.19	0.19	0.19	0.22	0.16	0.19	0.02	9.24
MgO	4.96	5.11	4.41	4.07	5.22	4.21	4.66	0.45	9.67
CaO	6.14	6.86	7.55	7.02	7.34	8.80	7.29	0.81	11.11
Na_2O	3.50	0.98	1.85	2.77	2.35	2.70	2.36	0.79	33.51
K_2O	0.02	1.70	0.67	0.43	0.01	0.60	0.57	0.57	99.04
P_2O_5	0.08	0.08	0.07	0.11	0.08	0.07	0.08	0.01	16.45
H_2O^+	3.9	4.6	4.0		4.0	3.9	4.1	0.3	6.47
S	0.09		0.04				0.07	0.03	38.46
CO_2	4.7	4.7	5.9		3.2	6.2	4.9	1.1	21.52
LOI	8.69	9.30	9.94	9.63	7.20	10.10	9.14	0.98	10.75
TOTAL	100.10	99.88	100.31	99.12	100.77	99.51	99.95	0.53	0.53
Ba ppm	20	711	403	46		145	265	260.9	98.45
Cr	68	54	57	70	148	130	88	37.0	42.10
Zr	101	111	104	107	111	92	104	6.6	6.30
Sr	141	56	102	71	224	88	114	56.1	49.33
Rb		53	17			12	27	18.3	66.82
Y	41	47	42	36	46	24	39	7.7	19.67
Nb		3					3	0.0	0.00
Zn	126	140	132	62	115	154	122	29.2	24.02
Ni	61	40	41		85	46	55	17.0	31.05
V	308	343	299	270	270	271	294	26.8	9.12
La	5.9	6.3	6.3	5.9	6.5	3.7	5.8	0.9	16.47
Ce	17.0	17.9	18.7	16.4	20.4	11.9	17.1	2.6	15.45
Nd	11.7	13.7	13.2	12.1	14.7	9.0	12.4	1.8	14.64
Sm	3.9	4.5	4.5	4.3	4.7	3.3	4.2	0.5	11.25
Eu	1.26	1.25	1.26	1.10	1.37	0.99	1.21	0.12	10.31
Tb	0.98	1.11	1.09	0.95	1.13	0.87	1.02	0.09	9.29
Dy	7.1	7.2	6.1	6.9	6.8	5.3	6.6	0.7	10.16
Ho	1.37	1.51	1.54	1.42	1.55	1.24	1.44	0.11	7.63
Yb	4.5	4.7	4.6	3.9	4.9	3.3	4.3	0.5	12.72
Lu	0.72	0.80	0.76	0.67	0.83	0.58	0.73	0.08	11.50
Ta	0.99	0.65	0.86	0.39	0.48	0.74	0.69	0.21	30.21
Th	0.51	0.62	0.51	0.56	0.70	0.51	0.57	0.07	12.50
U	0.12	0.16	0.19	0.10	0.17	0.12	0.14	0.03	22.31
Fe_T	10.23	11.15	10.43	9.20	10.67	9.35	10.17	0.69	6.81
Fe/Mg	2.06	2.18	2.37	2.26	2.04	2.22	2.18	0.11	5.11
La/Yb	1.31	1.34	1.37	1.51	1.33	1.12	1.34	0.11	8.59

Table 4.5.1f: Whole rock geochemistry, Spherulitic Flow, Dome Mine.

	D89-41	9500	P89-04	Mean	Std.Dev.	Co.Var.%
SiO_2	66.67	66.54	61.85	65.02	2.24	3.45
TiO_2	0.61	0.74	0.85	0.73	0.10	13.38
Al_2O_3	9.74	10.51	12.15	10.80	1.01	9.31
Fe_2O_3	0.38	1.20	2.05	1.21	0.68	56.35
FeO	9.59	6.78	6.42	7.60	1.42	18.65
MnO	0.17	0.18	0.10	0.15	0.04	23.73
MgO	1.35	2.23	2.30	1.96	0.43	22.06
CaO	2.68	2.86	4.58	3.37	0.86	25.39
Na_2O	1.80	0.24	3.54	1.86	1.35	72.47
K_2O	1.40	1.83	0.49	1.24	0.56	45.05
P_2O_5	0.14	0.17	0.14	0.15	0.01	9.43
H_2O^+	1.7		2.8	2.3	0.6	24.44
S						
CO_2	5.2		3.5	4.4	0.9	19.54
LOI	6.90	5.76	6.30	6.32	0.47	7.37
TOTAL	101.43	99.04	100.77	100.41	1.01	1.00
Ba ppm	46	58	76	60	12.3	20.55
Cr	13	20	30	21	7.0	33.22
Zr	283	293	252	276	17.5	6.32
Sr	46	32	54	44	9.1	20.66
Rb	31		5	18	13.0	72.22
Y	106	100	78	95	12.0	12.72
Nb	8		7	8	0.5	6.67
Zn	179	122	119	140	27.6	19.72
Ni			10	10	0.0	0.00
V		20	95	58	37.5	65.22
La	15.0	15.4	13.6	14.7	0.8	5.26
Ce	46.3	43.9	43.4	44.5	1.3	2.84
Nd	34.3	32.6	30.7	32.5	1.5	4.52
Sm	10.6	10.7	9.4	10.2	0.6	5.77
Eu	2.63	2.70	2.03	2.45	0.30	12.26
Tb	2.61	2.59	2.28	2.49	0.15	6.06
Dy	16.0	18.6	12.6	15.7	2.5	15.61
Ho	3.49	3.60	2.91	3.33	0.30	9.08
Yb	11.1	10.5	8.7	10.1	1.0	10.10
Lu	1.88	1.65	1.51	1.68	0.15	9.08
Ta	2.13	0.82	1.65	1.53	0.54	35.29
Th	1.56	1.38	1.46	1.47	0.07	5.02
U	0.42	0.38	0.32	0.37	0.04	11.01
Fe_T	9.93	7.85	8.24	8.67	0.90	10.40
Fe/Mg	7.35	3.52	3.58	4.42	1.79	40.52
La/Yb	1.35	1.47	1.56	1.45	0.09	5.96

Table 4.5.1g: Whole rock geochemistry, V10 subunit, Dome Mine.

	9491	P89-09	9494	D89-16	D89-17	Mean	Std.Dev.	Co.Var.
SiO_2	50.19	54.26	50.95	52.05	56.03	52.70	2.16	4.10
TiO_2	1.34	1.37	1.43	1.34	1.41	1.38	0.04	2.65
Al_2O_3	9.92	11.22	12.20	11.75	12.05	11.43	0.83	7.22
Fe_2O_3	0.30	2.00	1.27	1.61	1.54	1.34	0.57	42.55
FeO	14.68	12.12	12.00	14.16	12.14	13.02	1.16	8.88
MnO	0.28	0.17	0.18	0.18	0.12	0.19	0.05	27.96
MgO	2.61	2.50	2.41	2.72	2.41	2.53	0.12	4.75
CaO	6.67	4.46	6.24	5.54	4.04	5.39	1.01	18.68
Na_2O	0.86	2.94	2.63	2.03	1.70	2.03	0.73	35.93
K_2O	0.71	0.24	0.01	0.89	0.77	0.52	0.34	64.66
P_2O_5	0.56	0.66	0.53	0.45	0.47	0.53	0.07	13.94
H_2O^+		3.0		3.0	3.3	3.1	0.1	4.56
S								
CO_2		5.4		7.1	4.8	5.8	1.0	16.89
LOI	9.78	8.40	8.19	10.10	8.10	8.91	0.85	9.53
TOTAL	97.90	100.34	98.04	102.82	100.78	99.98	1.84	1.84
Ba ppm	36	77	40	24	59	47	18.7	39.55
Cr	20	11	30	57	44	32	16.5	50.85
Zr	150	167	192	160	183	170	15.2	8.94
Sr	64	104	73	49	38	66	22.7	34.55
Rb				11	11	11	0.0	0.00
Y	60	72	80	63	76	70	7.6	10.83
Nb		4		7	6	6	1.2	22.01
Zn	590	126	330	150	105	260	183.2	70.42
Ni				12		12	0.0	0.00
V	20		40	25	4	22	12.9	57.76
La	9.0	9.9	14.0	9.8		10.7	2.0	18.28
Ce	26.3	30.6	39.4	31.7		32.0	4.7	14.77
Nd	21.9	26.5	28.1	25.1		25.4	2.3	8.99
Sm	7.4	8.2	9.5	8.1		8.3	0.8	9.14
Eu	2.33	2.77	2.79	2.26		2.54	0.24	9.61
Tb	1.70	1.92	2.17	1.93		1.93	0.17	8.62
Dy	11.5	11.9	14.8	11.0		12.3	1.5	12.02
Ho	2.30	2.63	2.90	2.65		2.62	0.21	8.14
Yb	6.3	7.5	8.3	7.2		7.3	0.7	9.77
Lu	1.00	1.24	1.34	1.22		1.20	0.12	10.34
Ta	0.46	1.14	0.59	1.40		0.90	0.39	43.05
Th	0.67	0.78	0.94	0.90		0.82	0.11	12.88
U	0.17	0.27	0.26	0.31		0.25	0.05	20.27
Fe_T	14.95	13.90	13.13	15.59	13.51	14.21	0.92	6.45
Fe/Mg	5.73	5.56	5.45	5.73	5.61	5.62	0.11	1.91
La/Yb	1.43	1.32	1.69	1.36		1.46	0.14	9.78

Table 4.5.1h: Whole rock geochemistry, Amygdaloidal Pillow Lava (APL), Gold Centre Subgroup, Dome Mine.

	9496	P89-11	P89-12	Mean	Std.Dev.	Co.Var.%
SiO_2	45.85	46.08	46.61	46.18	0.32	0.69
TiO_2	1.20	1.10	1.21	1.17	0.05	4.24
Al_2O_3	13.04	12.93	13.69	13.22	0.34	2.54
Fe_2O_3	1.47	1.83	1.53	1.61	0.16	9.78
FeO	8.35	9.55	9.62	9.17	0.58	6.35
MnO	0.20	0.19	0.16	0.18	0.02	9.27
MgO	4.73	6.08	5.66	5.49	0.56	10.27
CaO	9.77	9.02	7.61	8.80	0.90	10.18
Na_2O	2.15	2.84	2.33	2.44	0.29	11.98
K_2O	0.32	0.11	0.58	0.34	0.19	57.10
P_2O_5	0.10	0.05	0.05	0.07	0.02	35.36
H_2O^+		4.6	4.7	4.7	0.1	1.08
S						
CO_2		6.1	5.3	5.7	0.4	7.02
LOI	11.03	10.70	10.00	10.58	0.43	4.06
TOTAL	98.21	100.48	99.05	99.25	0.94	0.94
Ba ppm	92	53	242	129	81.5	63.16
Cr	85	93	81	86	5.0	5.78
Zr	59	42	51	51	6.9	13.71
Sr	94	103	51	83	22.7	27.45
Rb			8	8	0.0	0.00
Y	24	20	24	23	1.9	8.32
Nb						
Zn	74	144	200	139	51.5	36.99
Ni		74	58	66	8.0	12.12
V	330	356	382	356	21.2	5.96
La	3.3	2.5	2.8	2.9	0.3	11.51
Ce	9.2	7.0	8.0	8.1	0.9	11.15
Nd	7.7	6.2	6.4	6.8	0.7	9.83
Sm	2.8	2.1	2.3	2.4	0.3	12.27
Eu	0.89	0.84	0.85	0.86	0.02	2.51
Tb	0.66	0.55	0.62	0.61	0.05	7.45
Dy	4.8	3.4	3.9	4.0	0.6	14.36
Ho	1.0	0.8	0.9	0.9	0.1	9.07
Yb	2.8	2.3	2.6	2.6	0.2	8.01
Lu	0.43	0.39	0.45	0.42	0.02	5.89
Ta	0.08	0.40	0.49	0.32	0.18	54.42
Th	0.19	0.27	0.18	0.21	0.04	18.88
U	0.10	0.10	0.11	0.10	0.00	4.56
Fe_T	9.66	11.18	10.98	10.60	0.67	6.37
Fe/Mg	2.04	1.84	1.94	1.93	0.08	4.30
La/Yb	1.18	1.09	1.08	1.12	0.05	4.10

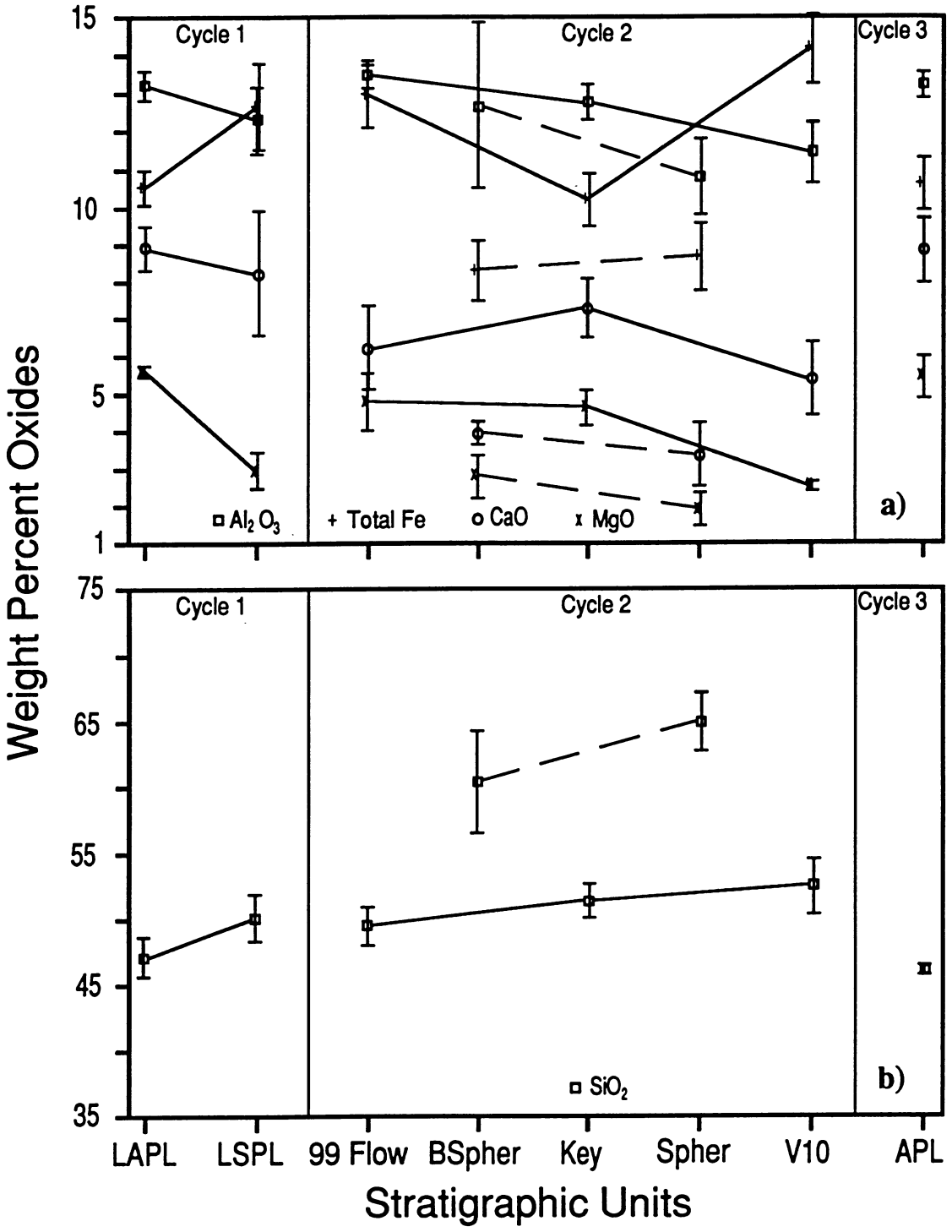

Figure 4.5.1: Averaged major element concentrations for various subdivisions of the Dome Mine stratigraphy (from Table 4.5.1). Three volcanic cycles are defined by the trends in the element concentrations. Error brackets are shown and equal twice the standard deviation. The anomalous units of the V8 subunit (dashed lines) are treated separately. Unit abbreviations are as follows: LAPL - Lower Amygdaloidal Pillow Lava, LSPL - Lower Spherulitic Lava, BSpher - Broken Spherulitic Flow, Spher - Spherulitic Flow, APL - Amygdaloidal Pillow Lava. a) Major oxides of Al, Fe (total as FeO), Ca and Mg. b) Plot for silica.

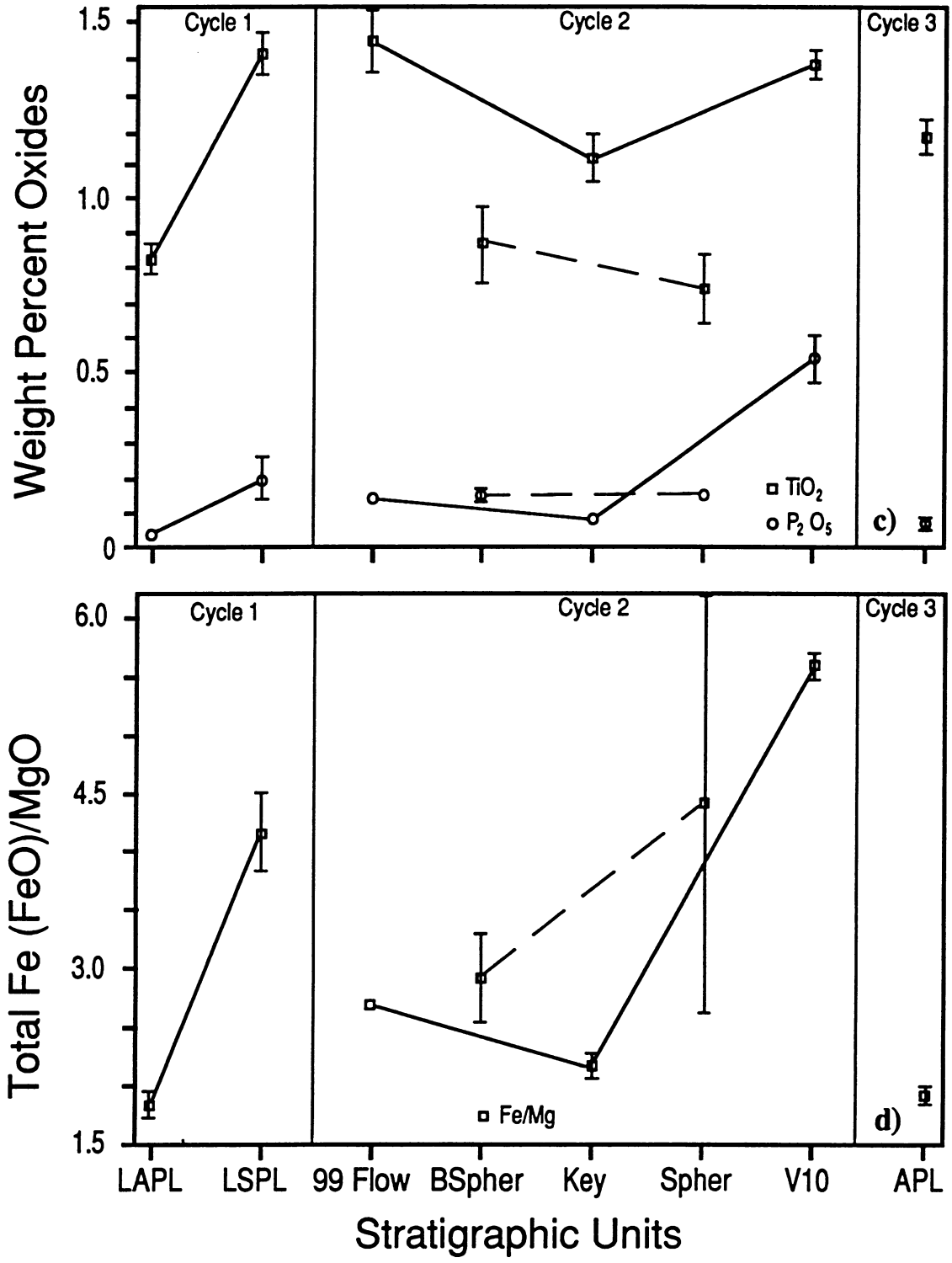

Figure 4.5.1 (con't): c)Oxides of Ti and P. d) Ratio of Fe to Mg in the whole rock.

cycle within the sampled section. From the 99 Flow of the V8 subunit to the top of the V10 subunit (Dacite Flow) there is a general progression to more acid composition. The SiO_2 content of the units increases slightly from an average 50 wt% in the 99 Flow to 51 wt% in the Key Flow, to 53 wt% in the V10 subunit. The oxides Al_2O_3 and MgO decrease consistently from 13.5 and 4.8 wt% respectively in the 99 Flow to 11.4 and 2.5 wt% in the V10 subunit. Total Fe, TiO_2, CaO, P_2O_5 and the Fe/Mg ratio have variable trends through the sequence, decreasing from the 99 Flow to the Key Flow and then increasing again in the V10 section. Overall, the V10 composition is the most acidic of all these examples.

Within the sequence of flows from the 99 Flow to the V10 subunit, there are interlayers which have anomalous compositions. These layers include the Broken Spherulitic and Spherulitic Flows at the Dome Mine and the pillowed flow with layered, coalesced varioles on the Porcupine Paymaster section. These flows are characterized by anomalously high SiO_2 content, up to 70 wt%, and low concentrations of TiO_2, total Fe oxides, and CaO relative to the surrounding units. In contrast, Al_2O_3 and P_2O_5 are relatively consistent with the overall trend in the sequence (Figure 4.5.1).

Only the lowermost part of the next cycle of differentiation is seen in the sampled section. The composition of this unit is more basic than the Vipond Subgroup, very similar to the LAPL. As there are no samples further upsection, the extent to which this cycle is differentiated is unknown. There is indication in the literature (Ferguson,1968; Mason and Brisbin, 1987) that a variolitic flow is found towards the top of the Gold Centre Subgroup, so some progression is assumed based on the composition of the variolites in the Vipond Subgroup.

The Jensen Cation plot has two apparent compositional trends for the Dome Mine area variolitic suite (Figure 4.5.2). The main trend is a typical tholeiite Fe enrichment trend, coarsely outlined from the LAPL to the V10 subunit, and starting again in the base of the overlying Gold Centre Subgroup (APL unit). There is considerable dispersion in this trend, possibly due to alteration effects, and it does not progress as far as the tholeiitic andesite field. However, samples of the Broken Spherulitic and Spherulitic Flows define trends to acidic compositions, at right angles to the overall trend of Fe enrichment and sub-parallel to the calc-alkaline trend (Jensen, 1976). Two samples from the anomalous units within the V8

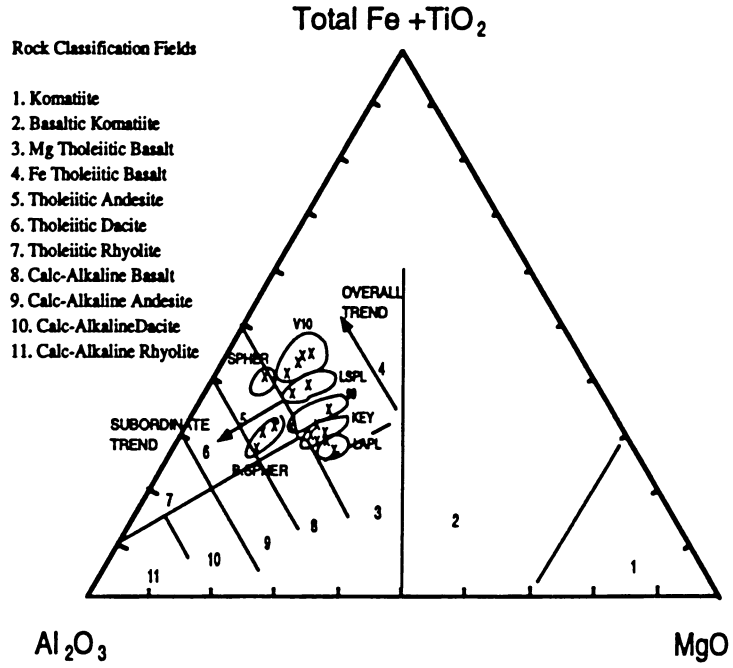

Figure 4.5.2: Jensen Cation plot for section in the Dome Mine area. Rocks are subdivided by the mine stratigraphy. Two trends are apparent: 1) an overall trend of Fe-enrichment (LAPL to V10 units), 2) a subordinate trend, parallel to the calc-alkaline trend, toward the units of anomalous composition in the V8 subunit of the Vipond Subgroup. The stratigraphic order of the units, from bottom to top, is as follows: 1) LAPL, 2) LSPL, 3) 99 Flow, 4) Broken Spherulitic Flow, 5) Key Flow, 6) Spherulitic Flow, 7) V10 subunit.

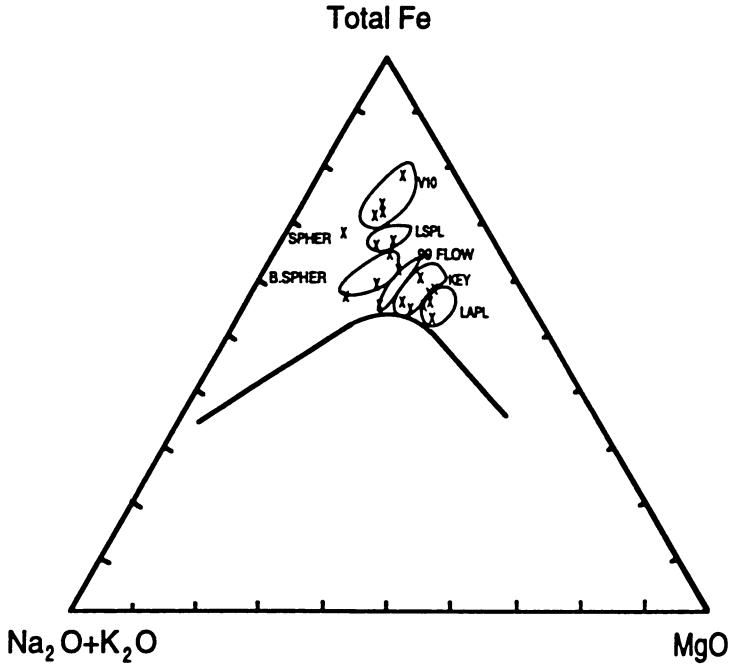

Figure 4.5.3: AFM diagram for the Dome Mine area section. Samples are grouped according to the mine nomenclature.

subunit plot as tholeiitic andesites. An Fe enrichment trend can be seen on an AFM plot of the Dome Mine area samples (Figure 4.5.3), however, the second trend is not as obvious, as it is probably masked by alkali mobility.

4.5.2 Trace Element Geochemistry of Units

As in the Harker Lake area, only the relatively immobile trace elements have been considered in order to "see" the primary igneous trends. The trace elements follow similar cyclical patterns to the major element data (Figure 4.5.4). In the lower cycle, culminating at the top of the LSPL, the compatible elements Cr, V, and especially Ni all decrease in concentration in the LSPL relative to the LAPL. The incompatible elements Zr, Y and Th all increase substantially. REE also increase from 6-10 times chondrite values in the LAPL to 20-25 times in the LSPL (Figure 4.5.5). La/Yb ratio jumps from an average value of 1.08 in the LAPL to 1.50 in the LSPL, indicating some fractionation of the REE towards the top of this volcanic cycle.

Trace element variations in the second cycle, from the 99 Flow to the V10 subunit, have trends indicative of differentiation towards the top of the sequence. Again, the compatible elements progressively decrease with height above the base of the cycle. Cr, Ni, and V decease from averages of 220 ppm, 90 ppm, and 350 ppm respectively in the 99 Flow to 30 ppm, 10 ppm, and 20 ppm in the V10 subunit. Zr, Y and Th increase from average values of 85 ppm, 30 ppm and 0.5 ppm respectively in the 99 flow to 170 ppm, 70 ppm and 0.8 ppm in the V10 subunit. REE in this section increase in concentration from 10-15 times chondrite values in the 99 Flow to 15-20 times in the Key Flow and finally abruptly increase to 30-50 times in the V10 subunit (Figure 4.5.5). The La/Yb ratio decreases from the 99 flow to the Key Flow before the increasing again in the V10 subunit to a value lower than that of the 99 Flow.

The anomalous interlayers have characteristics which reflect their more acid composition. These include lower concentrations of compatible elements (20 ppm Cr, <10 ppm Ni, 70 ppm V) and higher concentrations of the incompatibles (290 ppm Zr, 100 ppm Y, 1.5 ppm Th) than their surrounding units. The REE are also quite highly concentrated in these flows ranging from 40 to 80 times chondrite values. The REE profiles for these

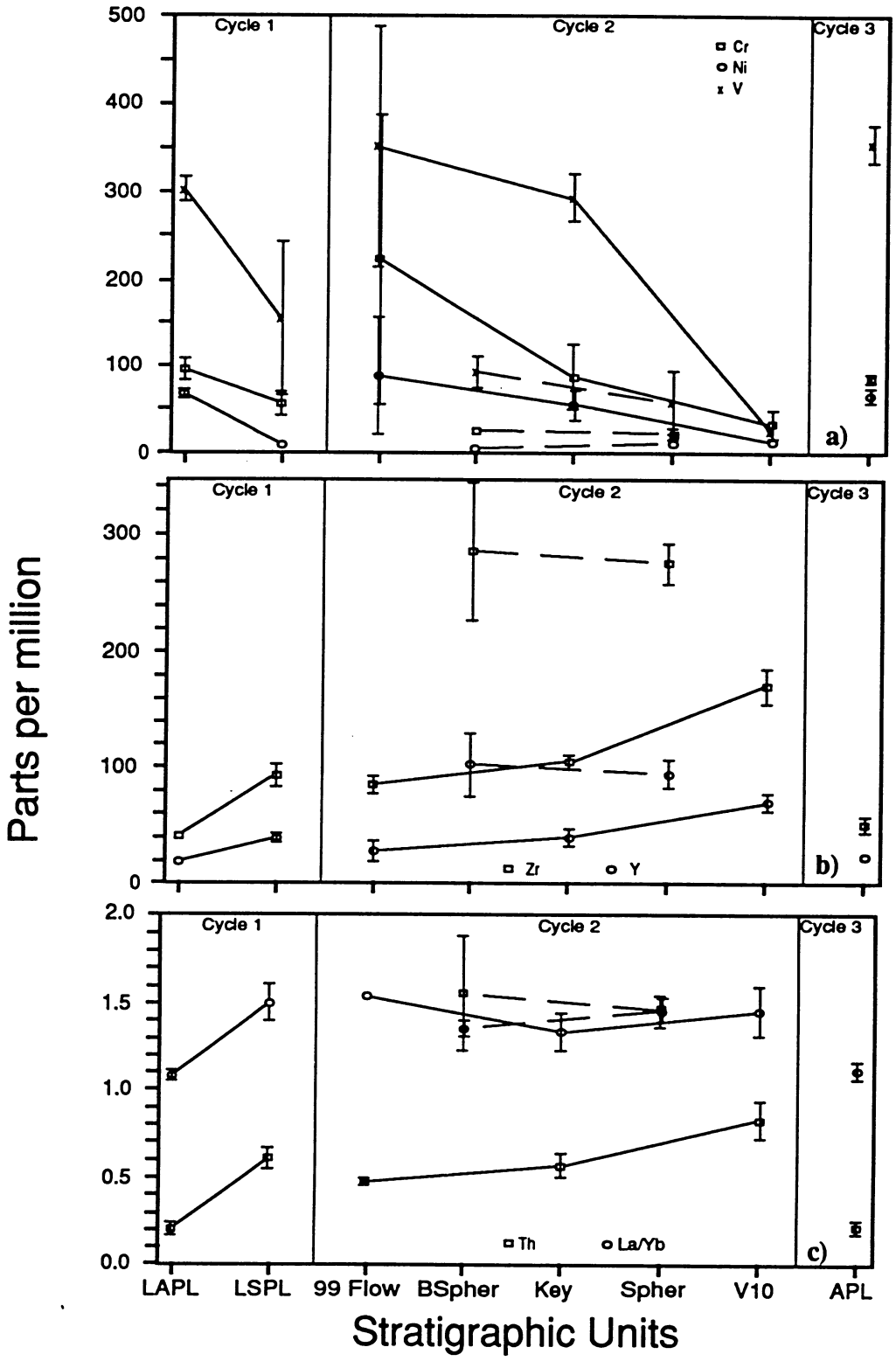

Figure 4.5.4:Averaged trace element concentrations for the various subdivisions of the Dome Mine section (Table 4.5.1). The trends corroborate the three cycles defined by the major element plots: a) compatible elements Cr, Ni, and V, b) incompatible elements Zr and Y, c) Th and La/Yb ratio. Units as defined for figure 4.5.1. Error bars represent 2 times the standard deviation.

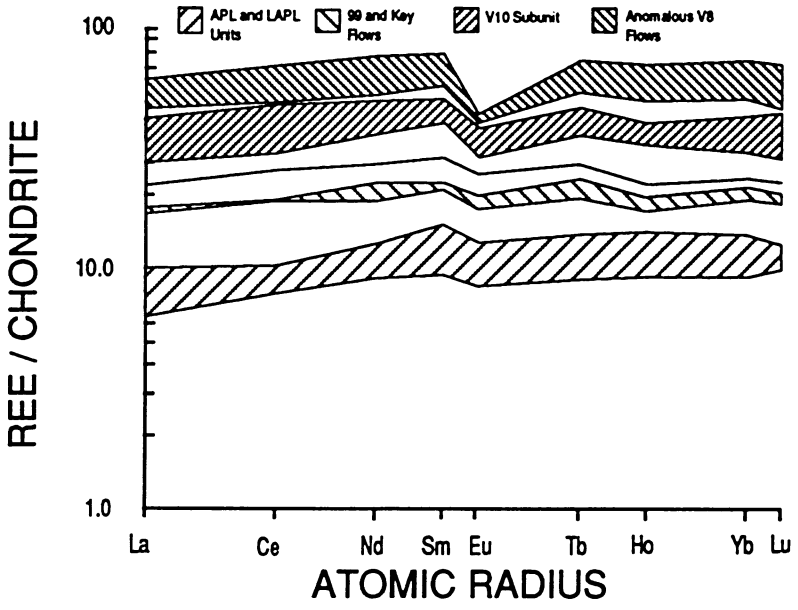

Figure 4.5.5: REE plots for selected samples from the Dome Mine section. Mine units are correlated with the appropriate profiles. The single line profile represents the LSPL unit.

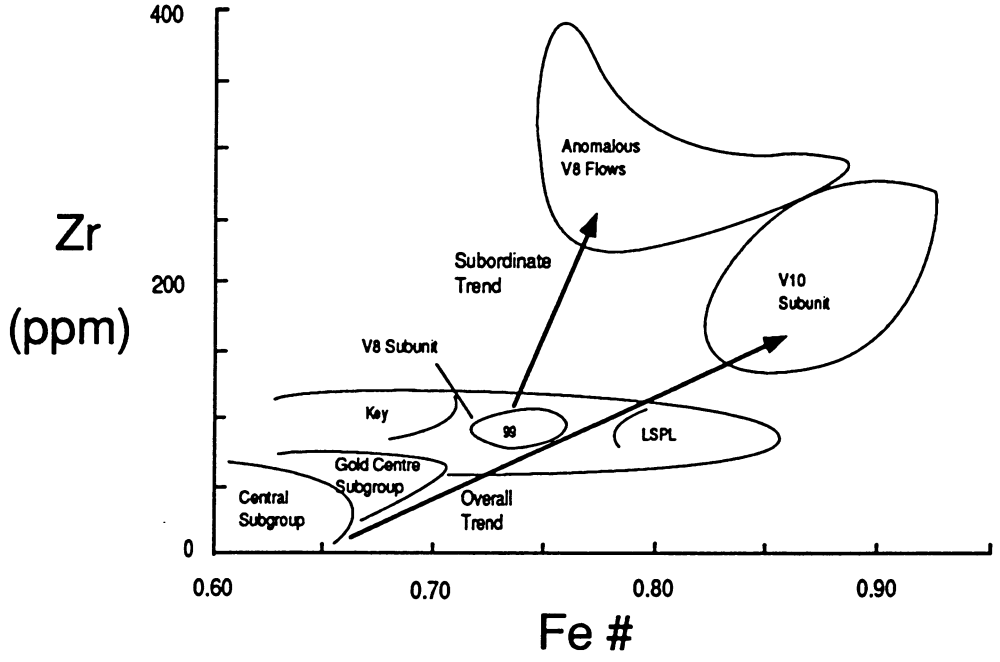

Figure 4.5.6: Zr vs Fe# diagram for the Dome Mine section. The diagram shows the progressive fractionation within the suite. Fields represent the mine units as labelled. The anomalous units of the V8 Subunit appear to be fractionated more along the Zr axis whereas the V10 Subunit rocks are fractionated more along the Fe# axis. This may indicate separation of a portion of the source magma at a certain point along its overall fractionation path as indicated by the arrows on the diagram.

intermediate flows are the only ones to have consistent and significant negative Eu anomalies. The two anomalous units also define trends within the overall volcanic cycle (Figure 4.5.4). However, the trend in concentration of the incompatible elements in the anomalous interlayers is opposite to their trend in the other units. It is interesting to note that despite being the most felsic rocks of the Vipond Subgroup, these flows have V content, La/Yb ratio and Fe/Mg ratio transitional between the V8 and V10 subunits. All the evidence above corroborates the major element information and supports an hypothesis that these units are the result of separation of a portion of magma at an intermediate stage in the development of the Vipond Subgroup (Figure 4.5.6).

The trace element data of the APL unit is quite similar to the LAPL unit at the base of the sampled sequence. Although the REE are more concentrated in the APL, 10-15 times chondrite values versus 6-10 times in the LAPL, the La/Yb ratio is essentially the same, indicating a similar source magma.

Figure 4.5.6 shows the relationship between Zr content and the Fe# in flows from the Dome Mine area. As in the Harker Lake area, the plot shows that there is progressive fractionation through the volcanic cycles. As indicated by the proximity of their fields, there is little difference between the LAPL and APL units (overlapping within the Gold Centre Subgroup field), whereas there is a direct positive slope relationship between the two variables for the variolitic Vipond suite. The V8 subunit has an apparently constant concentration of Zr, despite increasing Fe#. The other interesting point in this plot is the position of the intermediate flows of the V8 subunit which are obviously more fractionated than the V10 subunit with respect to the incompatible element Zr, and yet they are transitional between the V8 and the V10 subunits in terms of the Fe#.

4.6 Summary of Geochemistry

The effects of low grade metamorphism and deformation on the rocks discussed in this chapter have not created insurmountable problems for interpretation of the petrogenetic trends in the variolitic suites. The rocks from the Harker Lake area all fall into the the type 1) metamorphic assemblage (amphibole-chlorite-epidote) of Gélinas *et al* (1982) which have

little or no change in most primary igneous geochemical characteristics. The rocks in the Dome Mine area have been further altered and are generally categorized as type 2). In type 2) rocks, amphibole has been altered to chlorite, and changes in primary chemical abundances are evident. However, by restricting interpretations to elements of relative immobility, the petrogenetic trends of the Dome Mine area rocks can be discerned. The consistency and coherency of the elemental changes in the variolitic suites, described above, serves as further evidence that the primary chemistry of the rocks has not been too severely disturbed.

The general petrogenetic trends identified in the rocks at Harker Lake can be seen with equal clarity in the carbonatized rocks in the Dome Mine area. Despite the pervasive carbonate alteration common in the rocks in the Dome mine area, there is no evidence to suggest that there was preferential mobilization of the HFS elements and REE as reported by Hynes (1980) elsewhere. Comparison of the least altered example of the 99 Flow at the Dome Mine with a moderately altered sample (Figure 4.6.1) shows that there is no change at all in the REE patterns. In addition, the regional alteration and deformation in the Timmins area has not caused volume changes significant enough to alter the geochemical trends.

The REE in particular have very consistent patterns in the two study areas. The REE generally increase in total abundance and have no significant changes in La/Yb, with progressive differentiation. Negative Eu anomalies appear in the more evolved rocks. It is unlikely that significant REE mobilization has occurred because: 1) the REE patterns are smooth (i.e. consistent at the sample scale), 2) they appear to reflect igneous trends consistent at large scales (i.e. rock suites) and, finally, 3) the REE signature of variolitic suites is similar from area to area, despite differences in alteration intensity (i.e. between Harker Lake and Dome Mine areas).

In consideration of the geochemical data, it appears that the metamorphic effects on the variolitic suites for the most part can be considered isovolumetric and isochemical. Therefore, it may be concluded that careful interpretations regarding the nature of the primary chemistry and petrogenesis of these variolitic suites is possible.

The rocks of the variolitic suites in both areas have several distinct chemical characteristics. They define Fe enrichment trends typical of mafic tholeiitic suites and progress beyond the peak of Fe-enrichment to intermediate composition. The extent of Fe

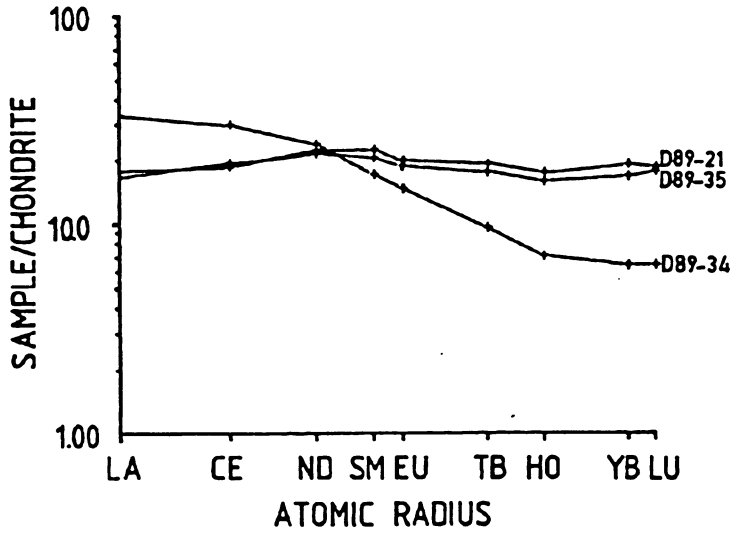

Figure 4.6.1: Chondrite normalized REE spectra for three samples from the 99 Flow, Dome Mine. Sample D89-21 is the least altered sample recovered in the Dome Mine area, having greenschist facies mineralogy, while D89-35 is a foliated, carbonatized example, more typical of the regional alteration present in the Timmins area. There is very little difference in the REE profiles of these two rocks, both having characteristics typical of Fe tholeiitic volcanics. Sample D89-34 is a highly altered example of the 99 Flow, only a few metres along strike from an ore body. Disturbance of the REE patterns is only recorded in the most altered samples of this study.

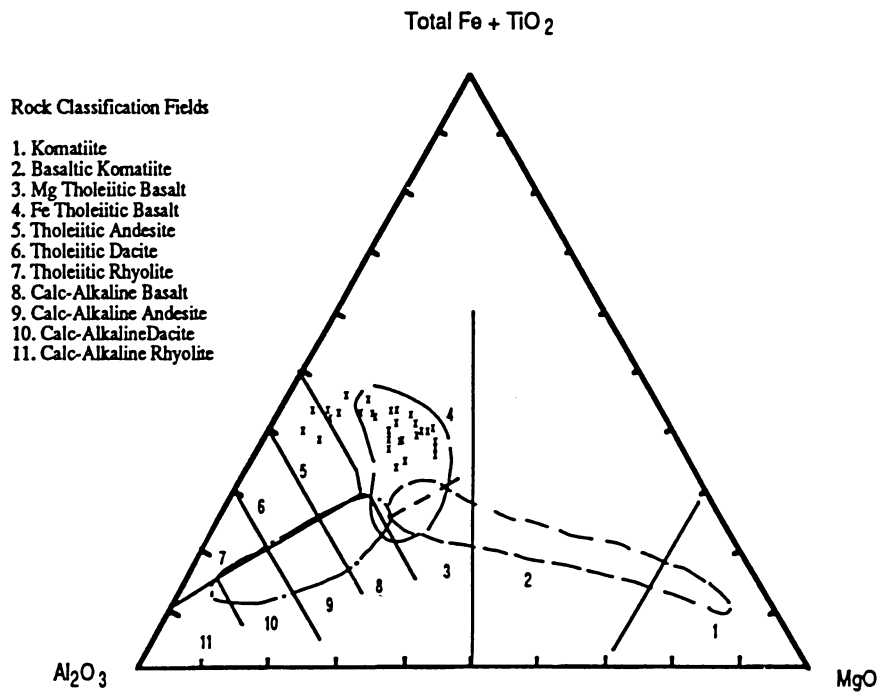

Figure 4.6.2: Jensen Cation plot of section from underlying Stoughton-Roquemare, through Kinojevis to Blake River Groups of the Harker area stratigraphy. Rocks from the Harker Lake section of this study are plotted as x's. Different Groups plot within fields shown on diagram: Stoughton-Roquemare Group, short dashes; Kinojevis Group, long dashes; Blake River Group, dot-dashes (modified after Jensen, 1978).

enrichment in variolites is quite anomalous in some units, such as the V10 subunit (see also Gélinas *et al*, 1976). Figure 4.6.2 shows a plot of samples from an approximately 6 kilometre stratigraphic section (Jensen, 1978) in Stoughton and Marriott Townships, about 20 kilometres east of the Harker Lake area. In addition to rocks from the tholeiitic Kinojevis Group, the section includes samples from the underlying komatiitic Stoughton-Roquemare Group, as well as, the overlying calc-alkaline Blake River Group. In comparison with the tholeiitic rocks in Figure 4.6.2, flows of the Harker Lake section occur well above the Mg tholeiite-Fe tholeiite dividing line, having significant Fe enrichment. The samples of Jensen's representative suite of tholeiitic rocks from the Kinojevis Group do not have the extent of differentiation indicated by the chemistry of the upper parts of the volcanic cycles in the Harker Lake section. It may be that the typically narrow intermediate sections within the Kinojevis Group were missed by the wider sample spacing in Jensen's regional study.

On a more local scale, Figure 4.6.3a shows a Jensen cation plot of the complete section across the Hurd property, outlined in Figure 2.1.1. This includes the Mg tholeiite rocks in the south half of the property. The evolved rocks of the Harker Lake section are the most acidic of any on the property. Also, the complete spectrum of rock compositions from Mg tholeiitic basalt to tholeiitic andesite is seen quite clearly on the plot of Zr versus Fe# (Figure 4.6.3b).

In the Timmins area, major element geochemical data from the sampled section in the Dome Mine area corresponds with the tholeiitic section of the Tisdale Group stratigraphy (Pyke, 1982) on a Jensen cation plot (Figure 4.6.4). The two sample sets have approximately equal scatter although the Vipond section is more evolved, is closer to intermediate composition and contains no Mg tholeiite examples. Davies *et al* (1979) have shown the Vipond sequence to be distinct from surrounding units in terms of trace element abundances. In trace element plots (i.e. Zr vs Y; TiO_2 vs Zr; TiO_2 vs Cr), the Vipond Subgroup is the most evolved section of stratigraphy in the tholeiitic rocks of the Timmins camp. The data from this study lies within the fields for the various units defined by Davies *et al* (1979) (Figure 4.6.5), and in the case of the anomalous V8 units, extends these fields.

The classification scheme of Melson *et al* (1976), based on whole rock geochemical data from modern tholeiitic basalts related to oceanic spreading centres, is quite applicable

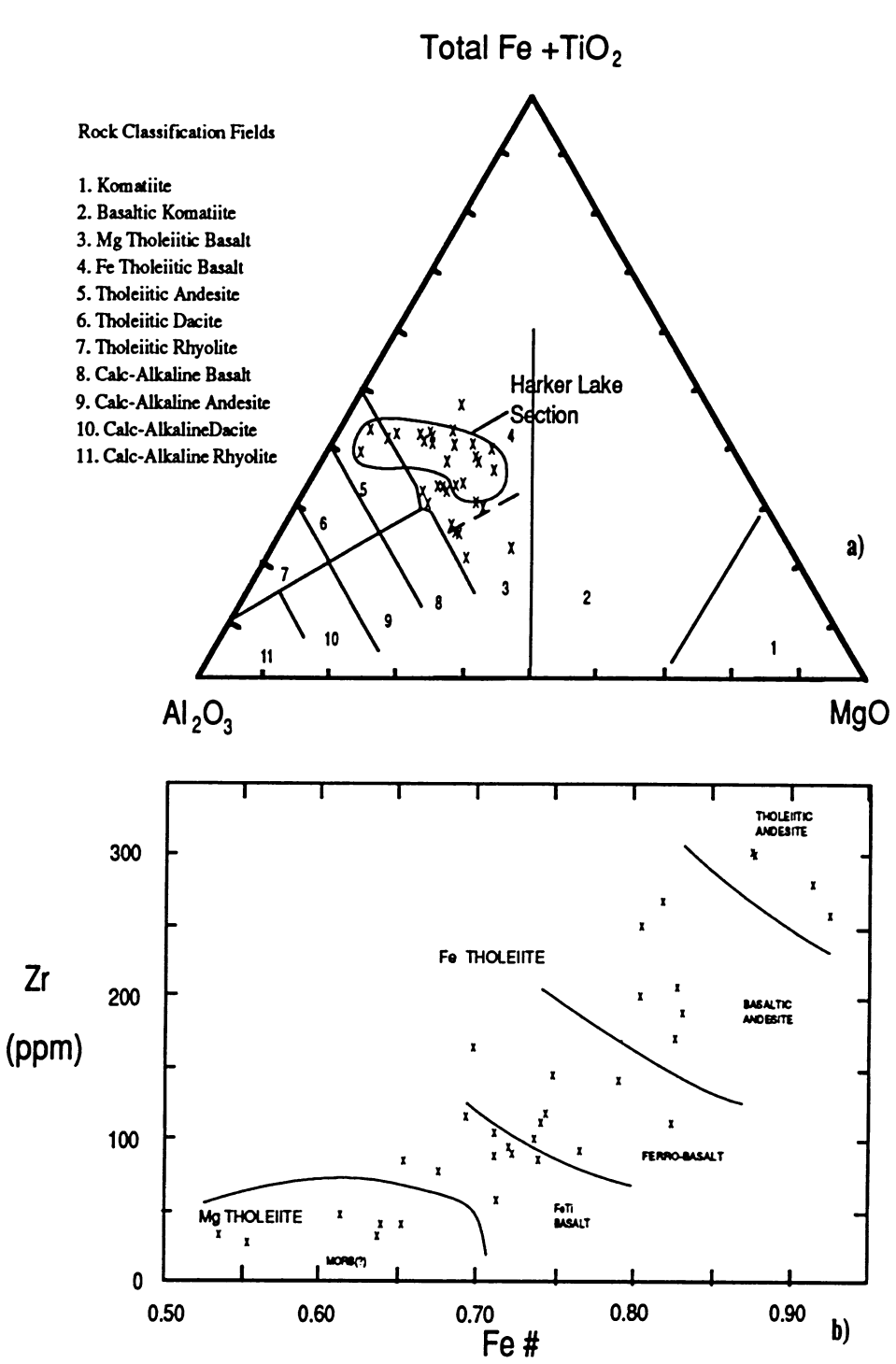

Figure 4.6.3: a) Jensen Cation plot for the Hurd Property complete section, including the Harker Lake section. Upper flows of the Harker Lake section are the most evolved on the property. The plot also includes the overlying Mg tholeiite section, to the south of the Harker Lake section. b) Zr vs Fe# plot, showing relative fractionation of rocks on the Hurd Property section, including the overlying Mg tholeiite section. Classification (Melson et al, 1976) of the rocks shows a complete suite from Mg tholeiitic basalt to tholeiitic andesite.

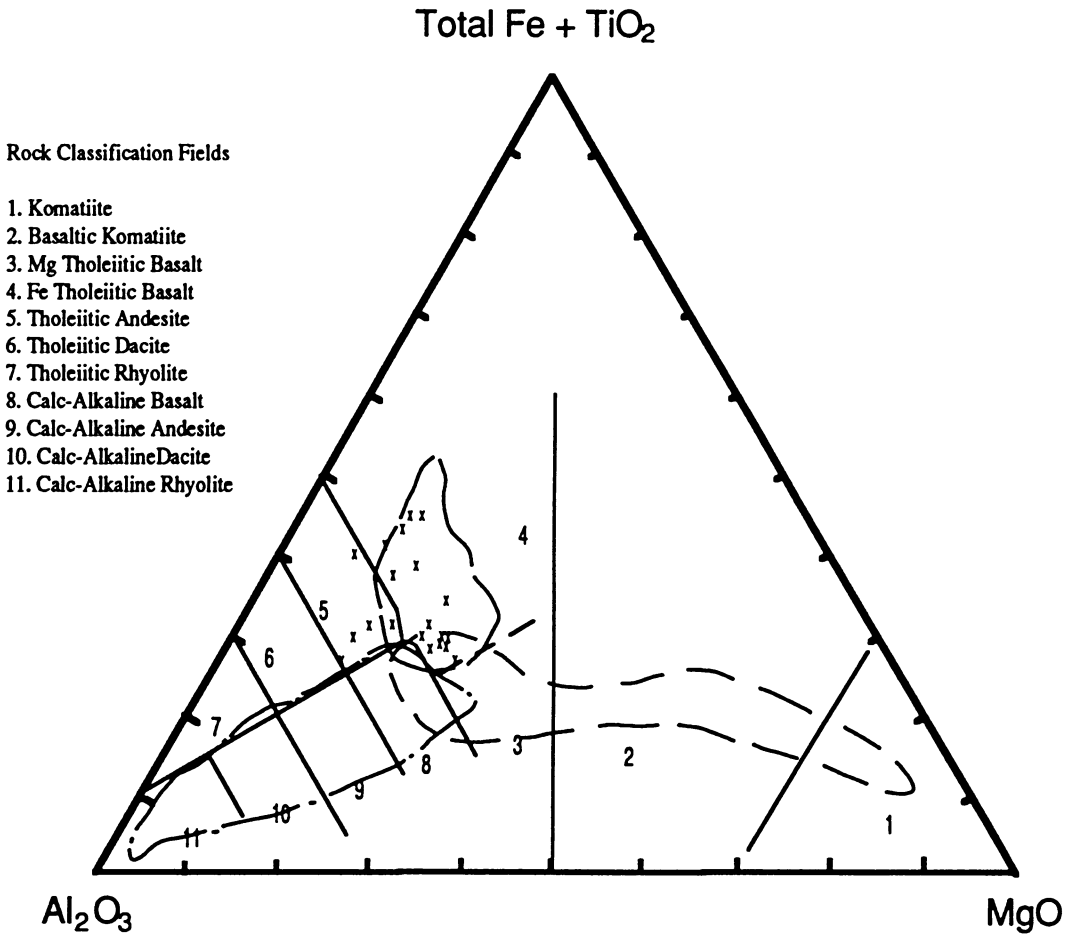

Figure 4.6.4: Jensen Cation plot of Tisdale Group volcanics, showing the fields of the lower, komatiitic section (short dashes), the tholeiitic section (long dashes), and the upper calc-alkaline section (dot-dashes) (modified after Pyke, 1982). Samples from the Dome Mine area used for this study are shown as x's.

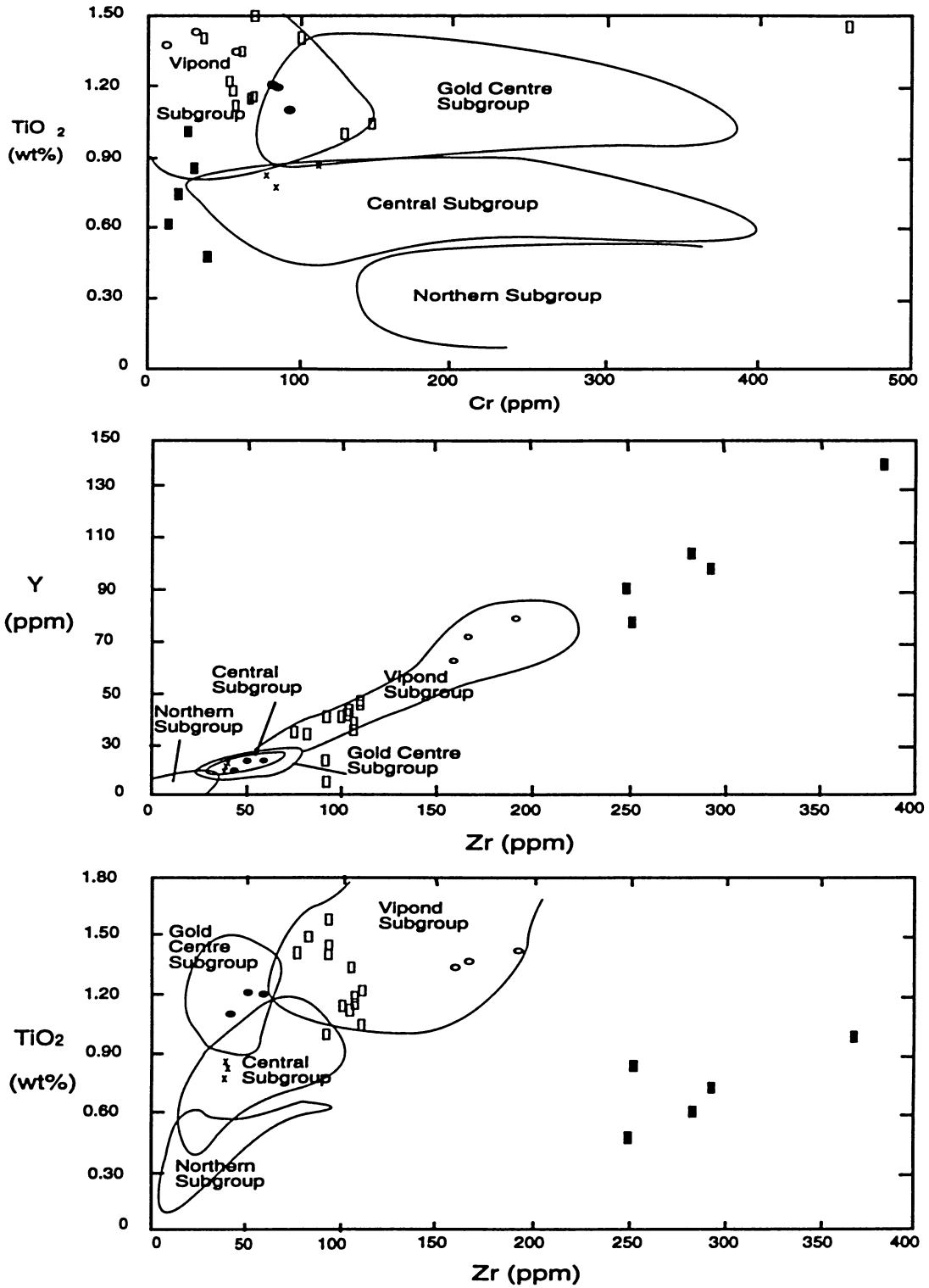

Figure 4.6.5: Plot comparing the Dome Mine section geochemical data with the fields defined by Davies et al (1979) for the mafic stratigraphic units in the Dome Mine area (Ferguson, 1968). Samples from this study are plotted and are represented by the following symbols: open circles-V10 subunit, open boxes- V8 subunit, closed boxes-anomalous units within the V8, X's-Central Subgroup, closed circles-Gold Centre Subgroup. All plots demonstrate that the Vipond Subgroup is the most evolved in the mafic stratigraphy of the Dome Mine area.

to the Archean variolitic suites in this study. The majority of the units within the variolitic suites would be classified as ferro-basalts or basaltic andesites. The uppermost flows in the Harker Lake area and the Dome Mine area may be classified as tholeiitic andesites. Only the non-variolitic flows in the Harker Lake area fit the requirements for FeTi basalts (total iron as FeO>12 wt%, TiO_2>2.0 wt%). Other flows, such as those in the Central and Gold Centre Subgroups in the Dome Mine area, are relatively similar to MORB rocks.

Detailed field mapping and sampling of these volcanic suites, shows the progression towards more acidic composition is somewhat irregular, with small cycles of enrichment building gradually to relatively felsic peaks. The trends in the concentration of the compatible and incompatible elements are complimentary and confirm the boundaries of these cycles.

There are indications of a weak, broad scale progression towards more acid composition in the variolitic suites, especially in the Harker Lake area, indicating a gradual evolution of the source magma with time. The ratios of Fe/Mg and, to a much lesser extent, La/Yb consistently increase through the suites. Al_2O_3 and P_2O_5 concentrations have consistent trends through the sequences, decreasing and increasing respectively towards the top. Also, the V concentration decreases consistently from bottom to top of the sequences. This temporal evolution of variolitic suites is unlike the development of the lava pile in eastern Iceland, studied by Wood (1976, 1978), where similar compositional variations are spatial, possibly caused by different lava viscosities or eruptive sites for the magmas. The variolitic suites of this study seem to be similar to the lava successions at the Isle of Skye, in Scotland (Thompson *et al*, 1972), and Thingmuli (Carmichael, 1964), in Iceland, which have both a spatial and temporal chemical variation.

The REE patterns from both the Harker Lake and Dome Mine areas have typical, flat tholeiitic profiles. They have a distinct progressive enrichment trend toward the top of the variolitic suite which provides further evidence that it was derived from an evolving source. This differentiation may be due to fractional crystallization. There is only minor fractionation within the REE despite an increase of as much as 10 times in their absolute abundance. Comparison of the REE patterns between the Harker Lake and Dome Mine areas, and between samples of the same unit within each area, shows that they are very similar in their absolute abundances, distribution, and profile. This is very important for stratigraphic

correlations in mining camps, such as the Timmins area, where host rock control on ore bodies is a possibility.

Varioles do not occur only in rocks with more acidic compositions. However, varioles do occur more commonly in the more evolved members of the tholeiitic suite (Figure 4.6.5), and correlate well with increased concentrations of incompatible elements, particularly Zr, Y, Th, and REE. The Fe/Mg ratio of the variolitic Key Flow would seem to indicate a more mafic composition than the 99 Flow despite the fact that the Key Flow is stratigraphically higher. However, the incompatible elements reflect the Key Flow's more differentiated nature (Figure 4.5.4). This contradiction may have something to do with the subordinate trend (subparallel to the calc-alkaline trend) which has been discussed above (Section 4.5.1).

4.7 **Formation and Classification of Variolitic Suites**

4.7.1 Differentiation of the Variolitic Volcanic Suites

The features of the variolitic suites discussed in this study are similar to other tholeiitic suites in the Archean (Thurston *et al*, 1986; Fowler and Jensen, 1989), and in more modern environments, such as eastern Iceland (Carmichael, 1964; Wood, 1976), Isle of Skye, in Scotland (Thompson *et al*, 1972) and the eastern Galapagos Rift (Perfit *et al*, 1983). All of these areas have differentiated geochemical progressions, especially noticeable as small cycles in volcanic flows, indicating differentiation of tholeiitic source magma. These cycles commonly begin with flows of essentially MORB composition, and evolve to FeTi basalt, ferro-basalt, basaltic andesite, andesite and even rhyolite (Carmichael, 1964; Fowler and Jensen, 1989), although rhyolites are volumetrically insignificant.

Progressive differentiation of a suite of rocks can be acheived several ways including assimilation, fractional crystallization, a combination of assimilation-fractional crystallization (AFC), and partial melting. Liquid imiscibility has been rejected because the suites are not bimodal. Assimilation is also assumed to be unlikely since there is no field evidence of it such as enclaves and xenoliths in the flows. In addition, the lithological homogeneity of the surrounding mafic terrane makes it unlikely that a rock of sufficiently felsic composition was present to create the more intermediate units by mixing with a mafic tholeiitic magma. REE

profiles do not reflect contamination of the source magma chamber by a more felsic host rock. One expects that with progressive contamination of the source magma (from, say, a tonalite, ave. La/Yb = 10 (Fowler and Jensen, 1989)) there should be significant fractionation in the REE, which would produce much higher La/Yb ratios near the top of the suite than near the base. The geochemical data do not support this as the REE have relatively flat profiles with very little fractionation associated with enrichment of REE abundances (Figures 4.4.6, 4.5.5). A process of AFC would also produce fractionation in the REE of the suite through assimilation of felsic rock. Assimilation of a local mafic terrane, such as in the Harker Lake area, would be difficult from a thermal standpoint given the similarity of rock composition to the magma. Even if possible, the effects would be minimal and so AFC is not considered important. Partial melting could be responsible for the original source magma (probably MORB-type) for these suites. It is unlikely that partial melting could produce the continuous progression of composition, or the small, repetitive cycles, found in the variolitic suites. Partial melts of a single source should become less felsic and exhibit LREE depletion with time.

In all the studies of tholeiitic suites listed above, fractional crystallization of a common tholeiitic source magma has been proposed for the development of the compositional range and geochemical characteristics of the suites. Processes other than fractional crystallization have played insignificant roles, if any. Commonly, special conditions such as high level emplacement of a portion of the magma in a relatively thick crust (i.e. away from the spreading centre), are required to explain the development of these suites by fractional crystallization. Whereas a relatively steady state may be achieved in a deep magma chamber, high level emplacement encourages further crystallization by cooling of the magma and decreasing pressure.

4.7.2 Modelling Fractional Crystallization

Because of the abundant evidence that the rocks in Harker Township and the Dome Mine Area, in Timmins, are representative of differentiated suites and because other methods of differentiation can be rejected, it was decided to evaluate the hypothesis that fractional crystallization was a mechanism of differentiation. This was done using two quantitative

techniques; the major element method of Pearce (1968), and the trace element method of Allégre *et al* (1977).

Pearce Element Ratio Plots (PER's):

The method of Pearce (1968) tests for fractionating phases in a suite of rocks. Traditionally, geochemical data are presented on variation diagrams in weight percent oxides, i.e. the oxide analyses for a particular sample are summed to 100%. The data represents a closed set, and as a consequence, variation in the abundance of one component oxide must affect the relative abundance (in wt%) of all the other components. Pearce (1968) has overcome this problem by ratioing the data by a constant, normally a conserved element. The abundance of the conserved element remains constant in the liquid in real terms (i.e. grams) during the process of differentiation. This results in the cancelling out of the "total" in the denominator wt% term (Ernst *et al*, 1988). Thus, changes in the abundance of elements involved in fractional crystallization are equivalent to the changes in the ratio of the concentrations of the unconserved and conserved elements because the mass terms cancel. This is expressed in the following relationship:

$$c^i_a/c^z_a = [(m^i_a/M_a)/(m^z_a/M_a)] = m^i_a/m^z_a \quad (1)$$

where "a" is a sample of mass, M_a, from a fractionating system, "i" and "z" are the compatible and incompatible elements respectively, and "c" and "m" are the concentration and mass of the elements. For instance, one can model the fractionation of olivine from an ultramafic melt by using the concentration of the compatible elements FeO+MgO as one axis coefficient and SiO_2 on the other axis. Al_2O_3 is not consumed in the fractionation of olivine. It is a conserved element and can be used as a normalizing factor for the axis coefficients. Based on the stoichiometry of the major oxides in the mineral phase, olivine fractionation will produce a line of slope equal to 1.0 on an X-Y plot using these axis coefficients. This line is referred to as the mineral vector. If a line of slope equal to 1.0 is produced by plotting the geochemical data on this diagram, one can assume simple olivine fractionation has taken place.

As shown in the example above, PER's are done with some knowledge of the mineral phases which may be important to the differentiation of the suite by fractional crystallization. They are designed to test for the separation of these specific minerals from an originally

homogeneous melt. Elements which do not take part in the fractionation are said to be conserved. Plot axis coefficients are determined by the stoichiometry of the fractionating minerals (Stanley and Russell, 1989). Separation of a specific phase will be represented by a unique mineral vector following the trend of the melt composition as fractionation progresses. If the data points of the members of a suite of rocks fall on a straightline this indicates that they are related by fractional crystallization of the mineral phases being tested. The slope of the straight line gives some quantitative information about the the amount of each phase involved. The mineral phases being tested by the PER can be rejected if the geochemical data define a trend which is inconsistent with the theoretical mineral vector, has low correlation, or passes through the origin of the plot.

PER's have been applied to the whole rock geochemical data of the rock suites from the two main areas in this study. The possibility that the members of the variolitic suites are related by fractional crystallization has been tested with two types of conserved constituent diagrams. Both plots compare the fractionation of clinopyroxene against plagioclase. Thorium has been chosen as the incompatible, or conserved, constituent in this study, because of its reliable analyses by instrumental neutron activation, its relative immobility in metamorphosed rocks and it is not likely to have been incorporated into fractionating minerals in these rocks. All of the axis coefficients described below are normalized by thorium.

In the first type of plot, the fractionation of clinopyroxene is compared to plagioclase. The axis coefficient for plagioclase is represented by only the concentration of Al_2O_3 which is not incorporated by any other mineral expected to be fractionating in a magma of basaltic composition. Separation of purely plagioclase will result in a mineral vector parallel to the Al_2O_3 axis. CaO content in a rock is used to isolate clinopyroxene fractionation and the axis coefficient for clinopyroxene (CPX) is defined by the formula:

$$SiO_2/6+2/3CaO-Al_2O_3/2-10/9P_2O_5$$

where the SiO_2, Al_2O_3 and P_2O_5 terms correct for CaO fractionation by plagioclase and apatite. Separation of only clinopyroxene from the melt would result in a vector parallel to the CPX axis.

The second plot compares the fractionation of the two minerals using SiO_2 for the y-axis coefficient and the silica mafic equivalent (SME) (Pearce, 1972) component for the x-

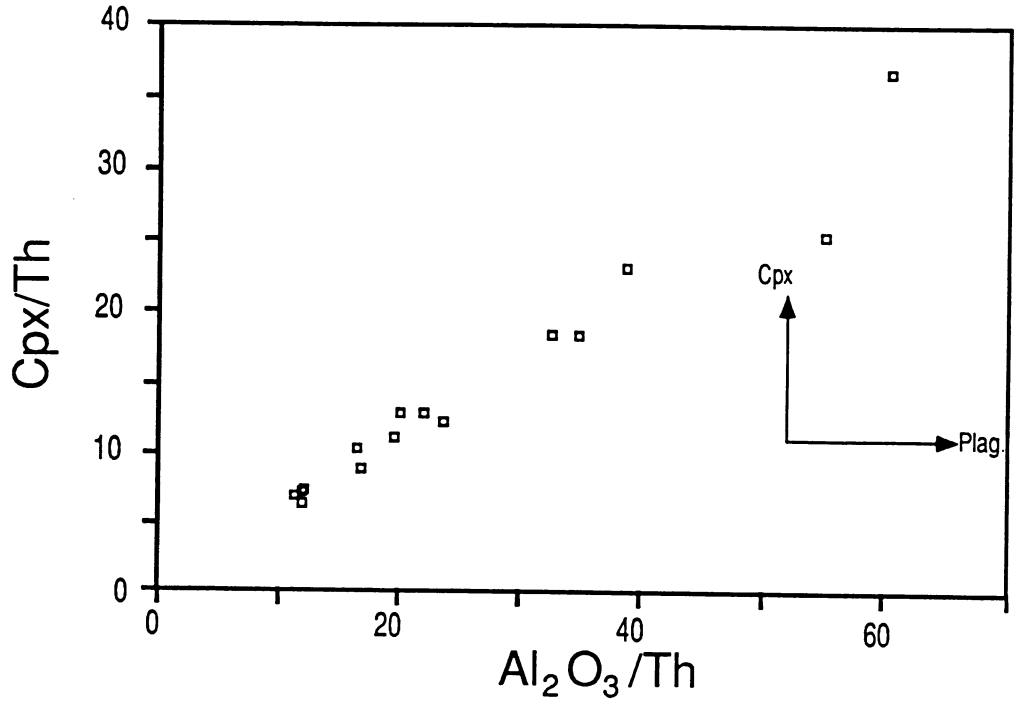

Figure 4.7.1: Pearce Element Ratio (PER) plot for the Harker Lake section, testing for fractionation of plagioclase and clinopyroxene. Linear regression (reduced major axes) gixes a slope of 0.55(0.03) and a y-intercept of 0.30(1.04) with r=0.97. The slope, representing a combination of fractionation of the two phases, lies between that indicating pure fractionation of either phase. The intercept is not significantly non-zero (see text). Cpx = SiO_2/6+2CaO/3-Al_2O_3/2-10P_2O_5/9.

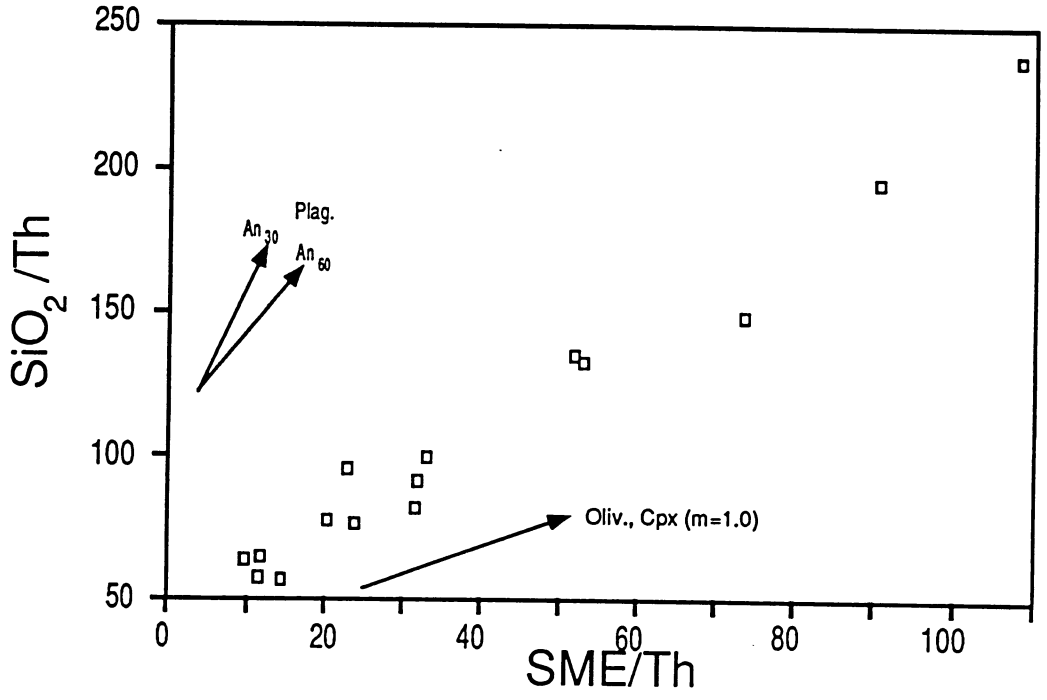

Figure 4.7.2: PER for Harker Lake section, again testing for fractionation of plagioclase and clinopyroxene but using different variables than Figure 4.7.1. The slope (1.78(0.09), r=0.98) again lies between that for pure fractionation of either phase. The y-intercept in this case is significantly non-zero (39.54(4.48)). SME = 0.5FeO + 0.5MgO + 1.5CaO.

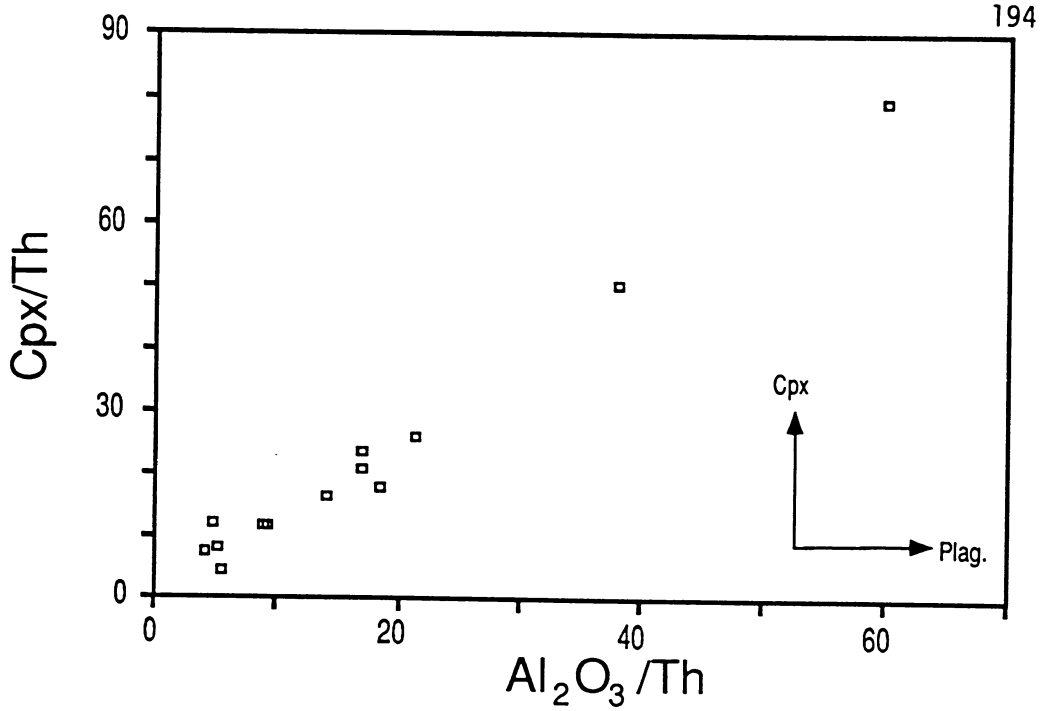

Figure 4.7.3: PER plot for the Dome Mine section, testing for fractionation of plagioclase and clinopyroxene. Linerar regression (reduced major axes) gives a slope of 1.32(0.07) with a y-intercept of 0.25(1.67) and a r value of 0.98. The slope indicates that fractionation of the two phases is possible, although again the y-intercept is not significantly non-zero. The Cpx term is defined in Figure 4.7.1.

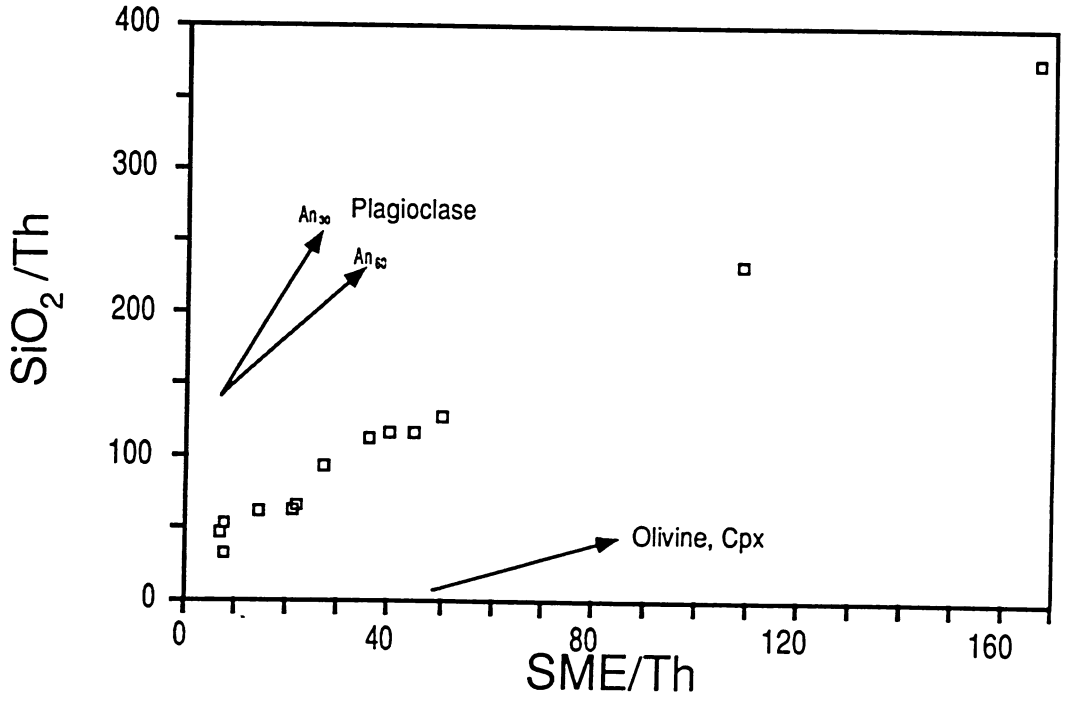

Figure 4.7.4: PER plot for the Dome Mine section, testing for fractionation of plagioclase and clinopyroxene. Linear regression (reduced major axes) gives a slope of 2.06(0.08) with a y-intercept of 30.17(4.95) and a r value of 0.99. This slope indicates that fractionation of the two test phases is possible. The SME term is defined in Figure 4.7.2.

axis coefficient. SME is defined by the following expression:

$$1.5CaO + 0.5MgO + 0.5FeO.$$

A component of plagioclase is present in both axis coefficients, but SiO_2 is dominant over CaO in plagioclase resulting in a mineral vector whose slope is greater than 1.0. The SME coefficient is intended to produce a slope of 1.0 for both olivine and clinopyroxene fractionation when plotted against SiO_2 so some experience with regard to the appropriate fractionating mineral phase must be applied to the interpretation of these vectors.

Interpretation of the PER's for the Harker Lake suite does not reject the hypothesis that it is a cogenetic series of rocks formed by progressive fractional crystallization (Figures 4.7.1, 4.7.2). Both diagrams have obvious straight line relationships between all members of the suite with good correlations. The slope of the line on both diagrams, occurring between the two mineral vectors, indicates a combination of plagioclase and clinopyroxene fractionation. The intercept in the CPX versus Al_2O_3 diagram is not a significant non-zero value and may represent a spurious trend, possibly related to metasomatism (e.g. Pearce, 1968).

The PER's for the Dome Mine suite (Figures 4.7.3, 4.7.4) do not reject the hypothesis of fractional crystallization for development of the suite. Once again the diagrams show well defined straight line relationships between the members of the suite (including the anomalous units of the V8 subunit) with very good correlations. The slopes of the best fit lines fall between the mineral vectors of the two axis coefficients indicating a combination of plagioclase and clinopyroxene fractionation has affected the development of the suite.

The importance of the non-zero intercept for the two CPX vs Al_2O_3 plots is mitigated by the fact that the two plots of SiO_2 vs SME do have no-zero intercepts (e.g. 40.46 and 30.60 for the Harker Lake and Dome Mine suites respectively). This fact plus the overall field, petrographic and geochemical evidence suggest a cogenetic history for the variolitic suites. It is possible that the starting composition of the fractionating magma was along the slope from the zero point of the plot.

Allégre's Technique:

The technique of Allégre *et al* (1977) considers the evolution of volcanic rock suites in terms of incompatible ($D<1$) and highly incompatible ($D<<1$) trace elements, where D is

the bulk rock distribution coefficient of the element. During fractional crystallization, the Rayleigh distillation equation best describes the changes in the concentration of elements in a residual melt (Neumann *et al*, 1954). The Rayleigh equation is:

$$C_l = C_o f^{D-1} \quad (1)$$

where C_l is the concentration of an element in the liquid, C_o is the initial concentration of the element in the liquid, and f is the weight fraction of the residual liquid. When D<<1:

$$C_l = C_o f^{-1}$$

and,

$$f = C_o/C_l.$$

Thus the Rayleigh equation can be rewritten, considering that D<<1:

$$C_l \approx C_o({}^*C_o/{}^*C_l)^{D-1} \quad (2)$$

where * indicates an element for which D<<1. Taking logs of both sides of equation (2), yields:

$$\log C_l = \log C_o + (D-1)\log {}^*C_o + (1-D)\log {}^*C_l \quad (3)$$

This is an equation of a straight line and on a graph of $\log {}^*C_l$ versus $\log C_l$, the slope equals the expression (1-D). As long as the slope is between 0.0 and 1.0, fractional crystallization is indicated. The technique involves some major assumptions which do not seem to adversely affect the results. The bulk D value, for both the highly incompatible element and the index element, is assumed to be constant throughout the differentiation process. Whereas this stipulation is quite plausible for highly incompatible elements not likely to be incorporated by any fractionating phase, it is not feasible for any element with moderate compatibility, such as minor oxides like TiO_2 or P_2O_5. Consequently, this technique works best comparing a highly incompatible element with another incompatible element.

Table 4.7.1 gives the results of regressions performed on plots of incompatible elements against the highly incompatible element thorium. All plots have slopes between 0.0 and 1.0, and have very good correlation coefficients, indicating fractional crystallization was the likely mechanism of differentiation in both the Harker Lake and Dome Mine suites. Figures 4.7.5 to 4.7.8 are examples of these plots, showing La and Zr versus Th for the two study areas. The table illustrates the decrease in slope with increasing distribution coefficient. The LREE, such as La, have larger ionic radii and are thus more difficult to incorporate into

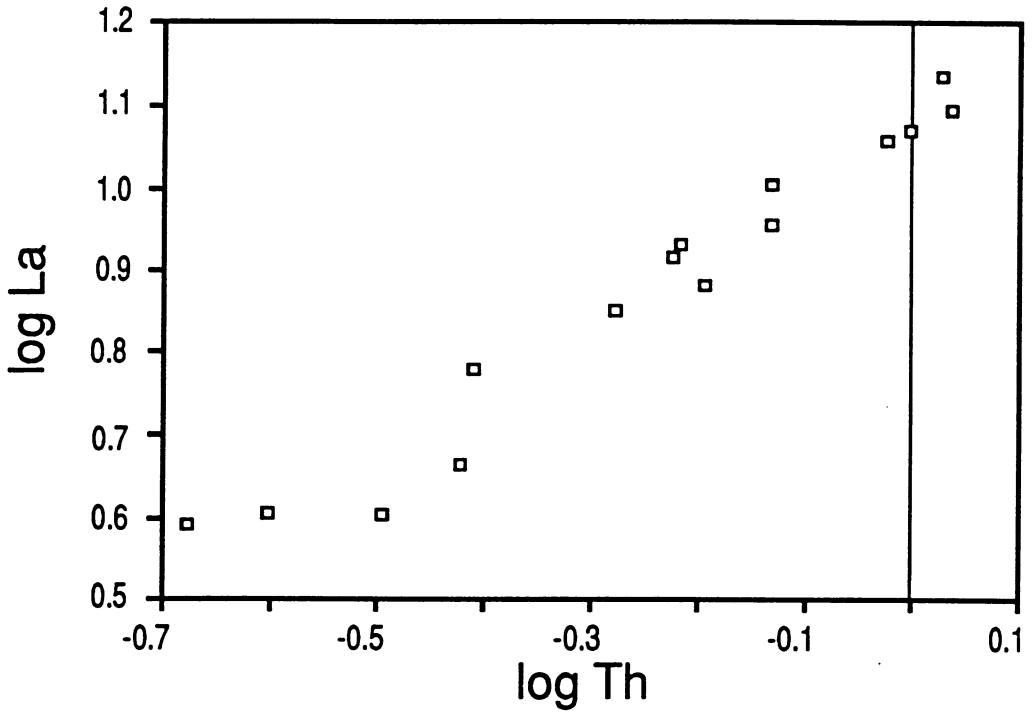

Figure 4.7.5: Plot of log La (incompatible element) vs Log Th (highly incompatible element) testing for differentiation of the Harker Lake suite by fractional crystallization. See text for discussion of technique and interpretation (from Allègre et al, 1977). For regression data, see Table 4.7.1.

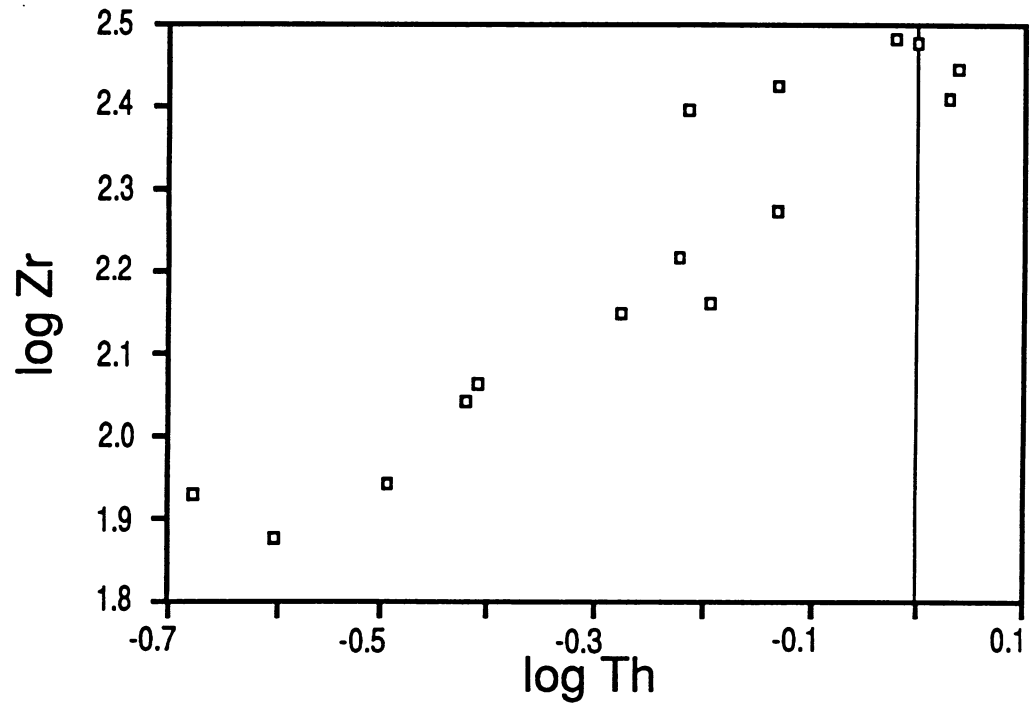

Figure 4.7.6: Plot of log Zr (incompatible element) vs log Th (highly incompatible element), testing for differentiation of Harker Lake suite by fractional crystallization. See text for discussion. For regression data, see Table 4.7.1.

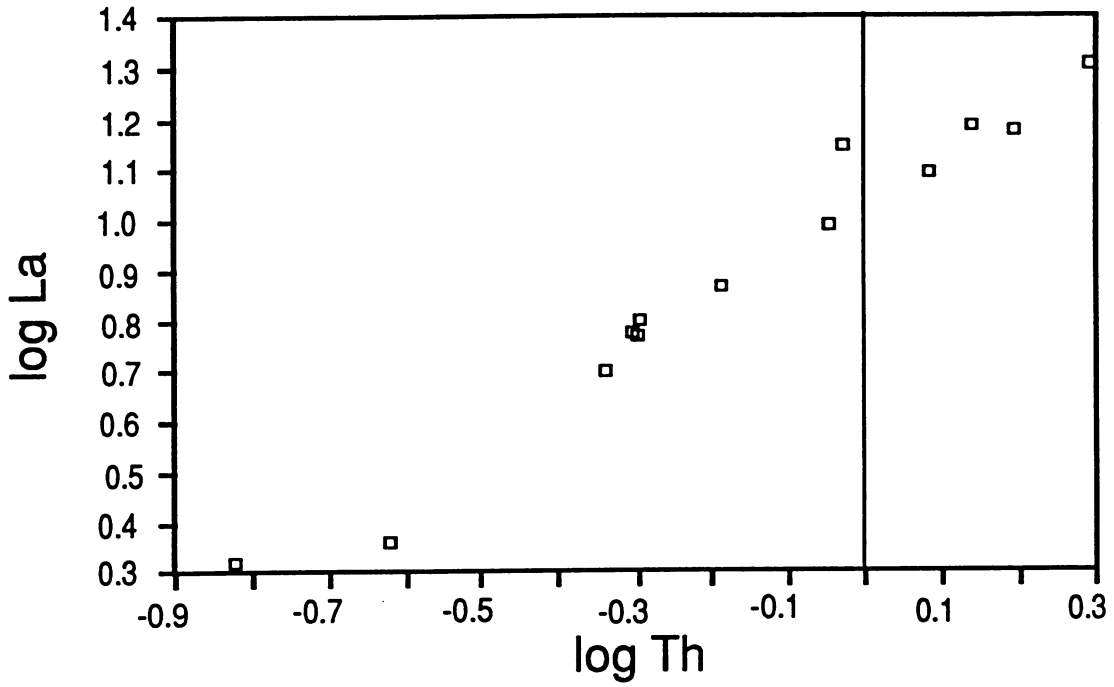

Figure 4.7.7: Plot of log la (incompatible element) vs log Th (highly incompatible element) testing for differentiation of the Dome Mine section by fractional crystallization. See text for discussion. Regression data in Table 4.7.1.

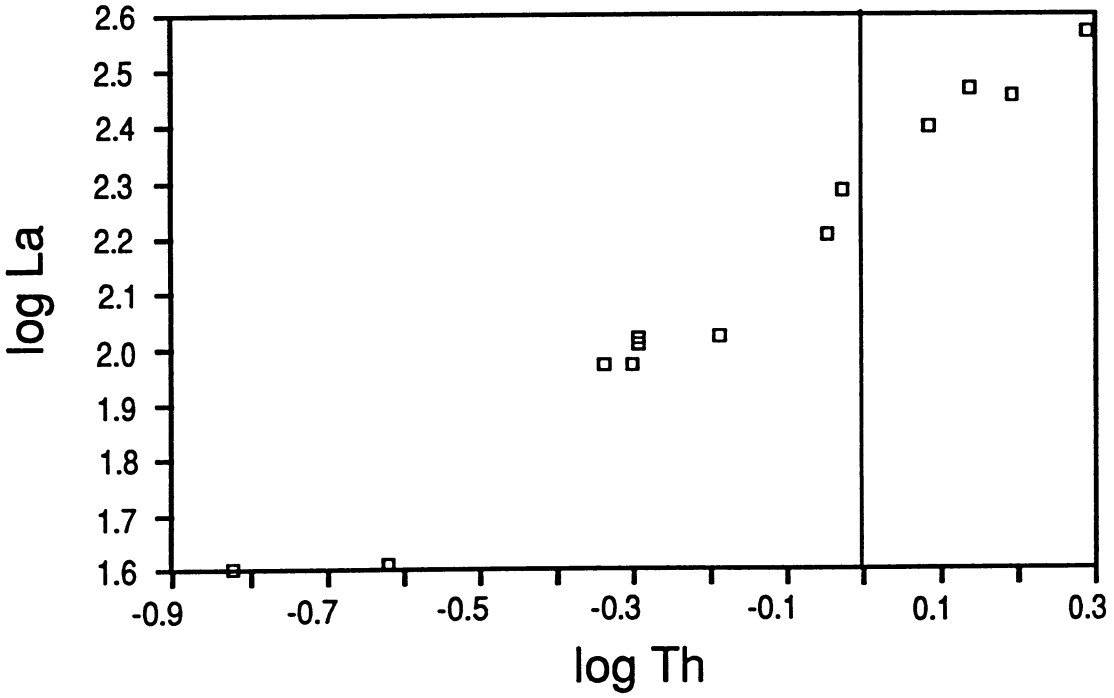

Figure 4.7.8: Plot of log Zr (incompatible element) vs log Th (highly incompatible element) testing for differentiation of the Dome Mine section by fractional crystallization. See text for discussion. Regression data in Table 4.7.1.

Table 4.7.1: Results of regression analysis of log-log plots of the whole rock concentrations of incompatible elements versus a designated highly incompatible element (Th) (Allégre et al, 1978). Note that the slope of the line decreases with increasing distribution coefficient, D. SiO_2 has also been included, although it is not an incompatible element.

a) Harker Lake Section

	n	intercept	slope	r	comments
log La vs log Th	15	1.08(0.04)	0.81(0.05)	0.98	Figure 4.7.5
log Sm vs log Th	15	0.97(0.04)	0.78(0.05)	0.98	
log Eu vs log Th	15	0.47(0.04)	0.60(0.05)	0.96	high D due to Eu^{+2} state
log Yb vs log Th	15	0.96(0.05)	0.74(0.05)	0.96	
log Zr vs log Th	15	2.44(0.07)	0.88(0.09)	0.94	Figure 4.7.6
log Y vs log Th	15	1.96(0.05)	0.66(0.06)	0.95	
log SiO_2 vs log Th	15	1.79(0.02)	0.16(0.02)	0.92	wt% vs ppm

b) Dome Mine Section

	n	intercept	slope	r	comments
log La vs log Th	13	1.05(0.06)	0.94(0.05)	0.98	see Fig. 4.7.7
log Sm vs log Th	13	0.90(0.05)	0.89(0.05)	0.98	
log Eu vs log Th	13	0.33(0.06)	0.71(0.05)	0.97	
log Yb vs log Th	13	0.89(0.05)	0.86(0.04)	0.98	
log Zr vs log Th	13	2.28(0.05)	0.95(0.05)	0.98	see Fig. 4.7.8
log Y vs log Th	13	1.83(0.15)	0.91(0.14)	0.89	D89-21 off line quite a bit
log Y vs log Th	11	1.87(0.05)	0.82(0.05)	0.98	minus D89-21, 9497
log SiO2 vs log Th	13	1.87(0.03)	0.11(0.03)	0.77	

mineral structures, lowering their distribution coefficient. The HREE are smaller, more easily incorporated, and thus have larger distribution coefficients. The slope associated with the HREE, Yb, is lower than that for the LREE, La, as well as, the moderate REE, Sm because the distribution coefficient for Yb is larger (Table 4.7.1). Eu has an anomalously low slope because of the ease with which it is reduced to Eu^{2+} which has a similar ionic radius to Ca^{2+} and is able to substitute in plagioclase, thereby increasing its distribution coefficient.

Although there are limiting assumptions associated with the Pearce Element Ratio and Allégre techniques, both failed to reject the hypothesis that the Harker Lake and Dome Mine suites are related by fractional crystallization and thereby confirm field relationships. Further, the conserved constituent diagrams (PER's) indicate that, as suspected, the mineral phases

being fractionated are, dominantly, plagioclase and clinopyroxene.

4.7.3 Comparison with Modern Environments

It has been noted that the variolitic suites of this study have similar geochemical characteristics and compositional range to certain modern tholeiites which are also thought to be due to fractional crystallization (Carmichael,1964; Thompson *et al*, 1972; Wood, 1976; Perfit *et al*, 1983). There are other similarities with the modern tholeiites as well. Perfit and Fornari (1983) and Perfit *et al* (1983) describe textures in the rocks from the eastern Galapagos Rift area which are remarkably like those preserved in the Archean variolites. They found weakly developed spherulitic, fasciculate, and variolitic (although their usage of this term is not defined) textures common in samples of FeTi basalts through to andesites. They also noted some phenocrysts in andesites. Plagioclase and pyroxene have crystallized together forming spherulitic or fasciculate textures, also observed in rocks from the Harker Lake section. Fine dendritic Fe-Ti oxides and branching pyroxenes indicative of rapid crystallization are common, as they are in the Archean variolitic suites. These textures are in accordance with Wood (1978), who states that the composition of these more evolved lavas requires them to be superheated when they reach the surface. This is consistent with the process of disequilibrium crystallization from an undercooled melt as insufficient nuclei would be present for equilibrium crystallization during surface cooling. From a mineralogical standpoint, Perfit and Fornari (1983) have noted apatite as a common mineral phase in more felsic rocks, again similar to the rock suites of this study. One more interesting point brought forward by Perfit and Fornari (1983) is that vesicularity increases in the more felsic rocks. Andesites appear frothy in comparison to basalts, due to increased volatile content in the more evolved lavas. This could be part of the explanation for the unusual thickness and continuity of the hyaloclastite unit near the top of the Harker Lake section.

It seems that a necessary condition for the compositional range and associated disequilibrium textures of these rock suites is the development of high level magma chambers. Portions of the source magma are moved to these chambers where they undergo further differentiation by fractional crystallization, resulting in rocks of more felsic composition (Carmichael, 1964; Perfit *et al*, 1983). This process may take place in several

stages (Perfit *et al*, 1983). Carmichael (1964) states that the volume of intermediate to acid lava in eastern Iceland could have been derived from an olivine tholeiite (MORB) parent by progressive fractional crystallization. At Harker Lake, there is a progression in the base level of elemental abundances of the individual cycles, perhaps indicative of temporal evolution in the source magma.

The interlayers of anomalous compositions found in the V8 subunit, may have been formed by a separate, possibly perched, magma chamber, connected to the main feeder source for the complete suite. A portion of the evolving magma source for the Vipond may have been separated and then fractionated further (due to volatile loss, cooling, pressure loss) before being erupted contemporaneously with the V8 subunit. As there are two anomalous flows in the Dome Mine sequence and only one at the Porcupine Paymaster, it is a possibility that the vent for this separate chamber was closer to the present site of the Dome Mine. The source system responsible for the development of the variolitic suites could be similar in geometry to that of the Kilauea volcanic complex in Hawaii (Wright and Fiske, 1971). Eruptive units of variable composition are erupted along Kilauea's East Rift from different high level magma chambers. All these chambers are related to a major magma source at depth, suggested by geochemical modelling (Stanley and Russell, 1989) and recordings of seismic activity (Wright and Fiske, 1971).

Wood (1976, 1978) notes two distinct lava types in eastern Iceland; a LIL depleted type (MORB), and a LIL enriched type, especially with respect to Fe, Ti, P, and K, called FETI type in Iceland. The chemical variation in eastern Iceland is spatial, not temporal, with the more evolved lavas present near the centre of the eruptive units, whereas the more mafic flows, olivine to transitional tholeiites, are found near the edges. These two types of lava are erupted at the same time, locally juxtaposed in succeeding flows, and are apparently continuously available for eruption throughout the development of the volcanic pile (i.e. no differentiation of source magma with time). Wood (1976) described two alternative explanations. The first has both types erupted from the same vent and subsequently separated by the effect of viscosity on the distance they flow. The second has the two types erupting from separate vents, similar to present day Hawaii and proposed for the V8 section of the Vipond Subgroup in this study.

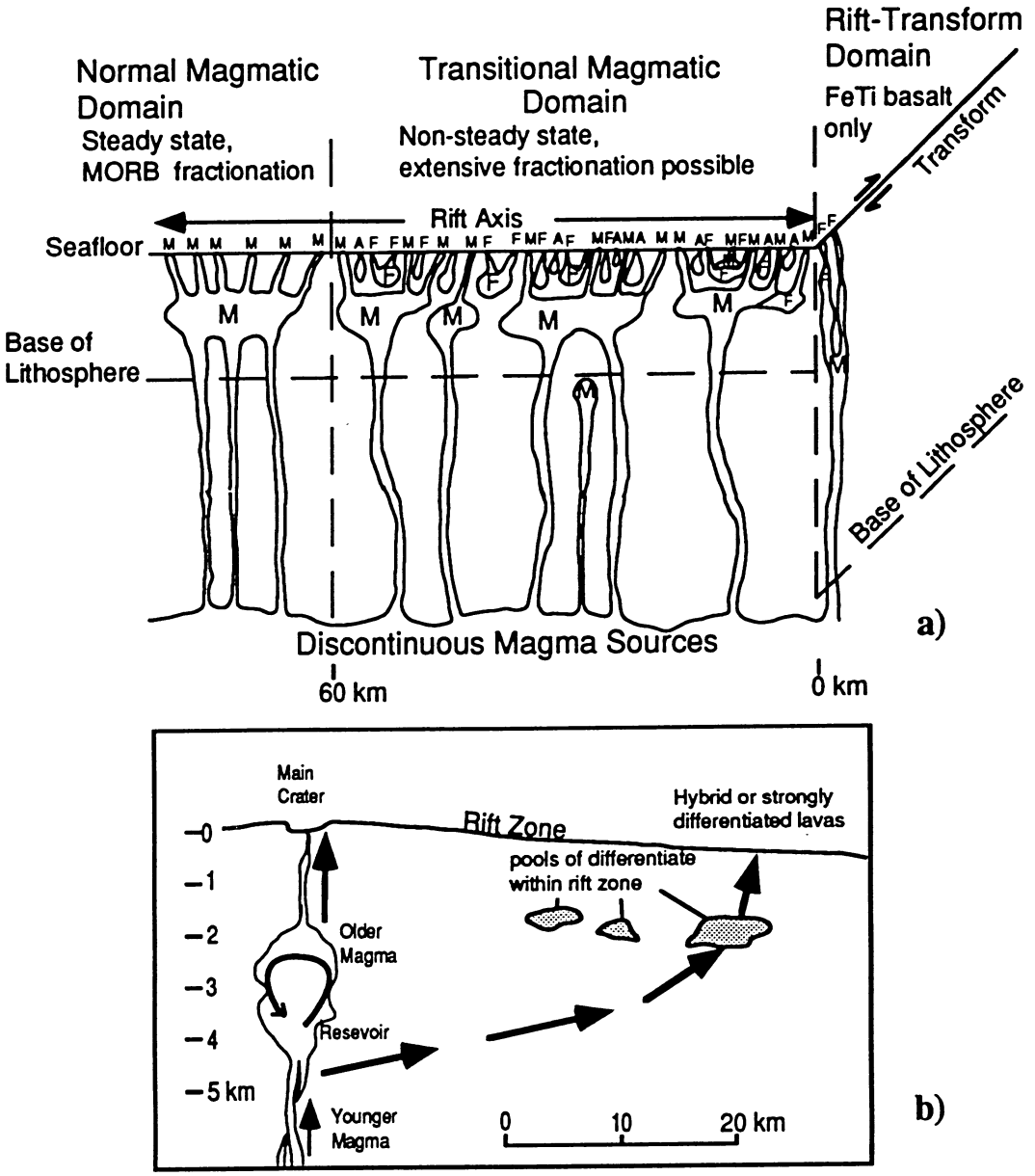

Figure 4.7.9: Conceptual models for the development of anomalously differentiated tholeiitic magmas: a) Magmatic domains in the vicinity of the intersection of a propagating rift and transform segment (after Perfit et al, 1983). The rift propagates from new (thin) to old (thick) crust. The intersection is marked as 0 km. The unstable transitional domain of the propagating rift, 0 to 60 km from intersection, has not re-equilibrated and is thermally and tectonically anomalous. Raised isotherms in this domain support the development of isolated, high level, highly differentiated magmas, resulting from low pressure fractionation which produce flows of wide ranging compositions. b) Development of isolated, high level pockets of differentiated magma in the rift zones of Kileauea Volcano, Hawaii, contributes to the mixed compositions of lava flows along the rifts (Wright and Fiske, 1971). The main crater erupts lavas more representative of the summit magma chamber. These features, including the primitive source magmas, anomalously differentiated suites of volcanic rocks, and a wide spectrum of lava compositions in a small area, match the sections examined in the Harker Lake and Dome Mine areas suggesting similar tectonic processes may have been acting in Archean time. Symbols are as follows: M-MORB, F-FeTi basalt, A-Andesite.

The studies of Perfit *et al* (1983) of samples along an off-ridge rift-transform segment in an accretionary zone, Carmichael (1964) and Wood (1976, 1978) of lavas from an oceanic island setting astride an active spreading centre, and Wright and Fiske (1972) from a mid-oceanic plate setting, all concern relatively thick oceanic crust in areas where rifting has facilitated the development of high level magma chambers (Figure 4.7.9). In addition, the heat provided by raised isotherms in unstable areas near the tip of propagating rifts and over hot spots provides energy to allow the liquids to evolve high in the crust. The high level magmas erupt frequently because of their tectonically active environment (e.g. East Rift at Kilauea). A wide variation in flow compositions in a short stratigraphic section is typical of the sections. This type of system may have played a part in the Archean tectonic environment represented by the variolitic suites in this study.

Figure 4.7.10 shows the geochemical data from the Harker Lake area and the Dome Mine area on a tectonic discrimination diagram designed by Pearce *et al* (1977). This diagram uses similar components to the Jensen cation diagram (Jensen, 1976). However, the data displayed are in weight percent rather than molecular percentages, and TiO_2 is not included. The fields on this diagram have been defined by statistical analysis of 8400 whole rock analyses of rocks from Archean to modern terranes. The discrimination fields are essentially representative of Cenozoic basaltic volcanic rocks, in particular, those with less than 60 wt% SiO_2. All samples from the two study areas have been plotted, even if their SiO_2 content exceeds the limits specified. Both areas have Fe enrichment trends, similar to the Jensen cation plots, contained within the field of continental tholeiites. The upper members of the suites plot in the field of spreading centre islands. In the Dome Mine area, the anomalous flows of the V8 subunit follow the trend of calc-alkaline orogenic rocks toward the Al_2O_3 apex within the spreading centre island field. The spreading centre island field is defined by rocks, such as those found in Iceland and the Galapagos Islands, which have anomalous differentiation, probably resulting from fractionation in high level magma chambers (Pearce *et al*, 1977). The geochemical data from this study plot in the fields of continental tholeiites and spreading centre islands which is consistent with the comparisons already made between the Archean variolitic suites and the modern oceanic suites found in areas of thickened crust.

In summary, the geochemical data and petrogenetic discussions above have shown that

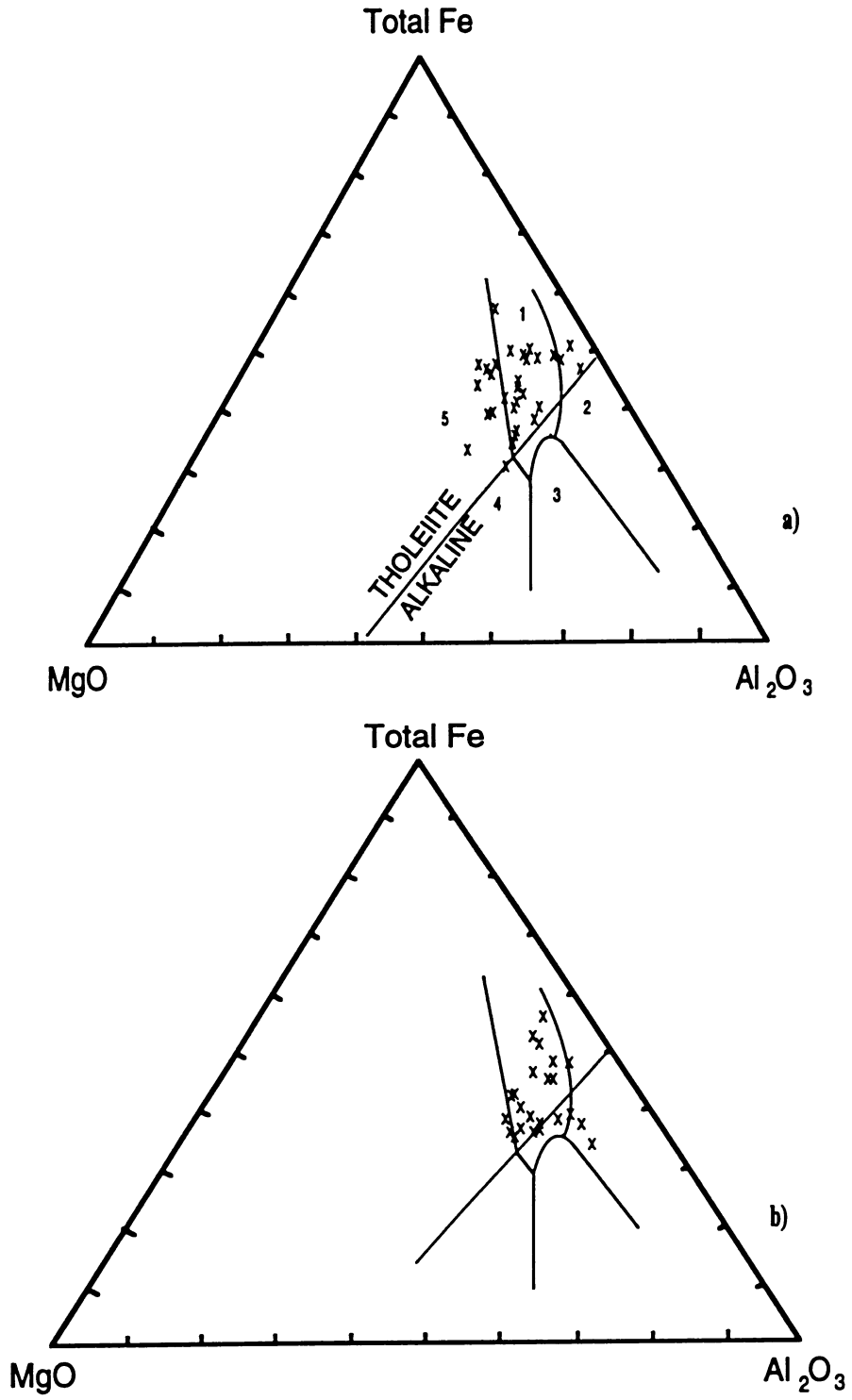

Figure 4.7.10: Tectonic discrimination plot (Pearce et al, 1977). a) The rocks of the Harker Lake section have characteristics similar to Cenozoic continental tholeiites, the upper flows resembling spreading centre island rocks. b) As figure a), showing the rocks of the Dome mine section. The subordinate trend identified in Figure 4.5.2 is also seen in this plot, within the spreading centre island field, projecting toward the alumina apex. Fields are defined as follows: 1. continental tholeiites, 2. spreading centre islands, 3. orogenic, 4. ocean ridge and floor, 5. ocean island.

variolitic suites are more evolved than their surrounding terrane, commonly high Fe and Ti basalts, and they have been developed primarily by fractional crystallization. They are very similar in compositional range, geochemical characteristics, and textures to modern oceanic tholeiitic suites developed in thicker crust than typical spreading ridge settings (i.e. off-ridge, accretionary zones, mid-plate hot spots). Archean continental crust is considered to have been similar to present day oceanic crust, but with higher heat flow to allow, for example, extrusion of komatiitic flows (Bickle, 1978; Wilks, 1988). After initial Archean crustal development of komatiitic through tholeiitic volcanic sequences from spreading ridges associated with mantle upwellings (Archean MORB equivalent?), it is possible that rift and/or hot spot related variolitic suites were formed in the thicker crustal setting. Considering the strike extent of some variolitic units, at least 30 kilometres in Timmins (D.Brisbin, pers. com.) and greater than 60 kilometres in Québec (Dimroth *et al*, 1973), they are more likely related to a rift-hosted source than a single volcanic centre. Also, there is a common association of variolitic suites with major lineaments in the Abitibi (such as the Destor-Porcupine Fault) which may have originated as deep seated rift features.

Rifting in Archean crust would allow elevation of an Archean MORB-type magma to multiple chambers at various levels in the crust and to the surface. The high level chambers would promote extensive fractional crystallization producing a lava series characterized by a wide compositional range and anomalous differentiation. They may form extensive hyaloclastite due to the elevated volatile content of the highly viscous, evolved lavas. Also, the evolved lavas are likely to develop disequilibrium textures, such as spherulitic, branching and dendritic features, because of the siliceous nature of the lava which limits intra-melt element diffusion and the high degree of undercooling due to a superheated, nucleus-free source (Wood, 1978; Fowler *et al*, 1987). If more of the comparative characteristics of modern ocean ridge and off-ridge basalts (i.e. MORB versus FeTi basalts and tholeiitic andesites) can be found in Archean suites, there may be a significant contribution possible to the understanding of Archean tectonics.

5. Alteration of Variolitic Suites

5.1 Introduction

The purpose of this chapter is to study the effects of alteration on variolitic suites of rocks, particularly the alteration related to Au mineralization at the Dome Mine and in the Harker Lake area. The alteration study was carried out within specific lithologic units of the Harker Lake and Dome Mine sections. Unit selection depended, to a certain extent on the availability of unaltered equivalents to the altered and mineralized rocks. This was determined by careful mapping of units in the Harker Lake area. At the Dome Mine, map plans provide detailed, level to level correlation of particular units in various parts of the mine. Although it is preferable to collect samples from a restricted area, this was not always possible at the Dome Mine because alteration zones are diffuse, coalesced, or cover large areas. As a result, the alteration study within a particular unit combines samples from various parts of the mine, chosen for their stratigraphic, geochemical, and textural similarities.

The geology, sample location, and petrography has been described in detail in Chapters 2 and 3. This chapter documents the results of whole rock geochemical studies of the alteration zones.

5.2 Evaluation of Metasomatism

5.2.1 Isocon Diagram

Gresens (1967) developed equations for determining the composition-volume change relationships of altered and unaltered rocks during metasomatism. His analysis is based on the assumption that some elements remain immobile during the alteration process. This provides the basis for calculation of changes in the concentration of other elements. Grant (1986) has rearranged Gresens' equations to calculate the changes in volume (or mass, in Grant's example), expressed in the following equation:

$$C^A_i = M^o/M^A(C^o_i + \Delta C_i) \quad (1)$$

where C^A_i and C^o_i are the concentrations of an element, i, in the altered and unaltered rocks

respectively, ΔC_i is the change in concentration of the element, and M^o/M^A is the ratio of equivalent masses before and after alteration. On a graph of the concentration of elements in an altered rock versus its unaltered equivalent (Figure 5.2.1), called an isocon diagram, a straight, "best fit" line passes through the origin and all the elements which have remained immobile during the alteration process (i.e. those elements whose mass has not changed). This line is called an isocon line, as it represents no change in element concentration ($\Delta C_i = 0$). The slope of the isocon line defines the overall mass change during metasomatism, and the volume change by the following equation:

$$V^A/V^o = M^A/M^o(g^o/g^A) \quad (2)$$

where V^A/V^o is the ratio of equivalent volumes before and after alteration, and g^o and g^A are the specific gravities of the unaltered and altered rock.

There are two main assumptions involved in the technique:

1) That the unaltered and altered samples were, in fact, identical prior to alteration.

2) That the isocon, or best fit line, represents no mass change for its constituent elements. Elements having similar chemical characteristics and behaviour (e.g. Ni and Cr) may also define straight lines, however, these can be avoided by careful examination of the components used for the isocon line. The isocon line could be drawn for constant volume during alteration, usually interpreted from field and petrographic evidence rather than immobile elements.

To facilitate viewing and interpretation of the isocon diagram most elements have been scaled to fit the graph (Figure 5.2.1). This is done to evenly distribute the major and trace elements along the diagram. In this study, consistent with Grant (1986), element concentrations in either parts per million for trace elements or weight percent for major oxides have been scaled to a maximum value of 30 for the graph axes (Grant, 1986). The scaling in no way affects the relationship of the elements to the isocon line. All components which have undergone an equivalent proportional gain, or loss, relative to the isocon (e.g. ΔC_i = +50%), will plot on a straight line radiating from the origin. In fact, these lines are identical in nature to the isocon which represents the value, $\Delta C_i = 0$ (Figure 5.2.1). Scaling of an element merely moves it out, or in, along one of these lines. Error in the element concentration must also be scaled, but again the scaling has no net effect relative to the

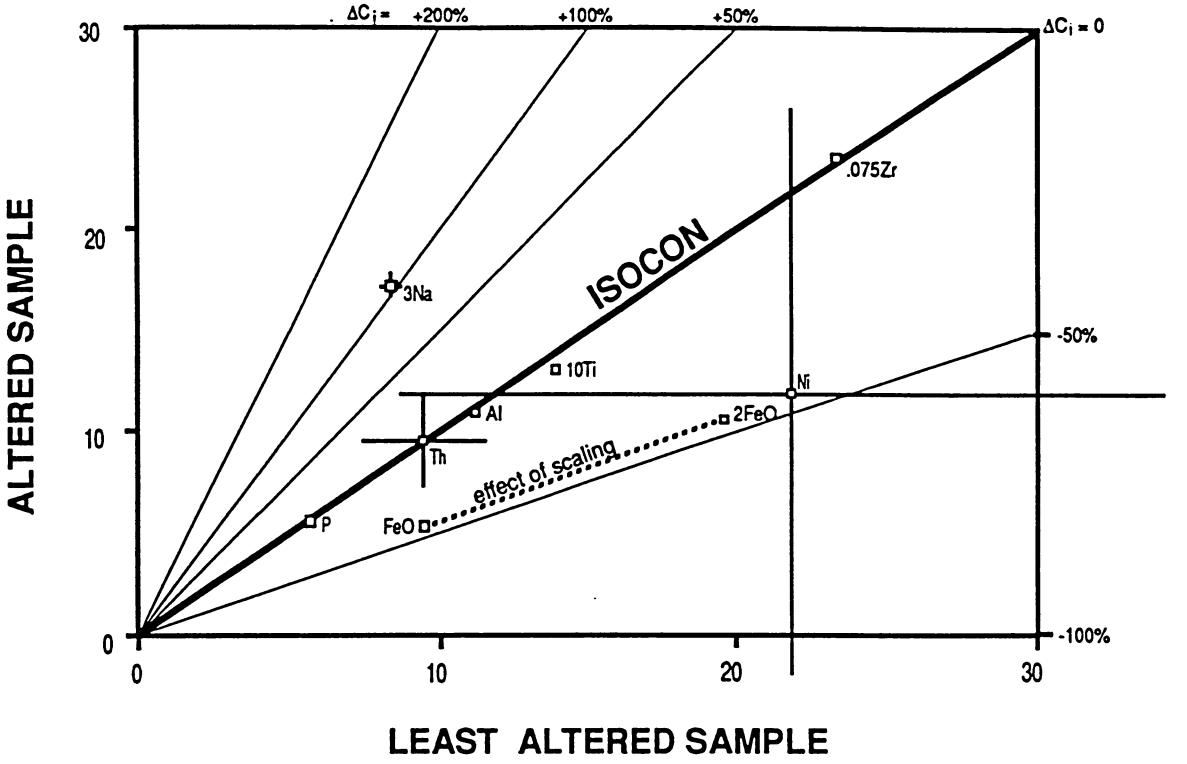

Figure 5.2.1: Explanatory figure for the isocon diagrams, shows effect of scaling on elements, lines of constant gain or loss, and error bars for selected elements. The isocon line passes through elements which have remained immobile during the metasomatic process, and in this case indicates no volume change (assuming that the specific gravities of the unaltered and altered samples are equal). Error bars are shown for Ni, Th, and Na_2O. The error in the in the value for Ni indicates that it cannot be considered to have been mobile, since the isocon line is within the error limits shown. The error for Na_2O, scaled equivalent to the component (3x), indicates that it was mobile, with an an enrichment of about 100% relative to the unaltered sample. Both the gains/losses of the components and their errors are expressed relative to the concentration present and, as a result, they can be compared directly on the diagram. Numbers before the elements are the scaling factors applied. Major oxides, except for iron oxides, are shown as simple elements (i.e. Si = SiO_2) to avoid cluttering the diagrams unnecessarily. The major oxides have been scaled to the axes in weight percent, trace elements in parts per million, and Au in parts per billion.

isocon. Quantification of gains and losses of elements during alteration can be done by simple graphical methods. By choosing a convenient value along the isocon, percentage gain or loss lines can be drawn by scaling vertically from the isocon line (Grant, 1986) and connecting the measured points to the origin.

The coefficients of variation ($100*\sigma/x$, where σ = standard deviation), calculated in Tables 4.4.1 and 4.5.1 for the various lithologic units, are used as expected background variance of the elements. These values include both sample variance as well as analytical error and represent the maximum variance expected in a particular unit. For the alteration study, only gains and losses greater than the element's variance for a particular lithologic unit are considered to be significant. The background variance can be related to the percentage gain and loss lines on the isocon diagram. For example, the position of Ni on the isocon diagram in Figure 5.2.1 indicates that it has been depleted by almost 50% from its original concentration. However, the background variance for Ni in this case, shown by the error bars (scaled by the same factor as the element), is greater than the total depletion. Therefore, it cannot be said with certainty that Ni has been depleted in the alteration process.

5.3 Geochemistry of Alteration

The results of the alteration studies using the isocon diagram are summarized, along with modal mineralogy (from Chapter 3), in Tables 5.3.1 to 5.3.3 for the Harker Lake area and Tables 5.3.4 to 5.3.6 for the Dome Mine area. The results are outlined, sample to sample, from the relatively unaltered country rock to the core of the alteration zone. This gradual approach shows any variation in the alteration style with changing alteration intensity. An overall summary from least to most altered rock is also given to characterize the most intensely altered part of the zone relative to background whole rock chemistry. Elemental gains or losses, listed in the following text, are in decreasing order of percentage change. Commonly, gains and losses, interpreted from the isocon diagrams, are expressed for the Fe_2O_3 which is not normally considered mobile. In fact, these results express a change in the overall oxidation state of the iron in the altered rocks as explained in the text.

5.3.1 Harker Lake Area

Line 28+00E Area, Intermediate Flows

Alteration of two flows was studied in the Line 28+00E area: the intermediate flow, just below the hyaloclastite unit, and the thick, massive flow just above the hyaloclastite, at the top of the section. Samples of the intermediate flow include H-27 (least altered), H-26 (moderately altered), and H-25 (most altered) (Table 5.3.1). Examination of samples H-27 and H-26 shows no macroscopic change, although microscopically, uralite and chlorite have been reduced and the proportion of plagioclase increased. The isocon diagram for these two samples (Figure 5.3.1a) reveals several isovolumetric chemical changes including an increase in the proportion of Fe_2O_3 relative to FeO (resulting from a change in the oxidation state), and gains in Na_2O and CO_2 content. There is also a small increase in Ta and, possibly, Th. The major losses recorded are in the concentrations of CaO, MnO and Zn. The decrease in CaO and increase in Na_2O is indicative of the breakdown of epidote and stabilization of albite in the rock. Oxidation of iron released by the elimination of uralite and chlorite has resulted in an increase in magnetite and possibly very fine grained hematite (though it is not in the mineral mode). Sample H-25 was taken from the bleached, veined and mineralized core of a small fault, where it crosscuts the flow. The isocon diagram for H-26 and H-25 (Figure 5.3.1b) indicates a small volume increase (+4%) but this value is not significant with respect to the error involved in the isocon. In addition to the changes noted in the previous stage of alteration, there is a large increase in S, Ba, K_2O, and Nb in sample H-25. Significant losses occur for H_2O, Zn and MnO. CO_2 content remains about the same as in H-26.

Overall, from the least altered to the most altered samples (H-27 to H-25) there is addition of S, Fe_2O_3, Na_2O, Sr, K_2O, Ta and CO_2, and depletion of H_2O, Zn, MnO, FeO, CaO, MgO and, possibly, Ni (Figure 5.3.1c). Volume does not appear to have changed significantly, despite the addition of veins in the core of the zone. This is supported by the lack of any shearing associated with the crosscutting structure. The significant addition of Na_2O resulting in the stabilization of albite and the formation of Na-bearing amphibole in the core of the zone indicates that the altering fluid was sodic rather than potassic. Oxidation of Fe^{2+} released by the mafic minerals resulted in a change of the proportion of Fe_2O_3 to the total amount of iron in the rock, and seems to be related to the increase in the amount of

Table 5.3.1: Comparative table of sample mineralogy and geochemistry for the alteration of the Variolitic Intermediate Flows, L28+00E area, Harker Lake section. Samples are ordered in the table from least to most altered (descriptions in the text).

Mineralogy	H-27	H-26	H-25	Overall(%)
uralite	X			- 10
chlorite	XXX	XXx	·	- 30
albite	XXXx	XXXXx	XXXXx	+ 10
quartz	X	X	XXX	+ 20
sphene/leucoxene	·	o	o	+ 1-5
epidote	o			- 1-5
carbonate	x	o	x	+ 2-3
magnetite	x	x	x	+ 2-3
hematite			o	+ 1-5
pyrite		o	o	+ 1-5
apatite			o	+ 1-5
Mg riebeckite			·	+ trace
talc			o	+ 1-5
Elemental Changes				Overall Changes
+ > 200 %			S	S
100 - 200			Sr,Ba	Fe_2O_3,Na_2O
50 - 100		Fe_2O_3,Na_2O,CO_2	K_2O,Fe_2O_3,Ni	Sr,K_2O,Ta,CO_2
20 - 50		Ta	Na_2O,Ta,Rb	
10 - 20		Th		
- > 75 %			H_2O,Zn	H_2O,Zn
50 - 75			MnO	MnO,FeO,Ni
20 - 50		Zn,CaO,FeO,MnO		CaO,MgO
10 - 20				
Au (ppb)	n.d.	n.d.	n.d.	
Specific Gravity	2.87	2.86	2.85	
Volume Change		0	+4%	+2%

Mineral modes are represented by the following symbols: X - 10%, x - 5-10%, o - 1-5%, · - trace.

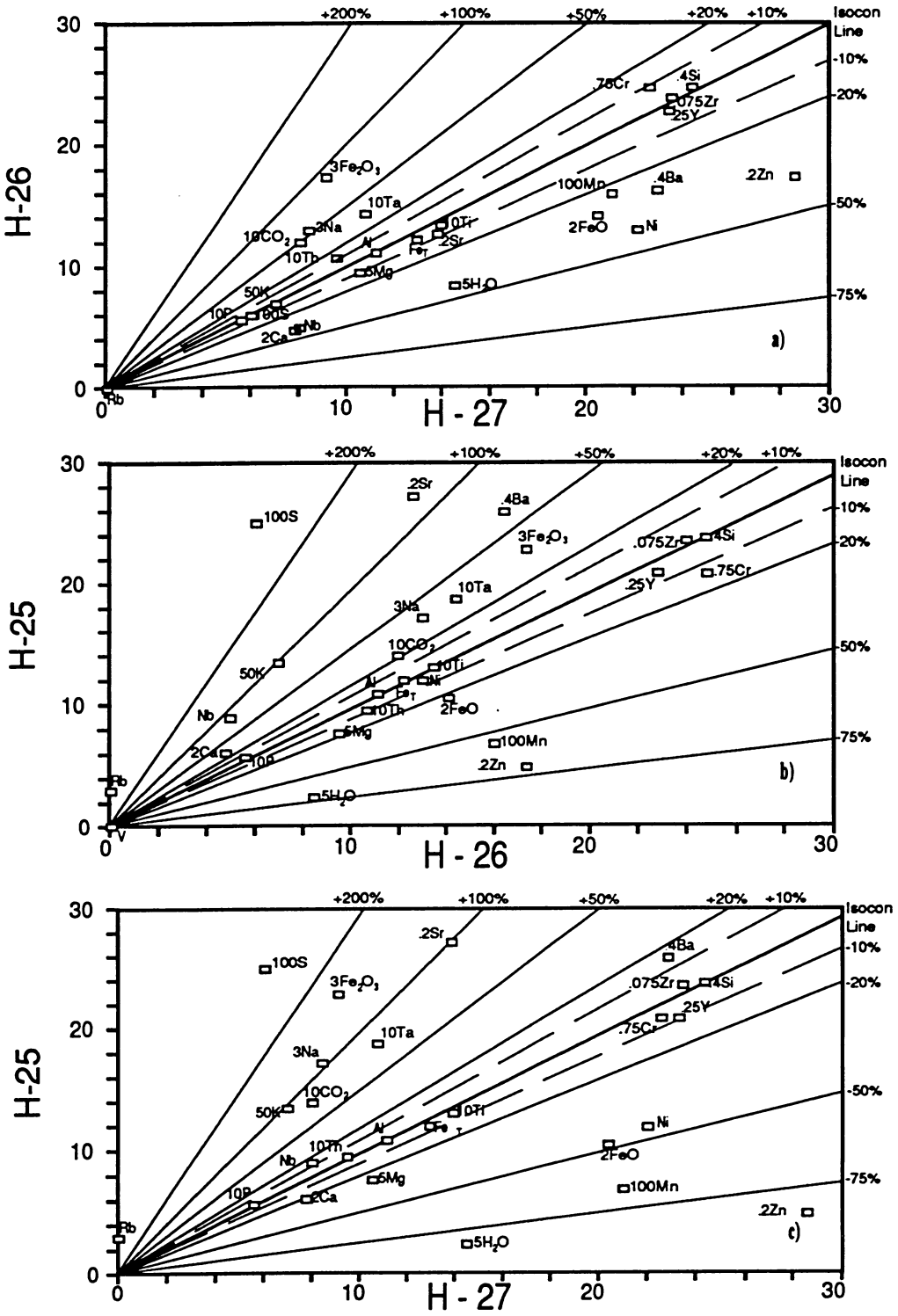

Figure 5.3.1: Isocon diagrams for the alteration of the Intermediate Variolitic Flow, L28+00E area, Harker Lake section. The alteration has very little volume change associated. a) Least (H-27) vs moderately (H-26) altered samples ($\Delta V = 0$). b) Moderately vs most (H-25) altered samples ($\Delta V = +4\%$). c) Least vs most altered samples ($\Delta V = +2\%$). Results are discussed in the text.

magnetite and hematite. This indicates that a relatively oxidized fluid reacted with the rock. The breakdown of amphibole and chlorite released MgO and H_2O which were subsequently lost with no significant secondary metasomatic phases to incorporate them in the altered rock. The breakdown of Ca-bearing plagioclase and epidote released some CaO and Al_2O_3. The Al_2O_3 was incorporated in the rock by formation of albite whereas not all the CaO was incorporated into carbonate and some was lost. Both Sr and Ba had significant gains during the metasomatic process which can be roughly correlated with the formation of carbonate. Another possibility is that some sulphate minerals were formed, due to the oxidizing effect of the fluid, incorporating Sr and Ba in the process. Sulphate minerals have not been identified in the alteration assemblage, perhaps because they are too fine grained or are mistaken for minerals having similar optical properties. Zn, due to its mobile nature, may simply have been removed by the altering fluid, giving an overall loss. A very minor increase in Ta is recorded, possibly incorporated by the formation of Fe oxides in the rock.

In the massive flow at the top of the section, samples H-29 (least altered), H-30, H-31, H-55 and H-55a (most altered) (Table 5.3.2 and Figure 5.3.2), were all taken in a section parallel to flow contacts, and perpendicular to the alteration zone, over a distance of 15 metres (Map 2.1.2a). Initial alteration from H-29 to H-30 (which appears fresh but is cryptically altered) involved minor addition of MgO and Na_2O, and depletion of CaO, and Fe_2O_3 (Figure 5.3.2a). Again, the elimination of epidote has probably contributed to the increase of albite in H-30. No volume change was expected according to field descriptions of the rocks, and this is corroborated by the isocon line which includes the elements P_2O_5, Al_2O_3, Th, TiO_2, and Zr. Sample H-31 (Figure 5.3.2b), which is bleached due to carbonatization and elimination of mafic minerals, has an insignificant volume increase (+4%) along with large additions of CO_2, Ba and Sr (>200%), as well as, lesser gains of Na_2O and, possibly, Ni (abundance of Ni close to detection limit). Ta seems to be enriched but the gain is close to the expected variance. Significant losses of H_2O, MnO, and FeO are recorded. MgO does not have a significant change despite the elimination of most of the mafic minerals. Some of the MgO released may have been incorporated by carbonate and the remaining chlorite which is more Mg-rich. Changes in the concentration of Fe_2O_3 and FeO indicate there has been oxidation of iron, reflected by the presence of hematite in H-31.

Table 5.3.2: Sample mineralogy and geochemistry for the alteration of the Upper Massive Flow, L28+00E area, Harker Lake section.

Mineralogy	H-29	H-30	H-31	H-55	H-55a	Overall
uralite	Xx	x				- 15%
chlorite	XX	XXx	X	x	·	- 20
albite	XXXX	XXXXx	XXXXx	XXXXx	XXXX	
quartz	X	X	Xx	Xx	XXX	+ 20
sph/lcxn	o	o	o	o	o	
epidote	o					- 2-3
carbonate	o	x	Xx	XX	X	+ 5-8
magnetite	X	x	x	o	x	- 2
hematite			o	o	o	+ 2
pyrite			o	x	x	+ 5-8
apatite	o	o	o	o	o	
Mg-rieb.			o	o	·	+ 1-2
talc				·	·	+ trace
zircon(?)	·	·	·	·		- trace
Element Changes						
+ > 200 %			CO_2	S,K,V,Au		S,Au,Ni, CO_2
100-200			Ba,Sr	Ni,CO_2	Fe^{3+}	Na
50-100			Na,Ni,Fe^{3+}	Fe^{2+},Cr	S,Ni	
20-50		Mg		Ca,P,Sr,Ba	Si	Sr,P
10-20		Na	Ta	Na		Si,Cr,Ta
- > 75 %		Ni		H_2O,Fe^{3+}	Ba,V	H_2O,Mg
50-75					Mg,Zn,Mn, Au,CO_2	Mn,Ba,Zn
20-50		Ca, Fe^{3+},K	H_2O,Mn,Fe^{2+}	Mg	Sr,Ca,Fe^{2+}	Fe^{2+}
10-20					Fe_T	Fe_T
Au (ppb)		26	n.d.	794	304	
Spec. Grav.		2.83	2.86	2.87	2.80	
Vol. Change			+4%	+6%	+8%	+14%

Mineral modes are represented by the following symbols: X - 10%, x - 5-10%, o - 1-5%, · - trace.

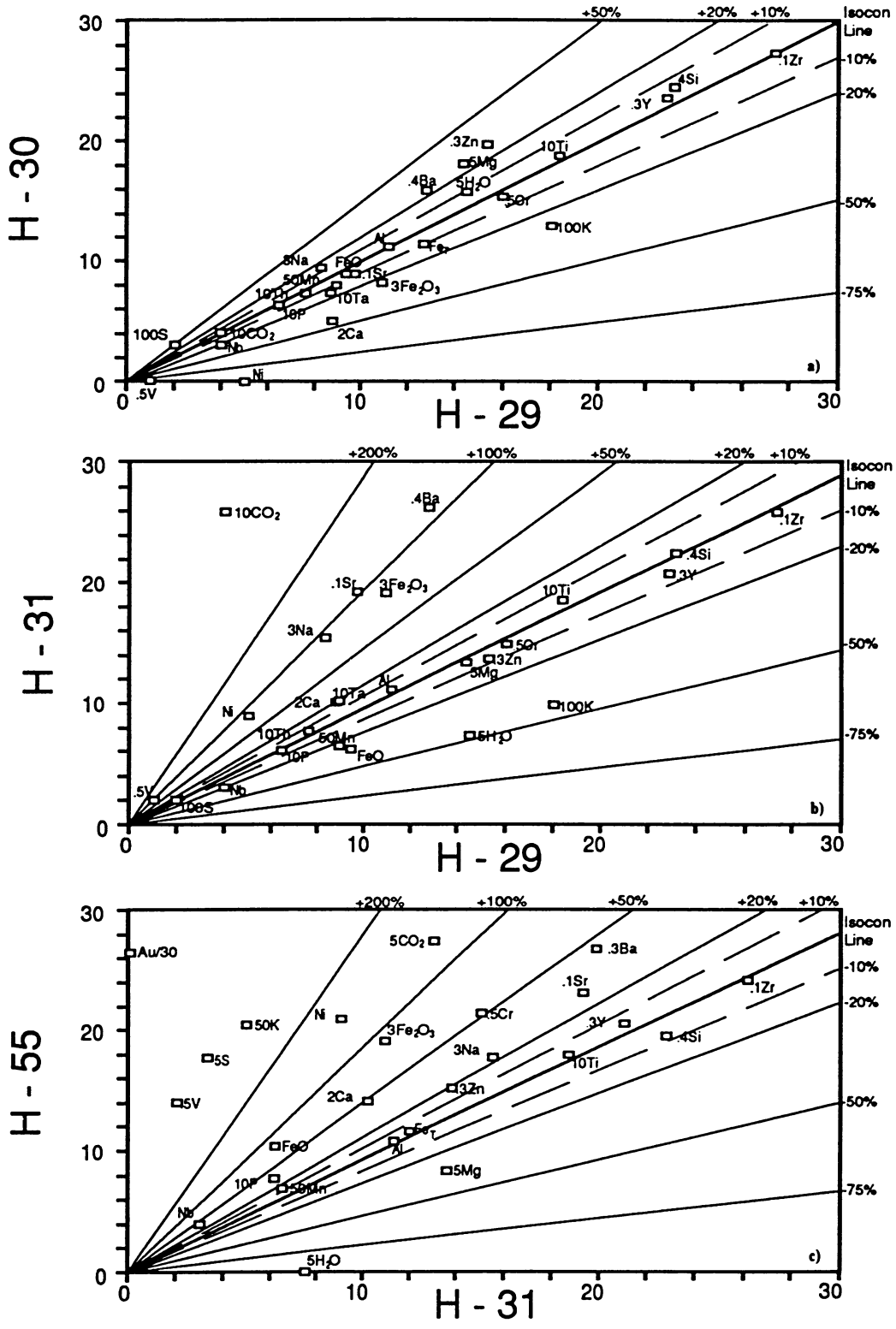

Figure 5.3.2: Isocon diagrams for the alteration of the Upper Massive Flow, L28+00E area, Harker Lake section. The overall volume change associated with alteration is approximately +14%. a) Least (H-29) vs cryptically (H-30) altered samples ($\Delta V = 0\%$). b) Least vs bleached zone (H-31, moderate to strong alteration) samples ($\Delta V = +4\%$). c) Bleached zone vs strongly (H-55) altered samples ($\Delta V = +6\%$).

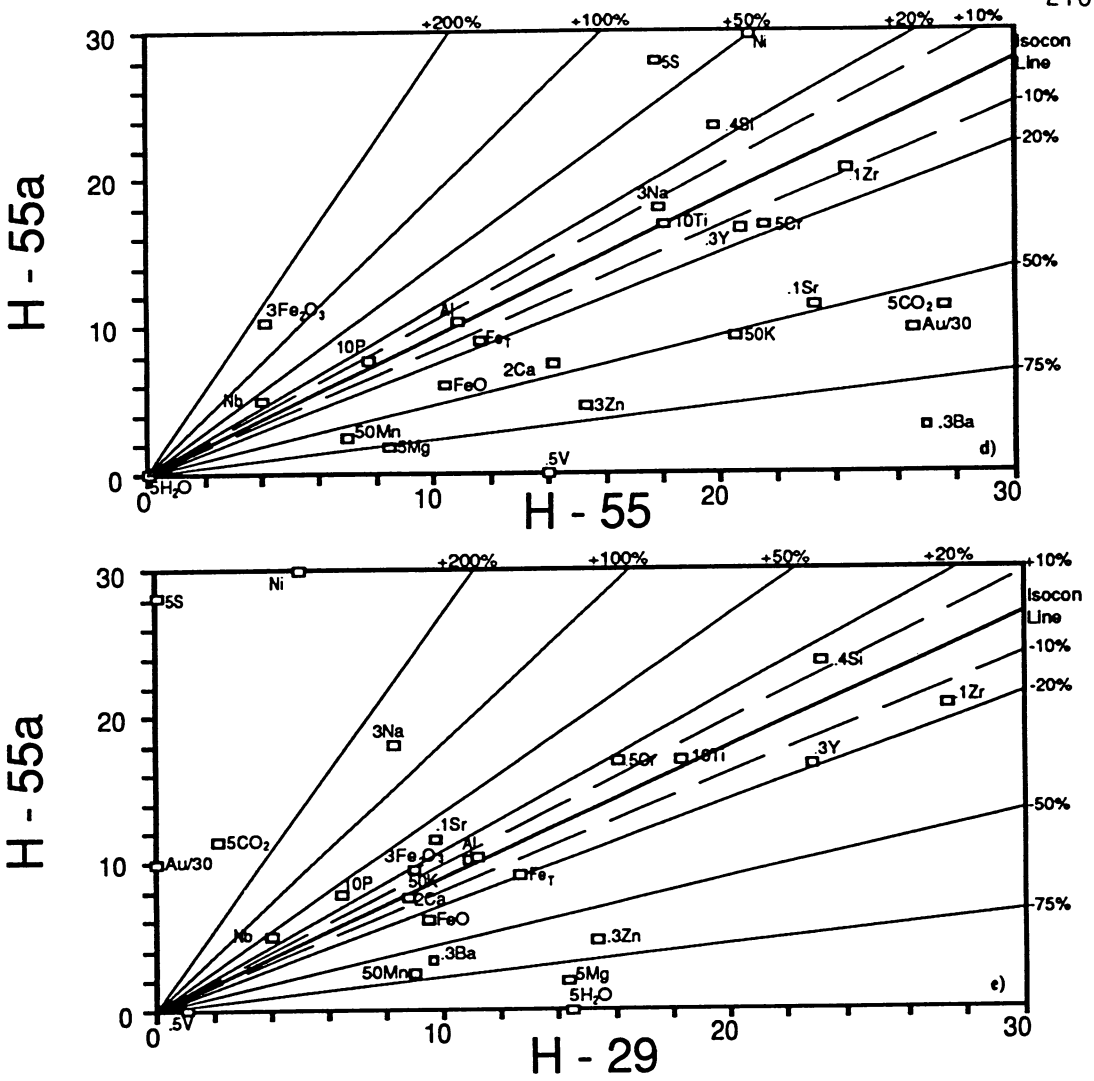

Figure 5.3.2 (con't.): d) Strongly altered (H-55) vs vein envelope (H-55a) samples (ΔV = +8%). c) Least (H-29) vs most (H-55a, vein envelope) samples (ΔV = +14%).

REE analyses are only available for these first three samples in the alteration profile (Figure 5.3.3). Sample H-31 has minor depletion evident in the HREE, relative to the least altered sample, H-29. Both H-30 and H-31 have insignificant LREE depletion considering the dilution effects possible.

Although H-31 occurs in relatively homogeneous, though pervasively altered, basalt away from veining, H-55 and H-55a are from the core of the alteration zone where there are abundant, small, anastomosing quartz veins. H-55 is a sample of altered wall rock between the veins, and H-55a is from a narrow envelope to a quartz vein, about 1.0 cm wide (Figure 3.1.1). Comparing sample H-31 to H-55 (Figure 5.3.2c), there is an estimated 6% volume increase and a large number of elements are enriched toward the core zone (H-55). There is a large increase in the concentration of S, and Au, in this zone, consistent with the significant increase in pyrite. K_2O, CO_2, and Sr are enriched in H-55, whereas the data for Ba and Na_2O are inconclusive. Ni and Cr are both enriched, though a reason is not immediately evident. Other lesser additions include CaO, P_2O_5, and possibly V. The proportions of ferrous and ferric iron indicate some reduction of iron relative to H-31, as a result of the formation of pyrite. The only significant loss at this stage of alteration is H_2O, as most of the hydrous phases have been eliminated, excepting minor amounts of chlorite, Na amphibole and talc.

A detailed comparison of sample H-55 with H-55a (Figure 5.3.2d) shows the isocon line is difficult to define using all the previously "immobile" elements, such as Al, Zr, and Ti. Because there is apparent elimination of zircon(?) in the vein envelope, it is possible that Zr was lost from sample H-55a. On the other hand, the content of plagioclase and magnetite, the primary residences for Al and Ti respectively, remained relatively constant in the two samples. This is corroborated by the Al_2O_3/TiO_2 ratio which is constant in all samples from the alteration study (Appendix 5.1b). For this reason, an isocon line including only Al_2O_3 and TiO_2 was chosen. The isocon line indicates a 7% volume increase from H-55 to H-55a. The oxidation of iron indicated by the isocon is suspect because of the large error associated with the titration method for ferrous iron (Wilson, 1955) in samples containing abundant pyrite. The increased presence of pyrite is reflected by a gain in the S content of H-55a. The only other significant addition to H-55a is SiO_2, and this is apparent from the petrographic work which showed a large increase in modal quartz. Many elements have been lost from H-55a,

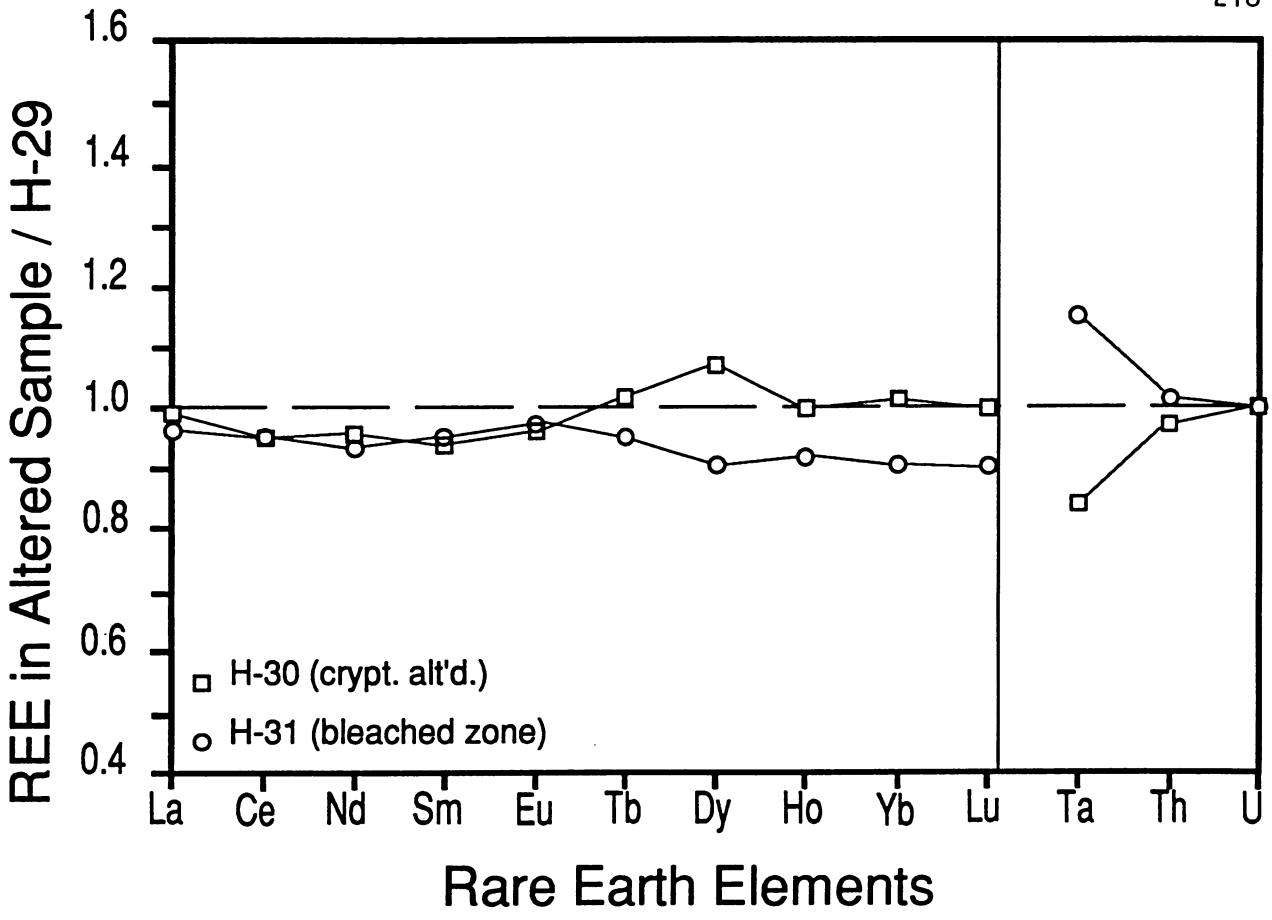

Figure 5.3.3: Rare Earth Elements, plus Ta, Th, and U, in the altered samples of the Upper Massive Flow normalized to the least altered equivalent (sample H-29). Data is available only for samples H-29, H-30, and H-31. The apparent HREE depletion in sample H-31, although possibly indicating a trend in more altered samples, is not greater than the error in the analyses (Table 4.2.1).

in particular, Ba, MgO, Zn, MnO, and CO_2, and to a lesser extent Sr, CaO, and total iron. There is a highly anomalous Au content in the vein envelope, as in H-55.

The alteration of flows in the Line 28+00E area was characterized by large additions of S, Au, CO_2, Na_2O and Ni with minor Sr, Cr, SiO_2, P_2O_5, and possibly Ta. The main losses have been MgO, H_2O, MnO, Ba, Zn, and minor total Fe. The ratio of ferric to ferrous iron was increased during alteration, indicating a relatively oxidizing fluid has interacted with the rock. Direct comparison of the least altered and most altered samples in the upper alteration profile (Figure 5.3.2e) is a bit misleading as there is more than one trend apparent within the sample sequence.

On a sample to sample basis, the alteration zone is characterized by an outer zone of oxidation, carbonatization and soda enrichment along with dehydration, followed by a zone of enrichment of S and Au, Ni and Cr, with further alkali enrichment (K, Na, Sr, and Ba), minor reduction of the oxidation state of iron and depletion of MgO toward the core. Finally, in the narrow envelopes to the central veins, there is silicification combined with depletion of several elements including CO_2, Mg, Zn, and total Fe. The alteration observed in the sample set for the intermediate flow below the hyaloclastite unit is not as well developed as in the upper massive flow and consequently only the first stage of oxidation, carbonatization and soda enrichment is observed.

Cryderman Zone:

The elemental gains and losses associated with the Cryderman Zone are summarized in Table 5.3.3 for the two small sample sections described in Section 3.1.2 (Figure 3.1.2). Altered samples are compared to sample 45722, from DDH 272-85-16, which is relatively unaltered and occurs between the two sections. The first section includes, from least to most altered, samples H-48, H-45, and H-44 (Figure 5.3.4) and the second section includes H-51, H-50, and H-49 (Figure 5.3.5). Because the Cryderman Zone parallels the volcanic stratigraphy, and sampling had to be done up section within the host flow, there is more potential for variability in the primary composition of the rocks, due to differentiation within the flow and the possibility that a flow contact is hidden by the alteration zone. Sample H-49 is taken from the core fault of the zone and there is evidence of quartz flooding and/or veining, plus brecciation, which distorts the host rock's geochemical characteristics, especially

Table 5.3.3a: Sample mineralogy and geochemistry for the alteration of the Non-variolitic Flows associated with the Cryderman Zone, Section I, Harker Lake section.

Mineralogy	45722	H-48	H-45	H-44	Overall
uralite	XXXX	XXXX			- 40 %
chlorite	o	x			- 2-3
albite	XXXX	XXXX	XXX	XXX	- 10
quartz			x	X	+ 10
sphene/lcxn	x	x	o	·	- 2-3
epidote		o			- 1-2
carbonate	o		XXXx	XXXx	+ 35
magnetite	x	x	o	o	- 2-3
hematite		o	Xx	Xx	+ 15
pyrite		·	o	o	+ 2-5
apatite			·	·	+ trace
chalcopyrite			·	·	+ trace
Elemental Changes		45722 to H-48	H-48 to H-45	H-45 to H-44	45722 to H-44
+ > 200 %		Ba	CO_2,S,Sr,Au	Au	CO_2,Au,S,Ba,Sr
100-200		Rb		Ni	Ni,Na
50-100		Cr,Na	Na,Ca,(Zr,Y)	S	Cr
20-50		P,Mn,Ni	Fe^{3+},P	Fe^{2+},(V,Cr)	Fe^{3+}
10-20		Zr, H_2O	Si		
- > 75 %			H_2O	H_2O,Ba,Rb	H_2O,Rb
50-75			Rb	K	K,Zn
20-50		Ca,Zn,CO_2	Fe^{2+},Mg,Cr	P,(Zr,Y)	Fe^{2+}
10-20					Ca,Fe_T
Au (ppb)		130	815	2600	
Spec. Grav.	3.08	2.99	2.87	2.90	
Vol. Change		-3%	+26%	-4%	+19.5%

Brackets indicate that the error in the element's value makes the observed elemental change uncertain. Mineral modes are represented by the following symbols: X - 10%, x - 5-10%, o - 1-5%, · - trace.

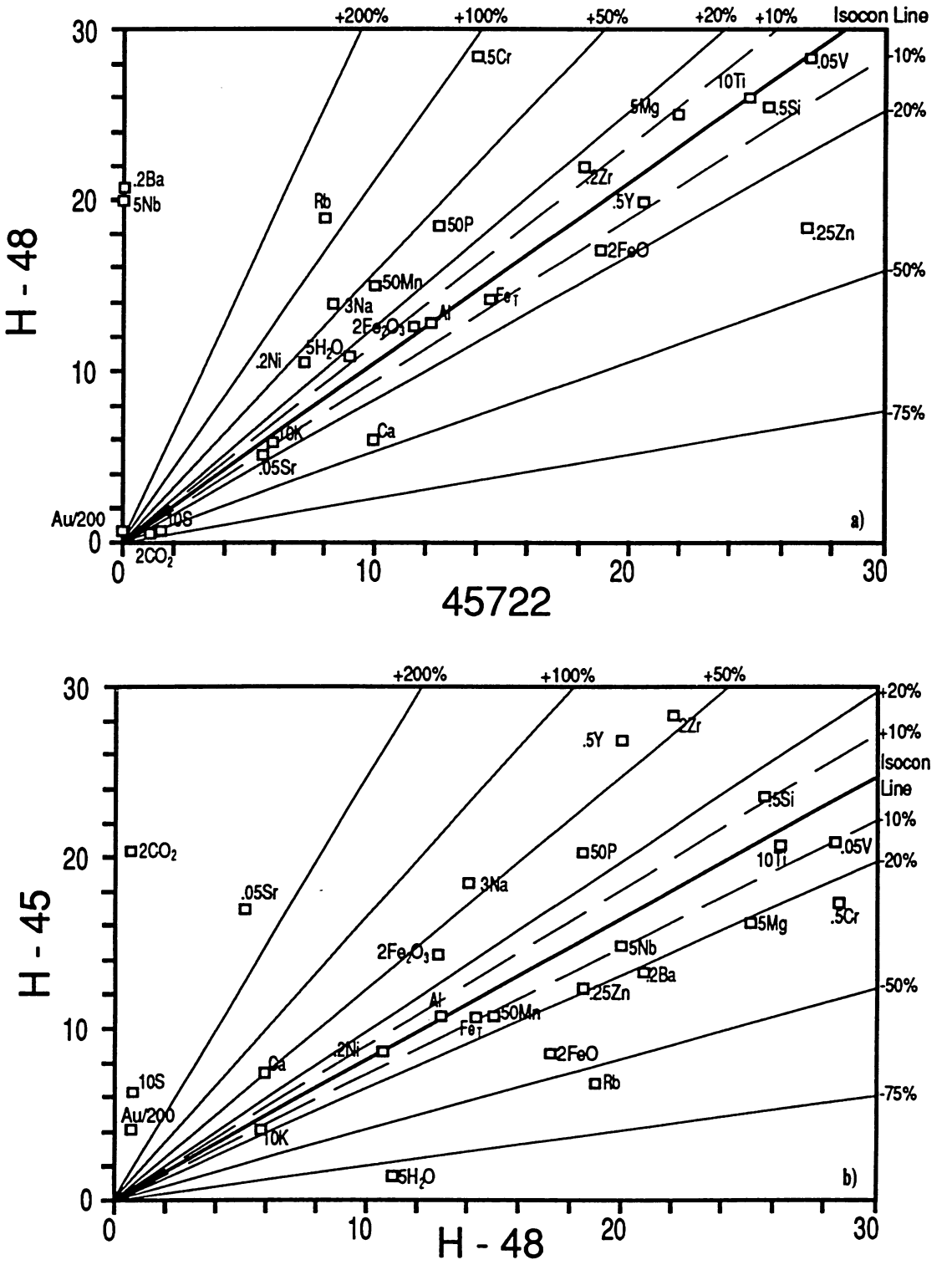

Figure 5.3.4: Isocon diagrams for alteration of the non-variolitic rocks on Section I, Cryderman Zone Harker Lake section (see Figure 3.1.2). Overall volume change from least (45722) to most (H-44) altered samples is approximately +20%. a) Least (45722) vs weakly (H-48) altered samples (ΔV = -3%). b) Weakly vs strongly (H-45) altered samples (ΔV = +26%).

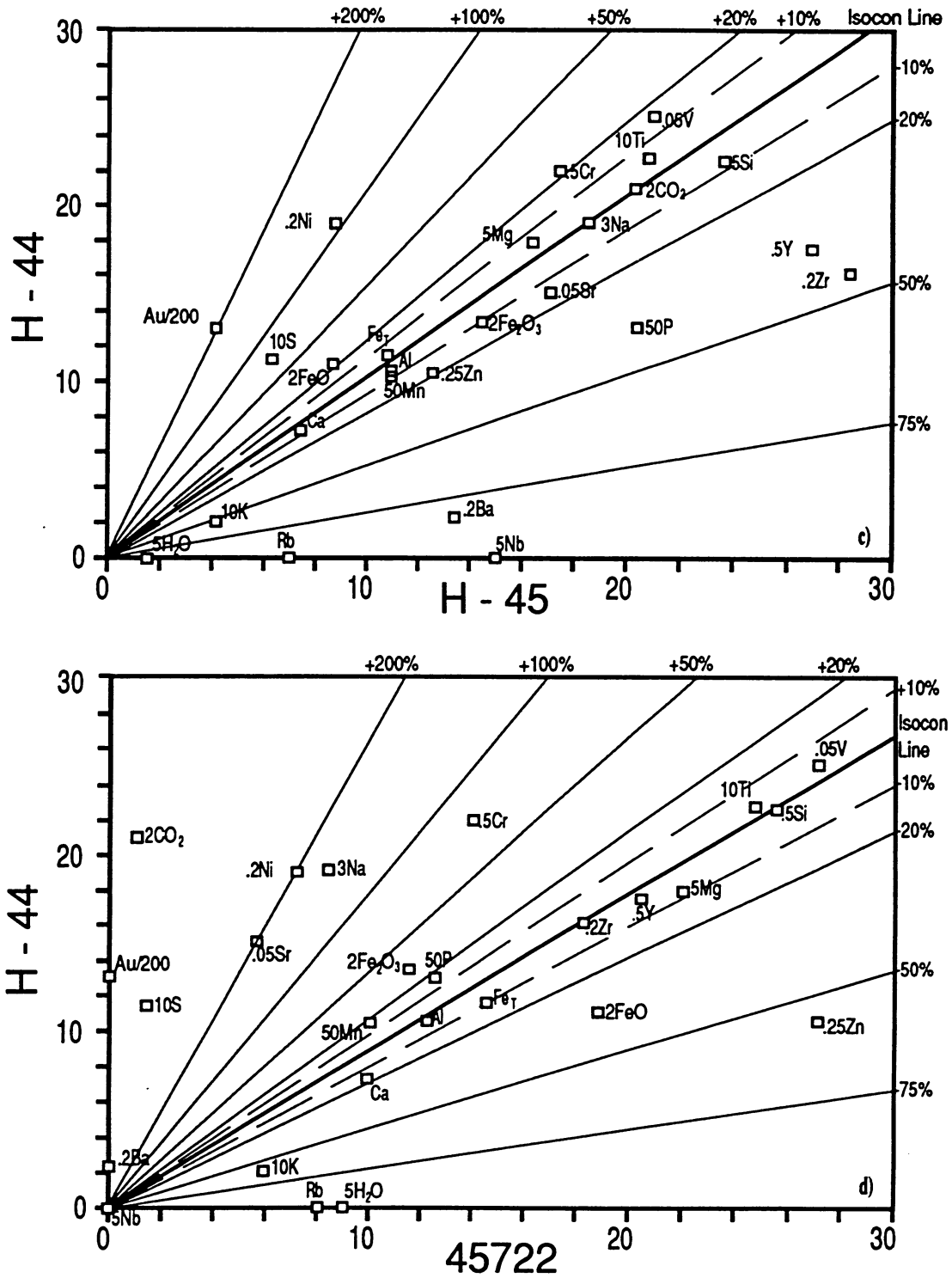

Figure 5.3.4 (con't): c) Strongly vs most (H-44) altered samples ($\Delta V = -4\%$). d) Least vs most altered samples ($\Delta V = +19.5\%$).

by dilution.

Alteration at the margin of the Cryderman Zone, as seen in sample H-48 relative to 45722 (Figure 5.3.4a), was characterized by isovolumetric ($\Delta V = -3\%$) addition of the alkalis, Ba, Rb, and Na_2O, plus Cr, P_2O_5, and MnO, as well as, losses of CaO, Zn, and CO_2. The loss of CO_2 is a bit misleading because the abundance is very small in both samples. There was also an addition of Zr which may be an artifact of primary variability within the flow as Zr would not be expected to be mobile at the low intensity of alteration represented by these samples. Oxidation of iron is not apparent in the geochemical data despite the presence of hematite in the mineral mode.

There is considerably more visible alteration in H-45 than H-48 and the isocon diagram reflects the increased intensity of alteration (Figure 5.3.4b). There is an increase in volume between the two samples of aproximately 26%, based on a "best-fit" isocon line through Al_2O_3, and close to total Fe, TiO_2, and Ni. Some of this volume increase may be attributable to tiny fractures which permeate the rock. As well, the isocon diagram indicates large additions of CO_2, S, Sr, and Au, along with less significant enrichments of Na_2O, CaO, Fe_2O_3 and possibly SiO_2. The development of large amounts of carbonate minerals coincides with a decrease in the proportion of albite as a result of dilution. This is different than the Line 28+00E area where albite is constant and carbonate are not developed to a great extent. Similar to the Line 28+00E area, introduction of Au is accompanied by a large gain in S and pyrite content. Losses of H_2O, Rb, FeO, and possibly Cr are recorded. MgO is somewhat depleted, although not as much as might be expected considering all mafic minerals are now eliminated. Hematization is coincident with the disappearance of chlorite and explains the consistent total iron abundance.

A constant Al_2O_3 isocon has been chosen despite the reduction of plagioclase and chlorite content in H-45 which should result in a loss of Al_2O_3. The apparent discrepancy is due to dilution of Si-Al minerals by carbonate minerals. At any rate, there is not another viable isocon line readily apparent and no consistent inter-element ratios within the samples from the alteration zone (Appendix 5.1) to indicate immobility of other elements. Enrichment of the generally immobile LIL elements, such as Zr, Y and P, in H-45 may be due to sampling from various levels in a flow or separate flows. Consistent inter-element ratios for

the various samples and overall chemical similarity suggests that these elements may be coupled, and possibly related to a differentiation process.

The last stage of alteration on this section, to the edge of the central quartz vein, occurs between H-45 and H-44 (Figure 5.3.4c). Visually, there is not that much difference between the two samples, although pyrite content is greater in H-44. Pyrite is especially associated with small, bleached patches in the darkly coloured rock. The isocon line indicates that there is an insignificant volume change (ΔV = -4%) between the two samples and this is corroborated by their textural similarity. Elements gained include Au, Ni, S, and FeO relative to Fe_2O_3 whereas components lost in H-44 include H_2O, Ba, Nb, Rb, K_2O, and, perhaps, SiO_2 and Sr. V and Cr increase in concentration, but not significantly above their intra-unit variance (Table 4.4.1c). The apparent decrease in the incompatible elements Zr, Y, and P_2O_5 in H-44 may be due to primary variations within the flow.

Comparing the least to most altered samples on this small section (45722 to H-44, Figure 5.3.4d) there is a volume change of about +20% based on an isocon defined by Al_2O_3, Zr, Y, TiO_2, SiO_2, and V. Enriched components include CO_2, Au, S, Ba, Sr (all >200%), Ni and Na_2O (100-200%), whereas depleted components include H_2O, Rb (>75%), K_2O, Zn (50-75%), and minor amounts of CaO and total Fe. Ba and Rb have been added at the fringe of the alteration zone and successively depleted in samples toward the core of the zone. Overall the proportion of Fe_2O_3 to FeO increases with alteration intensity indicating reaction of the rock with a relatively oxidizing fluid. The ferric-ferrous ratio does decrease at the core of the Cryderman Zone (H-45 to H-44) coincident with the highest pyrite content.

Results for the other small section in the Cryderman Zone (samples H-51, H-50, H-49) are similar. Figure 5.3.5 demonstrates that sample H-51 is more intensely altered than H-48, as is reflected on the isocon diagram in comparison with sample 45722 (Figure 5.3.5a). In particular, H-51 shows addition of >200% CO_2 not seen at all in H-48, along with Ba, Rb and Nb (low abundance). There is an increase in the proportion of ferric to ferrous iron in H-51 relative to 45722, which was not recorded for H-48. H-50 is similarly altered to H-45/H-44 with significant additions of S, CO_2, Au, Sr, Ni, CaO, and Na_2O over H-51 (Figure 5.3.5b).

An isocon diagram comparing H-49 with its nearest neighbour, H-50 (Figure 5.3.5c), has been done although choice of the isocon line on this diagram is difficult. Here, a line

Table 5.3.3b: Sample mineralogy and geochemistry for the alteration of the Non-variolitic Flows associated with the Cryderman Zone, Section II, Harker Lake area.

Mineralogy	45722	H-51	H-50	H-49
uralite	XXXX	X		
chlorite	o	XX		o
albite	XXXX	XXXX	XXX	XXx
quartz		o	X	Xx
sphene/lcxn	x	x	·	
epidote				
carbonate	o	x	XXXx	XXXx
magnetite	x	x	o	
hematite		x	Xx	Xx
pyrite		o	o	x
apatite			·	·
chalcopyrite			·	o
galena				o
Elemental Changes		45722 to H-51	H-51 to H-50	H-50 to H-49
+ >200 %		Ba,CO_2,Rb	S,CO_2,Au	Au
100-200			Sr,Ni	
50-100		Fe^{3+},Na,Mn,H_2O	V,Ca	Si,S,Cr
20-50		Sr,(Y)	Na	Zn
10-20			Ti	
- > 75 %				Fe^{3+},V,
50-75				
20-50		Ca,Fe^{2+},(V)	Zn,(P,Zr)	Fe_T,Ba,Rb,Zr
10-20			Al,Mg,Si	Y
Au (ppb)		10	1002	4970
Spec. Grav.		2.88	2.98	2.86
Vol. Change		+9%	+7%	+18%

Brackets indicate that the error in the element's value makes the observed elemental change uncertain. Mineral modes are represented by the following symbols: X - 10%, x - 5-10%, o - 1-5%, · - trace.

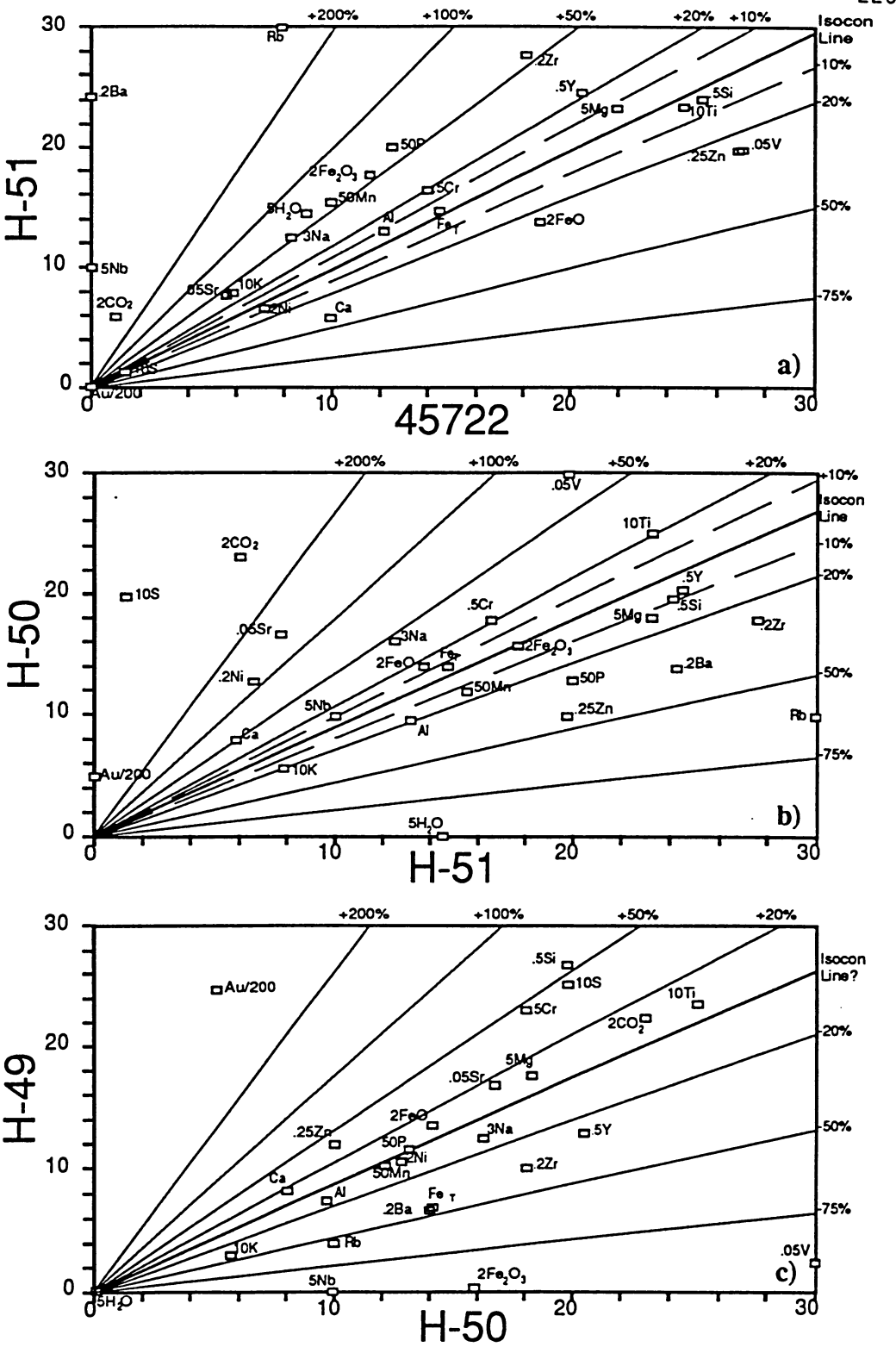

Figure 5.3.5: Isocon diagrams for alteration of the non-variolitic rocks on Section II, Cryderman Zone, Harker Lake section (see Fig. 3.1.2). a) Least (45722, same as SectionI) vs moderately (H-51) altered samples ($\Delta V = +9\%$). b) moderately vs strongly (H-50) altered samples ($\Delta V = +7\%$). c) Strongly altered sample vs Fault Zone sample (H-49) with strong Au and quartz enrichment and corresponding volume increase ($\Delta V = +18\%$). The isocon line for c) is not definite due to a lack of clearly immobile elements.

connecting MnO and P_2O_5 that passes close to Al_2O_3, TiO_2, Ni, MgO and FeO, giving an estimated volume increase of 18%, was selected indicating that SiO_2 has been added to H-49. This corresponds with petrographic information showing the sample to have abundant, brecciated, vein quartz. In addition, Au and S have been enriched in the fault zone. Zn is enriched in H-49, possibly due to leaching from the wall rock toward the fault zone. Although the Fe titration data show that extreme reduction of iron has taken place in the fault zone, there is no supporting mineralogical evidence, hematite being the main host for iron. The mineralizing fluid need not have been strongly reducing to stabilize pyrite. High sulphur fugacity will also stabilize pyrite, such that it is possible for pyrite to co-exist in equilibrium with hematite. Again, the Fe titration method is unreliable for samples containing more than 2-3% pyrite.

5.3.2 Dome Mine Area

The sampling of the alteration zones in the Dome Mine was less constrained than in the Harker Lake area, and as a consequence the geochemical background variance in the elements is expected to be greater than in the Harker Lake area. Here, the least altered samples are more strongly altered than those in the Harker Lake area, and have higher concentrations of volatiles and more strongly modified alkali element contents. In some cases, this higher background level of alteration reduces the contrast observed between altered and unaltered samples.

99 Flow, V8 subunit (Figure 5.3.6):

The geochemical alteration study of the 99 Flow is based on samples D89-21 (least altered), D89-35 (moderately altered), and D89-34 (most altered) (Table 5.3.4). Metasomatism has changed the "fresh" greenschist facies mafic mineral assemblage of amphibole-albite-epidote in D89-21 to one dominated by chlorite, carbonate and albite in D89-35. The extent of the deformation is much more pronounced in D89-35, resulting in reduced grain size and a volume increase of about 13% through the emplacement of carbonate minerals in dilatent zones. Despite the mineralogical changes between the two samples, there is not a great deal of difference in their whole rock geochemistry (Figure 5.3.6a). There is volatile enrichment (CO_2, H_2O, and S), minor alkali loss, and reduction of the overall oxidation state of iron.

Table 5.3.4: Sample mineralogy and geochemistry for the alteration of the 99 Flow, V8 subunit, Dome Mine, Timmins, Ontario.

Mineralogy	D89-21	D89-35	D89-34	Overall
uralite	XXX			- 30 %
chlorite	x	XXXx		- 5
albite	XXXX	XXXX		- 50
quartz	o	X	XXx	+ 20-22
carbonate	o	X	XXXXX	+ 35-38
magnetite	x	x		- 5
sphene/lcxn	o	o	o	
pyrite			o	+ 1-2
epidote	x	o		- 5
sericite			XX	+ 20
apatite	·			- trace
tourmaline			·	+ trace
Elemental Changes		D89-21 to 35	D89-35 to 34	D89-21 to 34
+ > 300 %			K,CO_2,Ba,Rb	CO_2,K,S,Ba
200-300		CO_2	Th,Ni,Cr	Th,Ca,Cr,Ni
100-200		H_2O,S	Ca,Zn	Zn
50-100				Mn,Ta
20-50		Ca,Sr	Mn	Mg
10-20		Fe^{2+}		Fe^{2+}
- > 75 %		K		Na,Fe^{3+}
50-75		Ba	Ti, Fe^{3+}	Ti
20-50		Na,Fe^{3+}	Y,P,Fe_T,(V,Sr)	Y,P,Fe_T
10-20		Ni	Si	H_2O
Au (ppb)	n.d.	n.d.	3	
Spec. Grav.	2.94	2.85	2.95	
Vol. Change		+13%	+16%	+33%

Brackets indicate that the error in the element's value makes the observed elemental change uncertain. Mineral modes are represented by the following symbols: X - 10%, x - 5-10%, o - 1-5%, · - trace.

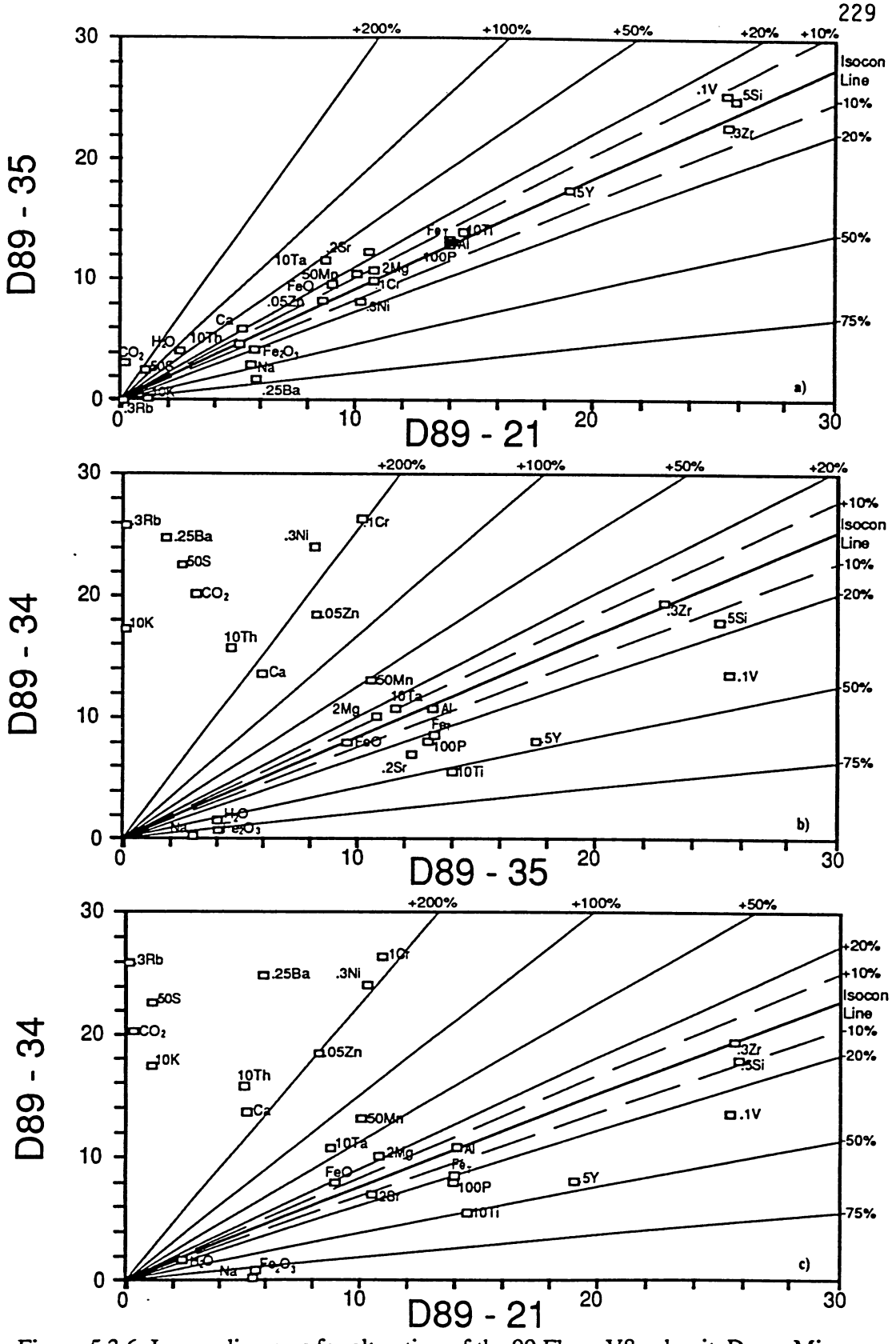

Figure 5.3.6: Isocon diagrams for alteration of the 99 Flow, V8 subunit, Dome Mine. The overall volume change for the alteration is approximately +33%. a) Least (D89-21) vs moderately (D89-35) altered samples (ΔV = +13%). b) Moderately vs most (D89-34) altered samples (ΔV = +16%). c) Least vs most altered samples (ΔV = +33%).

The difference in alteration between D89-35 and D89-34 is much more obvious visually and geochemically than between D89-21 and D89-35. The isocon line is drawn through FeO, Al_2O_3 and Zr and defines a volume increase of 16% for D89-35 to D89-34 (Figure 5.3.6b). Alteration is characterized by K enrichment, Na depletion, iron reduction, dehydration and minor silica depletion. Boron addition is assumed because of the presence of tourmaline, although there are no analyses available. Due to the simple mineralogy of D89-34, many relatively immobile elements, such as Ti, V, and P, have no significant mineral host in the rock and have been removed. Interestingly, D89-34 has a very significant enrichment of Cr and Ni, which are chemically similar, and also Zn. The host mineral for these elements is difficult to envisage based on the assemblage present in D89-34. One possibility is that Cr and Ni are present in micas, such as fuchsite. However, the mica in the sample does not have the distinctive green colour of fuchsite and XRD analysis (Appendix 3.2) indicates that it is actually muscovite. Nonetheless, muscovite may contain Cr, and possibly Ni, in quantities sufficient to account for the observed concentrations (Deer *et al*, 1980, pg. 202). Tourmaline, specifically dravite associated with serpentinized peridotitic and komatiitic rocks, has been found to be Cr-bearing in another study of Au deposits in the Timmins area (King and Kerrich, 1989). However, this study also found that Cr preferentially partitions into micas (e.g. fuchsite) when they are present in the rock with tourmaline. Zn may substitute for divalent cations in dolomite and muscovite, possibly accounting for its enrichment.

Figure 5.3.7 shows the REE abundances normalized to the least altered sample D89-21, which has a REE profile characteristic of primary tholeiitic rocks. Whereas very little change to the REE profile is evident in D89-35, other than minor dilution due to volume change, the profile for D89-34 has been strongly modified with LREE enrichment and HREE depletion. The presence of minor sphene (+/-leucoxene) in the core of the alteration zone would allow for the relative enrichment of the LREE to HREE in the rock (Grauch, 1989, Figure 15). However, the flattening of the profile in the HREE is not typical of sphene. The flattening could be attributed to the presence of muscovite (sericite) which has moderate and evenly distributed abundances of the REE. In addition, the presence of a very minor amount of zircon (Zr content is 65 ppm in D89-34) would add significantly to the HREE. The REE abundances in dolomite, the dominant mineral in D89-34, are not significant (Clark, 1984).

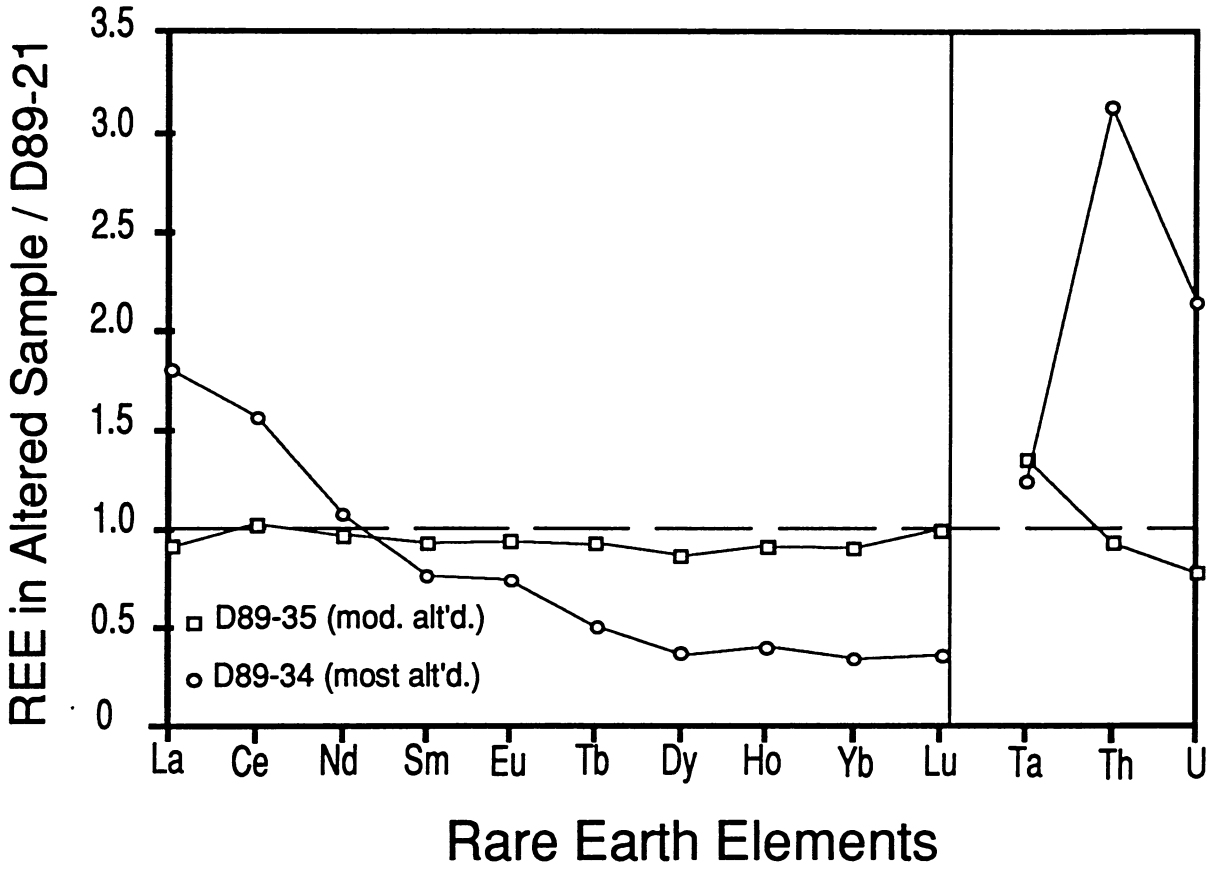

Figure 5.3.7: Rare Earth Elements, plus Ta, Th, and U, in the altered samples of the 99 Flow, V8 subunit,Dome Mine, normalized to the least altered sample (D89-21). The most altered sample, D89-34, shows significant alteration of the REE profile (even considering 30% dilution), with LREE enrichment (specifically La and Ce) and HREE depletion (from Tb).

Overall, the alteration associated with gold mineralization in the 99 Flow has highly significant gains in concentration for CO_2, K_2O, S, Ba, Th, CaO, Ni, Cr, Zn, MnO, Ta and perhaps MgO and losses in Na_2O, TiO_2, Y, P_2O_5, H_2O and minor loss of total iron (Figure 5.3.6c). The total volume increase between the least and most altered samples is 33%, which matches well with the sum of the two stages of alteration examined (+29%). The isocon line is drawn through Al_2O_3 and Zr, which both fall exactly on a line coincident with the origin and are immobile as indicated by their constant ratio in all samples (Appendix 5.1d). In addition, they are not chemically coupled, and occur in concentrations well above detection limits. The abundance of tourmaline in veins related to this alteration zone indicates that some Al may have entered the fluid from the country rock. However, the isocon diagram indicates that Al_2O_3 does not appear to have been leached from the local altered rocks. The simplicity of the mineralogy in D89-34 attests to the equilibration of the rock with a relatively simple fluid.

Key Flow, V8 subunit (Figure 5.3.8):

The alteration study for the Key Flow consists of two pairs of samples representing increasing alteration near an "ankerite vein" orebody subparallel with the upper contact of the unit. D89-08 and D89-07 were taken from the 1800 Level, and D89-39 and D89-40 were taken from the 2300 Level at approximately the same stratigraphic position within the Key Flow. D89-08 represents the least altered example whereas D89-40 is the most altered. Changes in mineralogy and elemental gains and losses between samples are summarized in Table 5.3.5.

Samples D89-39 and D89-07, representing moderate alteration, have no volume change with respect to D89-08 (Figures 5.3.8a and 5.3.8b). Addition of CO_2, K_2O, and Ba and depletion of MgO, Na_2O and H_2O are the main characteristics of this stage of alteration. This coincides with an increase in sericite and carbonate in the rock, and the elimination of chlorite and some albite. There is also reduction of the proportion of Fe_2O_3 relative to FeO in these samples compared to D89-08.

Before considering the geochemical differences between D89-39 and D89-40 (Figure 5.3.8c), it should be pointed out that D89-40 is a fine grained, non-variolitic rock, unlike the other samples in this alteration study. The isocon line, plotted using CaO, FeO, TiO_2, Al_2O_3,

Table 5.3.5: Sample mineralogy and geochemistry for the alteration of the Key Flow, V8 subunit, Dome Mine, Timmins, Ontario.

Mineralogy	D89-08	D89-39	D89-07	D89-40	Overall
uralite					
chlorite	XXx	XX	Xx	x	- 20 %
albite	XXXx	XXx	XXX	XXx	- 10
quartz	XX	XX	Xx	XX	
carbonate	Xx	XX	XXx	XXXX	+ 25
magnetite					
sphene/lcxn	x	o	o	o	- 2-3
pyrite	·		o	·	
epidote					
sericite		X	X	x	+ 10
apatite					
tourmaline			o	o	1-2
zircon(?)	·				
Elemental Changes		D89-08 to 39	D89-08 to 07	D89-39 to 40	
+ > 200 %		Rb,K,Ba	K		K,Ba
100-200			Ba	CO_2,S	CO_2
50-100			CO_2,S	Ni	
20-50		CO_2,Ca	Ca,Zn		Ca
10-20				Cr	Ni,Zn
- > 75 %					
50-75		S		Fe^{3+}	Fe^{3+}
20-50		Na,(Ni,Sr)	Fe^{3+},Mg,H_2O	H_2O	H_2O,Mg,Na
10-20		Mg	Fe_T,Fe^{2+}	Mn,Mg,Si,Sr	Si,Mn,Sr
Au (ppb)	2.82	2.80	2.81	2.89	
Spec. Grav.	+10%	0	-4%	-6%	-8%
Vol. Change					

Brackets indicate that the error in the element's value makes the observed elemental change uncertain. Mineral modes represented by the following symbols: X - 10%, x - 5-10%, o - 1-5%, · - trace.

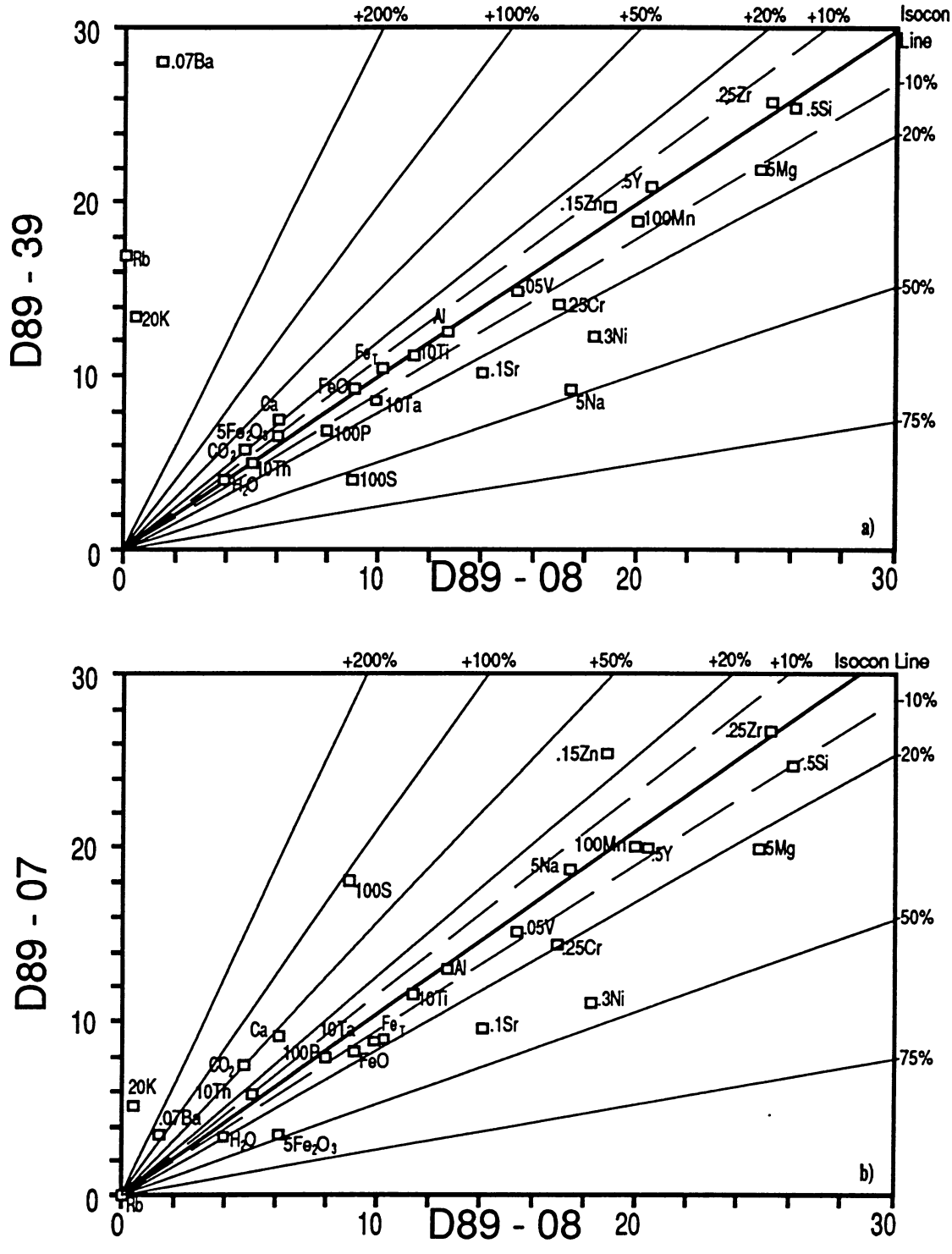

Figure 5.3.8: Isocon diagrams for alteration of the Key Flow, V8 subunit, Dome Mine. The overall volume change for the alteration is minor, possibly reflecting the strong foliation present in all the samples. a) Least (D89-08) vs moderately (D89-39) altered samples ($\Delta V = 0\%$). b) Least vs moderately (D89-07, 1.5m from ore) altered samples ($\Delta V = -4\%$).

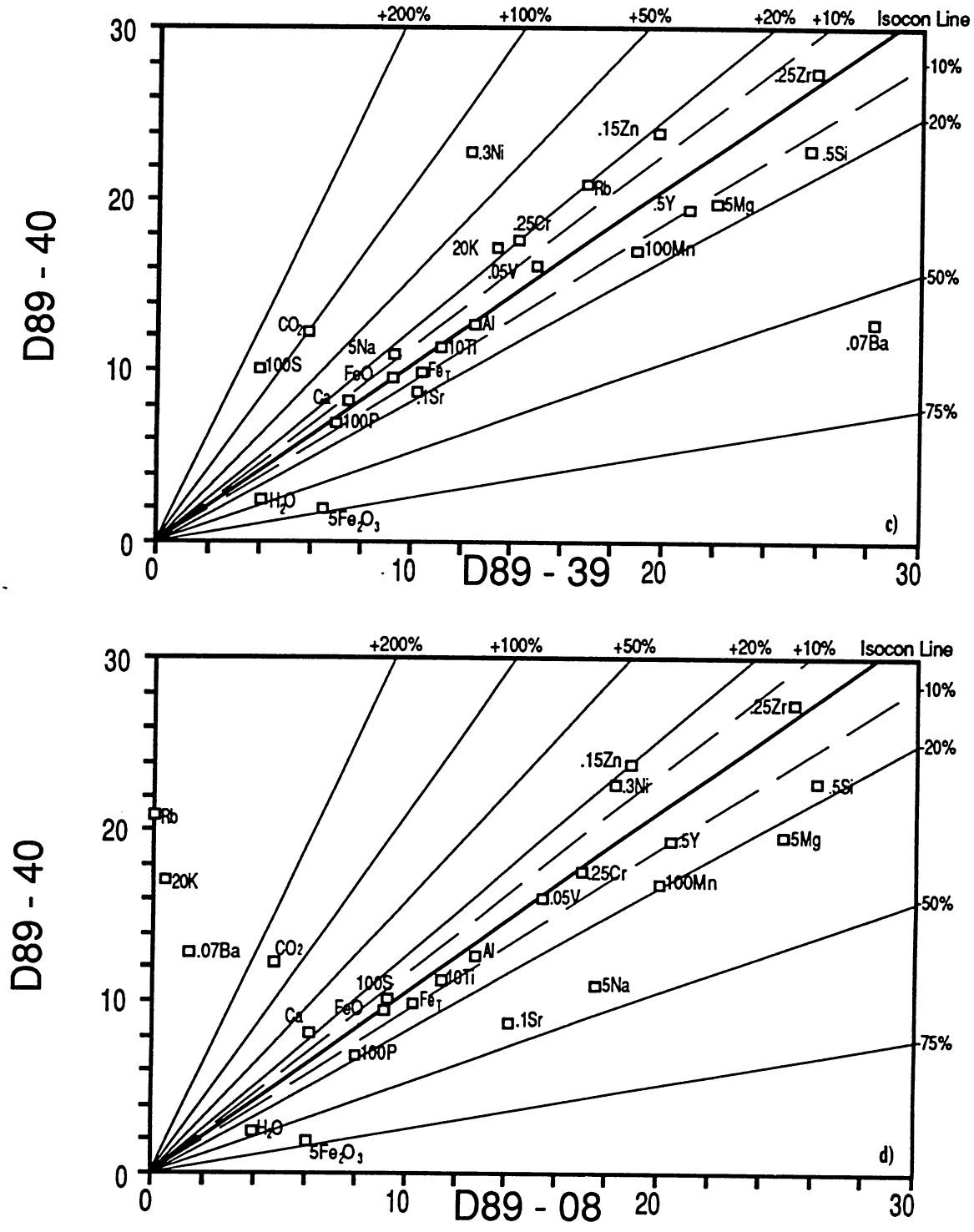

Figure 5.3.8 (con't.): c) Moderately (D89-39) vs most (D89-40) altered samples (ΔV = -6%). d) Least (D89-08) vs most (D89-40) altered samples (ΔV = -8%).

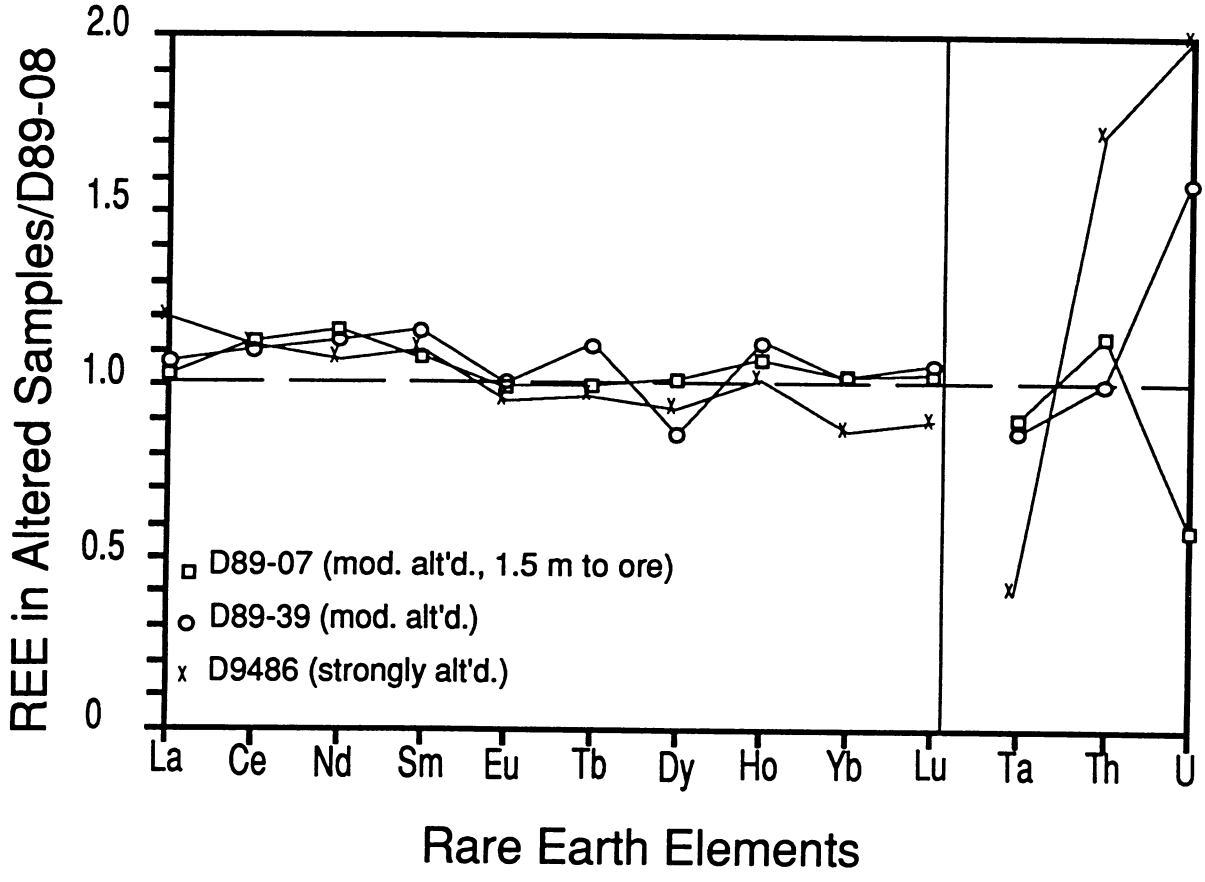

Figure 5.3.9: Rare Earth Elements, plus Ta, Th, and U, in the altered samples of the Key Flow, V8 subunit, Dome Mine, normalized to the least altered sample (D89-08). There is insignificant variation in REE abundances from least to most altered samples, especially considering the error involved in the analyses.

V, and Zr, indicates a volume decrease in D89-40 of about 6%. The largest gains in D89-40 are for the volatiles CO_2 and S, and for Ni, whereas losses occur for H_2O, MnO, MgO, SiO_2, and, possibly, Sr. The ratio of Fe_2O_3 to FeO is also further reduced from D89-39. The geochemical changes reflect a large increase in carbonate and elimination of some chlorite, albite and sericite.

Overall, from D89-08 to D89-40 (Figure 5.3.8d), the alteration of the Key flow in association with "ankerite vein" ore is characterized by strong gains in K_2O, Ba, and CO_2, and minor gains in CaO, Ni and Zn. Losses include H_2O, MgO, Na_2O, SiO_2, and MnO, as well as, a reduction in the ferric to ferrous iron ratio. The presence of tourmaline indicates that B was probably added to D89-40 as well. The REE spectra have not changed much in D89-39 and D89-07, only weak LREE enrichment to Sm is apparent (Figure 5.3.9). REE for D89-40 are not available, but another quite highly altered sample of the Key Flow, 9486, taken on the 1100 level, is included for comparison with D89-08. This sample has similar LREE enrichment to the other altered samples plus minor depletion in the heaviest REE, Yb and Lu.

An estimated volume loss of 8% for the alteration process was obtained from Figure 5.3.8d. This compares well with the sum of volume changes for the intermediate samples. Foliation is more pronounced in D89-08 than D89-40, despite the proximity of D89-40 to a shear hosted ore body. This may, in part, account for the volume loss between the two samples. Also, part of the change in volume may be explained by the textural differences in the rocks. For instance, another sample at the margin of an "ankerite vein", D89-07, had no volume gain with respect to D89-08 and, unlike D89-40, is texturally very similar to D89-08 and D89-39. It is possible that shearing in the variolitic rocks causes dilatencies to be formed in the pressure shadows created in the foliated matrix by the more competent varioles.

Dacite Flow, V10 subunit (Figure 5.3.10):

This alteration study involves two samples from the Dome Mine, D89-16 and D89-17, in proximity to "dacite ore", and one sample from the Porcupine Paymaster section, P89-09. A relatively unaltered sample of the Dacite Flow was not obtained at the mine during sampling in 1989 and follow-up work was not possible in 1990 due to a prolonged labour dispute. The Paymaster sample is included in the calculation of the coefficient of variance for the V10 subunit in Table 4.5.1. There is not a significant difference in alteration intensity

Table 5.3.6: Sample mineralogy and geochemistry for the alteration of the Dacite Flow, V10 subunit, Dome Mine, Timmins, Ontario.

Mineralogy	P89-09	D89-16	D89-17	Overall
uralite				
chlorite	XXX	XX	XXX	
albite	XXXX	XXXx	XXx	- 15
quartz	X	Xx	Xx	+ 5
carbonate	Xx	Xx	Xx	
magnetite	o			- 2-3
sphene/lcxn	o	x	x	+ 2-3
pyrite		o		+ 1
epidote				
sericite		o	x	+ 5
apatite	·	o		
tourmaline		·	·	+ trace
zircon(?)	·	·	·	
Elemental Changes		P89-09 to D89-16	P89-09 to D89-17	
+ > 200 %		Cr,K,S,(V)		Cr,K
100-200			Ba	
50-100				
20-50		CO_2,Ca		
10-20		Th		
- > 75 %			V	
50-75		Ba,Sr	S	Sr
20-50		Na,P	CO_2,Ca	Na,(Ba,Mn)
10-20			Mg,(Mn)	
Au (ppb)	n.d.	26	n.d.	
Spec. Grav.	2.87	2.86	2.85	
Vol. Change		0	-7%	-6%

Brackets indicate that the error in the element's value makes elemental change observed uncertain. Mineral modes represented by the following symbols: X - 10%, x - 5-10%, o - 1-5%, · - trace.

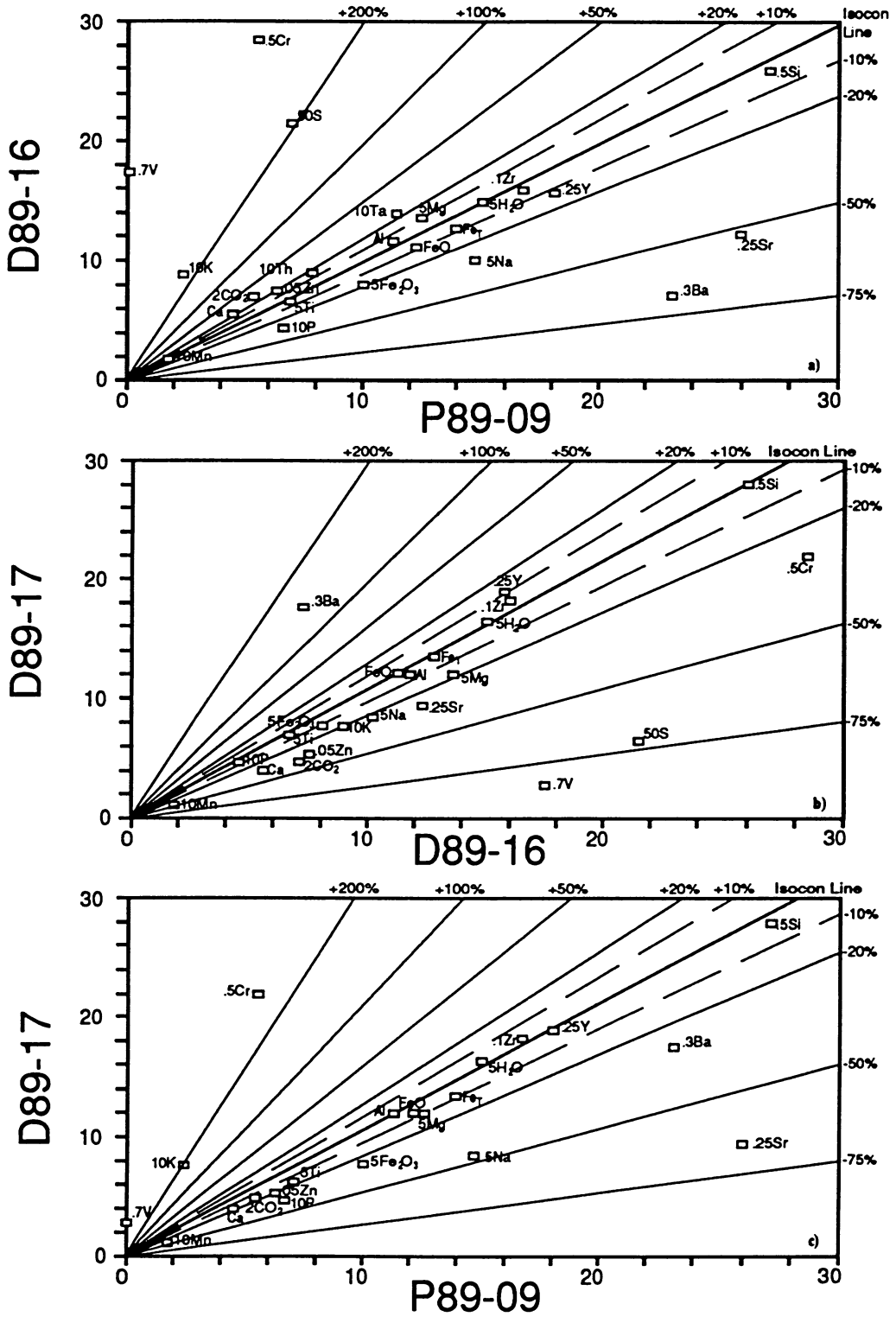

Figure 5.3.10: Isocon diagrams for alteration of the Dacite Flow, V10 subunit, Dome Mine. Overall, volume change as a result of alteration is quite small. The strongly altered samples, D89-16 and D89-17, may not be representative of the most intense alteration of the Dacite Flow as samples from the wall rock to quartz lodes were not accessible. a) Least (P89-09, see discussion in text) vs strongly (D89-16) altered samples ($\Delta V = 0\%$). b) Strongly (D89-16) vs strongly (D89-17, closer to ore) altered samples ($\Delta V = -7\%$). c) Least vs strongly (D89-17) altered samples ($\Delta V = -6\%$).

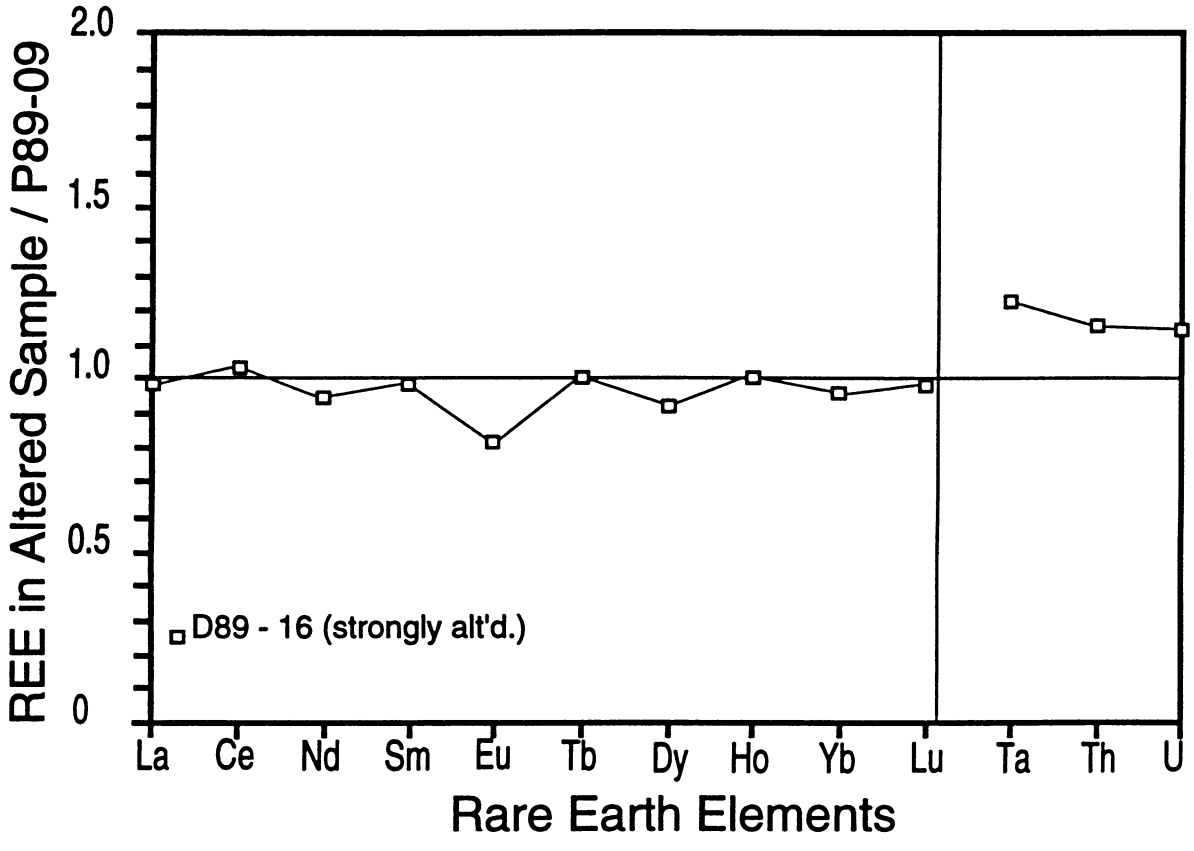

Figure 5.3.11: Rare Earth Elements, plus Ta, Th, and U, in altered sample D89-16 of the Dacite Flow, V10 subunit, Dome Mine, normalized to the least altered sample, P89-09, of the Porcupine Paymaster section. There is little to no variation in the REE profile from the least to most altered samples. The only noticeable change is a slight negative Eu anomaly.

between D89-16 and D89-17, despite the fact that D89-17 was sampled much closer to the 1340 ore body (Map 2.2.3).

Comparing P89-09 to D89-16 and D89-17 (Table 5.3.6, Figures 5.3.10a and 5.3.10c), there are large gains in K_2O, Cr, and S, and minor additions of CO_2, and CaO. Losses include Sr, Na_2O, P_2O_5 and, possibly, Ba. The gains correspond to significant sericite and pyrite development, along with minor carbonatization, at the expense of albitic plagioclase. The addition of S in D89-16 is important to note as this is the only sample with an anomalous Au concentration. The REE spectrum is not significantly altered, although the negative Eu anomaly characteristic of the Dacite Flow is slightly enhanced (Figure 5.3.11). The decrease in P_2O_5 may be due to intra-V10 subunit variation in concentration. In the Andesite Flow (lower V10 subunit) at the Dome Mine, P_2O_5 is at its highest concentration locally. Sample P89-09 is from the lower half of the V10 subunit on the Porcupine Paymaster section, whereas samples D89-16 and D89-17 are from the upper half. Consequently, the apparent depletion of P_2O_5 in D89-16 and D89-17, relative to P89-09, may be due to primary differences in concentration.

There is a volume loss of about 7% between samples D89-16 and D89-17 (Figure 5.3.10b). This is accompanied by a loss of S, CO_2, CaO, MgO and a gain in Ba in D89-17. The loss of volatiles may contribute to the volume change (i.e. less carbonate and sulphide in rock). D89-17 does not have a Au content above background despite being closer to an ore zone than D89-16.

The presence of abundant chlorite in the more altered Dacite samples is a good indication that the intensity of alteration is not as strong as in other units where chlorite is completely eliminated. Another possibility is that the chemistry of the Dacite Flow has stabilized chlorite more than the other units. Although the absence of a strongly altered sample of the Dacite Flow would limit the scope of the conclusions in this part of the alteration study, the trends which can be seen between sample P89-09 and samples D89-16 and D89-17 are similar to the alteration of other units at the Dome Mine.

5.4 Discussion

5.4.1 Harker Lake Area

In the Harker Lake area, mass balance calculations have shown that the alteration of variolitic, intermediate and non-variolitic flows is characterized by: oxidation; large addition of Na_2O, S, CO_2, Sr, Au, plus variable Ni, Ba, and minor Cr, P_2O_5, SiO_2 and Ta; significant depletion of H_2O, Zn, MgO, MnO and minor depletion of total Fe and, possibly, CaO. Generally, Al_2O_3, Zr, TiO_2, Th, and SiO_2 have been immobile in all cases, although SiO_2 has been added in the narrow envelope to anastomosing quartz veins. The REE have been relatively immobile although there is evidence of minor HREE depletion in the most altered sample for which REE analyses are available (H-31). This suggests that at the core of the alteration zone there may be significant alteration of the REE spectrum. Mass balance calculations have shown that both areas have volume increases associated with alteration. The fact that there is little to no shearing, indicates that the volume change is due to dilatencies caused by brittle reaction to stress.

The Fe^{3+}/Fe^{2+} has been increased due to oxidation of Fe released by the breakdown of uralite and chlorite and possibly Fe oxides, such as magnetite, to form hematite and rutile. The small decrease in Fe^{3+}/Fe^{2+} at the mineralized core of the alteration zones is due to formation of pyrite, rather than reduction of the iron due to changing oxidation state of the metasomatic fluid. Here, pyrite probably formed due to a high S fugacity.

The addition of Na_2O has resulted in albitization of metamorphosed plagioclase, to stabilize pure albite in the alteration zone. Reactions involving Na_2O eliminate epidote inclusions in oligoclase-albite resulting in clearer crystals and obvious albite twins (Section 3.1.2). Na alteration of chlorite (in conjunction with CO_2 and SiO_2) has also formed albite plus Fe dolomite and, likely, the Na amphibole of the intermediate flows.

The considerable enrichment of Sr is perhaps indicative of its partitioning into the added carbonate phases. The concentration of Sr correlates well with the trends of the carbonate minerals. Ba enrichment generally occurs further from the centre of the alteration zone than Sr enrichment. Both elements are commonly depleted at the core of the zones. In general, Sr and Ba addition coincides well with oxidation in the rocks. This effect is

pronounced in the Cryderman Zone where hematization is most prominent, indicating a very high fO_2.

Ni, and to a lesser extent Cr, have somewhat erratic behaviour but have generally been added, throughout the alteration zones. No depletion is apparent in the local altered rocks so it is assumed that these two elements were added from the metasomatic fluid. Ta was also added to the alteration zone in minor quantities. Cr and Ta could be associated with Fe-Ti oxides, which have variable concentrations in the alteration zone.

Locally, there is evidence of addition and depletion of P_2O_5. Most fluctuations are interpreted to be due to host rock variability, and possibly analytical error. For example, in the Cryderman Zone, P_2O_5 concentrations are close to detection limits.

The most common component lost during metasomatic alteration in the Harker Lake area is H_2O, due to the breakdown of the hydrous phases, amphibole and chlorite. MgO was also lost from the altered rocks due to the breakdown of ferromagnesian minerals. The amount of MgO depletion increases toward the centre of the alteration zone, where the most likely host for MgO is dolomite. MgO loss is especially noticeable in the Line 28+00E area, where dolomite is scarce. CaO is similarly related to the presence of carbonate. CaO was initially lost from epidote, then stabilized by the formation of calcite and dolomite. A minor amount of CaO was lost in the final, silicification stage in the envelope to the anastomosing veins in the Line 28+00E area. MnO loss recorded in the L28E area was due to the elimination of chlorite and sparse development of carbonate, especially in comparison to the Cryderman Zone. A minor amount of total iron was lost in both areas consistent with the elimination of amphibole and chlorite and the development of more Mg-rich chlorite toward the core of the alteration zone.

The enrichment of Zn in the core of the zones, may be a result of the breakdown of Fe-Ti oxides in the wall rocks. There is evidence of depletion of zinc in the wall rocks to the Cryderman Zone (Tables 5.3.3a and 5.3.3b) with enrichment occurring only in sample H-49, associated with the central quartz veins. Cu and Pb are present in the central veins, especially in the Cryderman Zone, although it is not assumed that these base metals were derived from the wall rocks.

In comparing the two alteration zones, there are two main points to note. The rocks

of the Cryderman Zone are non-variolitic, massive, more iron rich and more basic than the variolitic and intermediate flows which were analysed in the Line 28+00E area. These types of flows represent significant parts of variolitic suites as observed in this study. The alteration associated with the small structure in the Line 28+00E area is not apparently as strong as that associated with the Cryderman Zone. This difference in alteration intensity causes some uncertainty in comparison of the two areas. However, even by comparing the Line 28+00E area to moderately altered sections of the Cryderman Zone, there are significant differences.

An attempt to divide the alteration zone into segments of progressive alteration intensity was moderately successful only in the Line 28+00E area. The alteration consists of: 1) an outer cryptic zone, with no visible alteration but minor chemical changes relative to the unaltered equivalent rock, 2) a zone of bleaching resulting from the breakdown of mafic minerals and the addition of carbonate, and 3) at the core of the alteration zone a narrow (1.0 cm) silicified zone, characteristic of the envelope to the anastomosing quartz veins. The width of these segments is variable, the bleached part reaching as much as 8 metres in true width on the sample section in the upper massive flow, and as narrow as 5 centimetres in the intermediate flow below the hyaloclastite. In fact, the visible alteration associated with the structure disappears locally. The sampling of the Cryderman Zone did not show distinct zonation of the alteration, but rather a general trend to more intensely altered rock. The sampling is, perhaps, too widely spaced out to pick out all the mineralogical changes necessary to distinguish possible sub-zones.

The alteration mineral assemblages of the two areas are quite distinct. Strong hematization present in the Cryderman Zone is not seen in the Line 28+00E area. This may indicate a more oxidized fluid associated with the Cryderman Zone or perhaps the hematite content is related to the more Fe-rich original composition of the non-variolitic flows. Carbonatization is much more prominent in the Cryderman Zone. The Cryderman Zone is characterized by a relatively simple mineral assemblage in its most altered sections, whereas there are several minor minerals present in the Line 28+00E area including Na amphibole, talc, apatite and zircon(?). The last two minerals listed are a result of the evolved primary composition of the flows, rather than the alteration processes. Pyritization is at least as intense, though less extensive, in the L28E area than the Cryderman Zone.

The overall geochemical characteristics of the two zones are different, in conjunction with the mineralogy. Whereas the addition of Ni and Na_2O is about equal in the two zones, the addition of CO_2 is pronounced in the Cryderman zone. The oxidation of iron is about equal, both in percentage changes and ferric-ferrous ratio, but it is more obvious in the non-variolitic flows due to the extensive hematization. Sr and Ba enrichment is stonger and more consistent in the Cryderman Zone, though both areas have strong Ba enrichment at the margin of the visibly altered sections. The Cryderman Zone has significant K_2O loss, in contrast to the L28E area where small additions are noted locally. MgO and MnO losses are recorded in the L28E area, which are not observed in the Cryderman Zone (due to the presence of significant quantities of magnetite and dolomite). Actually, the intermediate stage of alteration rather than the most altered stage in L28E area more closely resembles the most altered samples in the Cryderman Zone in terms of elemental gains and losses.

5.4.2 Dome Mine Area

Mass balance calculations demonstrate that the alteration zones at the Dome Mine are characterized, with slight variations, by: significant addition of K_2O, S, CO_2, Ba, CaO and probably B (based on appearance of tourmaline); depletion of Na_2O, Sr, H_2O, plus minor depletion of total iron in extremely altered areas; and, reduction of the ferric-ferrous iron ratio. Apparently immobile elements include Al_2O_3, and Zr as well as, possibly, FeO. The immobility of Al_2O_3 and Zr is confirmed by their constant ratio within the various units studied (Appendix 5.1).

The REE elements at the Dome Mine remained immobile in most samples, their abundances mostly affected by the addition of components to the sheared rocks. However, they were mobile in very altered rocks. The best example of this is the pattern of REE present in sample D89-34, the most altered sample in the alteration study of the 99 Flow (Figure 5.3.7). In D89-34, there is significant LREE enrichment and HREE depletion relative to the least and moderately altered samples, D89-21 and D89-35. The depletion of the HREE is expected if the REE were leached from the rock since the HREE are more easily complexed by anions in solution, especially if the solutions contain abundant alkalis and HCO_3^- (Humphris, 1984). However, leaching does not account for the enrichment of the

LREE. Similar REE patterns of LREE enrichment and HREE depletion are reported for fenitization of quartzite by alkaline solutions (Martin *et al*, 1978). Because D89-34 is dominated by the effects of the metasomatic fluid (i.e. high fluid/rock ratio) it is expected that the characteristics of the fluid would be imparted to the rock. Because LREE complexes are less stable in the fluid, they may be "dumped" first into the secondary minerals resulting in LREE enrichment in the rock. It is probable that the REE concentrations in D89-34 were buffered by mineral chemistry (sphene, muscovite and, possibly, zircon(?)) and fluid chemistry, especially if it was alkaline. Assuming a common fluid for the various parts of the deposit, the other highly altered rocks in the Dome Mine should have similar features in their REE spectra. This is borne out by the other units studied, albeit to a much lesser degree of modification, and, also, by previous work (Kerrich and Fryer, 1979). Depletion of Y, Ti and P_2O_5 noted in highly altered samples, can be attributed to similar processes.

The addition of K_2O coincided with formation of sericite, and reduction of albite abundance in the alteration assemblage. The potassium may have been derived locally, in particular, from the abundant sedimentary rocks in the immediate vicinity of the Dome Mine (e.g. Porcupine Group, Pyke, 1982) which are also likely sources of Ba and B. CaO has been stabilized in the metasomatic regime by ferroan dolomite, $Ca_4(Fe,Mg)(CO_3)_2$, which is the dominant mineral in the highly altered areas of the mine.

Cr, Ni, and Zn appear to have been components of the fluid phase, having commonly been added, and only rarely depleted, in the host rocks of the Dome Mine. These elements may have been dissolved from spinels (e.g. Fe-Ti oxides) destroyed during the deformation and carbonatization of mafic and ultramafic rocks in the Timmins area. In general, addition of these elements is variable. Cr is significantly enriched in the altered zone of the Dacite Flow whereas Ni is enriched in the alteration of the Key Flow. Zn has very minor enrichment in both the Key and Dacite Flows. However, in the most altered areas of the 99 Flow (sample D89-34) there is a very large increase in all of Ni, Cr, and Zn. The most likely host for these elements is the sericite and carbonate present in the most altered zones, although there may be some incorporation of Cr, Ni, and Zn in tourmaline. Ta addition was minor, and was probably attributable to same process as the enrichment of Zn, Ni, and Cr as Ta is partitioned by Fe-Ti oxides.

Na_2O was lost due to the breakdown of albitic plagioclase in reaction with the potassic and CO_2-rich metasomatic fluid, resulting in sericite and carbonate. The loss is usually apparent in first stages of alteration and corresponds to K_2O enrichment. The reducing effects of the fluid resulted in an apparent loss of Fe^{3+} due to the breakdown of Fe oxides and subsequent formation of pyrite and ferroan dolomite. This transformation resulted in essentially no loss in the total iron content of the rock. TiO_2 was lost in only the most intensely altered samples, such as D89-34 where almost all sphene and Fe-Ti oxides have been eliminated. Generally, TiO_2 remained immobile as its mineral hosts were relatively persistent. Minor SiO_2 depletion occured in the most altered areas of the different units. This was probably the result of solution of silica released during the breakdown of the metamorphic mineral assemblage.

In general, FeO and MgO, released by the elimination of ferromagnesian minerals, has been maintained in the altered rocks by abundant dolomite. There was loss of H_2O associated with the elimination of hydrous phases, such as amphibole and chlorite, of the original unaltered greenschist facies assemblage. Overall, losses of H_2O were not large, compared to the Harker Lake studies for example, because muscovite is commonly present in the alteration assemblage at the Dome Mine. The loss of Sr in the alteration zones at the Dome Mine is a bit harder to explain. Whereas Sr was probably released during the breakdown of albite, its abundance should have been maintained by the abundant carbonate present in the altered rocks.

Although several common factors have been mentioned with respect to the alteration styles of the different units, there are also variations. The 99 Flow is the non-variolitic, most basic unit of the variolitic Vipond suite, similar in some ways to the non-variolitic host rocks of the Cryderman Zone in the Harker Lake area. Volume changes are different for the various units, mostly due to different styles of structural control. In the altered zone in the 99 Flow, the rock is intensely sheared, with massive carbonate addition, anastomosing quartz veins and a large volume increase, typical of "ankerite vein" orebodies. However, due to the intense foliation present in the relatively unaltered sample, D89-08, there is relatively little volume increase in the most altered samples in the alteration study of the Key Flow. In the Dacite Flow, the ore bodies have less deformation in their wall rocks, resulting in much smaller

volume changes, relative to their unaltered equivalents.

Comparisons of the alteration styles in the various Vipond units are important to see if rocks of variable composition react differently to what is assumed to be a common altering fluid. In common with the non-variolitic flows in the Harker Lake area, the mineralogy of the most altered sample of the 99 Flow is simpler than that of the more evolved flows of the section. The content of leucoxene, plagioclase and chlorite in the most altered samples increases up section whereas carbonate and sericite contents progressively decrease. This may in part be due to lesser alteration intensity in samples of the upper units. However, host rock composition may also be important. Carbonate may be expected to decrease upsection due to the decreasing MgO content which is directly correlated with CO_2 content in altered rocks at the Dome Mine (Roberts and Reading, 1981) and the increasing Fe/Mg ratio which controls, to a certain extent, the stability of carbonates (Bohlke, 1988). The increase in leucoxene in the upper flows may be related to the buildup of Fe and Ti in the melt as the suite evolved. Overall, the Ti-oxides, sphene and leucoxene, seem to persist in the alteration zones (see Table 5.3.6). The breakdown of albite in the presence of chlorite and calcite to produce sericite, ankerite and quartz was a common reaction in these types of rocks. The reaction has not apparently proceeded to a large extent in the more evolved rocks of the section.

Elemental gains and losses are not the same in all the rock types studied at the Dome Mine. MgO was added to the most altered rock in the 99 Flow, possibly partitioning into dolomite which dominates the mineral assemblage. The other units, the Key Flow and the Dacite Flow, have had consistent depletions of MgO content in progressively altered rocks. MnO was immobile except in the most intense stage of alteration in all cases. In the most altered samples, MnO was added in the 99 Flow, whereas it was lost in the Key Flow and Dacite Flow units. There was a small addition of FeO in the most altered sample of the 99 Flow, similar to MgO, but it was essentially immobile elsewhere. Cr and Ni were not consistently added in all units. The 99 Flow had strong additions of these elements whereas they had variable behaviour in the Key Flow and weak addition in the Dacite Flow. The lack of strong correlation between the two elements in the Dacite unit may be due to the low absolute abundances of the elements resulting in less precise analyses.

The discrepancies observed between the alteration style of the various units are possibly due to variable alteration intensities and the differences in the mineral assemblages which result. Part of the variation in alteration mineral assemblages, such as carbonate and albite content, is due to the primary chemistry of the units. Losses of Y, TiO_2, and P_2O_5 were recorded in the most altered sample of the 99 Flow, but these elements remained immobile in the other units. The mobilization of these three elements in only the 99 Flow may be another indicator that the alteration in D89-34 is more intense than has been sampled in the other units. Another indicator of variable alteration intensity is that the REE profile of the most altered samples was significantly disturbed only in the 99 Flow. Other studies of the REE in altered rocks at the Dome Mine (Kerrich and Fryer, 1979) have indicated similar REE fractionation, in particular HREE depletion, in units other than the 99 Flow.

5.4.3 Summary

The two study areas are similar in the nature of the mineralization (Au only) associated with the alteration, but not in terms of the amount and concentration of the mineralization. The Dome Mine is a large deposit, whereas the Harker Lake area is a small prospect. Both are situated in variolitic volcanic suites and are structurally controlled. The Destor-Porcupine Fault Zone passes very near both deposits and they are situated on its splay faults. Abundant pyritization is common to the mineralization in both areas, although at the Dome Mine the presence of quartz vein hosted Au is much more prevalent than in the Harker Lake area. There are some geochemical similarities in the alteration styles. The alteration zones in the Harker Lake and the Dome Mine areas both have significant additions of S, CO_2, Ni and/or Cr, and Au, significant depletions of MgO, H_2O, and minor depletions of total Fe, SiO_2, TiO_2, and Y, especially in the most altered sections. Al_2O_3 and Zr remain relatively immobile in the metasomatized rocks in both areas. The REE are generally immobile in both areas, but have signs of HREE depletion in the most altered samples.

The differences between the two zones are summarized in Table 5.3.7. Perhaps most obvious is that the Harker Lake area is characterized by a sodic, oxidative alteration style, whereas the Dome Mine has a potassic, reductive style. These two styles are reflected in the dominant minerals in the alteration zones. The reasons for the difference is related to the

Table 5.3.7 -Contrasting alteration characteristics, Harker Lake and Dome Mine areas.

Harker	vs	Dome
geochemical:		
-oxidation of iron		-reduction of iron
-Na enrichment		-K enrichment
-Sr enrichment		-Sr depletion
-Zn depletion		-Zn enrichment
-little LILE alteration, Ba variable		-B metasomatism, Ba added
and, overall:		
-smaller, less intense		-broader, more intense
-fresher host rocks		-generally carb'd, foliated
-dom.mafic terrane		-mixed volc./sed./plut. terrane
-brittle regime, frac. hosted		-dom. ductile regime, shears
-DPFZ nearby, on long splay		-DPFZ close, on short splay

overall country rock composition of the two areas. The Harker Lake area is dominated by relatively fresh, spilitized, mafic rocks, with only minor felsic intrusions in the region. Fluids passing through this terrane become sodic by reaction with the abundant albitic plagioclase in spilites, releasing Na^+ to the solution. The dominantly mafic terrane could also account for the comparatively small amount of LILE and Ba enrichment in the Harker Lake area, these elements more commonly associated with sedimentary or felsic plutonic rocks. There are diverse rock types in the immediate vicinity of the Dome Mine, including mafic and ultramafic volcanic and intrusive rocks, felsic volcanics, sediments, and felsic intrusions. Fluids passing through these rocks could easily acquire a potassic signature from the abundant sedimentary, felsic volcanic, and felsic intrusive rocks. These rocks could also have contributed the Ba and B which have been added to the altered rocks at the Dome Mine. The presence of a thick graphitic horizon at the top of the "Greenstone Nose" sequence may have

been enough to reduce the fluid. An important point regarding the rocks in the vicinity of the Dome Mine is that they have been deformed and a large proportion have been altered by a regional carbonatization event prior to being mineralized.

Another significant difference between the two areas, with implications for resulting fluid geochemistry, is the style of deformation asociated with the altered and mineralized zones. The alteration in the Harker Lake area is dominated by features characteristic of a brittle deformation regime, such as intense fracturing of the host rock and fault and fracture controlled alteration and mineralization. The alteration zones tend to be quite narrow, affecting relatively little country rock, and veining is generally as large, undeformed bodies or small, fault zone hosted anastomosing zones. In contrast, the Dome Mine is characterized by shear hosted ore bodies with wide, extensive alteration zones and abundant, anastomosing, commonly deformed veins. These features are more representative of a ductile to brittle-ductile regime. The widespread alteration at the Dome Mine, affecting a large volume of country rock, may indicate that the metasomatism took place at elevated temperatures and pressures, with respect to the Harker Lake area.

The nature of the host rocks and the morphology of the alteration and mineralization zones gives important information about what level in the crust these deposits were formed. The freshness of the local rocks, the brittle deformation, and the oxidative signature of the altering fluids suggest that the Harker Lake deposit was formed at fairly high levels. A fluid source similar to the local oxidized intrusions may have contributed to relatively oxidizing metasomatic fluids. The altered and deformed local terrane, the well developed penetrative fabrics associated with ore, and the reducing nature of the metasomatic fluids suggest that the Dome Mine deposit was formed at greater depth than those in the Harker Lake area. These factors may have implications for the size differences of the deposits.

6. Relationship to Epigenetic Au Mineralization

6.1 Chemical Reactions and Mineralogical Changes

6.1.1 Metamorphic and Metasomatic Changes

The metamorphic mineral assemblage is determined by a combination of original rock composition, temperature and pressure of metamorphism, composition of the metamorphic fluid and amount of fluid infiltration. The original mineral assemblage of the flows in this study probably consisted of: clinopyroxene, $Ca(Fe,Mg)Si_2O_6$; plagioclase, An_{65-45}; Fe-Ti oxides, 40-60 wt% ülvospinel or ilmenomagnetite; +/- apatite, zircon, xenotime (mostly in the upper flows). The unaltered metamorphic assemblage (i.e. at Harker Lake) consists mostly of uralite and albitic plagioclase, plus chlorite, epidote, magnetite, sphene, quartz. The mineral asssemblages reflect regional metamorphism by an H_2O-rich fluid (hydrous silicates such as amphiboles, epidote and chlorite) with Na_2O (albite) and CO_2 (sphene and calcite) components. The fluid involved in the greenschist facies metamorphic reactions could have been equilibrated locally with flows which had undergone seafloor metamorphism which added water and carbonate. The discussion in Section 4.3, of the chemical changes expected in low grade metamorphism, pointed out the geochemical characteristics of the original, unmetamorphosed equivalents of the rocks in this study have remained relatively undisturbed. The maintainance of the primary chemical composition of these rocks suggests metamorphism with very little fluid infiltration.

Metasomatism by hydrothermal fluids related to mineralizing events is a type of metamorphism which has resulted in significant changes in the chemical composition of the affected rocks in this study. Access for the fluid to the rock is of prime importance, and this is why primary permeability of volcanic rocks, such as flow top breccias are commonly altered (e.g. L28+00E area, Map 2.1.2). Permeability is commonly enhanced by the effects of faulting, such as the intense fracturing in the Cryderman Zone and the shearing in the Dome Mine deposit. Metasomatic alteration is most often a retrograde process, eliminating the minerals which were formed during peak metamorphism and, especially in the case of mafic rocks, creating a much simpler mineral assemblage. At the Dome Mine, the complex

mineralogy of the 99 Flow is reduced to a simple assemblage of essentially carbonate, quartz, and sericite by metasomatism. The retrograde process may be due to cooling fluid temperatures or changes in the fluid composition. Alteration zones are commonly characterized by several mineral assemblages representing increasing intensity of alteration such as the cryptic, bleached, and silicified zones in the Upper Massive Flow, L28+00E area, Harker Lake section. These changes towards the centre of an alteration zone reflect changing (usually increasing) volatile content in the rock pore fluids. In studying the following reactions which lead to the observed mineral changes, microprobe data is not available for most of the minerals, so well balanced reactions are not always possible.

One of the first retrogressive reactions to take place involves the conversion of titanite (from the metamorphic breakdown of ilmenomagnetite) to rutile and calcite by the addition of CO_2. This is possible in contact with a fluid with very low concentration of CO_2 (less than 0.1 X_{CO2} up to 525°C at 10 kbar (Graham et al, 1983) or 380°C at 3 kbar (Carmichael, 1991). The reaction occurs beyond the extent of visible alteration in the rock, 10's of metres from the metasomatic fluid conduit. Mafic minerals of the metamorphic assemblage are also broken down, commonly maintaining the relative abundances of Fe and Mg (Gélinas *et al*, 1982), by a reaction such as:

amphibole + epidote + CO_2 + H_2O = chlorite + calcite + quartz (1)

This corresponds to the regional alteration assemblage in the Timmins camp, and the outer alteration (cryptic) in the Harker Lake area. This style of retrograde alteration is much more widespread in Timmins due to the extensive access allowed by the penetrative foliation in that area. It shows that the regional carbonatization event is later than peak metamorphism and the deformation related to the foliation (Piroshco and Kettles, 1988; Hodgson *et al*, 1990).

With increasing proximity to the altered zone, the alteration intensity increases, and increasingly the mineral assemblage reflects the fluid composition. Stabilization of ankerite/dolomite toward the core of the alteration zone is a result of increasing X_{CO2} of the pore fluid (Roberts, 1987). Progressive protolysis of the mineral assemblage creates sericite (Dome Mine) and albite (Harker Lake area) depending on the mineral stabilities and the dominant cation present in the altering fluid. This process is illustrated by the following

generalized reactions, first at the Dome Mine:

$$\text{albite} + \text{chlorite} + \text{calcite} + K^+ = \text{sericite} + \text{ankerite/dolomite} + \text{quartz} + H_2O + Na^+ \quad (2)$$

or, alternatively, in the Harker Lake area:

$$\text{chlorite} + \text{calcite} + CO_2 + Na(OH) = \text{albite} + \text{ankerite/dolomite} + H_2O + O_2 \quad (3)$$

In some zones, leaching of Fe to form oxides and pyrite causes chlorite to become more Mg-rich (e.g. the Cryderman Zone). Progressively increasing X_{CO2} near the fluid conduit further destabilizes ferromagnesian minerals and results in the dominance of carbonate in the core of the more intense zones. In addition, the carbonatization of the rock results in simultaneous dehydration as the rocks were originally equilibrated with a water-dominated metamorphic fluid.

In the L28+00E area at Harker Lake, the combination of high Na^+/K^+, fairly high fO_2 (near magnetite/hematite buffer) in the fluid and the breakdown of chlorite results in the formation of magnesio-riebeckite (Ernst, 1960; Brown, 1974). The reaction would be similar to:

$$\text{chlorite} + Ca(OH)_{2(aq)} + \text{quartz} + Na^+ + CO_2 + O_2 = \text{Mg-riebeckite} + \text{dolomite} + H_2O \quad (4)$$

(the ferric/ferrous ratio in Mg-riebeckite is required to balance charge). The occurrence of magnesio-riebeckite in the L28+00E area and not the Cryderman Zone may be due to the higher Fe/Mg ratio of the more evolved host rocks in the L28+00E area, shown in Figure 6.1.1. This chemical control on the occurrence of Mg-riebeckite has been observed in iso-metamorphic terranes with interlayered blueschist and greenschist mineral assemblages (Dungan *et al*, 1983). Further alteration, with increasing CO_2 and H_2O at the core of the L28+00E zone, results in conversion of the magnesio-riebeckite to talc in the presence of carbonate releasing Na^+, Fe^{3+} and silica. At this stage, the increasing fS_2 of the altering fluid may have helped to destabilize magnesio-riebeckite and reduce iron for the formation of pyrite.

The occurrence of pyrite in the alteration zones of both the Harker Lake and Dome Mine areas is coincident with the addition of sulphur to the rock. Pyrite is most common near the centre of the zones where alteration is most intense. The presence of Au is also closely

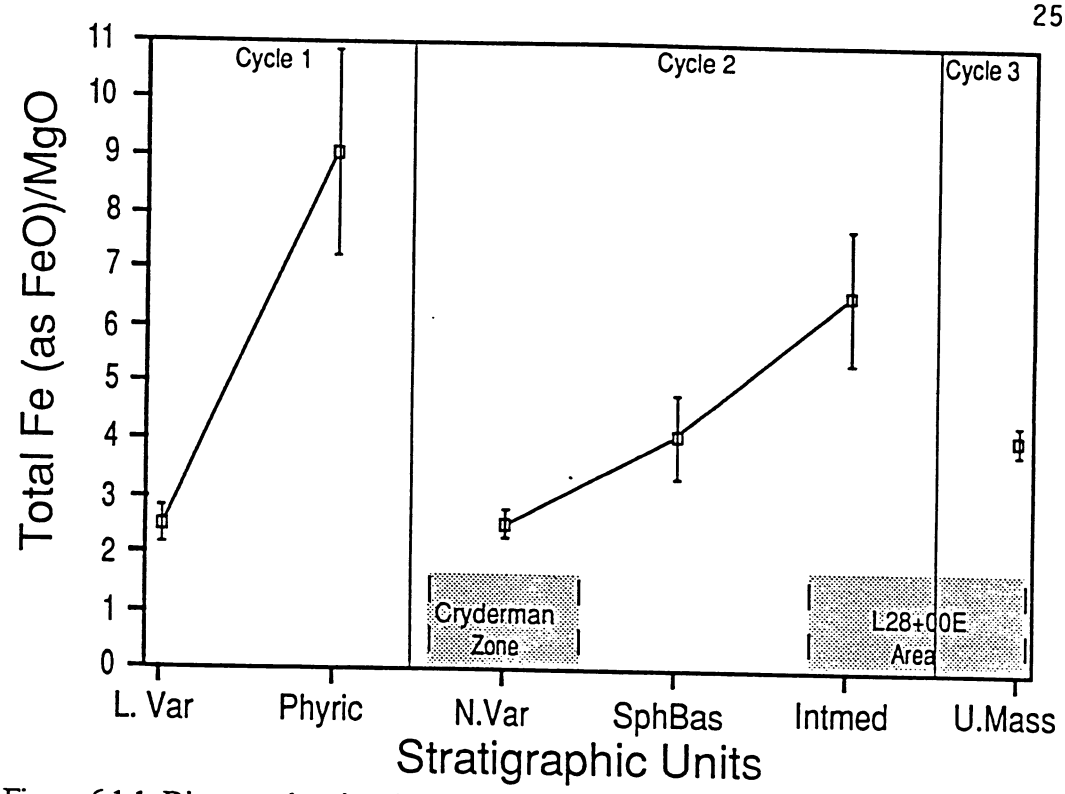

Figure 6.1.1: Diagram showing the increase in the Fe/Mg ratio within each volcanic cycle in the Harker Lake section. The upper, more evolved flows have quite high ratios relative to more average Fe tholeiite values (approx. 2.0 to 3.0). This is reflected in the mineral assemblages of the two alteration zones shown (see text). Error brackets are twice the standard deviation.

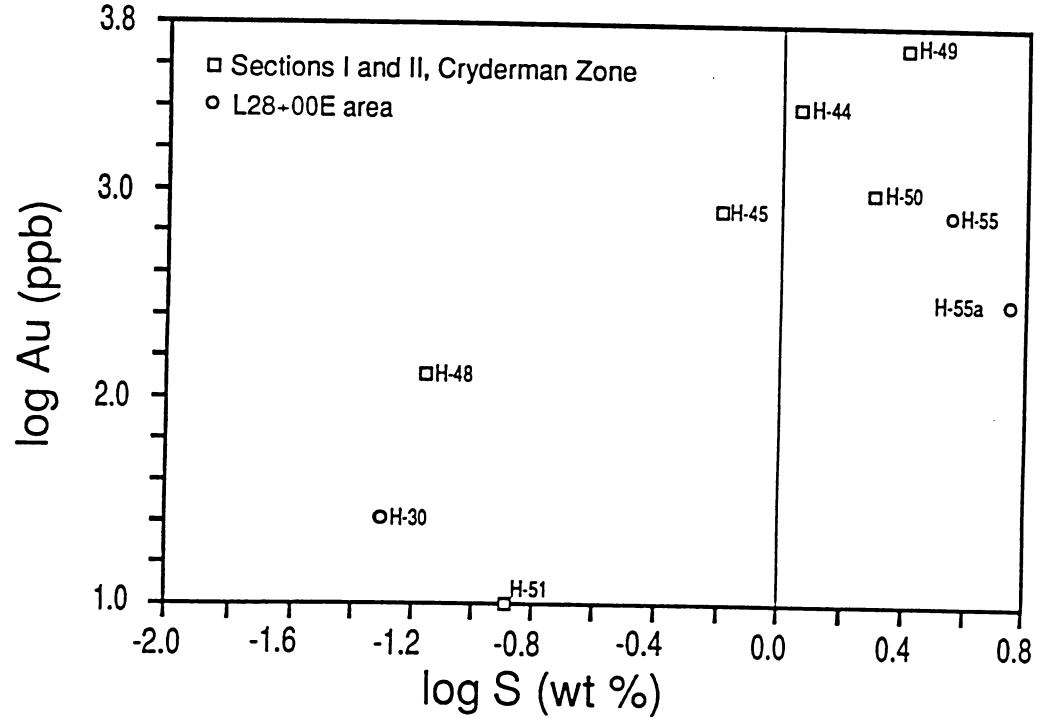

Figure 6.1.2: Diagram showing the relationship between the concentration of Au and S in mineralized rocks in the Harker Lake area. There is a definite, sympathetic relationship between the two variables.

related to sulphur addition in the altered rocks (Tables 5.3.1 to 5.3.6). This suggests that sulphur was an important component of the hydrothermal fluid and sulphidation reactions, such as:

$$Fe_3O_4 + 6H_2S = 3FeS_2 + 4H_2O + 2H_2 \quad (5)$$

played a role in the localization of Au mineralization. Indeed, at Harker Lake, where the sample control is best, there is a definite correlation between the content of sulphur and Au in the altered rocks (Figure 6.1.2).

6.1.2 Fluid Characteristics

As metasomatic fluids pass through the crust, they constantly re-equilibrate with local conditions of temperature, pressure and host rock composition. The mineral assemblages and reactions described above are indicative of the contrasting fluid compositions which have been suggested for the two study areas (section 5.4.3). Examination of the mineral assemblages and reactions can give a more detailed idea of the physical characteristics of the fluids which acted in the two areas. The predominance of carbonates in both study areas reflects a CO_2-rich fluid.

Mineral stabilities in the alteration zones are not always applicable where fluid/rock ratio is high (Colvine *et al*, 1988), so the use of experimental work by authors such as Liou *et al* (1974) on the stability relations of metamorphic minerals such as albite, actinolite and chlorite for temperature estimates must be carefully considered. Changes in hydrothermal fluid composition can give apparent retrograde effects not related to temperature. Geothermometry and geobarometry are beyond the scope of this study, so it was necessary to draw the possible parameters from the literature. Most temperature estimates for Archean lode gold deposits are obtained through fluid inclusion studies. There is a wide spread of estimated temperatures that may be applicable in the two areas of this study. The Dome Mine has been studied in some detail in the past. Kerrich and Fryer (1979) have determined a temperature of formation of the mineralization at the mine from several lines of evidence including isotopic, fluid inclusion and mineralogic data. They concluded that the deposit was formed at a temperature between 400 and 450°C and at a depth of about 6 km. However, nearby, at the Hollinger deposit, Wood *et al* (1986) have estimated temperature of formation

for that deposit at 270 +/- 48°C. There are no similar data available for the mineralization at Harker Lake. It has been estimated that the Kerr Addison deposit, about 45 kilometres to the south of the Harker Lake area, was formed at between 270 and 300°C (Kishida and Kerrich, 1987). This estimate may be a bit low. A study of H_2O-CO_2 inclusion data from Archean deposits by Brown and Lamb (1986) led them to conclude that many deposits were formed at pressures of 3-5 kb, higher than what has generally been reported (1-3 kb, Colvine *et al*, 1988), and temperatures of 350-450°C. There are some similarities in the style of alteration between the Kerr Addison and Harker Lake deposits. Both areas are characterized by strong Na enrichment in variolitic, mafic volcanics and have evidence of oxidation (hematization) present in the alteration zones. However, at the Kerr Addison deposit carbonatization is quite widespread (see CO_2/H_2O discussion below) and the style of deformation is more ductile than brittle. This seems to indicate that the temperature of formation estimated for the Kerr Addison deposit is higher than for the mineralization at Harker Lake. The Harker Lake deposit probably formed at the lower end of the range of temperatures and pressures discussed above.

The alteration assemblages at the Dome Mine and in the Harker Lake area indicate the Na^+/K^+ ratio was distinctly different in the two areas. Based on the mineral assemblages and the reactions written above, in particular reactions (3) and (5), the Na^+/K^+ of the metasomatic fluid appears to be higher in the Harker Lake area stabilizing albite rather than muscovite or potassium feldspar (Figure 6.1.3). According to Kishida and Kerrich (1987), in a study of similar rocks (variolitic basalts) at the Kerr Addison deposit, formation of an alteration assemblage dominated by carbonate and albite (@ 300°C) requires an $a(Na^+/K^+)$ ratio of greater than 10:1. This was based on the stability of albite and the absence of paragonite and potassium feldspar. At the Dome Mine, the Na^+/K^+ ratio is probably much less, considering that the most altered assemblages contain abundant sericite but little to no albite or paragonite.

The ratio of CO_2/H_2O in the fluid plays an important role in determining the mineral phases present in any alteration assemblage (Dubé *et al*, 1987). As metasomatic fluids move from the discharge area, or fluid conduit, into the pores of the surrounding rocks, they are progressively depleted in CO_2. This is because the rocks were equilibrated with a high $a(H_2O)$

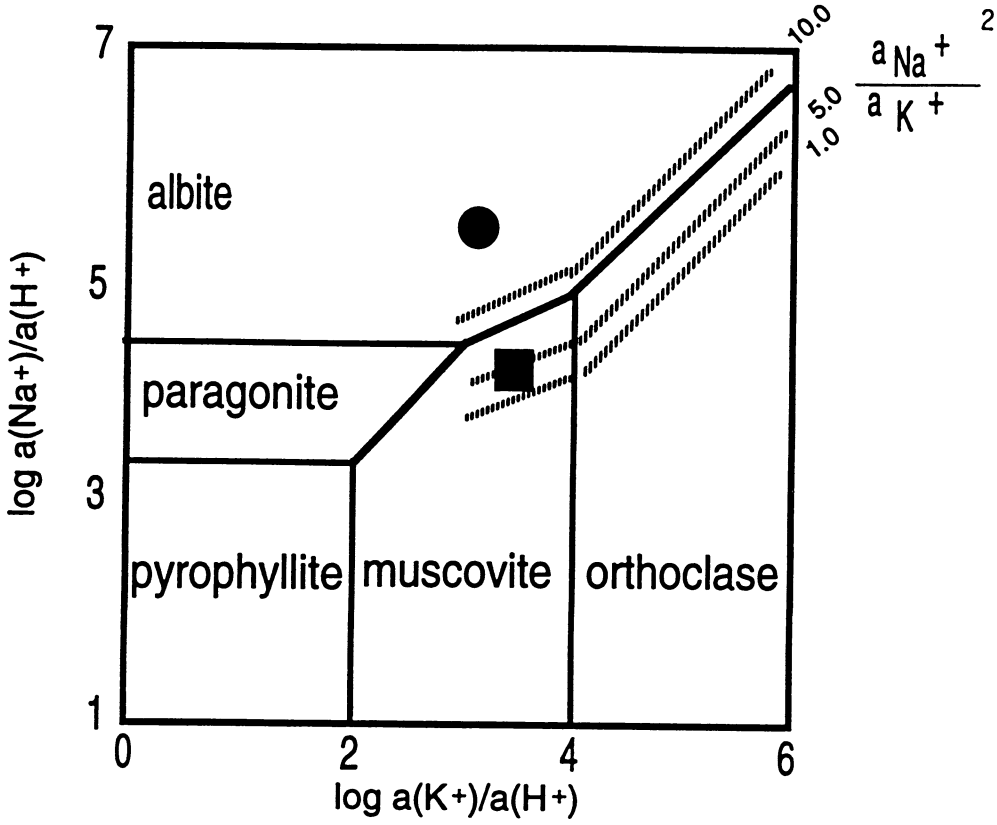

Figure 6.1.3: Activity-activity diagram showing the stabilities of silicate minerals at 350°C and 0.5 kb (from Beane and Titley, 1981). Dashed lines show the $a(Na^+)/a(K^+)$ for the solution. The circle indicates a possible composition for the metasomatic fluid in the Harker Lake area (albite stabilized) whereas the square represents a possible fluid composition at the Dome Mine (muscovite stabilized).

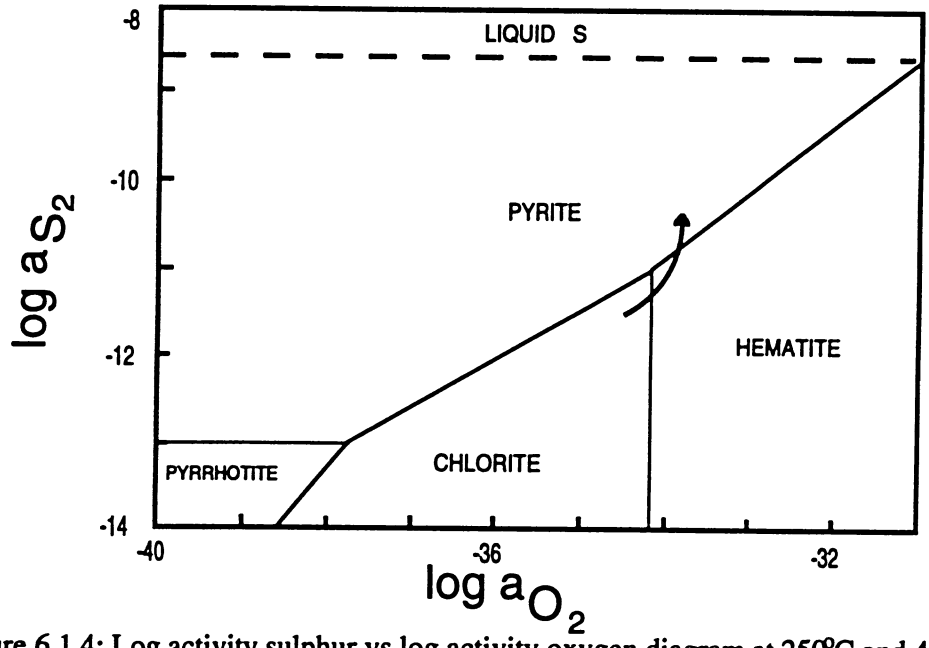

Figure 6.1.4: Log activity sulphur vs log activity oxygen diagram at 250°C and 40 bars (after Barton, 1984). Mineral stability fields are labelled. Arrow illustrates possible path of activty states in progressively altered wall rock in the Cryderman Zone, Harker Lake area. Alteration indicates that there is progressive oxidation and addition of sulphur in the wall rocks toward the centre of the zone.

fluid during metamorphism, so the relatively high X_{CO2} of the metasomatic fluid results in strong disequilibrium. This process of progressive depletion of CO_2 as the metasomatic fluid evolves by reaction with its host rocks can be interpreted on at least two scales. The first, sub-deposit, scale operates essentially laterally within the alteration zones found associated with mineralized veins or shear zones. Near the fluid conduit, where CO_2/H_2O is high, reduction occurs because of the dissociation of H_2O at higher temperatures which releases H_2 (Dubé *et al*, 1987). As the fluids continue to react, the ratio of CO_2/H_2O progressively decreases resulting in a chlorite (hydrous mineral) dominated, more oxidized, assemblages with magnetite and/or hematite, sphene, calcite and epidote.

The second, larger scale, can be imagined in terms of the position of the deposit in the upper earth's crust. At depth, the carbonatization reactions, such as (2) above, de-water the affected rocks, decreasing the CO_2/H_2O ratio in the fluid. As metasomatic fluids rise through the crust they react, cool and, possibly, boil (due to decreasing pressure). This results in a vertical progression of metasomatic assemblages related to the CO_2/H_2O ratio and oxidation potential of the metasomatic fluid on a crustal scale. Consequently at depth, more CO_2-rich fluid and hotter rocks may result in more widespread carbonatization and reduction, whereas near surface there would be more hydrous, oxidized assemblages and relatively restricted alteration. Of course, CO_2/H_2O ratio and redox state of the fluid can be controlled by other factors as well. For example, the presence of graphite in contact with the metasomatic fluid which would exert control on the carbon gas species present, such as CH_4 and CO, as well as, CO_2, resulting in a more reduced fluid.

The vertical pattern described above is suggested by the styles of alteration present at the Dome Mine and Harker Lake areas. The Dome seems to be part of a deeper metasomatic regime with extensive carbonatization, ductile deformation, and reduction associated with the mineralized zones (Fryer *et al*, 1979). The presence of graphitic sediments in the Dome Mine area probably contributed to a more reducing fluid in that deposit than in the Harker Lake area. In the Harker Lake area, the carbonatization associated with mineralization is restricted spatially, deformation is brittle, and the iron in the altered wall rocks is oxidized relative to the unaltered wall rocks, at least where pyrite has not been formed in high concentrations. Overall, the differing alteration styles suggest that the Harker

Lake deposit may have been formed in a higher crustal environment than the Dome Mine. This interpretation is consistent with the description above of the likely temperatures of formation for the two deposits.

The relative oxidation states of the metasomatic fluids at Harker Lake and at the Dome Mine can be estimated from the mineral assemblages. At the Dome Mine, the most altered assemblages consist of Fe-dolomitic carbonate, quartz, sericite and minor chlorite, rutile, pyrite and tourmaline. Almost all the iron present in the rock is in the ferrous state (e.g. $Fe^{2+}/(Fe^{2+}+Fe^{3+}) = 0.93$, D89-34). At no point is there an increase in the magnetite or hematite content of the rock, which would indicate the production of ferric iron. At Harker Lake, the alteration mineral assemblages are generally relatively oxidized, characterized by the persistence of magnetite, development of hematite, and the appearance of magnesio-riebeckite (Ernst, 1960; Brown, 1974). The presence of oxidized plutons in the Harker Lake area (Hattori, 1987), may indicate a similar oxidized source for the auriferous hydrothermal fluids which acted in that area (Rowins *et al*, 1991).

Pyrite occurs near the core of the alteration zones in the Harker Lake area, seemingly at the expense of the Fe-oxides. The appearance of pyrite in association with hematite and magnetite does not necessarily indicate that at some late stage the fluid became more reducing. Pyrite may form as a result of increasing fS_2 (Figure 6.1.4) possibly while fO_2 is also increasing. Thus the fS_2 likely increased toward the core of the alteration zone. Also, since the activity of sulphur in the fluid is not likely as high as CO_2 or H_2O, its effects would not be as widespread resulting in the concentration of pyrite at the centre of the zone. It is interpreted that there was only one fluid which affected the mineralized zones as there is no clear cut textural evidence to suggest a paragenetic sequence from carbonate to sulphide minerals, or visa-versa, in the rocks. In fact, the mineral textures are somewhat ambiguous, suggesting that the carbonate and sulphide minerals at the centre of the zones were contemporaneous and related to a single fluid.

It is considered likely that the fluids acting in both study areas were close to neutral pH. A fluid becomes acid by reactions such as hydration of wall rock minerals, adding $(OH)^-$ to the rock and releasing H^+ in the fluid. However, the metasomatic fluid has a large capacity to buffer the production of acid related to its high CO_2 content, as seen in the equilibrium

reaction:

$$HCO_3^- + H^+ = CO_2 + H_2O \text{ (all species aqueous)} \quad (6)$$

This will tend to maintain the neutrality of the fluid because there is almost always far more HCO_3^- in solution than metallic cations (Kerrich, 1983; Neall and Phillips, 1987). In addition, the salinity of these fluids is quite low, between 2.0 and 3.5 equivalent weight percent NaCl (Kishida and Kerrich, 1987). Immiscibility of the CO_2-H_2O-rich fluids may create two fluids for metasomatism, a brine and a CO_2-rich vapour, which would have very different effects on associated wall rocks. The alteration assemblages in the Harker Lake area do not show evidence of separation of the fluid components. At the elevated pressures and low fluid salinities generally associated with Archean lode Au deposits there is little likelihood that immiscibility would have occurred (Bowers and Helgeson, 1983).

In summary, some characteristics of the metasomatic fluids in the Harker Lake and Dome Mine areas were probably similar such as being neutral pH, H_2O and CO_2 rich, and low salinity. However, other properties of the fluids were apparently quite different. The temperature and pressure of formation of the Dome Mine mineralization are fairly well known, 400 to 450°C and 2 kb, or higher. The style of alteration and deformation in the Harker Lake area indicates that the mineralization there was formed at lower temperatures and lower pressures. H_2O/CO_2 and fO_2 were both higher in the metasomatic fluid in the Harker Lake area, the increases being possibly attributable to a higher crustal level. Additionally, the fluid sources could have been different, resulting in some differences in the overall fluid compositions.

6.1.3 Transportation of Au

Gold is insoluble as an ion in solution and so recognition of its principle ligands in hydrothermal solutions is important to understand the processes which could lead to Au deposition. Considering the conditions summarized above, Cl^-, HS^-, and HCO_3^- may have been present in sufficient quantities to have contributed significantly to large scale transport and concentration of Au (Phillips and Groves, 1983). Figure 6.1.5 shows the most common Au-complexing agents active in hydrothermal fluids at 300°C (after Seward, 1984). Clearly, at this temperature the HS^- complexes are the most soluble at all but very acid pH levels. HSO_4^-

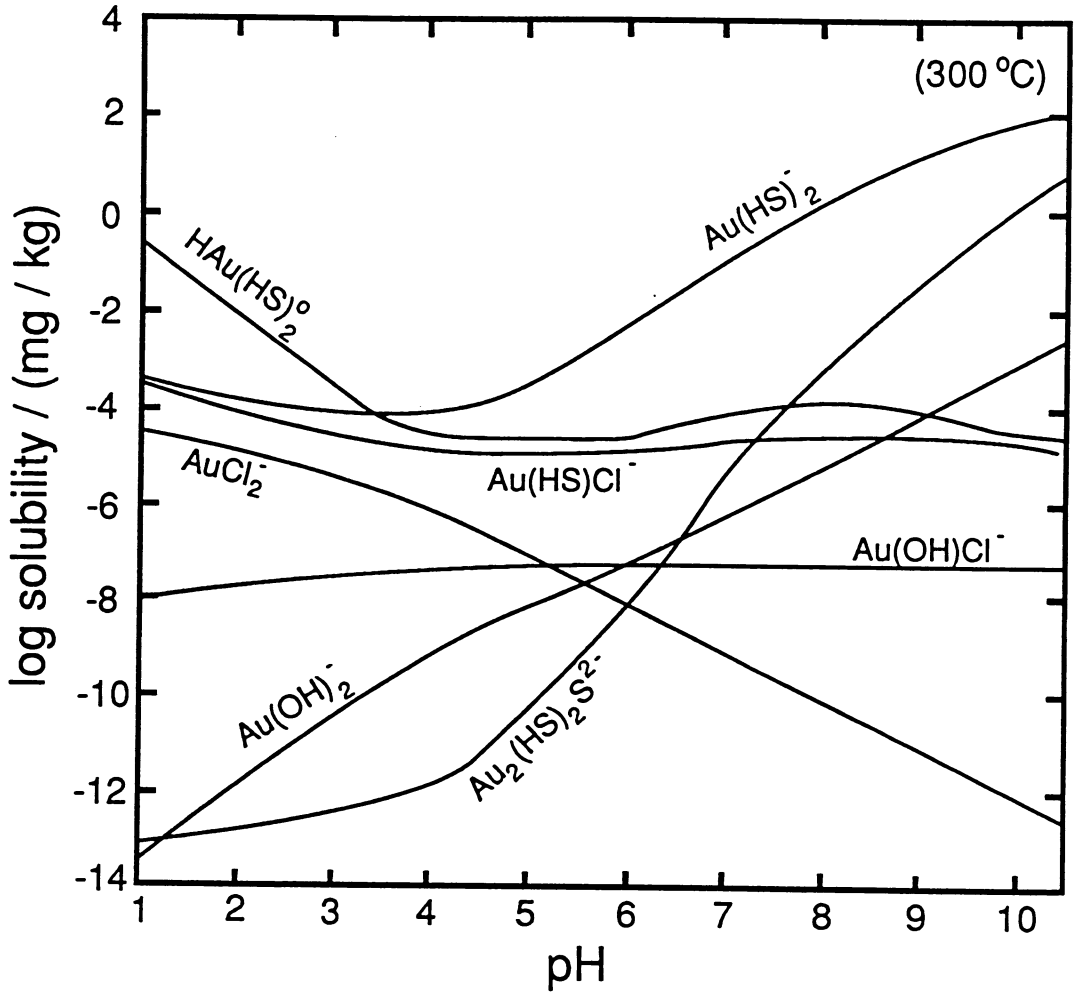

Figure 6.1.5: Solubility of Au complexes in equilibrium with pyrite and pyrrhotite (plus magnetite at high pH). HS^- complexes are the most common at all pH levels (after Seward, 1984).

and SO_4^{-2} may be significant at slightly higher fO_2 than is normally attributed to Archean Au deposits (Seward, 1984). The possibility exists that at higher temperature, greater than 350°C, chloride complexes are just as plentiful, if not more so, than the sulphur complexes (Figure 6.1.6). However, most fluid inclusion work on Archean lode Au deposits has shown that the fluids associated with mineralization are generally of very low salinity (Kishida and Kerrich, 1987; Groves and Phillips, 1987) suggesting that chlorine complexes of Au were not important.

Gold in solution is most commonly present in its +1 state. The large, weakly charged Au^{1+} ion preferentially forms bonds with large, polarisable ligands, such as HS^-, forming strong and stable complexes (Phillips and Groves, 1983). Small, non-polarisable bases, such as Cl^-, and F^- do not favour cations based on their ionic strength, and consequently tend to complex metals in proportion to abundance in the source rocks (Phillips and Groves, 1983). Metal complexing by small base ions tends to produce deposits with strong enrichments for several metals, with the particular metals depending on fluid temperature. Au deposits in the Archean tend to be Au-only, with significantly more enrichment of Au than other metals (Kerrich and Fryer, 1981), possibly indicating that the complexing agent was selective, preferring Au to other metals (e.g. HS^- ligand).

The anion, HCO_3^-, was probably strongly concentrated in the auriferous metasomatic fluids at both the Harker Lake and Dome Mine areas. This is due to their generally high fCO_2, evident by the ubiquitous carbonatization of wall rocks that were in contact with these fluids. However, the large areal extent of the carbonatization, in comparison to the restricted distribution of Au, and the apparent overprinting by other alteration types more closely related to Au, such as sulphidation, in Au deposits argues against carbonate as a major complexing agent of Au. The high concentration of the carbonate anion in solution, relative to Au, means that Au would probably never be saturated with respect to HCO_3^- even if the carbonate anion concentration was greatly reduced by carbonatization of a large volume of rock (Bohlke, 1988). This is demonstrated by the low to background abundance of Au in carbonate alteration zones surrounding gold lodes (Fyon and Crockett, 1983). At Alleghany, California, ore grade disseminated Au mineralization appears to be restricted to the alteration zones closest to veins, where the fCO_2 was likely very close to that in the fluid (Bohlke, 1988). In

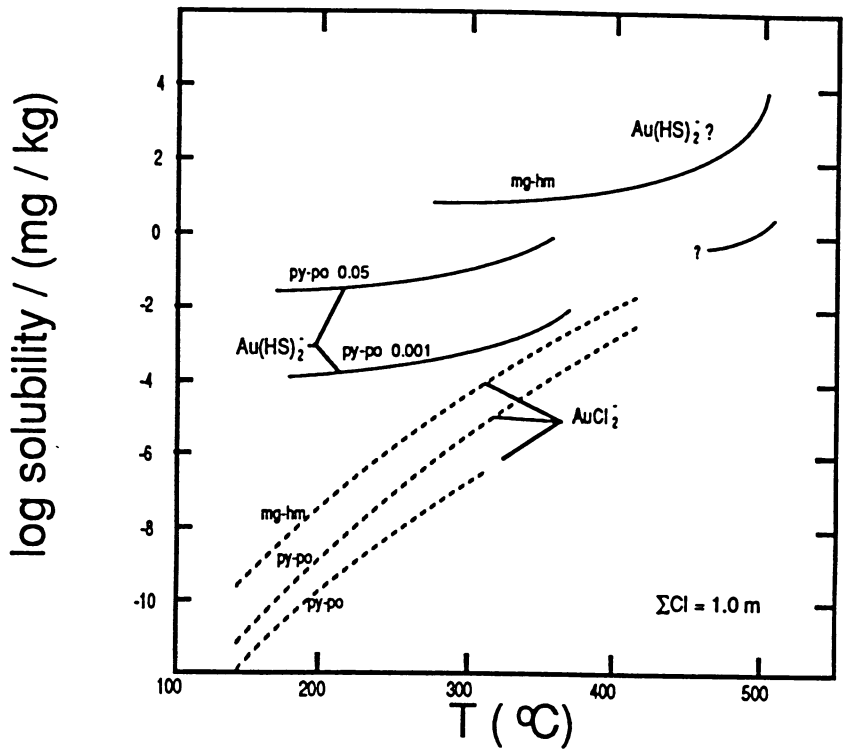

Figure 6.1.6: Solubility of Au versus temperature at variable conditions of ΣS and fO_2 for solutions with 1.0 m chloride and pH=6. Curves compiled by Seward (1984) from various experimental data. At lower temperatures, especially lower than 350°C, the HS^- Au-complex dominates the solutions whereas Cl^- may be more important at higher temperatures.

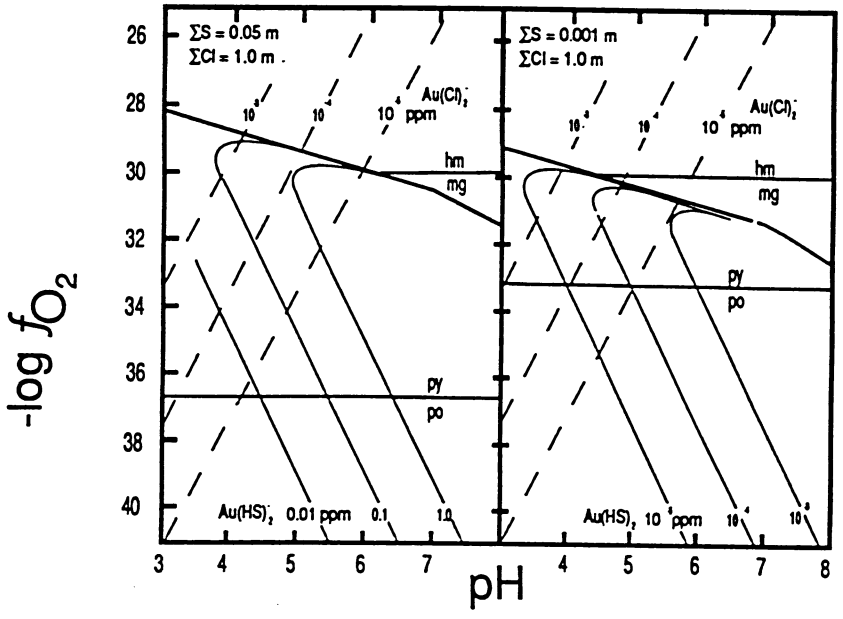

Figure 6.1.7: Gold solubility contours with respect to pH and oxygen fugacity for the complexes $Au(HS)_2^-$ and $AuCl_2^-$ at 300°C (modified after Seward, 1984). The stability fields for hematite (hm), magnetite (mg), pyrite (py), and pyrrhotite (po) are shown. For near neutral pH solutions, the bisulphide complex is more soluble, even if 1000 times less concentrated, than the chloride complex.

this alteration regime, destabilization of the carbonate ion would not have taken place, indicating that Au was probably being transported by another complexing agent.

The HS^- ion is likely the dominant Au complexing agent in auriferous metasomatic fluids which were involved in the formation of the mineralized zones examined in this study. The $Au(HS)_2^-$ complex is about three orders of magnitude more soluble in typical fluids (at 300°C) than the $AuCl_2^-$ complex, even considering a concentration of S about 20 times less than Cl (Figure 6.1.7). In addition, bisulphides are among the most stable complexes of Au over a wide range of temperatures, up to 350°C (Shenberger and Barnes, 1989). Finally, the close association of pyrite, and to a lesser extent other sulphides, with Au mineralization, suggests a link between the precipitation of sulphur and Au from solution (Neall and Phillips, 1987; Bohlke, 1988).

Figure 6.1.7 demonstrates that when the concentration of sulphur in solution is low enough, about three orders of magnitude less than Cl, solubility of the $Au(HS)^-_2$ is only slightly greater than $AuCl^-_2$. Therefore, the dominance of Au-sulphur complexes depends to a large extent on maintainance of a relatively strong activity of sulphur. This may be difficult in terranes dominated by rocks with abundant Fe (as in the Harker Lake area) which will tend to buffer the sulphur fugacity to low values (one reason why Au concentrations not as high in Harker Lake area as at the Dome Mine?). Fluids equilibrating with rocks having relatively low iron abundance, or Fe/Mg ratios, like komatiite or ultramafic rocks, are more likely to have high sulphur fugacity, leaching sulphur and associated metals, such as Au, from those rocks (Bohlke, 1988).

6.2 Deposition of Gold

6.2.1 Relative Importance of Au Deposition Mechanisims

One of the objectives of this study is to examine the relative importance of the influence of variolitic rocks on localization of Au mineralization. Lode Au deposits usually consist of several types of ore. Host rock influence is especially significant for Au mineralization disseminated in the rock, such as in pyritic alteration halos around veins and shear zones. An important point in the following discussion is that ore is not usually

deposited without the hydrothermal fluid carrying the ore metal being out of equilibrium with its environment, including wall rocks. Fluid-wall rock reactions may bring the ore metal(s) to saturation in the hydrothermal solution, at which point the metals are precipitated. The influence of the host rock composition on metal deposition is commonly dependent on the extent of disequilibrium with the altering fluid. The fluid-wall rock reactions may also have an influence on fluid equilibrium in the vein, or fluid conduit, although most vein components will be buffered by the infiltrating fluids.

Infiltration into the wall rock is restricted to a narrow envelope around the fluid conduit where the altered rocks may approach equilibrium with the fluid. Beyond this envelope is a reaction-dominated regime, a zone of disequillibrium, where material transfer takes place by diffusion, driven by activity gradients between the fluid and the unaltered wall rock (Rose and Burt, 1979). For example, the $a(CO_2)$ is generally much greater than the $a(S_2)$ in the hydrothermal fluids associated with Archean lode gold deposits and as a result of the different gradients, carbonatization is more widespread than sulphidation in the altered wall rocks.

One way to cause a hydrothermal fluid to precipitate components is to lower the fluid temperature. It is quite possible that in many Au deposits the wall rocks were considerably cooler than the metasomatic fluid. However, due to the restricted distribution of Au in the deposits examined in this study, it is considered that the temperature at the site of Au deposition was not significantly different than the fluid. In fact, if mineralization occurred at, or just past, the peak of deformation and metamorphism (as indicated by some ore deposit morphologies), it is likely that the host rocks would be the same temperature as the fluid. In this case, the apparent retrograde mineral changes documented in this study (i.e. sphene going to rutile and calcite) can be attributed largely to changes in the fluid X_{CO2}.

The solubility of the Au-bisulphide complex is greatest in a relatively reducing, slightly alkaline solution at temperatures appropriate to formation of mineralization in the study areas. The solubility contours in Figure 6.1.7 illustrate that several different changes to the fluid will tend to destabilize the Au-bisulphide complex. Either one of oxidation or reduction of the fluid will cause precipitation of sulphides and Au, if it is saturated with respect to the bisulphide complex. The more effective way to precipitate sulphides is to

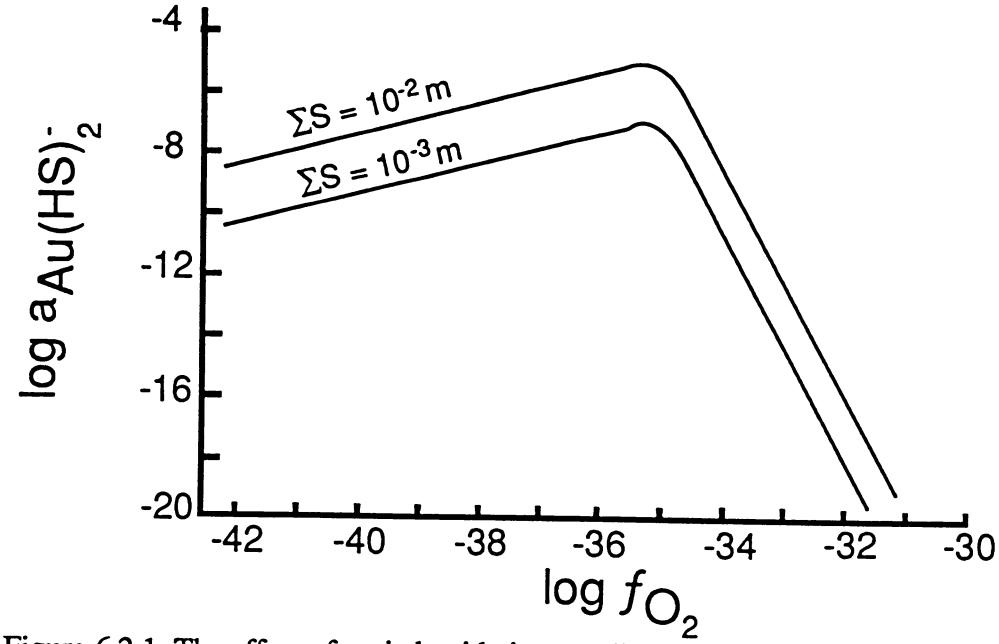

Figure 6.2.1: The effect of varied oxidation conditions on the solubility of Au at 250°C for total dissolved sulphur concentrations of 0.001 mole/l and 0.01 mole/l (pH = 6) (from Cameron and Hattori, 1987). The solubility of Au decreases with both increasing and decreasing fO_2. The solubility decrease is much more pronounced with increasing oxygen fugacity. There is little change in the pattern of Au solubility with respect to variation in total dissolved sulphur.

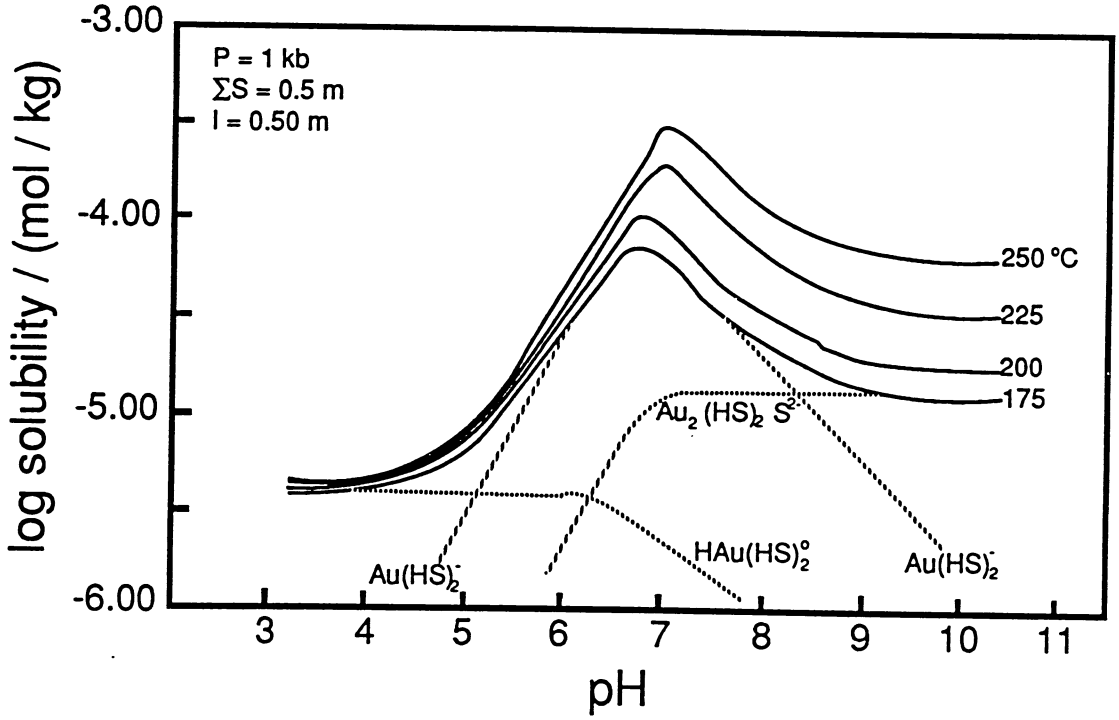

Figure 6.2.2: Solubility of Au-bisulphide complexes in sulphide solution as a function of pH and temperature (modified from Seward, 1984). A change of pH from near neutral conditions will decrease the solubility of the Au complexes. The pH effect on solubility is unchanged with small changes in temperature.

oxidize the fluid e.g. by reducing the wall rock, forming pyrite from Fe oxides(Figure 6.2.1).

Figure 6.2.2 shows the solubility of the bisulphide complex in relation to pH. A strong change in pH, especially to a more acid solution, will also destabilize the Au complex. However, hydrolysis reactions, common in alteration zones around Au mineralization, and the excess base related to the CO_2-HCO_3^- equilibrium (eq. 6) in the fluid tends to buffer the pH near neutral values reducing the importance of pH change as a depositional mechanism. Decreasing temperature has a variable effect on deposition of gold, depending on the pH-oxidation path of the fluid (Shenberger and Barnes, 1989).

Boiling of the metasomatic fluid can cause major changes to the fluid composition, upsetting an equilibrium which may have existed between the fluid and the wall rock. Boiling may occur when there is a sudden pressure decrease affecting the fluid, as when hydraulic fractures form, and propagate, in the wall rocks (Robert and Brown, 1986; Sibson *et al*, 1988). Removal of volatile species from solution by boiling will tend to cause rapid precipitation of complexed metals at the site of the boiling, namely in the vein formed by gangue deposition also related to fluid boiling. This may create high grade Au pockets in veins within deposits but is not likely to contribute substantially to wall rock deposition of disseminated Au with sulphides.

Equation (7) represents one of the major buffering equilibrium reactions in CO_2-rich solutions typical for Archean lode Au deposits:

$$CO_2 + H_2O = HCO_3^- + H^+ \text{ (aq.)} \qquad (7)$$

Driving off CO_2 by boiling will shift the equilibrium to the left, and reduce the H^+ in solution, provided there are enough HCO_3^+ ions (base). The resulting increase in the pH of the solution will affect the stability of Au-complexes in the fluid (Figure 6.1.5). In particular, the solubility of Cl^- based complexes is reduced by increased alkalinity.

In terms of destabilizing metal complexes, boiling has the least effect on bisulphide complexes. The solubility of Au-bisulphide complexes actually increases with H^+ consumption (Drummond and Ohmoto, 1985). The relationship can be seen by examining the equilibrium reaction:

$$8Au^o + 15H_2S + SO_4^{-2} = 8Au(HS)_2^- + 4H_2O + 6H^+ \text{ (aq.)} \qquad (8)$$

As seen in (7) above, H^+ consumption in solution is directly related to separation of CO_2 by

boiling and in (8) consumption of H^+ will shift the reaction to the right and increase the solubility of Au in the fluid. However, H_2S, on the left side of the reaction, may also boil, counteracting the effects of H^+ consumption on the equilibrium shown in equation (8). Consequently, deposition of Au from bisulphide complexes in solution is dependent on the relative amount and volatility of CO_2 and H_2S. If the molar consumption of H^+ is slow, less than 2.5 times faster than H_2S (see reaction (8) stoichiometry), the equilibrium will tend to shift to the left and precipitate Au. Since there is usually much more CO_2 in solution, which is substantially more volatile than H_2S (Figure 6.2.3), it is expected that molar H^+ consumption will generally be much greater than 2.5 times the molar consumption of H_2S due to boiling. Therefore, boiling will be an effective depositional mechanism for Au in the equilibrium reaction (8) only in certain cases, such as when there is an extraordinarily low total CO_2 in solution (therefore very little HCO_3^- to react with H^+), the temperature is high (> 400°C), or the system is completely closed to escaping volatiles. These special conditions do not seem to have been common in the formation of Archean lode Au deposits (Roberts, 1987; Colvine *et al*, 1988). It is possible that boiling may have been more important at the Dome Mine, where the temperature was higher, than in the Harker Lake area. The effects of boiling may partially account for the widely varied host rocks for Au ore at the Dome Mine.

There is another factor that may play a large role in the effect that boiling has on precipitating sulphur, and hence Au, from solution. The destabilization of chloride complexes by boiling of CO_2 would tend to cause the precipitation of iron from solution, since Fe-chloride complexes are quite soluble. There is a strong possibility that the iron would precipitate as pyrite, which has a very wide stability field, assuming sulphur is also available from the solution. This mechanism may cause the destabilization of Au-bisulphide complexes by reducing the fH_2S in the fluid. The overall effectiveness of this mechanism for Au precipitation is not certain owing to the generally low abundance of chloride ions present in solution, as evident in fluid inclusions from Archean lode Au deposits (Phillips and Groves, 1983; Kerrich and Kishida, 1987).

Probably the most efficient way to remove Au from solution is to remove the complexing agent. The process is controlled by the natural buffering charcteristics of the wall rock and results in disseminated sulphide mineralization extending away from the fluid

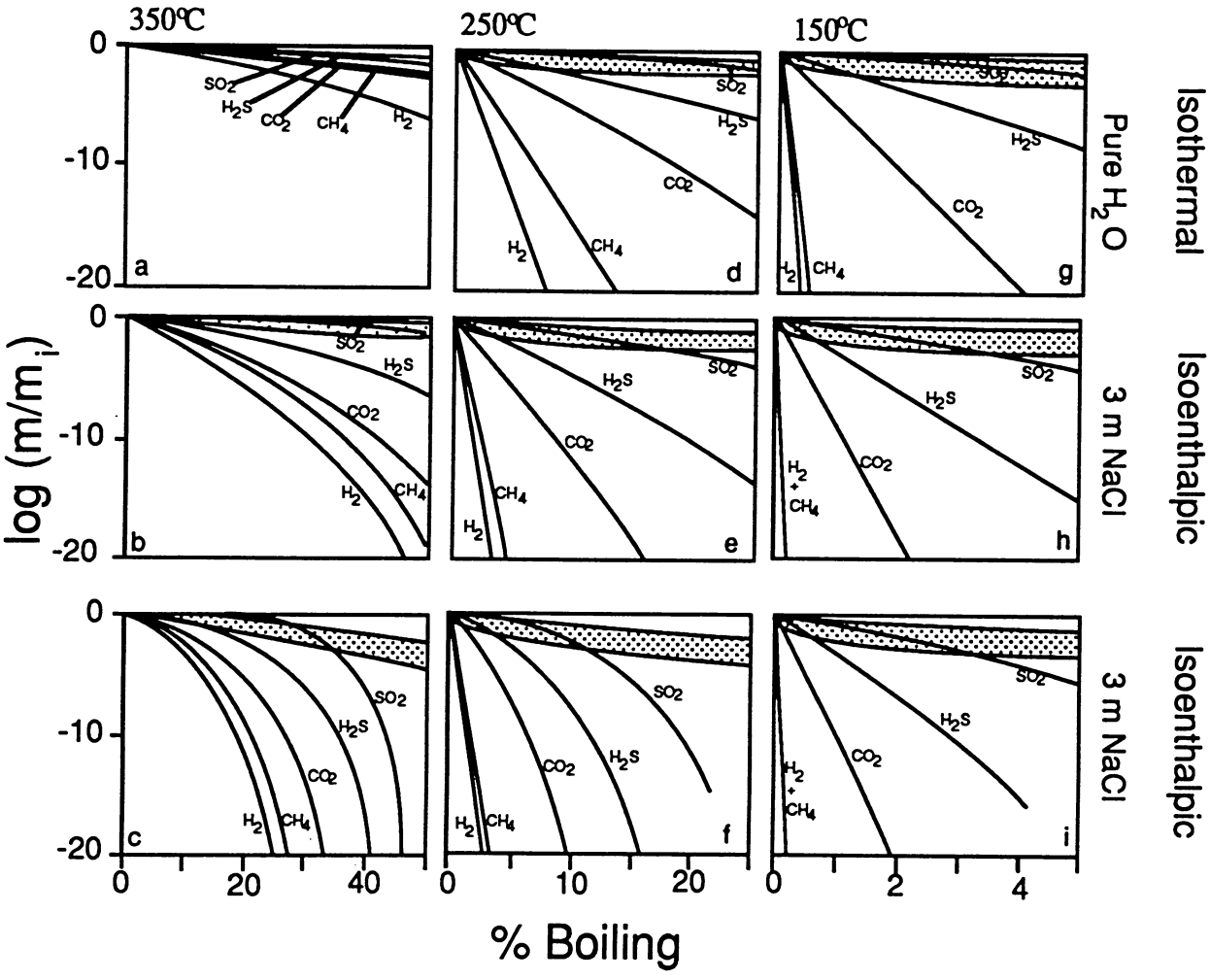

Figure 6.2.3: Dissolution paths for H_2, CH_4, CO_2, H_2S, and SO_2 from 350°C (a,b,c), 250°C (d,e,f), and 150°C (g,h,i) variable (as shown), boiling solutions (from Drummond and Ohmoto, 1985). Lines are from open boiling systems, whereas stippled areas represent the zone of all the closed boiling dissolution paths. The expression m/m_i represents the ratio of the gas molality of a liquid at any stage of boiling to the gas molality at the inception of boiling. In all cases above, the volatility of H_2S is less than CO_2 suggesting that equation (8) in the text will not lead to deposition of sulphides by boiling of H_2S.

discharge zone (or vein). Since bisulphide complexes are likely to have been the most important transport agent, and the inefficiency of precipitating bisulphide-complexed metals by boiling has been described, sulphidation of the wall rock is perhaps the most effective way of precipitating Au, given the proper conditions. According to Hodgson (1983), approximately 82% of Au deposits contain auriferous, hydrothermal pyritization of wall rock. The association of pyrite and anomalous Au concentrations in rocks has also been shown in this study (Tables 5.3.1 to 5.3.6, Figure 6.1.2). At the Hunt Mine, Kambalda, Australia, sulphidation of the wall rock has been demonstrated as thermodynamically sound, at elevated temperatures (350-400°C), by Neall and Phillips (1987). They found that the fH_2S decreased 30% across a pyritized alteration halo, resulting in mineralogical zoning (pyrite-pyrrhotite-magnetite progressively away from the vein), whereas the fO_2 and the fCO_2 did not change substantially. By calculation it was found that the decrease in the fH_2S would account for an 80% decrease in the solubility of Au. Typical reactions (Neall and Phillips, 1987) would involve magnetite, such as equation (5), or chlorite:

$$2Au(HS)_2^- + 2H^+ + FeO_{(chlorite)} = 2Au^\circ + 2H_2S + FeS_2 + H_2O \qquad (9)$$

resulting in a progressive increase in magnesium relative to iron in chlorite (Figure 6.2.4). This progression towards pyritic centres of alteration zones has been noted in both areas in this study. In addition to removing sulphur from solution, fluid oxidation and/or lowering of fluid pH during the sulphidation process will lead to saturation of Au with respect to the bisulphide complexes (Figure 6.1.7).

Deposition of Au indicates that it has become saturated in the fluid at the prevailing conditions. Saturation may come in stages and depends to a great extent on the amount of Au contained in the fluid. If Au is greatly undersaturated due to a poor source or an earlier event which caused the fluid to precipitate Au, then even significant interaction between the fluid and host rock may not be enough to deposit Au. Also, if Au is undersaturated in the fluid, then there may be a lag, either spatial or temporal, until sufficient deposition of gangue minerals causes Au to be saturated and subsequently precipitated (Bohlke, 1988).

Once sulphidation of the wall rock has occurred, other factors may also play a part in deposition of Au from solution. For example, the electrochemical and surface adsorption properties of pyrite have a tendancy to attract gold (Colvine *et al*, 1988). This helps to

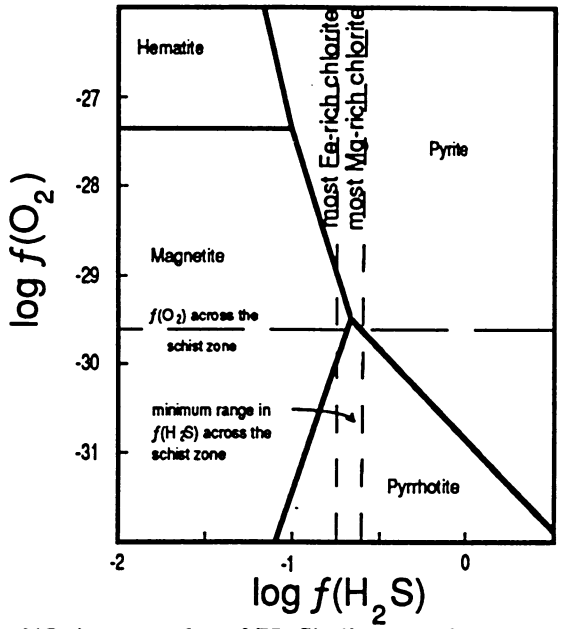

Figure 6.2.4: Log $f(O_2)$ versus log $f(H_2S)$ diagram from a study at the Hunt Mine, Kambalda, Australia (Neall and Phillips, 1987). The figure illustrates that Mg-rich chlorite is more stable than Fe-rich chlorite with increasing sulphur activity. The process of sulphidation of chlorite removes the Fe in the silicate for the formation of Fe sulphides, as noted in the L28+00E area.

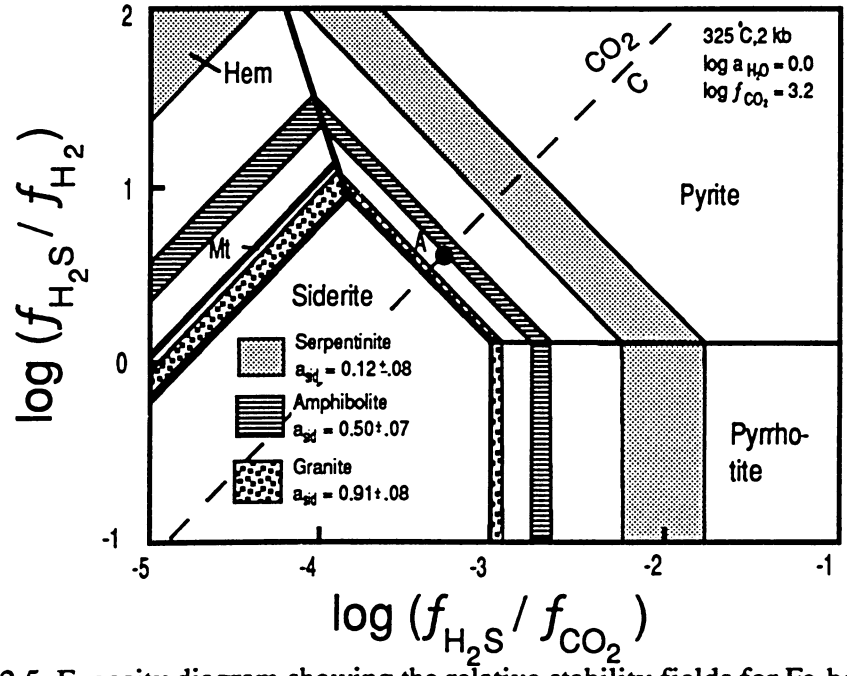

Figure 6.2.5: Fugacity diagram showing the relative stability fields for Fe-bearing phases at stated conditions (after Bohlke, 1989). Boundary of the siderite field shown for activities of $FeCO_3$ based on analyses of carbonates from the host rock types in the study. The activity of other phases is assumed to be unity. The stability field for siderite expands with decreasing host rock Fe/Mg ratio (for which serpentinite is the lowest and granite is highest). Note that a fluid of composition A would form differing alteration assemblages depending on the host rock type reacting with the fluid. The fluid would react with the serpentinite and the amphibolite to form magnesite-siderite carbonate whereas the fluid would form pyrite in contact with the granite.

explain the common occurrence of Au as coatings, or plates, on the grain and fracture surfaces of pyrite.

6.2.2 Variolites and Localization of Au

High iron rocks have been described as suitable hosts for Au mineralization related to sulphidation (Groves and Phillips, 1987). One of the most obvious examples of this process is altered Fe formation (Macdonald, 1984; Hall and Rigg, 1986). The theory is that the various Fe-enriched rocks provide the iron for reactions which produce pyrite and other sulphides. Mass balance studies in Au deposits generally indicate that iron has been preserved in the host rock whereas sulphur is an added component, presumably from the metasomatic fluid (Bohlke, 1988; this study). The variolitic suites examined in this study occupy the upper part of Fe-enrichment trends interpreted to result from fractional crystallization of tholeiitic rocks. The concentration of iron in the rocks commonly exceeds 15 wt.% which provides abundant material for sulphidation processes.

Furthermore, Bohlke (1989) points out that high iron content is not in itself sufficient to cause sulphidation of the host rock to occur. Rather it is the Fe/Mg ratio of the rock which exerts more control on the formation of disseminated sulphide ore zones. In these terms, the argument favouring localization of Au mineralization in high iron rocks does have some validity since these rocks commonly have a relatively high Fe/Mg ratio. However, in his study of Au mineralization and related alteration in various rock types of the Motherlode system, Alleghany, California, Bohlke (1989) found that Fe-poor granite (1.67 wt% FeO_{total}, Fe/Mg=10) was the preferred host rock for stratabound disseminated Au ore even though it was in contact with mafic amphibolite (6.08 wt% FeO_{total}, Fe/Mg=0.8). In a study of the alteration and mineralization of gabbro sills at the San Antonio Mine, Manitoba, Ames *et al* (1991) found that a leucogabbro, though poorer in total iron, was more effectively sulphidized during the mineralizing event than an adjacent melagabbro. Significantly, the leucogabbro has an Fe/Mg ratio of 3.16 compared to a ratio of 1.14 in the lesser mineralized melagabbro.

The reason that the ratio of iron and magnesium controls the formation of Fe sulphides, predominantly pyrite (due to its wide stability range), relates to the partitioning of iron between carbonates and sulphides (Bohlke, 1988). In general, mafic silicates, and

commonly Fe oxides, are not stable in the alteration zones associated with Au deposits, and this is true for the areas in this study. The partitioning of iron from these minerals between carbonates and pyrite depends on the prevailing Fe/(Fe+Mg) ratio of the system, usually controlled by the host rock in diffusion dominated environments (i.e. wall rocks, Rose and Burt, 1979). In rocks with a low Fe/(Fe+Mg) ratio, the alteration zone mineralogy is characterized by the magnesite-siderite solid solution series plus ankerite-dolomite. If the Fe/(Fe+Mg) ratio is high, pyrite and ankerite-dolomite are formed. The effect of rock types with various Fe/(Fe+Mg) ratios on the relative stabilities of siderite and pyrite is demonstrated in Figure 6.2.5. Clearly, under the conditions stated, the stability field of pyrite expands with increasing Fe/(Fe+Mg) ratio of the host rock.

The effectiveness of the process is dependent on several factors. Perhaps primary among them is the extent of disequilibrium between the fluid and the potential host rock. This is dependent on the fluid's history. Also important are fluid flow and, related to that, the amount of residence time for the fluid in the potential host rock to allow reactions to take place. As a fluid passes from a rock type with which it has equilibrated, into a chemically distinct rock type, the section immediately downstream from the contact represents the maximum contrast between fluid and host rock making potential sulphidation reactions most effective. Sulphidation and Au mineralization may not correlate exactly if the saturation level of the Au with respect to bisulphide complexes is not high. At the Hunt Mine in Kambalda, Australia, Phillips *et al* (1983) describe a two stage alteration zone, an outer, Au-poor, unbleached, pyritic zone and an inner, bleached, Au-rich, pyritic zone, possibly developed as a result of the lag in Au precipitation.

In light of the process outlined by Bohlke (1988), it is very significant that variolites commonly have higher than average Fe/Mg ratios for tholeiitic rocks. In general, Fe tholeiites are separated from Mg tholeiites by having an Fe/Mg ratio of 2.0 or better (Jensen, 1976). The V8 subunit of the Vipond Subgroup has a Fe/Mg ratio close to the average, between 2.0 and 3.0, whereas the V10 subunit has ratio values greater than 3.0 and commonly greater than 5.0. A similar range of values is found in the non-variolitic through intermediate units in the Harker Lake area stratigraphy. The ratios are generally progressively higher toward the top of the volcanic cycle (Figure 6.1.1). Based on the Fe/Mg ratio, variolitic suites, especially

their upper parts, are good candidates to host disseminated, auriferous pyritic mineralization under the right conditions. In addition, variolites are significantly enriched in iron which improves the extent to which pyritization can occur relative to other rocks with high Fe/Mg ratios but low total iron content, such as felsic volcanics and intrusives.

The mineralization in the two study areas reflects the differences in Fe/Mg ratio of the host rock. The "dacite" orebodies in the V10 subunit at the Dome Mine have diffuse, auriferous zones of pyritization (Ferguson, 1968) surrounding the central quartz veins (Figure 2.3.3). Further down the sequence, the "ankerite vein" orebodies found in the V8 subunit have quite narrow pyritic halos (< 1.0 m) and Au grades drop off abruptly. In the Harker Lake area the distinction is not as clear between the mineralization in the non-variolitic flows and the intermediate flows. However, considering that the zone in the L28+00E area is not as intensely altered as the Cryderman Zone, it has comparable pyrite content (Tables 5.3.1 to 5.3.3). The development of pyrite, with little carbonate alteration in the L28+00E area, is indicative of the higher Fe/Mg ratio of the upper flows in the Harker Lake sequence. The generally lower Au content is possibly indicative of the intensity of alteration.

Bohlke (1989) also points out that rocks with a high Fe/Mg ratio will be most effectively sulphidized in heterogeneous terranes where the fluid's history has brought it into equilibrium with rocks having low Fe/Mg ratio. In terranes having a low overall Fe/Mg ratio, such as lower Archean komatiitic through tholeiitic volcanic sequences, H_2S in the fluid will be buffered to relatively high levels by the dominance of the formation of magnesite-siderite over pyrite in altered wall rock to fluid conduits. In fact, the carbonate-sulphide equilibria in these terranes may cause sulphur to be leached from the rocks if the fS_2 is greater in the wall rock than in the fluid (Bohlke, 1988). This mechanism will increase the solubility of Au, by providing additional sulphur for bisulphide complexes. Where the fluid encounters rocks with high Fe/Mg ratio, such as differentiated igneous rocks (including variolites) and Fe formation, pyrite becomes stable and sulphur and Au are precipitated. The important factor here is that the favourable host rock must be in contrast with the rocks which have recently influenced the fluid equilibrium. The variolitic suites in this study have anomalous Fe/Mg ratios with respect to their surrounding rocks. They occur in the tholeiitic sequences which commonly overly (stratigraphically) komatiitic to tholeiitic lower volcanic suites. This situation exists

in the Dome Mine area, with the Vipond Subgroup occurring directly over the lower volcanic member (komatiitic to tholeiitic volcanics and intrusives) of Pyke (1982) and otherwise mostly surrounded by sediments and ultramafic intrusives, which generally have low Fe/Mg ratios as well. In the Harker Lake area, the variolitic suite is in the middle of the tholeiitic section of the regional stratigraphy (Kinojevis Group) and so the contrast with its surrounding rocks is not as great as in the Dome Mine area. As a result, the sulphidation process may not have been as effective at precipitating Au. This fact may be another reason why the mineralization at Harker Lake is not as intense as in the Dome Mine area.

A final point on the attributes of variolitic rocks for hosting disseminated Au mineralization relates to the relative competency of the rocks. Variolites are commonly evolved members of Fe tholeiitic suites, some flows containing as much as 65 wt% SiO_2. It is expected that a more felsic rock will react more competently than a more mafic rock under shear stress at greenschist facies conditions (Stesky *et al*, 1974). This is dependent on the mineralogy of the rocks as, for example, phyllosilicates will decrease the strength of a rock. Under greenschist facies metamorphism the more mafic rocks develope chlorite and/or serpentine which seriously decrease their strength and reduce brittle failure (Byerlee and Brace, 1968). More felsic rocks with elevated quartz content, such as the upper flows of the variolitic suites, are less likely to develope phyllosilicates and more likely to fail brittly (Stesky *et al*, 1974), thus creating permeability.

As a consequence of their more felsic nature, upper members of variolitic suites may be expected to react relatively more competently than surrounding rocks in a shear stress regime. Brittle failure under stress will tend to provide fluid access to a greater volume of the rock type allowing metasomatic reactions to be more pervasive. In the case of disseminated Au mineralization related to sulphidation of the host rock, brittle failure should increase the volume of mineralized rock, making the deposition process more effective in terms of the amount of Au precipitated. Phillips *et al* (1983) state that the best host rocks for disseminated sulphide-Au mineralization are high iron, less mafic, competent basaltic units which is a fairly accurate description of the characteristics of the variolitic suites.

The brittle nature of variolitic rocks may be illustrated at the Dome Mine where relatively homogeneous shear has acted on rocks of the Greenstone Nose. The crosscutting,

tension-gash vein morpholgy of the "dacite" ore bodies in the V10 flows, the uppermost unit of the Vipond Subgroup, is indicative of brittle failure (Figure 2.2.3). The "ankerite vein" ore bodies in the lower, more mafic flows are sheared, banded, anastomosing vein zones which have deformed in a ductile manner. The location of "ankerite vein" ore is controlled somewhat by the presence of flow top breccias and/or flow contacts, but they also crosscut the massive parts of flows. Widespread mineralization in the V10, and narrow zones of mineralization in the lower, less evolved V8 flows may be related to the prevalent style of deformation in the two units which is, in turn, partially related to the composition of the host rock.

6.2.3 Model

A model is envisaged for the creation of stratabound, disseminated sulphide-Au mineralization in variolitic wall rocks to discordant veins in Archean lode Au deposits. The processes which lead to such mineralization may have some effect within the vein as well, other factors notwithstanding. The model draws heavily on the relationship of magnesite-siderite and pyrite equilibrium as outlined by Bohlke (1988; 1989).

CO_2-rich fluid originates at depth (Groves and Phillips, 1987; Cameron, 1989) and rises through the crust due to thermal and hydraulic pressure gradients, possibly following deep-seated ductile shear zones, related to transcurrent faulting (Cameron, 1989). The fluid is focussed as it approaches the brittle-ductile transition and is brought into contact, and equilibrates, with Archean komatiitic through Mg tholeiitic volcanic sequences which may lie along the fluid pathway toward the variolitic section. The low Fe/(Fe+Mg) ratio of these primitive rocks leads to elevated concentrations of sulphur in solution, thereby increasing the solubility of Au by providing bisulphide for complexing (Bohlke, 1988). Base metals are not leached during this process due to the paucity of chloride anions in the fluid. The fluids may be channeled towards variolitic sequences along reactivated reverse faults (Hodgson *et al*, 1990), possibly including the structures which originally lead to the development of the variolitic suites by hosting high level intrusions (see Section 4.7.3).

At the brittle-ductile transition and above, cooling temperature reduces the fluid equilibrium and precipitation of gangue may take place. This could lead to sealing of the fluid

conduit, build-up of fluid pressure until lithostatic pessure is overcome, resulting in hydraulic fracturing of competent rocks and formation of veins. Structurally prepared and chemically distinct, high Fe/Mg ratio variolitic rocks stabilize pyrite in the wall rock to the veins, fractures and shears resulting in removal of sulphur, and consequently Au, from the fluid. This process may continue as long as fluids continue to infiltrate the rocks and access to the rocks is maintained by subsequent stages of hydraulic fracture and vein formation.

Progressive reactions between fluid and wall rocks as the surface is approached causes an increase in the fO_2, and changes the Na^+/K^+ and CO_2/H_2O ratios. Variable alteration assemblages in similar host rocks are formed in response to the changes in the fluid chemistry. Depletion of Au in the fluid eventually eliminates the possibility of formation of economic Au deposits downstream on the fluid path.

6.3 Comparison with Other Host Rock Controlled Deposits

6.3.1 Golden Mile, Kalgoorlie, Australia

The Golden Mile, at Kalgoorlie, Australia, is one of the largest Archean Au camps in the world. As is common to most lode Au deposits, there are important structural controls present, notably the Kalgoorlie Syncline and the Golden Pike and Golden Mile Faults. The largest proportion (80%) of mineralization is hosted by the Golden Mile Dolerite, a large, differentiated tholeiitic sill within the local greenstone belt (Phillips, 1986).

The Golden Mile Dolerite (GMD) has been subdivided into 10 units based on geochemical and petrographic information (Travis *et al*, 1971). Units 1 and 10 represent the upper and lower chilled margins to the sill and are characterized by "variolitic" texture. The rest of the sill is divided into two main sections which are chemically distinct (Figure 6.3.1). Units 2 to 5, and also unit 9, repesent an initial, more mafic pulse of magma which differentiated *in situ* (Travis *et al*, 1971), ranging in composition from basaltic komatiite (unit 2) to Fe tholeiite (unit 9). The other section of the sill, represented by units 6 to 8, is a later, more differentiated section, presumably from the same, but more fractionated, source magma as the initial pulse. This section is characterized by the appearance of Fe-Ti oxides and the units follow an Fe enrichment trend on the Jensen Cation Plot (Figure 6.3.1). The most

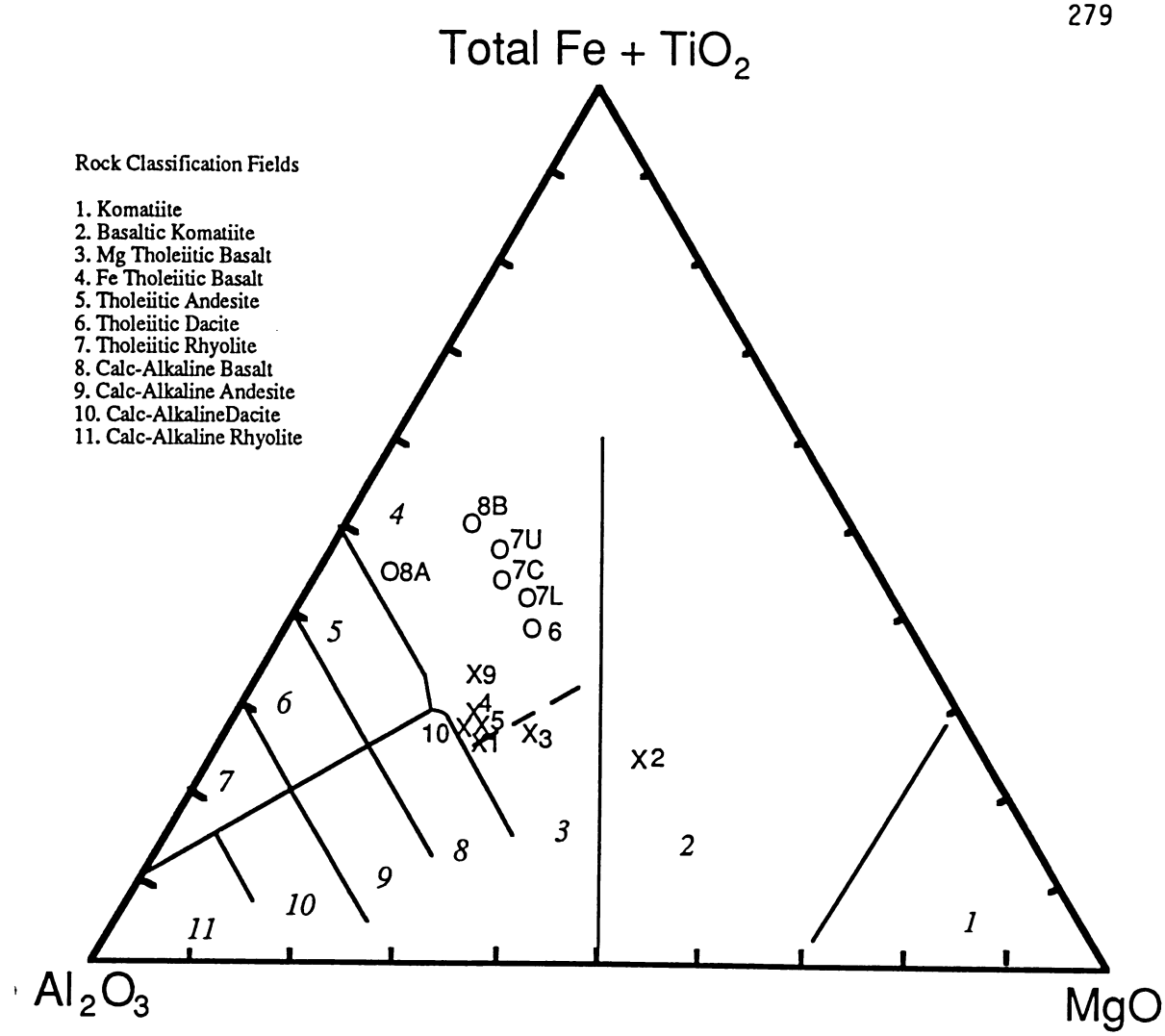

Figure 6.3.1: Jensen Cation plot of geochemical data for the ten subdivisions of the Golden Mile Dolerite, Kalgoorlie, Australia. The initial magma pulse is represented by the samples from units 1 through 5 and units 9 and 10 (plotted as x's). The second, more differentiated pulse is represented by units 6 through 8A (plotted as o's). Unit 8A, a granophyre, is the most differentiated rock in the

evolved unit (unit 8A, Travis *et al*, 1971) is a granophyre, of approximately andesitic composition, characterized by intergrowths of quartz and albite. This texture is likely quite similar to the myrmekitic texture described in the more evolved flows of both the Harker Lake and Vipond Subgroup sections in this study. The Fe enrichment trend in the GMD is very similar to the section in the Harker Lake area in the overall compositional range of the units and the local presence of Mg tholeiitic rocks (Figure 6.3.2). There are also strong similarities to the Vipond Subgroup compositional trend, although the possible presence of two magma sources in the Dome Mine area obscures the relationship somewhat (Figure 6.3.3).

Ore at the Golden Mile is typically grey, bleached and silicified, basalt or dolerite wall rock to veins, generally with 5-10% disseminated pyrite (Travis *et al*, 1971). Au is intimately associated with the pyrite in these wall rocks. In the most evolved unit (unit 8) exclusively, there is a separate ore type, more structurally controlled, in which mineralization is associated with a quartz stockwork, although the Au still occurs mostly in the wall rock. Textural and chemical evidence (Travis *et al*, 1971; Bartram and McCall, 1971) indicate that mineralization is a result of sulphidation of the iron in the wall rock. Bartram and McCall (1971) conclude that host rock control of ore in the Golden Mile is related to the deformation characteristics of favourable horizons (i.e. the more intermediate units react to stress in a brittle fashion, enhancing permeability). The chemical control of the GMD on the localization of ore, as indicated by the predominance of Au in wall rock sulphide zones, and the physical control on host rock permeability by the more evolved units of the sill make the GMD, and equivalent units, good exploration targets where they are cut by large, oblique structures (Travis *et al*, 1971). These controls are similar to the features apparently controlling the distribution of mineralization in the Harker Lake and Dome Mine areas. In the case of the Golden Mile Dolerite, structural control may be more obvious than its chemical control because of its massive, relatively homogeneous nature in comparison to the volcanic suites examined in this study.

6.3.2 Kerr Addison Deposit, Virginiatown, Ontario

Significant ore reserves are hosted in the variolitic volcanic rocks ("flow" ore) at the

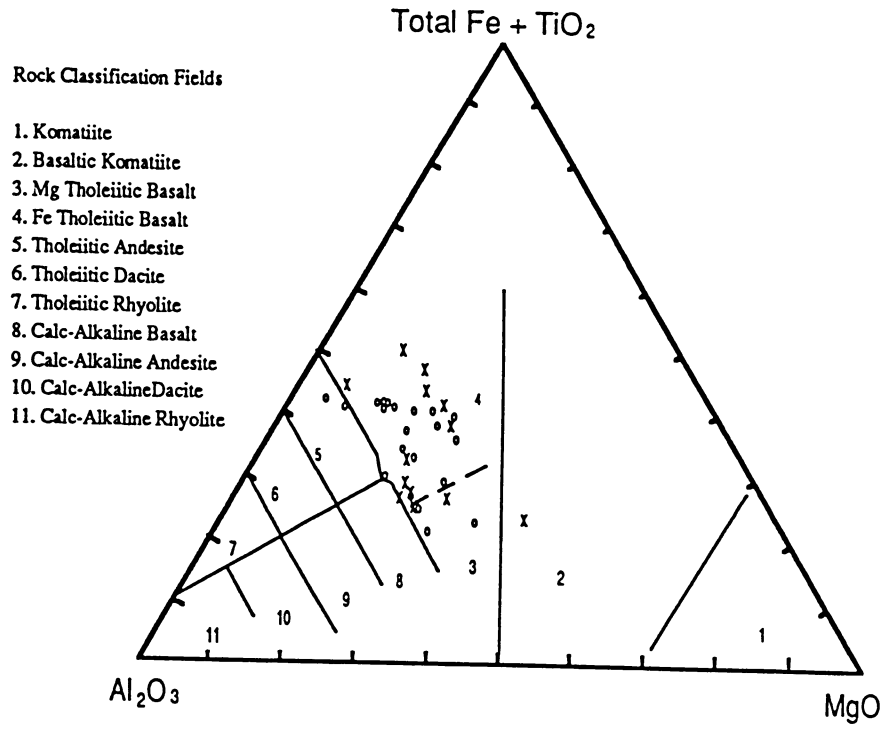

Figure 6.3.2: Jensen Cation plot comparing the section on the Hurd Property, (o's) including the variolitic Harker Lake section, and the section through the Golden Mile Dolerite (x's) (Travis et al, 1972). The general range of compositions in the two sections are quite similar,

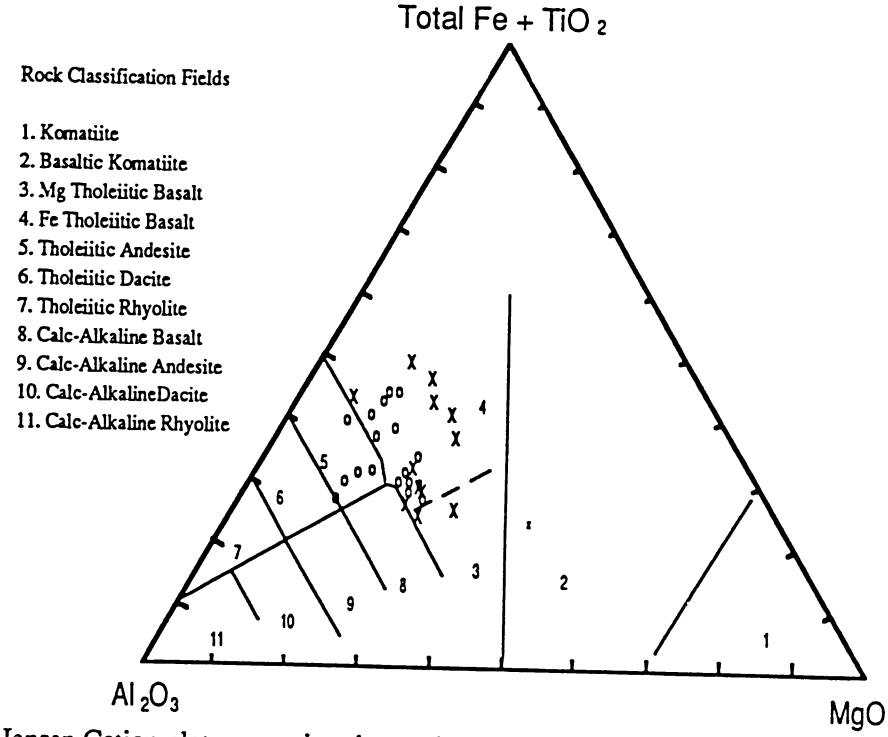

Figure 6.3.3: Jensen Cation plot comparing the section at the Dome Mine (o's) and the section through the Golden Mile Dolerite (x's) (Travis et al, 1972). In general the two sections are similar. The anomalous units of the V8 subunit of the Vipond Subgroup stand out from the rest of the samples, plotting as tholeiitic andesites.

Kerr Addison Mine near Kirkland Lake, Ontario. The other main host for ore is a large ultramafic unit ("carbonate" ore) which is in contact with the variolites. Ore in the variolitic rocks is predominantly auriferous disseminated sulphides in the altered wall rock to veins and shears (Kishida and Kerrich, 1987). In carbonate ore, Au tends to occur as the native metal in quartz-ankerite veins. In general, the flow ore is a higher grade and more evenly distributed than the carbonate ore (Thomson, 1941). The differences in the ore types reflects the differences in the host rock control on the localization of the mineralization. Another possibly important factor in the concentration of mineralization in the Kerr Addison deposit is the strong chemical contrast between the two main host rock types.

6.3.3 Banded Iron Formation

A common example given for host rock control on Au mineralization is banded iron formation (BIF) (Groves and Phillips, 1987; Macdonald, 1984). In this case, Fe-rich mesobands are replaced by sulphides where the BIF is crosscut by structures which have acted as fluid conduits. BIF is commonly quite siliceous, consisting of laminations of fine grained chert and magnetite, making it susceptible to brittle failure under stress, creating good access to the rock for altering fluids. However, the fine grained, siliceous nature makes BIF relatively impermeable and, overall, chemically inert. Therefore, the extent of mineralization in BIF is usually dependent on the density of the structures as replacement does not reach far from the source of the altering fluids (Macdonald, 1984). In comparison, variolitic volcanic rocks have more inherent permeability, such as cooling fractures, vesicles, flow tops and flow contacts, as well as, having a generally more reactive composition due to their high temperature of formation. This potentially allows more widespread alteration and mineralization in variolites than in BIF.

7. Summary and Conclusions

7.1 Summary of Data

7.1.1 Geology, Petrology, and Geochemistry of Variolites

Variolites are mafic to intermediate volcanic rocks, generally containing varioles. Variolites occur in the upper, more evolved parts of Fe-tholeiite volcanic sequences, especially near the peak of Fe enrichment. Varioles have been noted in rocks of more basic composition, such as Mg tholeiitic (Pirie, 1981) and basaltic komatiitic (Jensen, 1978) flows, but these compositions were not encountered in this study.

Variolitic suites have several characteristics which can be observed in outcrop. Flows are more felsic towards the upper parts of the suites. Varioles are not necessarily present in all flows and they are commonly concentrated in upper flows. This is reflected in the flow banding (so-called "flowy" texture) in the Spherulitic Flow of the Dome Mine and the layered varioles in the intermediate pillowed flow at the Paymaster. Another characteristic of these more felsic flows is their broken varioles, termed chicken feed texture, as typified by the Broken Spherulitic Flow and the brecciated flow top of the V10. The so-called "ropy texture" occurs at the top of the V10 subunit and is not found any where else in the Dome Mine section. A similar texture was found at the top of the most felsic flow in the Harker Lake section.

The unusual thickness and continuity of the hyaloclastite unit near the top of the Harker Lake section is interpreted to be a result of its more felsic composition. The high viscosity of the lava led to extensive brecciation and restricted degassing of the melt, thereby creating a frothy lava. The base of this hyaloclastite unit has pronounced flowbanding (Plates 2.1.2 and 2.1.3), characteristic of felsic flows.

The variolitic suites are characterized by disequilibrium textures attributable to crystal growth under diffusion limited conditions. Varioles are commonly composed of plagioclase spherulites, with or without skeletal plagioclase crystals and uralite (after pyroxene). Open plagioclase spherulites have been found in the massive parts of flows, in particular near the upper part of the variolitic suite. Dendritic and skeletal Fe-Ti oxides are found throughout the

suites, including within varioles. Hollow acicular and branching crystals of uralite, after pyroxene, are common in the massive and variolitic parts of flows. It is interpreted that the variolitic lavas were extruded from a shallow-level, super-heated magma which contained few, if any, nuclei for crystal growth (e.g. Fowler *et al*, 1987). After extrusion of the lava, the combination of few nuclei, high viscosity in the more evolved flows, and rapid cooling led to diffusion limited crystal growth in the melt. Diffusion in felsic liquids is reduced by the extensive polymerization of silica tetrahedra in the melt. Crystallization proceeded quickly once nuclei were established, leading to disequilibrium crystals, such as those described above, whose growth-habit was stabilized by the diffusion limiting conditions of the melt. A progression of textures with distance from the cooling surface has been documented in this study which relate to the degree of undercooling of the melt (e.g. Lofgren, 1974). The concentration of varioles in the more evolved flows relates to their formation under diffusion limited conditions.

The variolitic suites examined in this study have composition ranges beyond that normally associated with oceanic tholeiites. Variolites occur at and beyond the peak of Fe enrichment on the tholeiitic trend, extending to andesite composition. Varioles are commonly more concentrated in basaltic andesites. This correlates with the textures observed in the field characteristic of felsic flows. The variolitic suite contains elevated concentrations of incompatible elements such as Zr (up to 370 ppm), Y (up to 140 ppm), and REE (greater than 50 times chondrite values) and anomalously low concentrations of compatibles, such as V and Mg, especially in the upper flows of the sequence. Commonly, Si, Fe, Ti and P are elevated as well. The whole rock Fe/Mg ratio of variolites is generally anomalously high with respect to its host volcanic suite, usually greater than 3.0 in the upper flows. All these chemical attributes can be related to extensive differentiation of the source magma(s) of the variolitic suite.

7.1.2 Alteration Study

It is assumed that within the restricted areas studied, the complete suite of rocks in the deposits were subjected to alteration by metasomatic fluids of uniform composition. Thus, the mineralogical differences observed from one rock unit to another are primarily thought to be

due to changes in host rock composition or intensity of alteration. The upper, more evolved, members of variolitic suites tend to stabilize albite, chlorite and Fe-Ti oxides in their most intensely altered zones rather than carbonate which is predominant in the lower members. The more evolved flows also tend to have more complex mineralogy in their most altered zones than the lower units in the suites. In comparison to the lesser evolved flows, the higher Fe/Mg ratio of the upper flows, more easily enabled sulphidation of these rocks to form pyrite (e.g. Bohlke, 1988).

In the Harker Lake area, mass balance calculations (using the isocon diagram of Grant (1986)) demonstrate that the alteration associated with Au mineralization is characterized by oxidation of the host rock plus significant addition of Na_2O, S, CO_2, Sr and Au, and significant depletion of H_2O, Zn, MgO, MnO and, to minor extent HREE. At the Dome Mine alteration is characterized generally by reduction of the host rock, significant addition of K_2O, S, CO_2, Ba, CaO, B and LREE, and significant depletion of Na_2O, Sr, H_2O, and HREE.

Differences in the alteration styles between the two areas are due to several factors. The mineralized zones at Harker Lake probably formed at a shallower crustal level than the Dome Mine. This is especially evident in the style of deformation present in the two deposits. The Harker Lake area is characterized by brittle deformation in the mineralized zones as compared to the pervasive ductile deformation prevalent at the Dome Mine. The strong oxidation in the Harker Lake zones is possibly related to their crustal level or to crustal processes similar to those which produced the strongly oxidized local intrusions. Other factors which may have affected the nature of the alteration in the two deposits are the size and intensity of the mineralizing events (obviously much stronger at the Dome Mine), the influence of structure (shear zones allowing much more pervasive alteration at the Dome), and the local terrane (dominated by mafic volcanic rocks in the Harker Lake area, quite mixed felsic, mafic, ultramafic and sedimentary rocks in the Dome Mine area).

The metasomatic fluids in the Harker Lake and Dome Mine areas were quite different. The Dome Mine probably formed at the upper end of the range of temperatures and pressures for Archean lode Au deposits, that is 400-450°C and about 0.3 GPa (Kerrich and Fryer, 1979; Brown and Lamb, 1986). At Harker Lake, the style of alteration and deformation indicate lower mineralization temperatures, around 300°C, and lower pressure. H_2O/CO_2, Na/K, and

fO_2 were all higher in the metasomatic fluid at Harker Lake than at the Dome Mine. Alteration assemblages also indicate that the fluid was near neutral and that bisulphides were the dominant complexing agent in both areas.

7.2 Conclusions

7.2.1 Petrogenesis of Variolitic Suites

Based on field and geochemical evidence, it was assumed that partial melting and assimilation did not play a significant role in the observed differentiation of the variolitic suites. The hypothesis that the variolitic suites in this study were developed by fractional crystallization was tested using two modelling techniques (Section 4.7.2): the major element technique of Pearce Element Ratio Diagrams (Pearce, 1968) and the trace element technique of Allégre *et al* (1977). Both methods failed to reject the hypothesis that the two variolitic suites examined in this study (Harker Lake and Dome Mine) could be related by fractional crystallization. Intermittant extrusion of residual melt from a tholeiitic basalt magma that was undergoing progressive fractional crystallization of plagioclase and clinopyroxene is consistent with field relationships, petrography and the geochemical modelling. However, limited combined assimilation-fractional crystallization, magma mixing-fractional crystallization, or both, can not be entirely ruled out.

In comparison to Archean rocks of other areas, variolitic suites have a similar compositional range to the differentiated Golden Mile Dolerite sill in Kalgoorlie, Australia and, possibly, the mafic to felsic intrusive/extrusive suite at Kamiskotia, Ontario (Barrie, 1989). The variolitic suites are also similar to modern, evolved oceanic volcanic suites such as those found in the East Galapagos Rift area, the Thingmuli area in Iceland, and the East Rift of Kilauea Volcano, Hawaii. The compositional range of these suites results from the injection of tholeiitic magma along faults to high levels in the crust where fractional crystallization results in lavas more felsic than typical mid-ocean ridge basalts (Carmichael, 1964; Wright and Fiske, 1971; Perfit *et al*, 1983). Minor cooling as a result of emplacement in thicker crust allows extensive differentiation to take place. Heat energy provided by raised isotherms associated with the faults produces super-heated, nucleus-free, differentiated

extrusives which are essential to variole formation (Wood, 1976: Fowler *et al*, 1987).

Such suites are commonly related to rifting in thickened crustal settings, such as an oceanic island (Iceland), or a rift propagating from a thin oceanic plate into a thicker (cooler) plate (e.g. eastern Galapagos Rift into the Nazca Plate). In the case of Archean variolitic suites, the source tholeiitic magma was probably emplaced in rifts in earlier komatiitic to tholeiitic crust, likely analogous to modern oceanic plates.

7.2.2 Relationship to Au Mineralization

The objective of this study was not to discover the ultimate origin of Archean epigenetic Au deposits, but merely to examine one possible factor controlling the distribution of the mineralization, that is variolite-host control. This discussion is restricted to disseminated sulphide-Au mineralization in wall rocks to veins and shears. Disseminated mineralization results from disequilibrium between the wall rock and pore fluid. Au is deposited by destabilization of its main complexing agent, the bisulphide complex. Sulphidization of the wall rocks is one of the most effective ways to remove sulphur from solution thereby reducing the activity of the bisulphide complex. The association of sulphur addition to the wall rock and anomalous Au has been demonstrated in this study (Figure 6.1.2) and by others (e.g. Hodgson, 1983).

The hydrothermal fluids for Au mineralization could be derived from crustal processes (Groves and Phillips, 1987: Cameron 1989). The fluid is then transported from depth along faults, possibly including reactivated rifts originally related to the formation of the variolitic suites. As the fluid is focussed at the brittle-ductile transition, lower temperatures and pressure reduction-related fluid boiling change the fluid's equilibrium precipitating gangue minerals and bringing the bisulphide complexes and Au in solution closer to saturation. Brittle fractured and chemically distinct variolitic rocks, with high Fe/Mg ratios, react with the fluid and stabilize pyrite rather than carbonate in the wall rock to veins, fractures and shears (Bohlke, 1988). This results in destabilization of the bisulphide Au-complexes by removal of sulphur from the fluid to form pyrite. When Au has become saturated in the fluid, it too will precipitate. Due to their relatively felsic composition compared to the surrounding mafic units, variolites may have deformed as brittle bodies in shear zones, enhancing their

permeability, and allowing the metasomatic fluids access to a larger volume of rock. As a result, mineralization is potentially more extensive. This process will continue as long as access to fresh rocks is maintained and auriferous fluids continue to infiltrate them.

7.2.3 Exploration Applications

This study of variolites has documented certain facts that may be useful in the exploration for epigenetic lode Au deposits. The control exerted by variolites on gold mineralization relates to the effect their composition has on the precipitation of Au from solution. Bohlke (1988; 1989) has demonstrated that rocks which have anomalously high Fe/Mg ratios, relative to their surrounding terrane are preferential hosts for disseminated sulphide-Au mineralization. The present study shows that variolitic rocks commonly fit this criterion. In addition, the relatively felsic composition of the upper members of variolitic suites, such as the V10 subunit in the Timmins area, may cause them to fracture deform under stress, thereby enhancing their permeability. It should be pointed out that, in contrast to felsic rocks in general (which may also have a high Fe/Mg ratio and fracture under stress), variolites commonly contain high concentrations of iron which increases the amount of pyrite which can be developed in wall rock reactions. This also increases the amount of Au which can be precipitated as a consequence of pyritization leading to more significant mineralization in variolites than in felsic rocks (all other factors being equal).

The study shows that the intersection of major shear zones with evolved, high iron volcanic or intrusive rocks, especially when they are in contact with more magnesian (e.g. low Fe/Mg komatiitic) suites, should be considered priority exploration targets on a regional scale, in conjunction with other exploration parameters. However, the model is probably most useful in the detailed stages of an exploration program, when the most likely site for significant disseminated sulphide-Au mineralization is being sought within a area of altered and, possibly, weakly mineralized rocks. The results of this study suggest that variolites are one of the most suitable volcanic rocks to host disseminated sulphide-Au mineralization.

References

Allégre, C.J., Treuil, M., Minster, J., Minster, B. and Albarede, F., 1977. Systematic use of trace elements in igneous processes. Part 1. Fractional crystallization processes in volcanic suites: Contrib. Mineral. Petrol., v. 60, pp. 57-75.

Ames, D.E., Franklin, J.M. and Froese, E., 1991. Zonation of hydrothermal alteration at the San Antonio Gold Mine, Bissett, Manitoba, Canada: Ec. Geol., v. 86, pp. 600-619.

Barrie, C.T., 1989. Geology of the Kamiskotia area, Abitibi Subprovince, in Summary of Field Work and Other Activities 1989: Ont. Geol. Survey, Misc. Paper 146, pp. 144-152.

Barton, P.B., 1984. Redox reactions in hydrothermal fluids, Chapter 8 in Henley, R.W., Truesdell, H.H. and Barton, P.B., eds., Fluid-Mineral Equilibria in Hydrothermal Systems: Reviews in Economic Geology, v. 1, pp. 99-114.

Beach, A., 1980. Retrogressive metamorphic processes in shear zones with special reference to the Lewisian complex: Jour. Struc. Geol., v. 2, pp. 257-263.

Beane, R.E. and Titley, S.R., 1981. Porphyry copper deposits. Part 2. Hydrothermal alteration and mineralization: Ec. Geol., 75th Anniversary Vol., pp. 235-269.

Bickle, M.J., 1978. Heat loss from the earth: a constraint on Archean tectonics from the relation between geothermal gradients and the rate of plate production: Earth Planet. Sci. Letters, v. 40, pp. 301-315.

Bohlke, J.K., 1989. Comparison of metasomatic reactions between a common CO_2-rich vein fluid and diverse wall rocks: Intensive variables, mass transfer, and Au mineralization at Alleghany, California: Econ. Geol., v. 84, pp. 291-327.

Bohlke, J.K., 1988. Carbonate-sulphide equilibria and "stratabound" disseminated epigenetic gold mineralization: a proposal based on examples from Alleghany, California, U.S.A.: Applied Geochem., v. 3, pp. 499-516.

Bowers, T.S. and Helgeson, H., 1983. Calculation of the thermodynamic and geochemical consequences of non-ideal mixing in the system H_2O-CO_2-NaCl on phase relations in geologic systems: Metamorphic equilibria at high pressures and temperatures: Am. Mineral., v. 68, pp. 1059-1075.

Brodie, K.H., 1980. Variations in mineral chemistry across a shear zone in phlogopite peridotite: Jour. Struc. Geol., v. 2, pp. 265-272.

Brown, E.H., 1974. Comparison of the mineralogy and phase relations of blueschists from the North Cascades, Washington, and greenschists from Otago, New Zealand: Geol. Soc. America Bulletin, v. 85, pp. 333-344.

Brown, P.E. and Lamb, W.M., 1986. Mixing of H_2O-CO_2 in fluid inclusions; geobarometry and Archean gold deposits: Geochem. Cosmochem. Acta, v. 50, pp. 847-852.

Burrows, D.R. and Spooner, E.T.C., 1986. The M^{c}Intyre Cu-Au deposit, Timmins, Ontario, Canada, in Macdonald, A.J., ed., Proceedings of Gold '86: Toronto, Ont., pp. 23-39.

Byerlee, J.D. and Brace, W.F., 1968. Stick-slip, stable sliding, and earthquakes - effect of rock type, pressure, strain rate and stiffness: Jour. Geophys. Res., v. 73, pp. 6031-6037.

Cameron, E.M., 1989. Derivation of gold by oxidative metamorphism of a deep ductile shear zone: Part 1. Conceptual model: Jour. Geochem. Exploration, v. 31, pp. 135-147.

Cameron, E.M. and Hattori, K., 1987. Archean gold mineralization and oxidized hydrothermal fluids: Econ. Geol., v. 82, pp. 1177-1191.

Carmichael, D.M., 1991. Gold and the greenschist facies, in Robert, F., Sheahan, P.A., and Green, S.G., eds., Greenstone Gold and Crustal Evolution, NUNA Conference Volume (1990): Geol. Assoc. Canada Publication, pp. 142-143.

Carmichael, I.S.E, 1964. The petrology of Thingmuli, a Tertiary volcano in eastern Iceland: Jour. Petrology, v. 5, pp. 435-460.

Clark, A.M., 1984. Mineralogy of the REE, Chapter 2, in Henderson, P., ed., Rare Earth Element Geochemistry, Part of the Series, Developments in Geochemistry, Elsevier, Amsterdam, pp. 33-62.

Colvine, A.C., Fyon, J.A., Heather, K.B., Marmont, S., Smith, P.M., and Troop, D.G., 1988. Archean lode gold deposits in Ontario: Ontario Geological Survey, Miscellaneous Paper 139, 136 p.

Condie, K.C., Viljoen, M.J. and Kable, E.J.D., 1977. Effects of alteration on element distributions in Archean tholeiites from the Barberton greenston belt: Contrib. Mineral. Petrol., v. 64, pp. 75-89.

Corfu, F., Jackson, S.L. and Sutcliffe, R.H., 1991. U-Pb ages and tectonic significance of late Archean alkalic magmatism and non-marine sedimentation: Timiskaming Group, southern Abitibi belt, Ontario: Can. Jour. Earth Sci., v. 28, pp. 489-503.

Corfu, F., Krogh, T.E., Kwok, Y.Y. and Jensen, L.S., 1989. U-Pb geochronology in the southwest Abitibi greenstone belt, Superior Province: Can. Jour. Earth Sci., v. 26, pp. 1747-1763.

Davies, J.F., Grant, R.W.E., and Whitehead, R.E.S., 1979. Immobile trace elements and

Archean volcanic stratigraphy in the Timmins mining area, Ontario: Can. Jour. Earth Sci., v. 16, pp. 305-311.

Deer, W.A., Howie, R.A. and Zussman, J., 1980. An Introduction to Rock Forming Minerals (Twelfth edition): Longman Group Ltd., Great Britain, 528 p.

Dimroth, E., Boivin, P., Goulet, N. and Larouche, M., 1973. Tectonic and volcanological studies in the Rouyn-Noranda area: Québec Dept. Nat. Resources, Open-file Manuscript, G.M. 28491.

Drummond, S.E. and Ohmoto, H., 1985. Chemical evolution and mineral deposition in boiling hydrothermal systems: Ec. Geol., v. 80, pp. 126-147.

Dubé, B., Guha, J. and Rocheleau, M., 1987. Alteration patterns related to gold mineralization and their relation to CO_2/H_2O ratios: Mineral. and Petrol., v. 37, pp. 267-291.

Dungan, M.A., Vance, J.A. and Blanchard, D.P., 1983. Geochemistry of the Shuksan greenschists and blueschists, North Cascades, Washington: variably fractionated and altered metabasalts of oceanic affinity: Contrib. Mineral. Petrol., v. 82, pp. 131-146.

Ernst, R.E., Fowler, A.D. and Pearce, T.H., 1988. Modelling of igneous fractionation and other processes using Pearce diagrams: Contrib. Mineral. Petrol., v. 100, pp. 12-18.

Ernst, W.G., 1960. The stability relations of magnesioriebeckite: Geoch. Cosmoch. Acta, v. 19, pp. 10-40.

Ferguson, S.A., 1968. Geology and ore deposits of Tisdale Township, District of Cochrane: Ont. Dept. Mines, Geol. Report 58, 177 p.

Fowler, A.D. and Jensen, L.S., 1989. Quantitative trace-element modelling of the crystallization history of the Kinojevis and Blake River Groups, Abitibi Greenstone Belt, Ontario: Can. Jour. Earth Sci., v. 26, pp. 1346-1357.

Fowler, A.D., Stanly, H.E., and Daccord, G., 1989. Disequilibrium silicate mineral growth: Fractal and non-fractal features: Nature, v. 341, pp. 134-138.

Fryer, B.J., Kerrich, R., Hutchinson, R.W., Pierce, M.G. and Rogers, D.S., 1979. Archean precious-metal hydrothermal systems, Dome Mine, Abitibi greenstone belt. I. Patterns of alteration and metal distribution: Can. Jour. Earth Sci., v. 16, pp. 421-439.

Fyfe, W.S., Price, N.J. and Thompson, A.B., 1978. Fluids in the Earth's Crust: Elsevier, Amsterdam, 383 p.

Fyon, J.A. and Crockett, J.H., 1983. Gold exploration in the Timmins area using field and

lithogeochemical characteristics of carbonate zones: Ontario Geol. Survey, Study 26, 56 p.

Gelinas, L., Brooks, C. and Trzcienski, W.E., 1976. Archean variolites - quenched immiscible liquids: Can. Jour. Earth Sci., v. 14, pp. 2945-2958.

Gelinas, L., Mellinger, M. and Trudel, P., 1982. Archean mafic metavolcanics from the Rouyn-Noranda district, Abitibi Greenstone Belt, Quebec. 1. Mobility of the major elements: Can. Jour. Earth Sci., v. 19, pp. 2258-2275.

Gordon, G.E., Randle, K., Coles, G.G., Corliss, J.B., Beeson, M.H., and Oxley, S.S., 1968. Instrumental activation analysis of standard rocks with high resolution gamma ray detector: Geoch. Cosmoch. Acta, v. 32, pp. 369-396.

Graham, C.M., Grieg, K.M., Sheppard, S.M.F., and Turi, B., 1983. Genesis and mobility of the H_2O-CO_2 fluid phase during regional greenschist and epidote amphibolite facies metamorphism: A petrological and stable isotope study in the Scottish Dalradian: Jour. Geol. Soc. London, v. 140, pp. 577-599.

Grant, J.A., 1986. The Isocon Diagram - A simple solution to Gresens' Equation for metasomatic alteration: Econ. Geol., v. 81, pp. 1976-1982.

Grauch, R.I., 1989. Rare Earth Elements in Metamorphic Rocks, Chapter 6, pp. 147-168, in Lipin, B.R. and M^{c}Kay, G.A., eds., Geochemistry and Mineralogy of Rare Earth Elements: Mineralogical Society of America, Reviews in Mineralogy, v.21, 348 p.

Gresens, R.L., 1967. Composition-volume relationships of metasomatism: Chem. Geol., v. 2, pp. 47-55.

Groves, D.I. and Phillips, G.N., 1987. The genesis and tectonic control on Archean gold deposits of the Western Australian Shield - a metamorphic replacement model: Ore Geology Reviews, v. 2, pp. 287-322.

Groves, D.I., Phillips, N., Ho, S.E., Houstoun, S.M., and Standing, C.A., 1987. Craton scale distribution of Archean greenstone gold deposits: Predictive capacity of the metamorphic model: Econ. Geol., v. 82, pp. 2045-2058.

Hall, R.S and Rigg, D.M., 1986. Geology of the West Anticline Zone, Musselwhite Prospect, Opapimiskan Lake, Ontario, Canada, in Macdonald, A.J., ed., Proceedings of Gold '86, Toronto, Ontario, pp. 124-136.

Hattori, K., 1987. Magnetic felsic intrusions associated with Canadian Archean gold deposits: Geology, v. 15, pp. 1107-1111.

Hellman, P.L. and Henderson, P., 1977. Are rare earth elements mobile during

spilitization?: Nature, v. 267, pp. 38-40.

Hodgson, C.J., 1983. Preliminary report on a computer file of gold deposits of the Abitibi Belt, Ontario, in Colvine. A.C., ed., The Geology of Gold in Ontario: Ontario Geol. Survey, Miscellaneous Paper 110, pp. 11-37.

Hodgson, C.J., 1983b. The structure and geological development of the Porcupine camp - a re-evaluation, in Colvine, A.C., ed., The Geology of Gold in Ontario: Ontario Geological Survey, Miscellaneous Paper 110, pp. 211-225.

Hodgson, C.J. and M^{c}Geehan, P.J., 1982. Geological characteristics of gold deposits in the Superior Province of the Canadian Shield, in Hodder. R.W. and Petruk, W., eds., Geology of Canadian Gold Deposits: C.I.M.M., Special Vol. 24, pp. 211-232.

Hodgson, C.J., Hamilton, J.V. and Piroshco, D.W., 1990. Structural setting of gold deposits and the tectonic evolution of the Timmins-Kirkland Lake area, southwestern Abitibi Greenstone Belt, in Groves, D.I., et al , eds., Short Course on Abitibi Mineral deposits, Precambrian Geology, Perth, Australia, pp. 101-120.

Houstoun, S.M., 1987. Competency contrasts and chemical controls as guides to gold mineralization : An example from Barberton Mountain Land: University of Western Australia Publication, No. 11, pp. 147-160.

Hughes, C.J., 1977. Archean variolites - quenched immiscible liquids: Discussion: Can. Jour. Earth Sci., v. 14, pp. 134-139.

Hughes, C.J., 1973. Spilites, keratophyres, and the igneous spectrum: Geol. Magazine, v. 6, pp. 513-527.

Humphris, S.E., 1984. The mobility of rare earth elements in the crust, Chapter 9, in Henderson, P., ed., Rare Earth Element Geochemistry, Elsevier, Amsterdam, pp. 317-342.

Humphris, S.E., Morrison, M.A. and Thompson, R.N., 1978. Influence of rock crystallization history upon subsequent lanthanide mobility during hydrothermal alteration of basalts: Chem. Geol., v. 23, pp. 125-137.

Hutchinson, R.W., 1987. Metallogeny of Precambrian gold deposits: Space and time relationships: Econ. Geol., v. 82, 1993-2007.

Hutchinson, R.W. and Burlington, J.L., 1984. Some broad characteristics of greeenstone belt lodes, in Foster, R.P., ed., Gold '82: Geol. Soc. Zimbabwe, Special Publ. No. 1, pp. 339-372.

Hynes, A., 1980. Carbonatization and mobility of Ti, Y, and Zr in Ascot Formation

metabasalts, southeast Quebec: Contrib. Min. Pet., v. 75, pp. 79-87.

Irvine, T.N. and Baragar, W.R.A., 1971. A guide to the chemical classification of common volcanic rocks: Can. Jour. Earth Sci., v. 8, pp. 523-548.

Jackson, S.L. and Harrap, R.M., 1989. Geology of parts of Pacaud, Catherine, and southernmost Boston and M'Elroy townships, in Summary of Field Work and Other Activities, 1989: Ont. Geol. Survey, Miscellaneous Paper 146, pp. 125-131.

Jensen, L.S., 1978. Geology of Stoughton and Marriott Townships, District of Cochrane: Ont. Geol. Survey, Report 173, 72p.

Jensen, L.S., 1976. A new cation plot for classifying subalkalic volcanic rocks: Ontario Ministry of Natural Resources, Miscellaneous Paper 66, 22 p.

Jensen, L.S. and Langford, F.F., 1985. Geology and petrogenesis of the Archean Abitibi Greenstone Belt in the Kirkland Lake area, Ontario: Ont. Geol. Survey, Miscellaneous Paper 123, 130 p.

Jensen, L.S. and Langford, F.F., 1983. Geology and petrogenesis of the Archean Abitibi belt in the Kirkland Lake area, Ontario; Ont. Geol. Survey, Open File Rept. 5455, 512 p.

Jolly, W.T., 1980. Development and degradation of Archean lavas, Abitibi area, Canada, in light of major element geochemistry: Jour. Petrology, v. 21, pp. 323-363.

Karvinen, W.O., 1981. Geology and evolution of gold deposits in the Timmins area, Ontario, in Pye, E.G. and Roberts, R.G., eds., Genesis of Archean, Volcanic-hosted Gold Deposits: Ontario Geological Survey, Miscellaneous Paper 97, pp. 29-46.

Keays, R.R., 1984. Archean gold deposits and their source rocks: the upper mantle connection, in Foster, R.P., ed., Gold '82: Geol. Soc. Zimbabwe, Special Publ. No. 1, pp. 17-51.

Kennedy, G. and Fowler, A.D., 1983. Interference from uranium in neutron activation analysis of rare-earths in silicate rocks: Jour. Radioanalytical Chem., v. 78, pp. 165-169.

Kerrich, R., 1983. Geochemistry of gold deposits in the Abitibi greenstone belt: Can. Inst. Mining Metall., Special Vol. 27, 75 p.

Kerrich, R. and Fryer, B.J., 1981. The separation of rare elements from abundant base metals in Archean lode gold deposits: implications of low water/rock source regions: Ec. Geol., v. 76, pp. 160-166.

Kerrich, R. and Fryer, B.J., 1979. Archean precious-metal hydrothermal systems, Dome Mine, Abitibi greenstone belt. II. REE and oxygen isotope relations: Can. Jour. Earth Sci., v. 16, pp. 440-458.

Kerrich, R., Fyfe, W.S., Gorman, B.E. and Allison, I., 1977. Local modification of rock chemistry by deformation: Contrib. Mineral. Petrol., v. 65, pp. 183-190.

King, R.W. and Kerrich, R., 1989. Chromian dravite associated with ultramafic-rock-hosted Archean lode gold deposits, Timmins-Porcupine District, Ontario: Canadian Mineralogist, v. 27, pp. 419-426.

Kishida, A. and Kerrich, R., 1987. Hydrothermal alteration zoning and gold concentration at the Kerr Addison Archean lode gold deposit, Kirkland Lake, Ontario: Ec. Geol., v. 82, pp. 649-690.

Knight, C.W., 1924. Lightning River gold area: Ont. Dept. Mines, Annual Report, v. 33, part 3, 46 p.

Kretz, R., 1983. Symbols for rock-forming minerals: Am. Mineral., v. 68, pp. 277-279.

Liou, J.G., Kuniyoshi, S. and Ito, K., 1974. Experimental studies of the phase relations between greenschist and amphibolite in a basaltic system: Am. Jour. Sci., v. 274, pp. 613-632.

Lofgren, G.E., 1974. An experimental study of plagioclase crystal morphology: Isothermal crystallization: Am. Jour. Sci., v. 274, pp. 243-273.

Ludden, J.N. and Thompson, G., 1979. An evaluation of the behaviour of the REE during the weathering of seafloor basalt: Earth Planet. Sci. Letters, v. 43, pp.85-92.

Ludden, J.N., Gelinas, L. and Trudel, P., 1982. Archean metavolcanics from the Rouyn-Noranda district, Abitibi Greenstone Belt, Quebec. 2. Mobility of trace elements and petrogenetic constraints: Can. Jour. Earth Sci., v. 19, pp. 2276-2287.

Macdonald, A.J., 1984. Gold in Ontario: The role of banded iron formation, in Guha, J. and Chown, E.H., eds., Chibougamau - Stratigraphy and Mineralization: CIMM, Special Vol. 34, pp. 412-430.

Macdonald, A.J. and Fyon, J.A., 1986. Sulphidation - key to gold mineralization in banded iron formation: Gold '86 Poster Volume, pp. 96-97.

Martin, R.F., Whitley, J.E. and Woolley, A.R., 1978. An investigation of REE mobility: Fenetized quartzites, Borralan Complex, Northwestern Scotland: Contrib. Mineral. Petrol., v. 66, pp. 69-73.

Mason, R. and Brisbin, D.I., 1987. The geological setting of gold deposits in the Porcupine Mining Camp: Ont. Geol. Survey, Misc. Paper 136, pp. 215-223.

Mason, R., and Melnik, N., 1986. The anatomy of an Archean gold system - the M^{c}Intyre-Hollinger complex at Timmins, Ont, Canada, in Macdonald, A.J., ed., Proceedings of Gold '86, Toronto, Ont., pp. 40-55.

Melson, W.G., Vallier, T.L., Wright, G., Byerly, G. and Nelson, J., 1976. Chemical diversity of abyssal volcanic glass erupted along the Pacific, Atlantic and Indian Ocean seafloor spreading centres, in, Sutton, G., Manghnani, H., and Moberly, R., eds., The Geophysics of the Pacific Ocean Basin and Its Margin: American Geophysical Union, Geophys. Monogr. Series, v. 19, pp. 351-367.

Menzies, M.A. and Seyfried, W.J., 1979. Experimental evidence of rare earth element immobility in greenstones: Nature, v. 282, pp. 398-399.

Michard, A., Albarede, F., Michard, G., Minster, J.F. and Charlou, J.L., 1983. Rare earth elements and uranium in high temperature solutions from the East Pacific Rise hydrothermal vent field (13°N): Nature, v. 303, pp. 795-797.

Mortenson, J.K., 1987. U-Pb chronostratigraphy of the Abitibi greenstone belt [abstract]: Geol. Assoc. Canada, Program with Abstracts, v. 12, p. 75.

Murphy, J.B. and Hynes, A.J., 1986. Contrasting secondary mobility of Ti, P, Zr, Nb, and Y in two metabasaltic suites in the Appalachians: Can. Jour. Earth Sci., v. 23, pp. 1138-1144.

Neall, F.B. and Phillips, G.N., 1987. Fluid-wall rock interaction in an Archean hydrothermal gold deposit: A thermodynamic model for the Hunt Mine, Kambalda: Econ. Geol., v. 82, pp. 1679-1694.

Neumann, H., Mead, J. and Vitaliano, C.J., 1954. Trace element variation during fractional crystallization, as calculated from the distillation law: Geochem. Cosmochem. Acta, v. 6, pp. 90-99.

Nicollet, C. and Adriambololona, D.R., 1980. Distribution of transitional elements in crustal metabasic igneous rocks: Chem. Geol., v. 28, pp. 79-90.

Nunes, P.D. and Jensen, L.S., 1980. Geochronology of the Abitibi metavolcanic belt, Kirkland Lake area - progress report, in Pye, E.G., ed., Summary of Geochronology Studies, 1977-1979: Ontario Geological Survey, Miscellaneous Paper 92, pp. 32-39.

O'Hara, K., 1988. Fluid flow and volume loss during mylonitization: an origin for phyllonite in an overthrust setting, North Carolina, U.S.A.: Tectonophysics, v. 156, pp. 21-36.

Pearce, T.H., 1972. Chemical data as a critical test of differentiation mechanisms: the SME function: G.S.A. Cordilleran Section, 1972 Annual Meeting, Geol. Soc. America Abstracts, v. 4, p. 216.

Pearce, T.H., 1968. A contribution to the theory of variation diagrams: Contrib. Miineral. Petrol., v. 19, pp. 142-157.

Pearce. T.H., Gorman, B.E. and Birkett, T.C., 1977. The relationship between major element chemistry and tectonic environment of basic and intermediate volcanic rocks: Earth Planet. Sci. Letters, v. 36, pp. 121-132.

Perfit, M.R. and Fornari, D.J., 1983. Geochemical studies of abyssal lavas recovered by DSRV Alvin from Eastern Galapagos Rift, Inca Transform, and Ecuador Rift. 2. Phase chemistry and crystallization history: Jour. Geophysical Res., v. 88, pp. 10,530-10,550.

Perfit, M.R., Fornari, D.J., Malahoff, A., and Embly, R.W., 1983. Geochemical studies of abyssal lavas recovered by DSVR Alvin from Eastern Galapagos Rift, Inca Transform, and Ecuador Rift. 3. Trace element abundances and petrogenesis: Jour. Geophysical Res., v. 88, pp. 10,551-10,572.

Phillips, G.N. and Brown, I.J., 1987. Host rock and fluid control on carbonate assemblages in the Golden Mile Dolerite, Kalgoorlie gold deposits, Australia: Canadian Mineralogist, v. 25, pp. 265-273.

Phillips, G.N. and Groves, D.I., 1983. The nature of Archean gold-bearing fluids as deduced from gold deposits of Western Australia: Geol. Soc. Australia Jour., v. 30, pp. 25-39.

Phillips, G.N., Groves, D.I. and Clarke, M.E., 1983. The importance of host rock mineralogy in the location of Archean epigenetic gold deposits: Geol. Soc. S. Africa, Special Publication 7, pp.79-86.

Philpotts, A.R., 1977. Archean variolites - quenched immiscible liquids: discussion: Can. Jour. Earth Sci., v. 14, pp. 139-144.

Pirie, J., 1981. Regional geological setting of gold deposits in the Red Lake area, northwestern Ontario: pp. 71-93, in Genesis of Archean Volcanic-hosted Gold Deposits: Ont. Geol. Survey, Miscellaneous Paper 97. 175 p.

Piroshco, D.W. and Kettles, K., 1988. Geology of Tisdale and northern Whitney townships, in (various), eds., Summary of Field Activities, 1988: Ontario Geological Survey, Miscellaneous Paper 141, pp. 197-205.

Pyke, D.R., 1982. Geology of the Timmins area, District of Cochrane: Ont. Geol. Surv., Report 219, 141 p.

Robert, F. and Brown, A.C., 1986. Archean gold-bearing quartz veins at the Sigma Mine, Abitibi Greenstone Belt, Quebec: Part 2. Vein paragenesis and hydrothermal alteration: Ec. Geol., v. 81, pp. 593-616.

Roberts, R.G., 1987. Ore deposit models #11: Archean lode gold deposits; Geoscience Canada, v. 14, pp. 37-52.

Rogers, D.S., 1982. The geology and ore deposits of the No. 8 shaft area, Dome Mine, in Hodder, R.W. and Petruk, W., eds., Geology of Canadian Gold Deposits: C.I.M.M., Special Vol. 24, pp. 161-170.

Rose, A.W. and Burt, D.M., 1979. Hydrothermal alteration, Chapter 5 in Barnes, H.L., ed., Geochemistry of Hydrothermal Ore Deposits, Second Edition, John Wiley and Sons, New York, pp. 173-235.

Rowins, S.M., Lalonde, A.E., and Cameron, E.M., 1991. Magmatic oxidation in the syenitic Murdoch Creek Intrusion, Kirkland Lake, Ontario: evidence from the ferromagnesian silicates: Jour. of Geology, v. 99, pp. 395-414.

Satterly, J., 1951. Geology of Harker Township: Ont. Dept. Mines, Annual Report, v. 60, Part 7, 47 p.

Schandl, E.S. and Gorton, M.P., 1990. Is the mobility of REE associated with ore deposition of massive sulphides? Evidence from a REE-Zr-rich accessory mineral at Kidd Creek, Timmins, Ontario (revised abstract): 8th IAGOD Symposium, Proceedings with Abstracts, Ottawa, Ontario, p. A16.

Seward, T.M., 1984. The transport and deposition of gold in hydrothermal systems, in Foster, R.P., ed., Gold '82: Geol. Soc. Zimbabwe, Special Publ. No. 1, pp. 165-182.

Shelley, D., 1979. Manual of Optical Mineralogy: Elsevier, New York, 239 p.

Shenberger, D.M. and Barnes, H.L., 1989. Solubility of gold in aqueous sulphide solutions from 150 to 350°C: Geochem. Cosmochem. Acta, v. 53, pp. 269-278.

Sibson, R.H., Robert, F., and Poulsen, K.H., 1988. High-angle reverse faults, fluid-pressure cycling, and mesothermal gold-quartz deposits: Geology, v. 16, pp. 551-555.

Stanley, C.R. and Russell, J.K., 1989. Petrologic hypothesis testing with Pearce element ratio diagrams: derivation of diagram axes: Contrib. Mineral. Petrol., v. 103, pp.78-89.

Staudigal, H. and Hart, S.R., 1983. Alteration of basalt glass: Mechanisms and significance for the oceanic crust-seawater budget: Geoch. Cosmoch. Acta, v. 47, pp. 337-350.

Stesky, R.M., Brace, W.F., Riley, D.K. and Robin, P-Y.F., 1974. Friction in faulted rock at

high temperature and pressure: Tectonophysics, v. 23, pp. 197-203.

Studemeister, P., 1983. The redox state of iron: A powerful indicator of hydrothermal alteration: Geoscience Canada, v. 10, pp. 189-194.

Sun, S. and Nesbitt, R.W., 1978. Petrogenesis of Archean ultrabasic and basic volcanics: Evidence from rare earth elements: Contrib. Mineral. Petrol., v. 65, pp. 301-325.

Thompson, R.N., Esson, J., and Dunham, A.C., 1972. Major element chemical variation in the Eocene lavas of the Isle of Skye, Scotland: Jour. Petrology, v. 13, pp. 219-253.

Thomson, J.E., 1941. Geology of M^{c}Garry and M^{c}Vittie Townships, Larder Lake area: Ontario Dept. Mines Annual Rept., v.50, pt. 7, pp. 68-94.

Thurston, P.C., 1986. Volcanic cyclicity in mineral exploration; the caldera cycle and zoned magma chambers, in Wood, J. and Wallace, H., eds., Volcanology and Mineral Deposits: Ont. Geol. Survey, Miscellaneous Paper 129, pp. 104-123.

Thurston, P.C., 1985. Physical volcanology and stratigraphy of the Confederation Lake area, District of Kenora (Patricia portion): Ont. Geol. Survey, Report 236, 117 p.

Thurston, P.C., Ayres, L.D., Edwards, G.R., Gelinas, L., Ludden, J.N., and Verpaelst, P., 1985. Archean bimodal volcanism, in Ayres, L.D., Thurston, P.C., Card, K.D., and Weber, W., eds., Evolution of Archean Supracrustal Sequences: Geol. Assoc. Canada, Special Paper 28, pp. 7-22.

Travis, G.A., Woodall, R., Bartram, G.D., 1971. The geology of the Kalgoorlie goldfield: Geol. Soc. S. Africa, Special Publ. 7, pp. 175-190.

Wager, L.R. and Brown, G.M., 1968. Layered Igneous Rocks; Oliver and Boyd, Edinburgh, 588 p.

Wilks, M.E., 1988. The Himalayas; a modern analogue for Archean crustal development: Earth Planet. Sci. Letters, v. 87, pp. 127-136.

Wilson, A.D., 1955. A new method for determination of ferrous iron in rocks and minerals: Great Britain Geol. Survey Bull., v. 9, pp. 56-58.

Winkler, H.G.F., 1979. Petrogenesis of Metamorphic Rocks (Fifth Edition): Springer-Verlag, New York, 348 p.

Wood, D.A., 1978. Major and trace element variations in the Tertiary lavas of eastern Iceland and their significance with respect to the Iceland geochemical anomaly: Jour. Petrology, v. 19, pp. 393-436.

Wood, D.A., 1976. Spatial and temporal variation in the trace element geochemistry of the eastern Iceland flood basalt succession: Jour. Geophysical Res., v. 81, pp. 4353-4360.

Wood, P.C., Burrows, D.R., Thomas, A.V., and Spooner, E.T.C., 1986. The Hollinger-McIntyre Au-quartz vein system, Timmins, Ontario, Canada: geologic characteristics, fluid properties and light stable isotope geochemistry, in Macdonald, A.J., ed., Proceedings of Gold '86: Toronto, Ont., pp. 56-80.

Workman, A., 1986. Geology of the Holt-McDermott deposit, in Macdonald, A.J., ed., Proceedings of Gold '86: Toronto, Ont., pp. 184-190.

Wright, T.L. and Fiske, R.S., 1971. Origin of the differentiated and hybrid lavas of Kilauea Volcano, Hawaii: Jour. Petrology, v. 12, pp. 1-65.

Appendices

Appendix 3.1a: Microprobe analyses of sodic amphibole and talc from the L28+00E area, Harker Lake section.

Sample	H-55			
grain	1		2	
target	1 (core)	2 (rim)	3 (rim)	4 (core?)
SiO_2	56.02	62.52	56.36	56.58
TiO_2	0.15	0.01	0.18	0.11
Al_2O_3	0.51	0.26	0.50	0.79
FeO_{Tot}	19.94	6.19	20.58	10.05
MnO	0.17	0.01	0.02	0.55
MgO	11.37	27.82	10.43	17.17
CaO	0.61	0.04	0.50	11.84
Na_2O	6.17	0.02	6.61	0.68
K_2O	0.07	0.03	0.07	0.05
BaO	0.03	0.04	0.14	0.13
Cr_2O_3	0.06	0.00	0.03	0.03
ZnO	0.08	0.16	0.06	0.05
Total	95.20	97.13	95.54	98.41
Cations based on 24 oxygen, by stoichiometry				
Si	8.74	8.71	8.80	8.35
Ti	0.02	0.00	0.02	0.01
Al	0.09	0.04	0.09	0.14
Fe^{2+}	2.60	0.72	2.69	1.24
Mn	0.02	0.00	0.00	0.07
Mg	2.65	5.77	2.43	3.77
Ca	0.10	0.01	0.08	1.87
Na	1.87	0.00	2.00	0.19
K	0.01	0.01	0.01	0.01
Ba	0.00	0.00	0.01	0.01
Cr	0.01	0.00	0.00	0.00
Zn	0.01	0.02	0.01	0.01
F	0.00	0.02	0.03	0.17
Cl	0.00	0.00	0.00	0.00
Total	16.13	15.28	16.14	15.67
Mineral	Mg riebeckite	talc	Mg riebeckite	actinolite(?)

Targets:
1. amphibole, tourquoise-lavender pleochroism.
2. altered rim around target 1, yellowish, high birefringence.
3. amphibole grain, tourquoise-lavender pleochroism.
4. core of target 3 grain, lighter colour than 3.

Appendix 3.1b - Microprobe analyses of carbonate in sample H-50, Section II, Cryderman Zone, Harker Lake section.

Sample	**H-50**	
grain	1	2
target	veinlet	groundmass(w/py)
SiO_2	0.05	0.09
TiO_2	0.05	0.01
Al_2O_3	0.03	0.04
FeO_{Tot}	8.88	7.63
MnO	0.81	0.50
MgO	14.14	14.70
CaO	29.20	29.27
Na_2O	0.03	0.01
K_2O	0.01	0.00
BaO	0.04	0.04
Cr_2O_3	0.04	0.00
ZnO	0.01	0.00
Total	53.29	52.29
Cations based on 24 oxygen, by stoichiometry		
Si	0.02	0.03
Ti	0.02	0.00
Al	0.01	0.02
Fe^{2+}	2.93	2.54
Mn	0.27	0.17
Mg	8.32	8.71
Ca	12.35	12.47
Na	0.02	0.01
K	0.01	0.00
Ba	0.01	0.01
Cr	0.01	0.00
Zn	0.00	0.00
F	0.00	0.00
Cl	0.00	0.00
Total	23.97	23.96
Mineral	Fe dolomite-ankerite	ankerite-Fe dolomite

Grain:
1. carbonate in veinlet, large grain.
2. carbonate grain in groundmass of rock, in contact with pyrite.

Appendix 3.1c: Microprobe analyses of oxide minerals in samples from the Harker Lake section.

Sample	H-22			H-29				H-31							
grain	3			1		2		1		2			3		
target	1	2	3	1	2	3	4	1	2	3	4	5	6	7	8
SiO_2	0.65	29.72	29.40	15.79	28.52	26.98	0.64	0.20	31.05	0.17	0.17	31.51	0.09	0.11	0.21
TiO_2	0.40	32.75	29.03	33.11	34.76	32.22	1.16	0.02	35.05	0.02	0.06	35.79	86.94	0.29	0.00
Al_2O_3	0.17	3.08	4.45	1.08	1.67	1.52	0.03	0.01	1.29	0.04	0.01	1.20	0.00	0.03	0.00
Fe_2O_3	65.21	1.13	3.83	18.78	5.01	8.34	66.21	68.30	2.38	68.93	68.34	2.78	0.00	68.03	67.78
FeO	29.93	1.16	1.59	15.64	2.27	5.72	31.92	30.64	1.09	31.05	30.80	0.00	10.60	31.13	30.50
MnO	0.00	0.06	0.08	2.10	0.23	0.49	0.00	0.09	0.01	0.05	0.06	0.07	0.53	0.00	0.06
MgO	0.14	0.35	1.38	0.01	0.00	0.00	0.00	0.02	0.92	0.02	0.01	2.03	0.00	0.00	0.01
CaO	0.18	26.51	24.83	12.62	26.51	22.81	0.97	0.02	26.25	0.03	0.02	26.63	0.20	0.05	0.09
Cr_2O_3	12.89	1.59	1.14	0.93	0.75	0.00	0.05	0.03	0.20	0.17	0.05	0.00	1.07	0.00	0.17
Total	109.57	96.36	95.73	100.08	99.71	98.07	101.00	99.31	98.21	100.49	99.53	100.00	99.43	99.63	98.82
Cations based on total oxygen appropriate to oxide type, by stoichiometry															
Si	0.17	1.00	1.00	0.59	0.95	0.94	0.19	0.06	1.03	0.05	0.05	1.01	0.00	0.04	0.07
Ti	0.08	0.83	0.74	0.93	0.88	0.84	0.27	0.00	0.88	0.00	0.01	0.86	2.77	0.07	0.00
Al	0.05	0.12	0.18	0.04	0.07	0.06	0.01	0.00	0.05	0.02	0.00	0.05	0.00	0.01	0.00
Fe^{3+}	12.81	0.03	0.10	0.53	0.13	0.22	15.09	15.92	0.06	15.88	15.90	0.07	0.00	15.81	15.88
Fe^{2+}	6.54	0.03	0.05	0.49	0.06	0.17	8.09	7.94	0.03	7.95	7.96	0.00	0.38	8.04	7.94
Mn	0.00	0.00	0.00	0.07	0.01	0.01	0.00	0.02	0.00	0.01	0.01	0.00	0.02	0.00	0.01
Mg	0.05	0.02	0.07	0.00	0.00	0.00	0.00	0.01	0.05	0.01	0.01	0.10	0.00	0.00	0.00
Ca	0.05	0.96	0.91	0.50	0.95	0.85	0.31	0.01	0.94	0.01	0.01	0.91	0.01	0.02	0.03
Cr	2.22	0.04	0.03	0.03	0.02	0.00	0.01	0.01	0.01	0.04	0.01	0.00	0.04	0.00	0.04
Total	21.98	3.03	3.08	3.18	3.06	3.08	23.98	23.97	3.03	23.98	23.97	3.00	3.21	23.99	23.97
Mineral	mag/sp	tnt	tnt	tnt/mg	tnt	tnt	mag	mag	tnt	mag	mag	tnt	rut	mag	mag

Targets:

H-22 1. core of magnetite grain, unaltered, weak lamellae.
2. part of altered rim of grain, near the unaltered core.
3. altered rim of grain, near outer edge of grain.

H-29 1. altered-looking grain, magnetite(?), associated with amphibole grain, mixed results.
2. altered section of grain
3. grain, appears opaque, associated with amphibole grain.
4. as previous.

H-31 1. large, euhedral magnetite grain.
2. alteration at rim of grain.
3. euhedral magnetite grain.
4. euhedral grain, lighter colour than 3.
5. leucoxene grain.
6. acicular, ragged edged crystal, rutile.
7. small grain attached to rutile grain.
8. euhedral grain, magnetite colour.

Appendix 3.1d: Microprobe analyses of oxide mineral grains from sample D89-21, 99 Flow, Dome Mine.

Sample	**D89-21**					
grain	**1**	**1**	**1**	**1**	**1**	**3**
target	1	2	3	4	5	6
SiO_2	0.02	30.39	0.19	29.79	29.74	2.02
TiO_2	0.10	38.00	0.90	36.67	36.93	0.08
Al_2O_3	0.03	0.79	0.01	0.77	0.93	0.20
Fe_2O_3	69.46	1.39	67.32	2.38	3.13	64.60
FeO	31.36	0.02	31.79	1.41	0.83	28.71
MnO	0.04	0.04	0.00	0.03	0.06	0.08
MgO	0.02	0.00	0.06	0.00	0.00	0.31
CaO	0.01	28.48	0.36	27.15	27.78	0.13
Cr_2O_3	0.01	0.26	0.00	0.80	0.08	0.13
Total	101.06	99.37	99.67	99.01	99.47	98.11
Cations based on 24 oxygen, by stioichiometry						
Si	0.01	1.00	0.06	0.99	0.99	0.63
Ti	0.02	0.94	0.21	0.92	0.92	0.02
Al	0.01	0.03	0.00	0.03	0.04	0.07
Fe^{3+}	15.93	0.03	15.47	0.06	0.08	15.20
Fe^{2+}	8.00	0.00	8.11	0.04	0.02	7.51
Mn	0.01	0.00	0.00	0.00	0.00	0.02
Mg	0.01	0.00	0.03	0.00	0.00	0.15
Ca	0.00	1.00	0.12	0.97	0.99	0.04
Cr	0.00	0.01	0.00	0.02	0.00	0.63
Total	23.99	3.02	24.00	3.02	3.03	23.67
Mineral	mag	tnt	mag	tnt	tnt	mag

Targets:
1. pure rim, on grain with exsolution lamellae
2. exsolution bleb, within grain
3. exsolution lamellae
4. dark grey, non-opaque part of grain
5. non-opaque part
6. rim to opaque grain, no exsolution lamellae

Appendix 3.1e: Microprobe analyses of myrmekite and tourmaline in sample D89-25, Key Flow, Dome Mine.

Sample	**D89-25**		
grain	1		2
target	1	2	3
SiO_2	97.62	67.99	36.50
TiO_2	0.12	0.00	0.14
Al_2O_3	0.03	19.62	30.63
FeO_{Tot}	0.04	0.01	11.31
MnO	0.06	0.00	0.01
MgO	0.00	0.00	4.80
CaO	0.00	0.06	0.09
Na_2O	0.00	11.67	2.37
K_2O	0.00	0.03	0.02
Total	97.88	99.38	85.86
Cations			
Si	3.99	2.98	n.a.
Ti	0.00	0.00	n.a.
Al	0.00	1.02	n.a.
Fe^{2+}	0.00	0.00	n.a.
Mn	0.00	0.00	n.a.
Mg	0.00	0.00	n.a.
Ca	0.00	0.00	n.a.
Na	0.00	0.99	n.a.
K	0.00	0.00	n.a.
Total	4.00	5.00	n.a.
Mineral	quartz	albite	tourmaline

Targets:
1. vermicular intergrowths into plagioclase in myrmekite.
2. plagioclase in myrmekite.
3. bluish-green pleochroic grain in groundmass of rock, boron and volatiles missing from analysis.

Appendix 3.2a: X-ray powder diffraction camera data for a sample of sericite from D89-36, Broken spherulitic Flow, Dome Mine. Possible contaminating minerals include quartz and carbonate. Diffraction data for several minerals is shown for comparison, matches are highlighted.

Ring	Scale	Intensity	D-spacing	Muscovite	quartz	dolomite
		$I/I_m x100$	Å	2M1		
1	12.92	70	6.852	**3.73-18**	**4.26-35**	4.03-<5
2	21.10	40	4.211	**3.48-20**	3.34-10	3.69-5
3	23.84	15	3.732	**3.34-25**	**1.82-17**	2.89-100
4	25.36	15	3.512	**3.32-100**	**1.54-15**	2.67-10
5	26.74	100	3.334	**3.19-30**		2.54-10
6	28.28	5	3.156	**2.99-35**		2.41-10
7	30.02	10	2.977	2.86-25		2.19-30
8	31.75	20	2.818	**2.79-20**		2.02-15
9	35.09	60	2.559	**2.57-55**		1.80-20
10	36.48	15	2.463	**2.47-8**		1.79-30
11	37.66	15	2.388	**2.38-25**		1.57-10
12	39.81	20	2.264	**2.25-10**		1.55-10
13	42.48	10	2.128	2.15-16		
14	45.24	35	2.004	**2.13-20**		
15	50.26	25	1.815	**1.99-45**		
16	55.11	5	1.666	**1.65-25**		
17	59.72	25	1.584			
18	61.87	10	1.500	**1.50-30**		
19	67.94	25	1.380			

Appendix 3.2b: X-ray powder diffraction camera data for a sample of sericite from D89-34, the most altered sample of the 99 Flow, Dome mine. Possible contaminants include quartz and carbonate. Diffraction data is shown for these minerals as well as muscovite. Data that matches the sample is highlighted.

Ring	Scale	Intensity	D-spacing	muscovite	quartz	dolomite
		$I/I_{o}x100$	Å	2M1		
1	18.11	20	4.898	4.97-30	4.26-35	4.03-<5
2	19.85	90	4.473	**4.47-20**	3.34-100	3.69-5
3	22.98	5	3.871	**3.88-14**	1.82-17	2.87-100
4	23.96	10	3.714	**3.73-18**	1.54-15	2.67-10
5	27.00	85	3.302	3.48-20		2.54-10
6	28.30	20	3.153	3.34-25		2.41-10
7	30.26	10	2.934	**3.32-100**		2.19-30
8	31.67	15	2.825	**3.19-30**		2.02-15
9	32.52	5	2.753	2.99-35		**1.80-20**
10	35.11	100	2.556	2.86-25		**1.79-30**
11	37.70	15	2.386	2.79-20		1.57-10
12	42.34	20	2.135	2.60-16		1.55-10
13	46.20	15	1.965	**2.57-55**		
14	50.42	10	1.810	**2.38-25**		
15	56.03	20	1.641	**2.15-16**		
16	62.01	40	1.497	**2.13-20**		
				1.99-10		
				1.97-10		
				1.65-25		
				1.50-30		

Appendix 3.2c: X-ray powder diffraction camera data for a sample of carbonate from D89-34, the most altered sample of the 99 Flow, Dome Mine. The best fit is with dolomite. Diffraction data is also shown for possible contaminant minerals quartz and sericite (muscovite) with data matching the measured sample highlighted.

Ring	Scale	Intensity	D-spacing	dolomite	quartz	muscovite
		$I/I_m x100$	Å			2M1
1	21.58	10	4.118	4.03-<5	**4.26-35**	4.97-30
2	24.83	20	3.586	3.69-5	**3.34-100**	4.47-20
3	26.63	60	3.347	**2.89-100**	**1.82-17**	3.88-14
4	27.82	20	3.207	**2.67-10**	**1.54-15**	3.73-18
5	31.21	100	2.866	**2.54-10**		3.48-20
6	33.37	10	2.685	**2.41-10**		**3.32-100**
7	35.21	10	2.549	**2.19-30**		**3.19-30**
8	37.05	25	2.426	**2.02-15**		2.99-35
9	40.99	30	2.202	**1.80-20**		2.86-25
10	45.02	30	2.014	1.79-30		2.79-20
11	50.35	50	1.812	1.57-10		2.60-16
12	60.17	25	1.538	1.55-10		2.57-55
						2.38-25
						2.13-20
						1.99-45
						1.65-25
						1.50-30

Appendix 4.1: Whole rock geochemical data for samples used for plotting Jensen Cation (Jensen, 1976) and AFM (Irvine and Baragar, 1971) diagrams. For sample locations, see Maps 2.1.1 and 2.1.2.

	H-02	H-03	H-05	H-05a	H-06	H-07	H-08	H-09	H-10	H-33	H-34	H-35
SiO_2	49.75	61.09	52.17	57.28	53.17	50.84	47.84	45.99	47.22	54.74	52.94	63.85
TiO_2	3.13	1.76	2.02	1.98	2.03	2.83	2.59	2.23	2.64	1.69	1.70	0.90
Al_2O_3	12.90	13.06	12.43	11.85	12.78	11.51	13.35	13.48	13.12	12.98	13.48	12.33
Fe_2O_3	6.46	1.56	4.19	2.54	4.89	6.19	4.37	4.27	4.64	2.81	3.04	2.99
FeO	10.48	6.87	9.88	9.24	9.09	9.86	12.24	11.92	12.24	9.44	10.53	8.73
MnO	0.25	0.18	0.22	0.19	0.22	0.22	0.26	0.21	0.19	0.18	0.22	0.23
MgO	4.28	3.86	4.92	4.21	4.50	4.78	6.20	7.66	7.34	5.13	5.82	1.05
CaO	6.79	7.17	10.29	7.13	8.86	7.40	9.10	8.41	7.92	7.71	7.94	5.15
Na_2O	4.89	3.57	1.85	3.16	3.37	4.95	2.20	1.98	2.06	3.02	3.12	4.21
K_2O	0.42	0.73	0.32	0.43	0.23	0.26	0.75	0.96	0.95	0.35	0.55	0.23
P_2O_5	0.38	0.24	0.21	0.25	0.23	0.30	0.26	0.19	0.26	0.21	0.21	0.32
Total	99.73	100.09	98.50	98.26	99.37	99.14	99.16	97.30	98.58	98.26	99.55	99.99
Ba	nd	111	15	32	14	nd	44	34	39	40	48	58
Cr	nd	78	56	57	59	56	71	122	80	73	120	30
Zr	127	111	148	147	145	92	94	69	89	165	116	280
Sr	60	110	191	66	124	178	99	73	84	110	99	62
Rb	10	20	4	4	nd	nd	26	34	22	7	10	nd
Y	46	51	65	62	63	33	32	27	35	72	51	107
Nb	14	2	5	5	4	nd	nd	nd	6	4	3	7
Zn	65	46	98	73	70	66	149	40	20	69	83	48
Ni	nd	47	36	36	44	6	34	79	41	43	66	31
V	416	278	544	523	551	498	570	513	577	392	435	nd
La		6.7	7.7	7.3	7.6					8.2	6.0	12.4
Ce		18.7	22.4	22.3	21.7					24.2	18.8	39.3
Nd		14.4	18.8	19.1	18.3					21.1	14.7	30.8
Sm		4.8	6.3	6.2	6.0					6.7	4.7	10.4
Eu		1.59	1.91	1.71	1.84					2.18	1.60	2.86
Tb		1.20	1.66	1.48	1.54					1.71	1.24	2.68
Dy		6.8	9.3	9.1	8.9					10.3	6.8	15.2
Ho		1.57	2.10	2.00	1.90					2.30	1.61	3.60
Yb		4.8	6.5	6.0	6.0					6.6	5.3	10.7
Lu		0.81	1.05	1.00	1.08					1.16	0.80	1.80
Ta		1.36	1.29	1.42	1.01					1.12	0.77	2.29
Th		0.56	0.66	0.62	0.64					0.60	0.39	1.09
U		0.14	0.20	0.15	0.16					0.13	0.21	0.39
FeO_{Tot}	16.29	8.27	13.65	11.53	13.49	15.43	16.17	15.76	16.42	11.97	13.27	11.42
Fe_T/Mg	3.81	2.14	2.77	2.74	3.00	3.23	2.61	2.06	2.24	2.33	2.28	10.88

Sample descriptions:
H-02 - Non-variolitic Flow, massive, coarse grained
H-03 - plagioclase phyric pillow basalt
H-05 - Lower Variolitic pillow basalt, near rim of pillow
H-05a - Lower Variolitic pillow basalt, core area of pillow
H-06 - Lower Variolitic pillow basalt, massive section
H-07 - Non-variolitic pillow basalt
H-08 - Non-variolitic massive basalt, basal chill margin
H-09 - Non-variolitic massive basalt, coarse grained section
H-10 - Non-variolitic massive basalt, fine grained section near top of flow
H-33 - Lower Variolitic Flows, massive flow
H-34 - Lower Variolitic Flows, aphantic, amygdaloidal, varioles parallel to flow contact
H-35 - Phyric Intermediate section, lower massive part

Appendix 4.1: con't.

	H-36	H-37	H-38	H-39	H-11	H-12	H-14	H-15	H-16	H-17	H-18	H-19
SiO_2	62.25	60.33	47.45	50.05	58.40	52.23	57.96	61.24	59.09	54.75	54.48	55.70
TiO_2	0.98	1.01	2.88	2.45	1.99	2.51	1.58	1.47	1.69	2.10	2.24	2.09
Al_2O_3	12.76	12.48	12.14	12.15	11.68	12.17	11.51	11.27	11.42	11.75	12.18	11.79
Fe_2O_3	2.75	3.10	3.47	4.40	4.96	4.87	1.21	5.37	2.49	3.78	3.59	3.86
FeO	9.20	10.68	13.12	11.32	9.03	11.48	12.93	7.43	12.31	9.79	10.26	10.57
MnO	0.26	0.26	0.32	0.28	0.19	0.24	0.18	0.19	0.25	0.19	0.17	0.20
MgO	1.70	1.07	6.54	5.78	3.25	4.16	1.89	1.74	2.73	2.67	4.17	3.08
CaO	4.93	6.14	8.72	7.43	5.07	6.15	3.86	4.25	3.73	5.25	5.88	6.88
Na_2O	4.58	1.36	2.58	3.54	3.27	2.56	4.21	4.44	2.16	3.36	2.87	2.42
K_2O	0.41	0.82	0.38	0.67	0.18	0.61	0.23	0.08	0.08	0.11	0.35	0.10
P_2O_5	0.30	0.38	0.35	0.29	0.53	0.37	0.62	0.58	0.68	0.52	0.42	0.51
Total	100.12	97.63	97.95	98.36	98.55	97.35	96.18	98.06	96.63	94.27	96.61	97.20
Ba	93	269	nd	78	65	142	58	17	26	6	66	nd
Cr	28	34	132	55	50	38	35	33	41	34	30	27
Zr	256	258	88	111	249	141	311	304	299	188	214	267
Sr	74	236	92	197	159	139	114	64	188	84	137	122
Rb	6	18	3	22	nd	14	nd	nd	nd	nd	6	nd
Y	98	105	41	40	69	52	90	91	83	65	66	81
Nb	7	10	nd	5	6	5	5	7	5	4	3	9
Zn	54	216	91	73	89	111	96	68	148	98	95	96
Ni	7	14	101	47	24	16	12	14	8	nd	26	28
V	nd	nd	521	568	42	225	nd	nd	nd	3	276	184
La	11.1	13.6	4.0	4.6	8.5	7.1	11.1	11.4	12.0	9.0	9.0	10.1
Ce	35.3	38.7	12.5	13.9	23.5	18.6	31.2	35.3	34.9	27.0	26.8	29.0
Nd	27.8	30.2	9.9	11.0	21.7	15.6	26.8	28.7	29.1	20.8	21.2	23.3
Sm	9.5	10.2	3.5	3.8	6.9	5.1	9.1	9.1	9.1	7.1	7.0	8.1
Eu	2.78	3.31	1.50	1.52	2.58	2.04	2.88	2.91	3.03	2.47	2.41	2.77
Tb	2.47	2.52	0.90	1.02	1.72	1.25	2.30	2.27	2.26	1.68	1.77	2.07
Dy	13.70	15.00	5.50	6.00	9.90	7.80	12.90	13.20	14.20	10.20	10.60	11.70
Ho	3.50	3.50	1.31	1.25	2.30	1.57	3.00	2.90	2.80	2.20	2.40	2.70
Yb	9.9	10.5	3.5	3.9	6.8	5.3	8.7	8.9	9.0	6.4	6.7	8.0
Lu	1.68	1.71	0.58	0.66	1.17	0.85	1.49	1.51	1.54	1.11	1.13	1.30
Ta	1.77	1.47	0.39	0.67	0.98	0.57	0.97	1.22	0.80	0.75	0.86	0.99
Th	0.92	1.07	0.32	0.38	0.61	0.53	0.91	0.95	0.87	0.74	0.68	0.74
U	0.17	0.24	nd	0.09	0.21	0.13	0.26	0.22	0.26	0.18	0.18	0.12
FeO_{Tot}	11.67	13.47	16.24	15.28	13.49	15.86	14.02	12.26	14.55	13.19	13.49	14.04
Fe_T/Mg	6.87	12.59	2.48	2.64	4.15	3.81	7.42	7.05	5.33	4.94	3.24	4.56

Sample descriptions:
H-36 - Phyric Intermediate section, pillowed?
H-37 - Phyric Intermediate section, near upper contact
H-38 - Non-variolitic massive flow, epidote alteration
H-39 - Non-variolitic flow, footwall to Cryderman Zone
H-11 - Upper Massive Flow, coarse grained
H-12 - Upper Massive Flow, near base of flow
H-14 - Variolitic Intermediate Flows, hyaloclastite unit
H-15 - Variolitic Intermediate Flows, blocky breccia
H-16 - Variolitic Intermediate Flowss, variolitic section
H-17 - Spherulitic Basalt Flows, massive, chlorite amygdules
H-18 - Spherulitic Basalt Flows, massive, magnetic, weakly amygdaloidal
H-19 - Spherulitic Basalt Flows, massive, dark green

Appendix 4.1: con't.

	H-20	H-22	H-23	H-24	H-40	H-41	45722
SiO_2	46.86	48.01	52.03	49.05	64.38	62.05	50.88
TiO_2	2.32	2.80	2.53	2.46	1.42	1.54	2.47
Al_2O_3	13.00	12.52	12.49	12.25	10.71	11.40	12.17
Fe_2O_3	2.40	2.57	1.87	3.14	4.51	4.47	5.87
FeO	13.17	13.29	11.48	12.69	7.60	7.69	9.23
MnO	0.20	0.20	0.25	0.21	0.16	0.16	0.20
MgO	7.24	6.42	4.96	5.41	1.31	1.63	4.39
CaO	7.42	7.42	7.34	8.60	3.76	3.16	9.92
Na_2O	1.43	2.00	2.39	2.27	3.70	3.98	2.78
K_2O	0.37	0.10	0.44	0.35	0.09	0.10	0.59
P_2O_5	0.22	0.33	0.27	0.25	0.60	0.56	0.25
Total	94.63	95.66	96.05	96.68	98.24	96.74	100.55
Ba	19	nd	42	34	13	41	nd
Cr	103	76	56	97	29	25	28
Zr	76	105	114	85	282	300	91
Sr	85	100	79	69	61	50	112
Rb	8	nd	7	7	nd	nd	8
Y	37	43	44	40	84	91	41
Nb	nd	4	4	5	5	6	nd
Zn	109	112	112	93	80	93	108
Ni	81	45	48	68	5	6	36
V	478	447	519	540	nd	nd	542
La	4.0	5.1	4.7	3.9	10.5	11.7	
Ce	12.2	15.3	14.8	12.0	31.9	35.6	
Nd	9.8	12.2	11.2	10.0	25.7	29.8	
Sm	3.1	4.2	3.9	3.3	8.0	9.3	
Eu	1.23	1.66	1.42	1.31	2.85	3.08	
Tb	0.82	1.06	0.98	0.87	2.04	2.34	
Dy	4.8	5.9	6.0	5.2	11.8	13.2	
Ho	0.92	1.36	1.29	1.12	2.70	3.30	
Yb	3.2	4.0	4.1	3.4	8.2	8.6	
Lu	0.53	0.66	0.68	0.60	1.38	1.50	
Ta	0.24	0.43	0.54	0.57	0.93	1.44	
Th	0.25	0.44	0.34	0.21	0.76	1.00	
U	0.07	0.08	0.11	0.08	0.17	0.21	
FeO_{Tot}	15.33	15.60	13.16	15.52	11.66	11.71	14.45
Fe_T/Mg	2.12	2.43	2.65	2.87	8.90	7.19	3.29

Sample descriptions:
H-20 - Non-variolitic massive flow, coarse grained
H-22 - Non-variolitic massive flow
H-23 - Non-variolitic flow
H-24 - Non-variolitic massive flow
H-40 - Variolitic Intermediate Flows, coalesced varioles in blocky breccia
H-41 - Variolitic Intermediate Flows, massive section of hyaloclastite unit
45722 - Non-variolitic flow, footwall to Cryderman Zone

Appendix 4.2: Whole rock geochemical data from the Dome Mine section for samples used in plotting the Jensen Cation and AFM diagrams in Chapter 4. For sample locations, see Maps 2.2.1 to 2.2.6.

	9494	9497	9499	9500	D89-8	D89-16	D89-21	D89-23	D89-30	D89-32	D89-39	D89-41
SiO_2	50.95	48.25	52.32	66.54	52.26	52.05	51.56	55.93	48.94	52.42	51.43	66.67
TiO_2	1.43	1.58	1.15	0.74	1.14	1.34	1.45	1.01	0.77	1.34	1.12	0.61
Al_2O_3	12.20	13.54	12.07	10.51	12.74	11.75	14.06	15.75	13.05	13.21	12.50	9.74
Fe_2O_3	1.27	3.33	1.40	1.20	1.22	1.61	5.62	1.53	0.85	7.37	1.31	0.38
FeO	12.00	7.27	7.96	6.78	9.15	14.16	8.94	7.77	9.07	6.66	9.27	9.59
MnO	0.18	0.27	0.19	0.18	0.20	0.18	0.20	0.11	0.25	0.20	0.19	0.17
MgO	2.41	3.50	4.07	2.23	4.96	2.72	5.38	2.95	5.70	3.08	4.41	1.35
CaO	6.24	8.11	7.02	2.86	6.14	5.54	5.14	4.27	8.29	6.06	7.55	2.68
Na_2O	2.63	1.72	2.77	0.24	3.50	2.03	5.52	0.82	2.97	3.55	1.85	1.80
K_2O	0.01	1.12	0.43	1.83	0.02	0.89	0.22	2.51	0.01	0.06	0.67	1.40
P_2O_5	0.53	0.16	0.11	0.17	0.08	0.45	0.14	0.17	0.04	0.25	0.07	0.14
H_2O^+	nd	nd	nd	nd	3.90	3.00	2.50	4.10	4.10	3.20	4.00	1.70
Total	89.85	88.85	89.49	93.28	95.31	95.72	100.73	96.92	94.04	97.40	94.37	96.23
La	14.0	5.0	5.9	15.4	5.9	9.8	6.0	20.4	2.1	7.4	6.3	15.0
Ce	39.4	14.1	16.4	43.9	17.0	31.7	16.9	62.1	6.9	23.0	18.7	46.3
Nd	28.1	10.7	12.1	32.6	11.7	25.1	13.6	47.0	5.5	16.3	13.2	34.3
Sm	9.5	3.5	4.3	10.7	3.9	8.1	4.1	14.6	1.7	5.3	4.5	10.6
Eu	2.79	1.17	1.10	2.70	1.26	2.26	1.39	3.15	0.60	1.71	1.26	2.63
Tb	2.17	0.80	0.95	2.59	0.98	1.93	0.92	3.53	0.43	1.29	1.09	2.61
Dy	14.8	5.9	6.9	18.6	7.1	11.0	5.8	21.9	3.2	7.3	6.1	16.0
Ho	2.90	1.21	1.42	3.60	1.37	2.65	1.25	5.22	0.65	1.58	1.54	3.49
Tm	1.08	0.39	0.50	1.40	nd	nd	nd	nd	nd	nd	nd	nd
Yb	8.3	3.3	3.9	10.5	4.5	7.2	3.9	15.0	1.9	4.8	4.6	11.1
Lu	1.34	0.51	0.67	1.65	0.72	1.22	0.64	2.53	0.35	0.81	0.76	1.88
Ta	0.59	0.28	0.39	0.82	0.99	1.40	0.87	2.15	0.44	1.33	0.86	2.13
Th	0.94	0.46	0.56	1.38	0.51	0.90	0.50	1.96	0.15	0.65	0.51	1.56
U	0.26	0.11	0.10	0.38	0.12	0.31	0.17	0.55	0.06	0.20	0.19	0.42
Y	80	nd	36	100	41	63	15	139	19	43	42	106
V	40	nd	270	20	308	25	548	101	281	86	299	nd
Ba	40	166	46	58	20	24	4	137	20	18	403	46
Sr	73	109	71	32	141	49	264	65	55	188	102	47
Zr	192	93	107	293	101	160	93	369	40	105	104	283
Cr	30	nd	70	20	68	57	458	26	86	62	57	13
Zn	330	330	62	122	126	150	203	109	110	92	132	179
Cu	12	11	66	9	nd	nd	nd	nd	nd	nd	nd	nd
Rb	nd	nd	nd	nd	nd	11	nd	66	nd	nd	17	31
Nb	nd	nd	nd	nd	nd	7	26	12	nd	4	nd	8
Ni	nd	nd	nd	nd	61	12	182	2	57	nd	41	nd
CO_2	nd	nd	nd	nd	4.7	7.1	.2	3.3	6.3	3.4	5.9	5.2
Au	5	10	5	5	1	29	nd	nd	nd	nd	3	8
FeO_{Tot}	13.14	10.27	9.22	7.86	10.25	15.61	14.00	9.15	9.83	13.29	10.45	9.93
Fe_T/Mg	5.45	2.93	2.27	3.52	2.07	5.74	2.60	3.10	1.73	4.32	2.37	7.36

Sample descriptions:
9494 - Dacite Flow (1100 L), massive, foliated, homogeneous
9497 - 99 Flow (1200 L), dark green, massive, foliated
9499 - Key Flow (1200 L), variolitic, pillowed flow (Plate 1.1.1b)
9500 - Spherulitic Flow (1200 L), massive section, tiny qtz eyes, lt green
D89-08 - Key Flow (1800 L), strong foliation, variolitic pillowed flow
D89-16 - Dacite Flow (1200 L), lt grey-green, massive, foliated, tr. pyrite
D89-21 - 99 FLow (2300 L), dark green, massive, medium grained
D89-23 - Broken Spherulitc Flow (2300 L), heterogeneous, intensely foliated, variolitic
D89-30 - LAPL (2900 L), grey, massive, strong foliation
D89-32 - LSPL (2900 L), dark green, med. grained, strongly magnetic
D89-39 - Key Flow (2900 L), variolitic, strongly foliated
D89-41 - Spherulitic Flow (2900 L), grey, fine grained, foliated

Appendix 4.2: con't.

	9496	P89-02	P89-04	P89-06	P89-09	P89-12	P89-13	9491
SiO_2	45.85	47.89	61.85	53.08	54.26	46.61	44.98	50.19
TiO_2	1.20	1.49	0.85	1.04	1.37	1.21	0.82	1.34
Al_2O_3	13.04	12.62	12.15	13.23	11.22	13.69	13.83	9.92
Fe_2O_3	1.47	3.44	2.05	2.98	2.00	1.53	1.40	16.61
FeO	8.35	10.61	6.42	8.02	12.12	9.62	9.55	nd
MnO	0.20	0.19	0.10	0.22	0.17	0.16	0.24	0.28
MgO	4.73	3.61	2.30	5.22	2.50	5.66	5.61	2.61
CaO	9.77	8.41	4.58	7.34	4.46	7.61	9.71	6.67
Na_2O	2.15	2.63	3.54	2.35	2.94	2.33	3.10	0.86
K_2O	0.32	0.43	0.49	0.01	0.24	0.58	0.08	0.71
P_2O_5	0.10	0.12	0.14	0.08	0.66	0.05	0.03	0.56
H_2O^+	nd	3.90	2.80	4.00	3.00	4.70	5.40	nd
Total	87.18	95.34	97.27	97.57	94.94	93.75	94.75	89.75
La	3.3	5.5	13.6	6.5	9.9	2.8	2.4	9.0
Ce	9.2	16.7	43.4	20.4	30.6	8.0	6.8	26.3
Nd	7.7	11.4	30.7	14.7	26.5	6.4	5.7	21.9
Sm	2.8	3.9	9.4	4.7	8.2	2.3	1.8	7.4
Eu	0.89	1.23	2.03	1.37	2.77	0.85	0.60	2.33
Tb	0.66	1.10	2.28	1.13	1.92	0.62	0.52	1.70
Dy	4.8	5.9	12.6	6.8	11.9	3.9	3.4	11.5
Ho	1.00	1.21	2.91	1.55	2.63	0.90	0.71	2.30
Tm	0.33							0.81
Yb	2.8	4.1	8.7	4.9	7.5	2.6	2.3	6.3
Lu	0.43	0.66	1.51	0.83	1.24	0.45	0.39	1.00
Ta	0.08	0.66	1.65	0.48	1.14	0.49	0.50	0.46
Th	0.19	0.52	1.46	0.70	0.78	0.18	0.22	0.67
U	0.10	0.08	0.32	0.17	0.27	0.11	0.06	0.17
Y	24	34	78	46	72	24	21	60
V	330	280	95	270	nd	382	304	20
Ba	92	82	76	nd	77	242	33	36
Sr	94	114	54	224	104	51	44	64
Zr	59	82	252	111	167	51	42	150
Cr	85	70	30	148	11	81	80	20
Zn	74	138	119	115	126	200	128	560
Cu	nd	nd	nd	nd	nd	nd	nd	17
Rb	nd	3	5	nd	nd	8	nd	nd
Nb	nd	nd	7	nd	4	nd	nd	nd
Ni	nd	21	10	85	nd	58	70	nd
CO_2	nd	6.5	3.5	3.2	5.4	5.3	7.0	nd
Au	10	3	8	2	1	3	6	1
FeO_{Tot}	9.67	13.71	8.26	10.70	13.92	11.00	10.81	14.95
Fe_T/Mg	2.04	3.80	3.59	2.05	5.57	1.94	1.93	5.73

Sample Descriptions:
9496 - APL (1200 L), attenuated pillows, strong foliation
P89-02 - lower V8 subunit, massive, fine grained
P89-04 - mid-V8 subunit, variolitic pillowed flow, large pillows, layered varioles
P89-06 - mid-V8 subunit, variolitic pilowed flow, scattered varioles (Plate 2.2.1)
P89-09 - V10 subunit, massive, fine to medium grained
P89-12 - Gold Centre Subgroup, massive flow, dark green, fine grained
P89-13 - Central Subgroup, pillowed flow, dark green, moderate foliation, chloritic amygdules
9491 - Andesite Flow, masive, med. grained, foliated, homogeneous

Appendix 4.3: Whole rock geochemical data for the sampled section at M^{c}Diarmid Lake. For sample locations, see Map 2.3.1.

	MCD-01	MCD-04	MCD-05	MCD-07	MCD-10	MCD-12	MCD-14
SiO_2	56.09	57.70	57.19	57.42	54.54	56.22	56.03
TiO_2	0.93	0.97	0.95	0.94	0.94	0.96	0.98
Al_2O_3	14.02	13.79	13.52	13.85	14.46	13.59	13.92
Fe_2O_3	3.03	1.98	2.16	2.23	1.88	2.69	1.88
FeO	5.91	6.94	7.52	6.33	7.79	7.13	7.41
MnO	0.13	0.17	0.17	0.16	0.19	0.16	0.18
MgO	5.07	5.50	5.06	5.24	6.54	5.74	5.30
CaO	9.42	6.80	6.81	8.39	6.19	6.64	6.89
Na_2O	1.36	3.40	2.85	2.50	3.59	2.32	3.68
K_2O	0.02	0.03	0.04	0.08	0.07	0.11	0.03
P_2O_5	0.06	0.06	0.07	0.07	0.08	0.07	0.06
H_2O^+	4.10	3.10	3.20	3.20	3.60	3.80	3.50
Total	100.14	100.44	99.54	100.41	99.87	99.43	99.86
Ba	42	100	62	74	82	111	37
Cr	115	180	126	144	187	116	151
Zr	183	186	193	161	143	193	168
Sr	161	111	111	148	94	120	70
Rb	nd	nd	nd	nd	nd	nd	nd
Y	77	75	80	65	61	82	68
Nb	2	3	5	3	3	9	7
Zn	79	124	174	131	134	96	86
Ni	30	92	32	56	58	34	52
V	257	277	258	263	284	264	298
La	11.0	12.0	12.8	10.2	8.9	13.1	10.8
Ce	34.3	36.2	39.4	31.5	25.6	39.2	33.5
Nd	25.6	25.7	28.2	21.5	18.8	28.0	24.5
Sm	8.4	8.9	9.2	7.5	6.3	8.7	7.9
Eu	1.87	1.94	1.99	1.70	1.39	2.04	1.71
Tb	2.06	2.15	2.23	1.82	1.58	2.16	2.00
Dy	12.6	12.9	13.8	11.3	10.3	14.2	12.2
Ho	2.84	2.93	3.24	2.37	2.03	2.95	2.73
Yb	8.4	8.8	9.3	7.5	6.6	9.6	8.0
Lu	1.43	1.44	1.58	1.26	1.08	1.56	1.33
Ta	1.57	1.20	1.25	1.05	0.68	1.00	1.16
Th	1.09	1.16	1.18	0.95	0.87	1.13	1.02
U	0.29	0.31	0.26	0.29	0.19	0.22	0.25
Au	nd	2	nd	11	4	2	nd
FeO_{Tot}	8.64	8.72	9.46	8.34	9.48	9.55	9.10
Fe_T/Mg	1.70	1.59	1.87	1.59	1.45	1.66	1.72

Sample descriptions:
MCD-01 - Flow 1, massive, fine grained, near base, lt green
MCD-04 - Flow 2, brecciated flow top to massive transition, variolitic
MCD-05 - Flow 2, upper spherulitic massive part, lt green, epidote
MCD-07 - Flow 2, basal chilled margin, lt green
MCD-10 - Flow 3, upper variolitic pillowed part, massive sample, spherulitic
MCD-12 - Flow 2, central massive part, lt green, fine grained
MCD-14 - Flow 3, variolitic pilowed section, sample from pillow core

Appendix 5.1a: Major and trace element data for the alteration study of the Variolitic Intermediate Flow, L28+00E area, Harker Lake section.

	H-27	H-26	H-25
SiO_2	60.82	61.93	59.68
TiO_2	1.39	1.35	1.31
Al_2O_3	11.14	11.17	10.98
Fe_2O_3	3.04	5.78	7.60
FeO	10.19	7.08	5.28
MnO	0.21	0.16	0.07
MgO	2.11	1.91	1.55
CaO	3.89	2.40	3.06
Na_2O	2.80	4.34	5.76
K_2O	0.14	0.14	0.27
P_2O_5	0.56	0.56	0.57
H_2O^+	2.9	1.7	0.5
S	0.06	0.06	0.25
CO_2	0.8	1.2	1.4
TOTAL	100.05	99.78	98.28
Ba ppm	57	41	65
Cr	30	33	28
Zr	312	319	315
Sr	69	63	136
Rb	0	0	3
Y	93	91	84
Nb	8	5	9
Zn	143	87	25
Ni	22	13	12
V	0	0	0
Ta	1.07	1.44	1.88
Th	0.95	1.07	0.96
Fe_T	12.89	12.22	12.04
Spec.Grav.	2.87	2.86	2.85
Au ppb	0	0	0
FeO/Fe_T	0.79	0.58	0.44
Al_2O_3/TiO_2	8.0	8.3	8.4
Zr/Y	3.4	3.5	3.8
Ti/Zr	44.6	42.3	41.6
Al_2O_3/Zr	357.1	350.2	348.6
Fe_T/Fe_T+MgO	0.86	0.86	0.89

Appendix 5.1b: Major and trace element data for the alteration study of the Upper Massive Flow, L28+00E area, Harker Lake section.

	H-11	H-29	H-30	H-31	H-55	H-55a
SiO_2	58.40	57.70	61.52	56.67	49.33	59.47
TiO_2	1.99	1.83	1.88	1.86	1.80	1.70
Al_2O_3	11.68	11.17	11.28	11.31	10.88	10.34
Fe_2O_3	4.96	3.62	2.78	6.42	1.35	3.42
FeO	9.03	9.44	9.00	6.24	10.41	6.16
MnO	0.19	0.18	0.16	0.13	0.14	0.05
MgO	3.25	2.86	3.64	2.71	1.68	0.40
CaO	5.07	4.39	2.48	5.11	7.08	3.82
Na_2O	3.27	2.77	3.18	5.16	5.94	6.04
K_2O	0.18	0.18	0.13	0.10	0.41	0.19
P_2O_5	0.53	0.65	0.64	0.62	0.77	0.78
H_2O^+	2.5	2.9	3.2	1.5		
S	0.02	0.01	0.05	0.66	3.54	5.62
CO_2	0.1	0.4	0.4	2.6	5.5	2.3
TOTAL	101.17	98.10	100.34	101.09	98.83	100.29
Ba ppm	65	32	40	66	90	11
Cr	50	32	31	30	43	34
Zr	249	273	275	261	243	209
Sr	159	97	90	193	232	116
Rb					8	0
Y	69	76	79	70	69	56
Nb	6	4	3	3	4	5
Zn	89	51	66	46	51	16
Ni	24	5		9	21	30
V	42	2		4	28	0
Ta	0.98	0.89	0.75	1.03		
Th	0.61	0.76	0.74	0.77		
Fe_T	13.44	12.66	11.47	11.95	11.61	9.20
S.G.	2.90	2.88	2.83	2.86	2.87	2.80
Au ppb	0	0	26	0	794	301
FeO/Fe_T	0.7	0.8	0.8	0.5	0.9	0.7
Al_2O_3/TiO_2	5.9	6.1	6.0	6.1	6.0	6.1
Zr/Y	3.6	3.6	3.5	3.7	3.5	3.7
Ti/Zr	79.9	67.0	68.4	71.3	74.1	81.3
Al_2O_3/Zr	469.1	409.2	410.2	433.3	447.7	494.7
P_2O_5/Zr	21.3	23.8	23.3	23.8	31.7	37.3
Al_2O_3/P_2O_5	22.0	17.2	17.6	18.2	14.1	13.3
Fe_T/Fe_T+MgO	0.81	0.82	0.76	0.82	0.87	0.96

Appendix 5.1c: Major and trace element data for the alteration study of the Non-variolitic Flows associated with the Cryderman Zone, Harker Lake section.

	45722	H-48	H-51	H-45	H-44	H-50	H-49
SiO_2	50.88	51.21	48.09	47.19	45.13	39.43	53.64
TiO_2	2.47	2.62	2.33	2.08	2.27	2.51	2.36
Al_2O_3	12.17	12.85	13.16	10.91	10.59	9.66	7.45
Fe_2O_3	5.75	6.39	8.85	7.23	6.77	7.93	0.15
FeO	9.39	8.60	6.85	4.34	5.52	7.05	6.80
MnO	0.20	0.30	0.31	0.22	0.21	0.24	0.21
MgO	4.39	5.03	4.64	3.28	3.59	3.65	3.53
CaO	9.92	5.95	5.82	7.42	7.19	8.05	8.34
Na_2O	2.78	4.66	4.15	6.19	6.36	5.40	4.19
K_2O	0.59	0.58	0.79	0.42	0.21	0.56	0.31
P_2O_5	0.25	0.37	0.40	0.41	0.26	0.26	0.23
H_2O^+	1.8	2.2	2.9	0.3			
S	0.14	0.07	0.13	0.63	1.14	1.98	2.52
CO_2	0.5	0.3	3.0	10.2	10.5	11.5	11.2
TOTAL	101.23	101.13	101.42	100.81	99.73	98.23	100.94
Ba ppm	0	104	121	67	12	70	34
Cr	28	57	33	35	44	36	46
Zr	91	110	138	142	81	90	51
Sr	112	103	155	342	301	334	338
Rb	8	19	30	7	0	10	4
Y	41	40	49	54	35	41	26
Nb	0	4	2	3	0	2	0
Zn	108	74	79	50	42	40	48
Ni	36	53	33	44	95	64	53
V	542	568	395	420	501	600	50
Fe_T	14.50	14.28	14.72	10.76	11.54	14.10	6.93
S.G.	3.08	2.99	2.88	2.87	2.90	2.98	2.86
Au ppb		130	10	815	2600	1002	4970
FeO/Fe_T	0.65	0.60	0.47	0.40	0.48	0.50	0.98
Al_2O_3/TiO_2	4.9	4.9	5.7	5.2	4.7	3.9	3.2
Zr/Y	2.2	2.8	2.8	2.6	2.3	2.2	2.0
Ti/Zr	271.4	238.2	168.8	146.7	280.5	278.6	463.1
Al_2O_3/Zr	1337.4	1168.2	953.6	768.5	1307.7	1073.6	1461.8
Fe_T/Fe_T+MgO	0.77	0.74	0.76	0.77	0.76	0.79	0.66

Appendix 5.1d: Major and trace element data for the alteration study of the 99 Flow, V8 subunit, Dome Mine.

	D89-21	D89-35	D89-34
SiO_2	51.56	50.17	35.82
TiO_2	1.45	1.40	0.55
Al_2O_3	14.06	13.15	10.76
Fe_2O_3	5.62	4.16	0.66
FeO	8.94	9.56	7.90
MnO	0.20	0.21	0.26
MgO	5.38	5.39	5.02
CaO	5.14	5.91	13.55
Na_2O	5.52	3.06	0.20
K_2O	0.22	0.02	3.46
P_2O_5	0.14	0.13	0.08
H_2O^+	2.5	4.1	1.6
S	0.02	0.05	0.45
CO_2	0.2	3.1	20.1
TOTAL	100.95	100.41	100.41
Ba ppm	23	7	99
Cr	108	101	264
Zr	85	76	65
Sr	105	123	70
Rb	0	0	86
Y	38	35	16
Nb	0	0	0
Zn	172	164	369
Ni	34	27	80
V	254	255	136
La	6	5.5	10.8
Ce	16.9	17.2	26.3
Nd	13.6	13.2	14.6
Sm	4.1	3.8	3.1
Eu	1.39	1.30	1.03
Tb	0.92	0.85	0.46
Dy	5.8	5.0	2.1
Ho	1.25	1.13	0.50
Yb	3.9	3.5	1.3
Lu	0.64	0.63	0.22
Ta	0.87	1.16	1.07
Th	0.50	0.46	1.56
U	0.17	0.13	0.36
Fe_T(FeO)	13.94	13.26	8.49
spec grav	2.94	2.85	2.92
Au ppb	0	0	0
FeO/Fe_T	0.64	0.72	0.93
Al_2O_3/TiO_2	9.7	9.4	19.6
Zr/Y	2.2	2.2	4.1
Ti/Zr	170.6	184.2	84.6
Al_2O_3/Zr	1654.1	1730.3	1655.4
Fe_T/Fe_T+Mg	0.72	0.71	0.63

Appendix 5.1e: Major and trace element data for the alteration study of the Key Flow, V8 subunit, Dome Mine.

	D89-07	D89-08	D89-39	D89-40
SiO_2	49.41	52.26	51.43	45.93
TiO_2	1.16	1.14	1.12	1.14
Al_2O_3	13.06	12.74	12.50	12.75
Fe_2O_3	0.68	1.22	1.31	0.38
FeO	8.36	9.15	9.27	9.59
MnO	0.20	0.20	0.19	0.17
MgO	3.98	4.96	4.41	3.95
CaO	9.14	6.14	7.55	8.26
Na_2O	3.75	3.50	1.85	2.19
K_2O	0.26	0.02	0.67	0.86
P_2O_5	0.08	0.08	0.07	0.07
H_2O^+	3.3	3.9	4.0	2.5
S	0.18	0.09	0.04	0.10
CO_2	7.5	4.7	5.9	12.3
TOTAL	101.06	100.1	100.31	100.19
Ba ppm	49	20	403	184
Cr	58	68	57	71
Zr	107	101	104	110
Sr	96	141	102	88
Rb	0	0	17	21
Y	40	41	42	39
Nb	0	0	0	0
Zn	170	126	132	160
Ni	37	61	41	76
V	304	308	299	323
Ta	0.89	0.99	0.86	
Th	0.58	0.51	0.51	
FeT(FeO)	8.96	10.23	10.43	9.93
S.G.	2.81	2.82	2.80	2.89
Au ppb	0	1	3	8
FeO/Fe_T	0.93	0.89	0.89	0.97
Al_2O_3/TiO_2	11.3	11.2	11.2	11.2
Zr/Y	2.7	2.5	2.5	2.8
Ti/Zr	108.4	112.9	107.7	103.6
Al_2O_3/Zr	1220.6	1261.4	1201.9	1159.1
Fe_T/Fe_T+MgO	0.69	0.67	0.70	0.72

Appendix 5.1f: Major and trace element data for the alteration of the Dacite Flow, V10 subunit, Dome Mine.

	P89-09	D89-16	D89-17
SiO_2	54.26	52.05	56.03
TiO_2	1.37	1.34	1.41
Al_2O_3	11.22	11.75	12.05
Fe_2O_3	2.00	1.61	1.54
FeO	12.12	11.30	12.14
MnO	0.17	0.18	0.12
MgO	2.50	2.72	2.41
CaO	4.46	5.54	4.04
Na_2O	2.94	2.03	1.70
K_2O	0.24	0.89	0.77
P_2O_5	0.66	0.45	0.47
H_2O^+	3.0	3.0	3.3
S	0.14	0.43	0.13
CO_2	5.4	7.1	4.8
TOTAL	100.48	100.39	100.91
Ba ppm	77	24	59
Cr	11	57	44
Zr	167	160	183
Sr	104	49	38
Rb	0	11	11
Y	72	63	76
Nb	4	7	6
Zn	126	150	105
Ni	0	12	0
V	0	25	4
Ta	1.14	1.4	
Th	0.78	0.9	
U	0.27	0.31	
Fe_T	13.90	12.73	13.51
spec grav	2.88	2.85	2.86
Au ppb	1	29	3
FeO/Fe_T	0.87	0.89	0.90
Al_2O_3/TiO_2	8.2	8.8	8.6
Zr/Y	2.3	2.5	2.4
Ti/Zr	82.0	83.8	77.1
Al_2O_3/Zr	671.9	734.4	658.5
Fe_T/Fe_T+Mg	0.85	0.82	0.85